

University of Alberta

Intracellular regulation of matrix metalloproteinase-2 activity:
The roles of caveolin-1 and troponin I phosphorylation.

by

Ava Kalyca Chow

A thesis submitted to the Faculty of Graduate Studies and Research
in partial fulfillment of the requirements for the degree of

Doctor of Philosophy
in
Medical Sciences- Paediatrics

©Ava Kalyca Chow

Fall, 2010

Edmonton, Alberta

Permission is hereby granted to the University of Alberta Libraries to reproduce single copies of this thesis and to lend or sell such copies for private, scholarly or scientific research purposes only. Where the thesis is converted to, or otherwise made available in digital form, the University of Alberta will advise potential users of the thesis of these terms.

The author reserves all other publication and other rights in association with the copyright in the thesis and, except as herein before provided, neither the thesis nor any substantial portion thereof may be printed or otherwise reproduced in any material form whatsoever without the author's prior written permission.

EXAMINING COMMITTEE

Supervisor: Dr. Richard Schulz, Paediatrics and Pharmacology

Committee Members: Dr. Edwin E. Daniel, Pharmacology
Dr. Shairaz Baksh, Paediatrics
Dr. Zamaneh Kassiri, Physiology

External Examiner: Dr. Pascal Bernatchez, Anesthesiology, Pharmacology and
Therapeutics, University of British Columbia

*This thesis is dedicated to the memory and spirit of my mother who gave me the ability,
opportunity, drive and courage to pursue my dreams.*

ABSTRACT

Matrix metalloproteinase-2 (MMP-2) was recently revealed to have targets and actions within the cardiac myocyte. In ischemia/reperfusion (I/R) injury, MMP-2 is activated and degrades troponin I (TnI) and α -actinin. The regulation of intracellular MMP-2 activity is relatively unknown and is thus the subject of this thesis.

The localization of MMP-2 in caveolae of endothelial cells suggests that caveolin-1 (Cav-1) may play a role in regulating MMP-2. Whether Cav-1 is responsible for regulating MMP-2 in the heart is unknown.

A Cav-1 knockout mouse model was used to explore the role Cav-1 may play in the regulation of MMP-2 activity. The initial studies found that MMP-2 and Cav-1 were co-localized in cardiomyocytes and that MMP-2 activity in Cav-1^{-/-} hearts was markedly enhanced. Additionally, the caveolin scaffolding domain inhibited MMP-2 activity in a concentration-dependent manner.

To explore whether increased MMP-2 in Cav-1^{-/-} hearts translates to impaired cardiac function, Cav-1^{+/+} and Cav-1^{-/-} isolated working hearts were physiologically challenged with increasing increments of left atrial preload followed by increasing concentrations of isoproterenol. Cav-1^{-/-} hearts show similar or better cardiac function compared to Cav-1^{+/+} hearts following preload challenge or β -adrenergic stimulation *in vitro*, and this appears unrelated to changes in MMP-2.

Though the function of Cav-1^{-/-} hearts appears similar to that of Cav-1^{+/+} hearts during physiological situations, whether this is the case during I/R injury is not known. Cav-1^{+/+} and Cav-1^{-/-} isolated working mouse hearts exposed to global, no-flow ischemia

showed no functional differences. However, Cav-1^{-/-} hearts had significantly higher levels of both TnI and α -actinin following I/R than Cav-1^{+/+} hearts.

Post-translational modifications of the intracellular MMP-2 substrates could alter susceptibility to MMP-2 proteolysis. Isolated working mouse hearts were exposed to isoproterenol and/or I/R injury to examine the phosphorylation status of TnI. Isoproterenol and I/R both result in the phosphorylation of TnI, however, isoproterenol lead to a more highly phosphorylated form of TnI than that observed in hearts exposed I/R alone.

These and subsequent studies will further reveal the molecular mechanisms that underlie the complex interactions between Cav-1 and MMP-2. This may eventually lead to a novel avenue of therapeutic intervention for heart diseases.

ACKNOWLEDGMENTS

Firstly, I would like to thank my supervisor *Dr. Richard Schulz* not only for the opportunity to do my Ph.D, but for allowing me the independence and freedom to explore, experiment and make mistakes! And of course for steering me back on track when I have strayed too far off course. Your guidance, time and advice have been invaluable and you have shown me the true spirit of science.

I am also deeply grateful to my committee members. *Dr. Edwin Daniel*, you have truly been an inspiration, both in research and in life. *Dr. Shairaz Baksh*, your advice and support, both for the Ph.D and the next stage of my career, are greatly appreciated.

I would also like to thank the numerous members of the Schulz lab, past and present that have been a part of this journey. In particular, thank you to *Drs. Jonathan Cena* and *Ahmed El-Yazbi*. Thanks so much for crazy fun experiments, deep intellectual thoughts and the requisite insanity that is so necessary in completing a Ph.D! Thanks also go out to *Woo Jung Cho*, not only for his hard work on the micrographs in the thesis, but for his willingness to share his vast knowledge and enthusiasm about science.

I'd also like to express my appreciation to the members of the Cardiovascular Research Centre who have helped me throughout this adventure. The people that I have met, and the friendships that have formed during my time here more than make up for all the blood, sweat and tears that went into this Ph.D. Thanks especially to *Mary-Jo Boeglin* for administrative (and especially) moral support.

And finally, I would like to thank my husband, *Kirby Chan*, who was dragged along for this incredible journey and whose unwavering support, love and sense of humor were essential for my sanity. I know that our next big adventure has already begun, and his name is *Korbin*.

TABLE OF CONTENTS

CHAPTER 1 INTRODUCTION

1.1: Matrix metalloproteinases.....	2
1.1.1: Classification	3
1.1.2: Structure	3
1.1.3: Function	4
1.1.4: Regulation	5
1.2: Tissue inhibitors of metalloproteinases.....	8
1.3: Pharmacological inhibitors of MMPs.....	9
1.4: MMPs in heart development and angiogenesis	11
1.5: MMPs in inflammatory heart disease.....	12
1.6: MMPs in ischemia/reperfusion injury	15
1.7: Intracellular MMPs.....	19
1.7.1: Sarcomeric MMP-2	20
1.7.2: Cytoskeletal MMP-2.....	20
1.7.3: Nuclear MMP-2.....	21
1.8: Caveolins	21
1.8.1: Classification	22
1.8.2: Structure	23
1.8.3: Function	24
1.8.4: Regulation	26
1.8.5: Caveolin knockout models.....	26
1.9: Working hypothesis	27
1.10: Thesis objectives	28
1.10.1: Caveolin regulation of MMP-2 in the heart (Chapter 2).....	28
1.10.2: MMP-2 and caveolin localization in the heart (Chapter 3).....	28
1.10.3: Physiological and pharmacological challenges to caveolin-1 knockout mouse heart (Chapter 4).....	28
1.10.4: Ischemia/reperfusion injury in the caveolin-1 knockout mouse heart (Chapter 5)	29
1.10.5: Troponin I phosphorylation in response to ischemia/reperfusion injury and/or β -adrenergic stimulation in the isolated working mouse heart	29
1.11: Conclusion.....	29
1.12: References	38

CHAPTER 2
CAVEOLIN REGULATION OF MMP-2 IN THE HEART

2.1: Introduction	72
2.2: Materials and methods.....	73
2.2.1: Animals.....	73
2.2.2: Tissue collection and preparation of heart extracts	73
2.2.3: Gelatin zymography	74
2.2.4: Western blot analysis.....	74
2.2.5: Immunohistochemistry	75
2.2.6: In vitro MMP-2 kinetic assay.....	76
2.2.7: In vitro degradation of tubulin.....	77
2.2.8: Collagen content of Cav-1 ^{+/+} and Cav-1 ^{-/-} mouse hearts	78
2.2.9: In silico analyses.....	79
2.2.10: Statistical analysis	79
2.3: Results.....	79
2.3.1: Caveolin binding domains in MMP-2	79
2.3.2: Confocal of MMP-2 and Cav-1	80
2.3.3: In vitro MMP-2 kinetic assay.....	80
2.3.5: MMP-2 activity and protein in lipid rafts of hearts	81
2.3.6: Tubulin in Cav-1 ^{+/+} and Cav-1 ^{-/-} mouse hearts	81
2.3.7: Collagen content of Cav-1 ^{+/+} and Cav-1 ^{-/-} mouse heart extracts.....	82
2.4: Discussion	82
2.5: References	107

CHAPTER 3
MMP-2 AND CAVEOLIN LOCALIZATION IN THE HEART

3.1: Introduction	114
3.2: Materials and methods.....	116
3.2.1: Animals.....	116
3.2.2: Tissue preparation	117
3.2.3: Cryosectioning	117
3.2.4: Double immunofluorescent labeling	117
3.2.5: Confocal microscopy.....	118
3.2.6: Electron microscopy.....	119
3.3: Results.....	120
3.3.1: General distribution of MMP-2.....	120
3.3.2: MMP-2 and Cav-1 co-localization in cardiomyocytes.....	120
3.3.3: Localization of MMP-2 and Cav-2 in cardiomyocytes.....	121
3.3.4: Localization of MMP-2 and Cav-3 in cardiomyocytes.....	121

3.3.5: Localization of MMP-2 in FAK positive fibroblasts	122
3.3.6: Localization of MMP-2 in DDR-2 positive fibroblasts	122
3.3.7: MMP-2 in capillary endothelial cells.....	122
3.3.8: MMP-2 in interstitial Cajal-like cells	123
3.3.9: Co-localization of Cav-1 and Cav-2	123
3.3.10: Co-localization of Cav-1 and Cav-3	123
3.3.11: Co-localization of Cav-2 and Cav-3	124
3.3.12: FAK-positive fibroblasts and co-localization with Cav-1	124
3.3.13: vWF-positive capillary endothelial cell and its co-localization with Cav-1	124
3.3.14: DDR-2-positive fibroblast and its co-localization with Cav-1.....	124
3.3.15 c-Kit-positive ICLCs and its co-localization with Cav-1	125
3.3.16: FAK-positive fibroblast and its relationship with Cav-2	125
3.3.17: c-Kit-positive interstitial Cajal-like cell and its relationship with Cav-2	125
3.3.18: FAK-positive fibroblasts and its co-localization with Cav-3	125
3.3.19: DDR-2-positive fibroblasts and its co-localization with Cav-3	126
3.3.20: vWF-positive capillary endothelial cells and its relationship with Cav-3.....	126
3.3.21: c-Kit-positive ICLCs and its co-localization with Cav-3	126
3.3.22: FAK and vWF are not associated.....	126
3.3.23: Association between DDR-2 and c-Kit	127
3.3.24: Cardiomyocyte electron microscopy	127
3.3.25: Capillary endothelial cell electron microscopy	128
3.3.26: Fibroblast electron microscopy	128
3.4: Discussion	129
3.5: References	154

CHAPTER 4
PHYSIOLOGICAL AND PHARMACOLOGICAL CHALLENGES TO CAVEOLIN-1 KNOCKOUT
MOUSE HEART

4.1: Introduction	162
4.2: Materials and methods.....	164
4.2.1: Animals.....	164
4.2.2: Isolated working mouse heart	164
4.2.3: Langendorff mouse hearts.....	166
4.2.4: Tissue preparation	166
4.2.5: Western blotting	167
4.2.6: Gelatin zymography	167
4.2.7: Data analysis	167
4.2.8: Statistics	168
4.3: Results.....	168
4.3.1: Response of caveolin-1 knockout mouse hearts to preload challenge	168
4.3.2: Response of caveolin-1 knockout mouse hearts to isoproterenol challenge...	169
4.3.3: MMP-2 activity and protein content in Cav-1 ^{-/-} mouse hearts following preload and adrenergic challenges	169

4.3.4: Sarcomeric and cytoskeletal protein levels in Cav-1 ^{-/-} mouse hearts following preload and isoproterenol challenges	170
4.3.5: MMP-2 activity in Cav-1 ^{-/-} mouse hearts Langendorff perfused for 10 or 90 minutes	170
4.4: Discussion	170
4.5: References	184

CHAPTER 5

ISCHEMIA/REPERFUSION INJURY IN THE CAVEOLIN-2 KNOCKOUT MOUSE HEART

5.1: Introduction	191
5.2: Materials and methods.....	192
5.2.1: Animals.....	192
5.2.2: Isolated working mouse heart	193
5.2.3: Tissue preparation	194
5.2.4: Western blotting	195
5.2.5: Gelatin zymography	195
5.2.7: Statistics	196
5.3: Results.....	196
5.3.1: Cav-1 ^{-/-} hearts are not functionally different from Cav-1 ^{+/+} hearts following 15 min of ischemia and reperfusion	196
5.3.2: MMP-2 activity and protein content in Cav-1 ^{-/-} and Cav-1 ^{+/+} mouse hearts after 15 min of ischemia followed by reperfusion	197
5.3.3: Sarcomeric and cytoskeletal protein levels in Cav-1 ^{-/-} mouse hearts is greater than that in Cav-1 ^{+/+} hearts after 15 min of ischemia followed by reperfusion	197
5.3.4: Cav-1 ^{-/-} hearts are not functionally different from Cav-1 ^{+/+} hearts following 17 min of ischemia	198
5.3.5 MMP-2 activity and protein content in Cav-1 ^{-/-} and Cav-1 ^{+/+} mouse hearts after 17 min of ischemia followed by reperfusion	199
5.3.6: Sarcomeric and cytoskeletal protein levels in Cav-1 ^{-/-} mouse hearts is greater than that in Cav-1 ^{+/+} hearts after 17 min of ischemia followed by reperfusion	199
5.4: Discussion	199
5.5: References	221

CHAPTER 6

TROPONIN I PHOSPHORYLATION IN RESPONSE TO ISCHEMIA / REPERFUSION INJURY AND/OR β-ADRENERGIC STIMULATION IN THE ISOLATED WORKING MOUSE HEART

6.1: Introduction	227
6.2: Materials and methods.....	230
6.2.1: Animals.....	230
6.2.2: Isolated working mouse heart	230

6.2.3: Heart extracts.....	232
6.2.4: Western blotting	232
6.2.5: Gelatin zymography	233
6.2.6: Data analysis	234
6.2.7: Statistics	234
6.3: Results.....	234
6.3.1: Functional measures	234
6.3.2: MMP-2 activity and protein content	235
6.3.3: Troponin I levels.....	235
6.3.4: Phospho Troponin I levels.....	236
6.4: Discussion	237
6.5: References	259

**CHAPTER 7
CONCLUSIONS**

7.1: Conclusions	268
7.2: Limitations	271
7.2.1: Experimental design limitations	271
7.2.2: Technique limitations	273
7.3: Future directions.....	277
7.4: References	281

LIST OF TABLES

<u>Table 1.1:</u>	Intracellular MMP-2 substrates	37
<u>Table 3.1:</u>	Antibodies and sera used in experiments.....	151
<u>Table 3.2:</u>	Protein co-localization in Cav-1 ^{+/+} myocardium.....	152
<u>Table 5.1:</u>	Differences in functional parameters between the final aerobic measurement and the final measurement obtained during reperfusion, within each group for hearts exposed to 15 min ischemia.....	217
<u>Table 5.2:</u>	Differences in functional parameters between the final aerobic measurement and the final measurement obtained during reperfusion, within each group for hearts exposed to 17 min ischemia.....	219
<u>Table 6.1:</u>	Difference in functional parameters between the final aerobic measurement and the final measurement obtained during reperfusion, within each group.....	257

LIST OF FIGURES

<u>Figure 1.1:</u>	MMP structure	31
<u>Figure 1.2:</u>	Activation mechanisms of MMP-2	33
<u>Figure 1.3:</u>	Intracellular targets and binding partners of MMP-2 in the cardiomyocyte	35
<u>Figure 2.1:</u>	Caveolin binding domains in MMP-2.....	87
<u>Figure 2.2:</u>	Cav-1 localizes with MMP-2 in cardiac myocytes in left ventricular sections	89
<u>Figure 2.3:</u>	CSD inhibition of MMP-2 in a kinetic assay	91
<u>Figure 2.4:</u>	MMP-2 proteolytic activity and protein, and TIMP-2 and -4 protein in Cav-1 ^{+/+} and Cav-1 ^{-/-} hearts	93
<u>Figure 2.5:</u>	Characteristics of lipid raft enriched fractions from Cav-1 ^{+/+} and Cav-1 ^{-/-} hearts	95
<u>Figure 2.6:</u>	α -tubulin degradation and content in Cav-1 ^{-/-} mouse hearts.....	97
<u>Figure 2.7:</u>	Immunohistochemical staining for tubulin in Cav-1 ^{+/+} and Cav-1 ^{-/-} mouse ventricle	99
<u>Figure 2.8:</u>	Collagen content Cav-1 ^{+/+} and Cav-1 ^{-/-} mouse heart as determined by Sircol assay.....	101
<u>Figure 2.9:</u>	CSD binding motifs on MMP-2	103
<u>Figure 2.10:</u>	Sequence alignment of rat, mouse, human, pig, turkey medaka and zebrafish MMP-2 proteins	105

<u>Figure 3.1:</u>	MMP-2 in Cav-1 ^{+/+} and Cav-1 ^{-/-} left ventricular myocardium	133
<u>Figure 3.2:</u>	MMP-2 localization with caveolins in Cav-1 ^{+/+} and Cav-1 ^{-/-} left ventricular myocardium	135
<u>Figure 3.3:</u>	MMP-2 co-localization with FAK, DDR-2, vWF and c-Kit in Cav-1 ^{+/+} and Cav-1 ^{-/-} myocardium.....	137
<u>Figure 3.4:</u>	Co-localizations of caveolins in Cav-1 ^{+/+} and Cav-1 ^{-/-} myocardium	139
<u>Figure 3.5:</u>	Cav-1 localization with FAK, DDR-2, vWF and c-Kit in Cav-1 ^{+/+} and Cav-1 ^{-/-} myocardium	141
<u>Figure 3.6:</u>	Co-localization of Cav-2 with FAK and c-Kit in Cav-1 ^{+/+} and Cav-1 ^{-/-} myocardium	143
<u>Figure 3.7:</u>	Co-localization of Cav-3 with FAK, DDR-2, vWF and c-Kit in Cav-1 ^{+/+} and Cav-1 ^{-/-} myocardium.....	145
<u>Figure 3.8:</u>	FAK, vWF, DDR-2 and c-Kit in Cav-1 ^{+/+} and Cav-1 ^{-/-} myocardium	147
<u>Figure 3.9:</u>	Electron micrographs of cardiomyocytes, fibroblasts and capillary endothelial cells in Cav-1 ^{+/+} and Cav-1 ^{-/-} myocardium.....	149
<u>Figure 4.1:</u>	Functional measurements of isolated working hearts in response to step-wise increase in preload pressure from Cav-1 ^{+/+} and Cav-1 ^{-/-} mice	174
<u>Figure 4.2:</u>	Functional measurements of isolated working hearts from Cav-1 ^{+/+} and Cav-1 ^{-/-} mice challenged with varying concentrations of DL-isoproterenol (Iso)	176
<u>Figure 4.3:</u>	MMP-2 activity and protein from Cav-1 ^{+/+} and Cav-1 ^{-/-} mouse hearts following preload and isoproterenol challenges	178

<u>Figure 4.4:</u>	Levels of sarcomeric and cytoskeletal proteins in Cav-1 ^{+/+} and Cav-1 ^{-/-} following preload and isoproterenol challenges	180
<u>Figure 4.5:</u>	MMP-2 activity in Cav-1 ^{+/+} and Cav-1 ^{-/-} mouse hearts perfused for 10 min or 90 min.....	182
<u>Figure 5.1:</u>	Experimental design for Cav-1 ^{+/+} and Cav-1 ^{-/-} hearts exposed to I/R injury.	203
<u>Figure 5.2:</u>	Functional measurements of isolated hearts from Cav-1 ^{+/+} and Cav-1 ^{-/-} subjected to 15 min of global no-flow ischemia.....	205
<u>Figure 5.3:</u>	MMP-2 protein and activity in Cav-1 ^{+/+} and Cav-1 ^{-/-} subjected to 15 min I/R.....	207
<u>Figure 5.4:</u>	Levels of sarcomeric and cytoskeletal proteins Cav-1 ^{+/+} and Cav-1 ^{-/-} subjected to 15 min I/R.....	209
<u>Figure 5.5:</u>	Functional measurements of isolated hearts from Cav-1 ^{+/+} and Cav-1 ^{-/-} subjected to 17 min of global no-flow ischemia.....	211
<u>Figure 5.6:</u>	MMP-2 protein and activity in Cav-1 ^{+/+} and Cav-1 ^{-/-} subjected to 17 min I/R.....	213
<u>Figure 5.7:</u>	Levels of sarcomeric and cytoskeletal proteins Cav-1 ^{+/+} and Cav-1 ^{-/-} subjected to 17 min I/R.....	215
<u>Figure 6.1:</u>	Experimental design for mouse hearts exposed to isoproterenol and/or I/R.....	241
<u>Figure 6.2:</u>	Peak systolic pressure and pulse pressure of isolated mouse hearts exposed to isoproterenol and/or I/R.....	243

<u>Figure 6.3:</u>	Coronary flow and aortic output of isolated mouse hearts exposed to isoproterenol and/or I/R.....	245
<u>Figure 6.4:</u>	Heart rate and rate pressure product of isolated mouse hearts exposed to isoproterenol and/or I/R	247
<u>Figure 6.5:</u>	Cardiac output and cardiac work of isolated mouse hearts exposed to isoproterenol and/or I/R.....	249
<u>Figure 6.6:</u>	MMP-2 protein and activity in isolated mouse hearts exposed to isoproterenol and/or I/R.....	251
<u>Figure 6.7:</u>	Levels of total and phosphorylated cTnI in isolated mouse hearts exposed to isoproterenol and/or I/R.....	253
<u>Figure 6.8:</u>	Levels of phosphorylated cTnI in isolated mouse hearts exposed to isoproterenol and/or I/R using a Phos-tag TM acrylamide gel.....	255

LIST OF NON-STANDARD ABBREVIATIONS

AP-1	activated protein-1
ATP	adenosine-5'-triphosphate
b.i.d.	<i>bis in die</i> (twice a day)
cAMP	cyclic adenosine monophosphate
Cav	caveolin
Cav-1 ^{-/-}	cav<tm 1 M Is>/J- caveolin-1 knockout mouse
Cav-1 ^{+/+}	B6 129 SF2/J- control mice for Cav-1 ^{-/-}
CBD	caveolin binding domain
CSD	caveolin scaffolding domain
CSD-X	caveolin scaffolding domain control peptide
cTnC	cardiac troponin C
cTnI	cardiac troponin I
DAPI	4',6-diamidino-2-phenylindole
DDR-2	discoidin domain receptor-2
DMSO	dimethyl sulfoxide
eNOS	endothelial nitric oxide synthase
FAK	focal adhesion kinase
GM-6001	N-[(2R)-2-(hydroxamidocarbonylmethyl)-4-methylpentanoyl]-L-tryptophan methylamide
GSH	glutathione
GTP	guanosine-5'-triphosphate
ICLC	interstitial Cajal-like cells
IgG	immunoglobulin G

IL-1 β	interleukin-1 β
i.p.	intraperitoneal
I/R	ischemia and reperfusion
Iso	DL-isoproterenol
IU	international units
kb	kilobases
kDa	kilodalton
λ_{em}	emission wavelength
λ_{ex}	excitation wavelength
MLC-1	myosin light chain-1
MMP	matrix metalloproteinase
mRNA	messenger ribonucleic acid
MT-MMP	membrane type matrix metalloproteinase
NF- κ B	nuclear factor - κ B
nNOS	neuronal nitric oxide synthase
ONOO $^-$	peroxynitrite
PBS	phosphate buffered saline
PD-166793	N-[(4'-Bromo[1,1'-biphenyl]-4-yl)sulfonyl]-L-valine
PKA	protein kinase A
PKC	protein kinase C
PVDF	polyvinylidene fluoride
SDS-PAGE	sodium dodecyl sulfate polyacrylamide gel electrophoresis
SEM	standard error of the mean
TIMP	tissue inhibitor of metalloproteinase

TnC	troponin C
TNF- α	tumor necrosis factor- α
TnI	troponin I
TTBS	Tris-Tween buffered saline
vWF	von Willebrand factor

CHAPTER 1

INTRODUCTION

Portions of this chapter have been published in the following reviews:

Chow AK, Cena J, Schulz R. Acute actions and novel targets of matrix metalloproteinases in the heart and vasculature. *Br J Pharmacol* 2007; 152:189-205.

Kandasamy AD, Chow AK, Ali MA, Schulz R. Matrix metalloproteinase-2 and myocardial oxidative stress injury: beyond the matrix. *Cardiovasc Res* 2010; 83: 413-423.

1.1: Matrix metalloproteinases

Matrix metalloproteinases (MMPs) were initially discovered in 1962 as collagenolytic activity released during the process of extracellular matrix protein degradation required for resorption of the tadpole tail¹. Since then, the MMP family has grown to include 25 members. Though many MMPs were subclassified based on their ability to degrade various proteins of the extracellular matrix, they also play other important roles such as the activation of cell surface receptors and chemokines². MMPs have been shown to play significant roles in a number of physiological processes, including embryogenesis³ and angiogenesis⁴, but also contribute to pathological processes such as tumor metastasis⁵, inflammation and arthritis⁶. Of this diverse family of enzymes, MMP-2 and -9 (also known as gelatinase A and gelatinase B, respectively) have emerged as important players in a number of cardiovascular diseases, including atherosclerosis, stroke, heart failure, ischemic heart disease and aneurysm⁷⁻¹⁰. Though MMPs are best known for their actions in extracellular matrix remodeling, recent evidence has shown that MMPs, in particular MMP-2, also play important roles intracellularly, particularly in response to enhanced oxidative stress including ischemia and reperfusion (I/R) injury of the heart¹¹⁻¹³.

In the heart, MMPs are predominantly found in their full-length zymogen form closely associated with their natural endogenous inhibitors, the tissue inhibitors of metalloproteinases (TIMPs)¹⁴. MMP-2 is ubiquitously expressed in the cells which comprise the heart and is found in normal cardiomyocytes, as well as in the endothelium, vascular smooth muscle cells, and fibroblasts^{11,15}. Similarly, MMP-2 is found in human arteries¹⁶ as well as in normal human umbilical and femoral vein

endothelial cells¹⁷. MMP-9 is an enzyme whose expression is first induced under conditions of immune activation (i.e. in response to pro-inflammatory cytokines) and is normally associated with activated leukocytes and macrophages¹⁸, human endothelial cells¹⁹ and H9c2 embryonic cardiomyocytes²⁰.

1.1.1: Classification

MMPs are a large family of zinc-dependent endopeptidases that have been classified in a number of different ways. MMPs are given numerical designations²¹ and archetypal classification of the MMPs is based on the extracellular matrix substrates which they proteolyze, primary structure, and subcellular localization²². Groups of MMPs include the collagenases (MMPs -1, -8, and -13), stromelysins (MMPs-3 and -10), matrilysins (MMPs-7 and -26), membrane-type MMPs (MT-MMPs, 1 through 8), and the gelatinases (MMPs-2 and -9) (Figure 1.1). It is, however, becoming increasingly apparent that this classification scheme is arbitrary, particularly as a number of MMPs do not fit into the aforementioned groups, and previously classified MMPs have been shown to proteolyze other substrates in addition to the ones for which they were originally named.

1.1.2: Structure

All MMPs are initially synthesized in an enzymatically inactive or zymogen form ("pro-MMPs"²³). MMP structure (Figure 1.1) consists of a signal peptide at the N-terminal region which is considered to promote the translocation of the enzyme into the endoplasmic reticulum and subsequent secretion out of the cell. Adjacent to the signal peptide is a hydrophobic propeptide domain that shields the neighboring catalytic domain which contains a Zn²⁺ ion. The catalytic domain in the gelatinases is unique from

that of other MMPs in that it contains three fibronectin type II-like domains which form a collagen binding domain, allowing for the binding and subsequent cleavage of type IV collagen or denatured collagen (gelatin)²⁴. Activation of proMMPs requires the dissociation of the binding between the cysteinyl sulphhydryl in the propeptide domain and the catalytic Zn²⁺ ion. This critical cysteine residue and the Zn²⁺ catalytic domain are common to all MMPs. The so-called “cysteine switch” is believed to be a common mechanism of activation for all MMPs²⁵. The hemopexin-like C-terminal region is connected to the catalytic domain by a flexible hinge region and can allow for the binding of other proteins which may serve to alter the activity of the MMP (Figure 1.1).

1.1.3: Function

MMPs were first described in relation to their ability to degrade extracellular matrix proteins, and as such, their roles in extracellular matrix remodeling in a variety of physiological and pathophysiological processes in the cardiovascular system are well described (see 1.4-1.6). In addition, MMPs have been shown to play essential roles outside the cardiovascular system in pathological processes such as tumor metastasis⁵, arthritis development⁶ and cirrhosis²⁶.

Traditional examinations of MMPs have focused on their ability to degrade extracellular matrix substrates and consequently, these processes are best described. The collagenase activity of MMP-1, -8 and -13 has been shown to act upon the triple helical structure of fibrillar collagen. MMP-1 distinctly cleaves fibrillar collagen three quarters of the distance from the N terminal end, which then leaves the collagen fragments vulnerable to cleavage by other MMPs (eg. gelatinases)²⁷.

The degradation of type IV collagen, an essential component of the basement membrane, is effected by the gelatinase members of the MMP family. Purified MMP-2 and MMP-9 have been shown to degrade various preparations of type IV collagen *in vitro*²⁷⁻³². Both MMP-2 and MMP-9 can cleave type IV collagen into two fragments of unequal size, with the activity of the enzymes being temperature dependent^{29;30;32}. Further studies revealed that MMP-2 tends to cleave type IV collagen between Gly and X residues, provided that X is either a hydrophobic or polar charged residue³³.

1.1.4: Regulation

The activity of MMPs can be regulated at the levels of gene transcription and translation, by post-translational modifications and by interaction with endogenous inhibitors such as the TIMPs. Despite their functional similarity, the promoters for MMP-2 and -9 are structurally distinct. The MMP-9 promoter contains a downstream TATA box and an activated protein-1 (AP-1) binding site slightly upstream. A nuclear factor- κ B (NF- κ B) binding site is located far upstream and allows this gene to be responsive to various cytokines. The promoter for MMP-2 does not contain a TATA box and, therefore, allows for multiple sites of transcription. MMP-2 transcription is mainly controlled by the binding of transcription factors to a downstream GC box. The MMP-2 promoter lacks a proximal AP-1 binding site; however, studies investigating transcription-regulation have revealed a functional AP-1 consensus binding sequence³⁴. For a more comprehensive review on the gene regulation of MMPs please see Yan and Boyd (2007)³⁵. Contrary to previous thought, MMP-2 is not a constitutive enzyme and its expression can be actively upregulated in cardiac cells in response to hypoxia, angiotensin II, endothelin-1 or interleukin 1 β via JunB and FosB^{34;36}. At the mRNA level, MMP-2 can be regulated by a variety of stimuli, including hypoxia and reoxygenation. In

endothelial cells, a short duration (6 h) of hypoxia inhibited MMP-2 mRNA synthesis whereas a longer duration (24 h) resulted in an increase. Reoxygenation following hypoxia was found to increase MMP-2 mRNA as well³⁷. Moreover, in cardiac microvascular endothelial cells, MMP-2 protein and mRNA levels were stimulated by pro-inflammatory cytokine-dependent mechanisms³⁸.

The exact nature of the effects of post-translational modifications on MMP activity is not yet fully elucidated. Maeda's group demonstrated that MMP-1, -8 and -9 can be activated by the pro-oxidant species peroxynitrite (ONOO^-) without requiring the removal of the inhibitory propeptide domain^{39;40} (Figure 1.2). Low concentrations of ONOO^- (1 to 10 μM) cause the S-glutathiolation of the cysteine containing the PRCGVPD sequence within the propeptide domain which then results in an increase in proteolytic activity⁴⁰. As all members of the MMP family contain this highly conserved sequence in their propeptide domain, it is likely that S-glutathiolation may play a role in the regulation of the activities of other MMPs in the presence of ONOO^- (Figure 1.2). Glutathiolation is an increasingly recognized mechanism of post-translational control of protein activity⁴¹⁻⁴⁴. Higher levels of ONOO^- (> 100 μM) have, in contrast, been shown to inactivate MMPs⁴⁵, possibly via the nitration of tyrosine residues⁴⁶. Likewise, it was shown that full length human recombinant MMP-2 (72 kDa) is activated by low levels of ONOO^- (0.3-10 μM , peak at approximately 1 μM) but concentrations in excess of 100 μM inactivate it⁴⁷. Addition of glutathione flattened and shifted the concentration-response curve of ONOO^- -induced MMP-2 activation rightward and abrogated MMP-2 inactivation at higher concentrations. Extensive modifications of MMP-2 by ONOO^- , including S-glutathiolation of Cys-65 and Cys-102, hydroxylation of Phe-583, and nitration of Tyr-244 were revealed by mass spectrometric analysis⁴⁷. Hence, the

commonly used terminology of “pro” versus “active” MMPs, based on their molecular weights as seen by SDS-PAGE zymography (72 kDa “proMMP-2” and 64 kDa active MMP-2; 92 kDa “proMMP-9” and 84 kDa active MMP-9) is misleading as under conditions of oxidative stress the full length form of the MMP may also be proteolytically active.

Another posttranslational modification which may play a significant role in the regulation of MMP activity is phosphorylation. It was shown that MMP-2 may be phosphorylated on S32, S160 and S365, T250, and Y271 and phosphorylation of MMP-2 by protein kinase C greatly reduces its activity⁴⁸. *In silico* analysis of the MMP-2 protein sequence shows that several kinases, including protein kinase A, protein kinase C, and glycogen synthase kinase-3 may be able to phosphorylate MMP-2 and consequently modulate its activity. The protein kinases and phosphatases responsible for changing MMP-2 phosphorylation status *in vivo* are yet unknown. The role of phosphorylated MMP-2 in the heart is not yet known, though protein kinase A⁴⁹, protein kinase C⁵⁰ and glycogen synthase kinase-3⁵¹ have all been shown to play important roles in myocardial preconditioning.

The activation of MMPs can occur within the cell by oxidative stress⁵², at the cell surface or extracellularly. Cell surface activation of 72 kDa MMP-2 occurs as a result of its interaction with MT1-MMP and TIMP-2. A second molecule of MT1-MMP then interacts with the MMP-2/TIMP-2/MT1-MMP complex and cleaves the propeptide domain from MMP-2 resulting in 64 kDa “active” MMP-2⁵³. The binding of other proteins to the hemopexin domain of MMP-2 has been shown to expedite its activation. The interaction of the integrin $\alpha_v\beta_3$ with MMP-2^{54;55} facilitates this complex process of

proteolytic MMP-2 activation. In addition, other proteins such as heparin⁵⁶, thrombin⁵⁷ and factor Xa⁵⁸ also play important roles in the activation of MMP-2, though the mechanisms by which they act are not yet fully elucidated. In contrast MMP-2 has been found in caveolae and is likely maintained in an inhibited state by its interaction with caveolin-1 (Cav-1) to which it co-localizes⁵⁹ (see Chapter 2).

1.2: Tissue inhibitors of metalloproteinases

Activity of the MMPs may also be modulated by the endogenous TIMPs. The TIMPs are small proteins (~23 kDa) that inhibit MMP activity by binding to them in a 1:1 stoichiometric ratio⁶⁰. The four members of the TIMP family (TIMP-1 through -4) are cysteine rich proteins stabilized by disulfide bonds⁶¹. They are composed of a large N-terminal domain responsible for MMP inhibition and a smaller C-terminal domain. The TIMPs in general do not demonstrate specificity for any particular MMP⁶⁰, though TIMP-2 shows some degree of preference for MMP-2 and TIMP-1 for MMP-9⁶². All four TIMPs have been found in the heart and in cardiomyocytes⁶³ with TIMP-1 and TIMP-2 being the best characterized. TIMP-1 expression is induced by a variety of different stimuli, including pro-inflammatory cytokines⁶³ and angiotensin II⁶⁴, while TIMP-2 expression in the heart is constitutive⁶³. TIMP-3 is reduced in failing hearts⁶⁵ and has thus far been found exclusively in the extracellular matrix⁶⁶. Its unusually robust adherence to extracellular matrix components renders it difficult to isolate⁶⁶. TIMP-4 is abundantly expressed in the heart⁶⁷ and is found in the intracellular space together with MMP-2 in the thin myofilaments of the cardiomyocyte sarcomere⁶⁸. As the heart is the tissue

where TIMP-4 mRNA is most abundantly found^{67,69}, this suggests that it may play essential roles in the protection of the heart against oxidative stress injury^{68,70}.

1.3: Pharmacological inhibitors of MMPs

In addition to the TIMPs, a number of pharmacological inhibitors of MMPs are now available that are of significant utility, not only as experimental tools, but also as potential therapeutic agents in the treatment of cancer and inflammation as well as cardiovascular disease. *o*-Phenanthroline is a small organic compound that potently inhibits a broad range of MMPs. Its ability to readily pass through the cell membrane and inhibit MMPs makes it ideal for experimental use. Caution must be used in interpreting results obtained as a consequence of inhibition with *o*-phenanthroline as it may have other effects, including scavenging of reactive oxygen species, which are less well documented. Like *o*-phenanthroline, many other MMP inhibitors such as batimastat, marimastat, GM-6001 (ilomastat or gelardin), and PD-166793, share its mechanism of inhibitory action by virtue of their potent Zn²⁺ chelation properties⁷¹.

Though MMP inhibitors have shown great promise as inhibitors of inflammation⁷² and tumor angiogenesis⁷³ in experimental animal models, early clinical trials for the treatment of cancer with the MMP inhibitor marmistat were beset by unanticipated side effects. In particular, a tendonitis-like fibromyalgia developed in late-stage cancer patients treated with MMP inhibitors, which appears to be unrelated to the ability of these compounds to inhibit MMPs⁷⁴.

Selective inhibition of the gelatinases MMP-2 and MMP-9 has been accomplished with the use of inhibitory peptides which are speculated to bind to the

hydrophobic substrate pocket, thereby preventing access of the substrate to the active site, though the susceptibility of these peptides to proteolysis^{75;76} greatly diminishes their potential as effective experimental and pharmacological tools. In experimental models, MMP-2 neutralizing antibodies have also shown protective actions in hearts exposed to pro-inflammatory cytokines⁷⁷ or I/R injury⁷.

One class of MMP inhibitor which may be of significant clinical utility is the tetracycline class of antibiotics. While investigating a rat model of gingival inflammation and periodontitis, Golub and his co-workers recognized that the tetracyclines possess MMP inhibitory activity⁷⁸ independent of their antimicrobial properties⁷⁹. Further studies revealed that doxycycline is the most potent MMP inhibitor of the tetracyclines and that chemically modified tetracyclines which are devoid of antimicrobial properties still inhibit MMP activity⁸⁰. Doxycycline for example is able to inhibit MMP activity at plasma concentrations lower than that required for its antimicrobial action⁸¹. Though the tetracycline class of antibiotics are powerful Zn²⁺ chelators⁷¹, their inhibition of MMP activity may also include other mechanisms. Doxycycline has been shown to inhibit MMP-7 activity by binding proximally to the catalytic Zn²⁺ and disrupting the structural Zn²⁺ and Ca²⁺ ions which are necessary for the maintenance of MMP-7 tertiary structure⁸². Regardless of the mechanism of doxycycline action, its inhibition of MMP activity may improve the outcome of inflammatory diseases where MMPs play important pathological roles^{83;84}. To date, the only MMP inhibitor approved for clinical use by the U.S. Food and Drug Administration and Health Canada is a subantimicrobial dose formulation of doxycycline (20 mg bid) that has been shown to significantly improve the outcome of periodontal inflammation⁸⁵. Use of MMP inhibitors for other

conditions in which MMPs are known to be activated, such as aortic aneurysms⁸⁶ and colorectal cancer⁸⁷ has shown beneficial effects.

1.4: MMPs in heart development and angiogenesis

The presence of MMPs in the heart has been implicated in early heart development. Of particular significance is the role of MMP-2 in heart tube formation. Inhibition of MMP-2 in chick embryos using either an MMP-2 neutralizing antibody or ilomastat produces severe heart defects, including cardia bifida, abnormal left-right patterning and a disruption in the looping direction⁸⁸. There is evidence that the presence of MMP-2 may play an essential role in the tissue remodeling and cell migration that is necessary in the emergent heart. Extensive MMP-2 activity is observed in areas of the developing heart where migration of neural crest cells and formation of the tunica media for the great vessels requires remodeling of the extracellular matrix⁸⁹. Moreover, inhibition of MMP activity using doxycycline, GM-6001 or α -phenanthroline disrupts the localization of β -catenin in cultures of neonatal rat cardiomyocytes (A.K. Chow, E. Ehler & R. Schulz, unpublished observations), a protein that is important in the signaling pathways of heart organogenesis⁹⁰.

MMP-2 has also been shown to play important roles in angiogenesis⁹¹ and heart valve development⁹². For instance, PEX, a natural byproduct of MMP-2 breakdown (amino acids 445-637), is the C-terminal hemopexin-like fragment of MMP-2 that lacks catalytic activity. PEX is able to block MMP-2 binding with integrin $\alpha\beta 3$ and thereby disrupts angiogenesis⁹³. In heart valve development, blockade of MMP activity with GM-6001 blocks cell invasion necessary for normal heart valve development, resulting in

a truncated axis⁹⁴. Furthermore, introduction of MMP-2 antisense morpholino oligonucleotides into the developing zebrafish severely disrupts their early development⁹⁵. In contrast, MMP-2 deficient mice are viable at birth although upon closer examination, they have a number of problems that distinguish them from their wild-type littermates. For example MMP-2 knockout mice display significantly retarded growth compared with their wild-type controls⁹⁶. MMP-2 null mice also display lower bone mineral density, a loss of articular cartilage, and abnormal bone and craniofacial development⁹⁷. Additionally, MMP-2 knockout mice can respond differently to experimental stimuli when compared with their wild-type controls. For instance, MMP-2 knockouts displayed a significantly more severe response and earlier onset of experimental autoimmune encephalomyelitis than controls⁹⁸. MMP-2 knockout mice also display impaired neovascularization in a hindlimb ischemia model when compared with controls⁹⁹. The MMP-2 knockout phenotype, however is relatively benign. It has been speculated that the mild phenotype of the MMP-2 deficient mouse, when compared to MMP-2 knockdown in zebrafish, may be a result of additional compensatory mechanisms in the more complex mammalian system.

1.5: MMPs in inflammatory heart disease

Myocarditis and/or pericarditis are characteristic features of a number of diseases including rheumatic fever, Kawasaki disease and bacterial or viral infection of the heart. Acute inflammation of the heart may lead to structural alterations and/or impairment of contractile function. MMPs have also been implicated in the pathogenesis of acute myocardial inflammation.

One common pathway by which MMPs are stimulated in these inflammatory diseases is through the production of pro-inflammatory cytokines. Both tumor necrosis factor- α (TNF- α) and interleukin-1 β (IL-1 β) have been shown to affect the expression and activity of MMPs. IL-1 β and TNF- α both regulate the expression of collagenase in human fibroblasts via an AP-1 responsive element of the gene¹⁰⁰. Similarly, IL-1 β stimulates the expression and enhanced activity of MMP-2, but not MMP-9, in cardiac microvascular endothelial cells¹⁰¹ and fibroblasts¹⁰².

Kawasaki disease is an acute inflammatory syndrome that primarily affects children. It manifests itself as a systemic vasculitis along with coronary artery dilation and aneurysm. Similar to I/R injury of the heart, patients in the acute phase of Kawasaki disease have increased serum levels of both MMP-9 and TIMP-1, which have been implicated in the formation of aortic aneurysms, a severe consequence of this disease¹⁰³. Children with Kawasaki disease have elevated MMP-3 and TIMP-1 serum levels when compared with healthy children¹⁰⁴. Additionally, autopsy of children who died from Kawasaki disease reveals prominent immunohistological localization of MMP-2 in the neointima of coronary artery aneurysms when compared to sections obtained from patients who died of other causes¹⁰⁵. All of these observations suggest that, similar to I/R injury, serious manifestations of Kawasaki disease may be a result of an imbalance between MMPs and TIMPs leading to a net positive proteolytic activity in the coronary vasculature.

Acute viral myocarditis can occur in young and otherwise healthy patients, resulting in dilated cardiomyopathy with no effective treatment besides supportive therapy. Patients can develop viral myocarditis following infection with Coxsackievirus

B3 and both direct infection of the cardiomyocyte by the virus, or immune reaction following infection can lead to impaired heart function¹⁰⁶. Overexpression of TIMP-1 in a mouse model of Coxsackievirus B3 -induced myocarditis significantly reduced both MMP-2 and MMP-9 activity in hearts¹⁰⁷. Another group studied a mouse model of Coxsackievirus B3 -induced myocarditis and discovered that MMP-2, -9 and -12 transcription and translation, as well as gelatinolytic activity were increased during acute myocarditis in cardiac ventricles. This was accompanied by a significant reduction in the mRNA levels of TIMP-3 and -4 without change in TIMP-2¹⁰⁸.

The majority of the research in acute myocarditis has focused on the role of MMPs acting on extracellular matrix proteins of the heart, however, this does not preclude a possible intracellular role of MMPs in the pathogenesis of inflammatory heart disease. In this regard, isolated, working rat hearts were exposed to pro-inflammatory cytokines and it was found that MMP-2 activation was accompanied by the loss of TIMP-4 from hearts. The cytokine-induced loss of contractile function as well as myocardial troponin I (TnI) content were prevented by MMP inhibitors⁷⁷. In patients with Kawasaki disease, increased levels of TnI (and its fragments) were found in serum in acute phases of myocarditis^{109;110}. TnI levels and/or degradation products in serum may be a useful diagnostic tool for Kawasaki disease, although this was contradicted in another study¹¹¹. Elevated serum TnI is also commonly observed in patients with idiopathic acute pericarditis¹¹². In addition, a high level of circulating intact TnI in the blood is able to elicit an autoimmune response that can subsequently lead to myocardial inflammation, fibrosis and increased mortality rates in mice¹¹³.

1.6: MMPs in ischemia/reperfusion injury

Stunning injury of the heart as a result of ischemia followed by reperfusion is defined as a temporary, reversible loss of contractile function without necrotic cell death¹¹⁴. The feature common to all events which induce stunning is a reduction in coronary blood flow that deprives the myocardium of oxygen. If the reduction of coronary flow is prolonged, the myocardium can transition into a hibernating state¹¹⁵ where myocytes can undergo dedifferentiation¹¹⁶. Ischemia is necessary but not sufficient to cause myocardial stunning as the injury occurs during the acute phase of reperfusion when blood flow through the ischemic myocardium is reestablished. In isolated rat hearts perfused with physiological salt solutions, stunning can occur after approximately 15-25 min of global, no-flow ischemia, depending on the Ca^{2+} concentration and other components in the perfusate. If ischemia is extended to over 30 min, irreversible functional impairment occurs as cells can also undergo necrosis¹¹⁷.

The exact mechanism responsible for myocardial stunning has yet to be fully elucidated, however, it is known that reactive oxygen and nitrogen species, including ONOO^- , are generated in the myocardium in a burst-like manner in the first seconds of reperfusion and are central in the pathogenesis of stunning injury^{117;118}. As the generation of ONOO^- may not only activate MMPs^{39;40} but also inactivate TIMPs^{119;120}, their involvement in the isolated rat heart subjected to I/R injury was investigated. Both 72 and 64 kDa MMP-2 are released at a basal rate into the perfusate of normal, aerobically perfused rat hearts, whereas there was a marked increase in this release during the first minutes of reperfusion following ischemia¹³. There was a positive correlation between increasing duration of ischemia, enhanced release of MMP-2 at

reperfusion, and a reduction in cardiac mechanical function during reperfusion¹²¹. Administration of MMP inhibitors such as α -phenanthroline, doxycycline or a neutralizing MMP-2 antibody functionally protected hearts from stunning injury¹³. In the isolated, perfused rabbit heart, 15 min of ischemia are insufficient to cause the release of MMP-2 into the perfusate during reperfusion. However with 60 min of ischemia significant amounts of MMP-2 were found in the coronary effluent during reperfusion¹³.

An imbalance between TIMPs and MMPs in the heart may be one of the contributing factors to acute I/R injury. In a Langendorff rat model of I/R, TIMP-4 was also found to be acutely released into the perfusate during the initial reperfusion phase. Though it is released in conjunction with MMP-2, there is an overall shift towards enhanced proteolytic activity in the heart tissue as revealed by *in situ* zymography⁶⁸. The export of MMP-2 during reperfusion may likely be a protective mechanism of the heart to diminish the net cellular proteolytic activity by reducing the myocardial MMP/TIMP ratio¹³. Levels of both MMP-9 and TIMP-1 are increased in the plasma of patients following myocardial infarction¹²². Right atrial biopsies from patients undergoing cardiopulmonary bypass for coronary artery bypass grafting, obtained within ten min of aortic cross-clamp release (a mild form of reperfusion injury), show a dramatic increase in both MMP-2 and MMP-9 activities and a decrease in TIMP-1 during reperfusion¹²³. The increase in MMP-2 and -9 activities positively correlates with the duration of cross clamp and inversely with cardiac mechanical function 3 h after cross clamp release. In contrast TIMP-1 levels correlated positively with cardiac mechanical function at this time and correlated negatively with the duration of cross clamp

placement¹²³. Plasma activities of both MMP-2 and MMP-9 were also seen to be elevated 1 min following release of the aortic cross clamp¹²³.

Ischemic preconditioning reduces this I/R-induced release of MMP-2 into the perfusate of isolated rat hearts¹²⁴, providing further evidence that MMP-2 may play an important role in the development of myocardial stunning injury. In a related study, hyperlipidemia caused by feeding rats a diet enriched with 2% cholesterol was shown to prevent the protective effects of preconditioning. This was demonstrated by the ability of hyperlipidemia to reverse the protective effects of preconditioning-mediated inhibition of MMP-2 activation and release¹²⁵. Interestingly, high density lipoprotein which is known to be cardioprotective, prevents MMP-2 activation and release in ischemic-reperfused rat hearts¹²⁶.

It is likely that the alteration in MMP activities is a result of the increased oxidative stress which occurs most evidently during reperfusion following ischemia. During the first minute of reperfusion, cardiotoxic levels of ONOO⁻ are generated in the heart¹¹⁸. Direct infusion of ONOO⁻ into aerobically perfused isolated rat hearts caused a time-dependent loss in cardiac mechanical function which was preceded by evidence of MMP-2 activation (released into the perfusate) and which was prevented by a MMP inhibitor¹¹. At these levels, ONOO⁻ is likely capable of activating MMP within the cardiomyocyte without necessitating proteolytic removal of the propeptide domain⁴⁶. Furthermore, exposure of isolated adult rat cardiomyocytes to ONOO⁻ resulted in a time and concentration dependent loss of contractile function which can be abrogated in the presence of the MMP inhibitors doxycycline or PD-166793¹²⁷.

In addition to affecting MMP activity, ONOO⁻ may also stimulate proteolytic activity in the heart via its direct action on TIMPs. Concentrations of ONOO⁻ as low as 50 μM inhibited TIMP-1 activity while above 500 μM resulted in its degradation¹¹⁹. TIMP-2 activity was also shown to be reduced in the presence of ONOO⁻¹²⁸, though whether this is a result of direct inhibition of TIMP-2 or a disruption of TIMP-2/MMP-2 binding is unclear. The ability of TIMP-4 to inhibit MMP-2 activity and prevent the invasiveness of both microvascular endothelial cells and tumour cells was reduced by ONOO⁻ treatment¹²⁰.

Other models of oxidative stress in the heart have also shown that MMP-2 and MMP-9 may play important roles in the development of cardiac dysfunction. In particular, doxorubicin-induced cardiotoxicity involves the generation of reactive oxygen and nitrogen species¹²⁹ and increased myocardial MMP-2 activity is observed in mice administered doxorubicin¹³⁰. Other groups have found that doxorubicin also increases MMP-2 and MMP-9 transcripts in mouse hearts¹³¹ and that antioxidants such as dexrazoxane and carvedilol prevent doxorubicin-induced increases in MMP-2 and MMP-9 mRNA in H9c2 myocyte cells²⁰.

Recent studies have investigated the transcriptional activation of MMP-2 and MMP-9 as a result of I/R injury of the heart. There is a rapid activation of the MMP-2 promoter as early as 30 min of reperfusion following global ischemia in isolated hearts from transgenic mice containing the MMP-2 promoter linked to a β-galactosidase reporter³⁶. This was observed in cardiac myocytes, fibroblasts and endothelial cells. The transcription factors JunB-FosB bind to a distinct, functional AP-1 site which activates the MMP-2 promoter in this setting^{34;36}. Using these same mice in a myocardial infarct

model, as well as mice to which the MMP-9 promoter was linked to β -galactosidase, revealed that the MMP-2 promoter was induced within one day of infarct whereas the MMP-9 promoter was first detected after three days and peaked seven days after myocardial infarct¹³². Given the rapid activation of MMP-2 in the acute reperfusion phase following ischemia (see above), resulting in its activation and release on a minutes timescale and subsequent release from the heart, it is not surprising that these measures would then occur to replenish MMP-2 levels in the myocardium.

The development of cardiac specific MMP-2 transgenic mice also lends credence to the role of MMP-2 in I/R injury. In fact, 4 month old MMP-2 transgenic mice that are not exposed to insult, already display cardiac myocyte abnormalities, including disruption of sarcomeric architecture, disintegration of Z bands and myofilament lysis¹³³. When compared with their controls, 6 month old heterozygous MMP-2 transgenic mice display larger infarct size and greater functional impairment following 30 min of ischemia followed by 30 min of reperfusion in a paced, Langendorff model¹³⁴.

1.7: Intracellular MMPs

In accordance with the abundant evidence linking MMPs with cardiac remodeling and inflammatory heart diseases such as rheumatic fever, Kawasaki disease and endocarditis (reviewed in¹³⁵), most researchers focus on the long term proteolytic effects of MMPs on extracellular matrix proteins¹³⁶. However, MMP-2 was found to contribute to acute cardiac mechanical dysfunction in heart pathologies before collagen matrix changes were observed^{13;77}. Since ONOO⁻ levels are acutely enhanced during reperfusion of the ischemic heart¹¹⁸, and MMP-2 is closely associated with the

sarcomere in cardiomyocytes^{11;15}, and can be activated by ONOO⁻¹³⁷, the hypothesis is that in acute myocardial injury associated with enhanced oxidative stress, the detrimental effect of MMP-2 is primarily within the myocyte, though extracellular MMP-2 may also play a role.

1.7.1: Sarcomeric MMP-2

Various methodological approaches provided compelling evidence for the localization of MMP-2 to the sarcomere of cardiac myocytes, including: (i) immunogold electron microscopy with anti-MMP-2, which showed a distinct sarcomeric staining pattern in rat heart sections; (ii) highly purified preparations of thin myofilaments (which include TnI) prepared from hearts showed both 72 and 64 kDa MMP-2 gelatinolytic activities as well as MMP-2 protein; (iii) immunoprecipitated TnI from I/R heart homogenates revealed 72 and 64 kDa MMP-2 gelatinolytic activities by zymographic analysis and (iv) confocal microscopy, which demonstrated the colocalization of MMP-2 with TnI¹¹. MMP-2 in the cardiac sarcomere is accompanied by TIMP-4 as shown using immunogold electron microscopy and other biochemical evidence for its association with the thin myofilaments⁶⁸. It is likely that the TIMP-4 found within cardiomyocytes is an important means to regulate intracellular MMP-2 activity.

1.7.2: Cytoskeletal MMP-2

Myocardial stunning injury in isolated guinea pig hearts is accompanied by the degradation of the cytoskeletal proteins desmin, spectrin, and α -actinin¹³⁸, though the protease(s) responsible was not identified. α -Actinin and desmin (but not spectrin) were found to be susceptible to degradation by MMP-2 *in vitro*. Infusion of ONOO⁻ into

isolated, perfused rat hearts caused activation of MMP-2 with concomitant loss of myocardial α -actinin content, which was prevented by MMP inhibition¹³⁹. Moreover, MMP-2 was found to co-localize with α -actinin in cardiac myocytes^{15;139}.

1.7.3: Nuclear MMP-2

The nucleus has a matrix that resembles the extracellular matrix and provides structural and organizational support for various nuclear processes. Various biological processes such as apoptosis¹⁴⁰, cell cycle regulation¹⁴¹, and nuclear matrix degradation¹⁴² involve the proteolytic processing of nuclear proteins. MMP-2 was found in the nucleus of human cardiomyocytes¹⁴³. Indeed both MMP-2¹⁴³ and MMP-3¹⁴⁴ carry a putative nuclear localization sequence. Si-Tyaeb et al.¹⁴⁴ reported that an active, truncated fragment of MMP-3 was localized to the nucleus of several human cancer cell lines. The full-length MMP-3 remained cytosolic, whereas the truncated form translocated to the nucleus and a nuclear localization sequence was demonstrated to be essential for this translocation¹⁴⁴. Although the Schulz group found that MMP-2 was able to proteolyze the nuclear DNA repair enzyme, poly(ADP-ribosyl) polymerase *in vitro*¹⁴³, the role of MMP-2 and other MMPs within the nucleus remains to be discovered.

A summary of the potential intracellular targets and/or binding partners of MMP-2 in the cardiomyocyte is illustrated in Figure 1.3. Known intracellular substrates of MMP-2 are listed in Table 1.1.

1.8: Caveolins

One potential modulator of MMP-2 activity in the cardiomyocyte is caveolin. The caveolins are proteins found within lipid rafts in the plasma membrane. Though the

existence of lipid rafts is not universally accepted¹⁴⁵, most groups define lipid rafts as microdomains of the plasma membrane that are highly enriched with cholesterol, glycolipids and sphingolipids¹⁴⁶. Lipid rafts have properties that are believed to be unique from those of the surrounding plasma membrane. In particular, their low density facilitates their separation from the adjacent plasma membrane by sucrose gradient centrifugation^{147;148}. Additionally, lipid rafts are resistant to non-ionic detergents such as Triton X-100 and Brij-98 at 4°C¹⁴⁹, though the significance of this property is also not universally agreed¹⁵⁰.

1.8.1: Classification

The caveolin family is composed of three members: caveolin-1 (Cav-1), Cav-2 and Cav-3. Caveolins are proteins essential for the formation of caveolae, which are small cell membrane invaginations found in many cell types, including endothelial cells and cardiomyocytes. They appear to play significant roles in signal transduction¹⁵¹, cholesterol homeostasis¹⁵² and vesicular transport¹⁵³. The first discovered and consequently best characterized caveolin is Cav-1. Two distinct isoforms of Cav-1 have been identified (α and β) and are the result of an alternate internal translational start site that results in the truncated β isoform¹⁵⁴. Cav-1 levels have been found to be highest in adipocytes, fibroblasts, smooth muscles and endothelial cells as well as in cardiomyocytes¹⁵⁵, though the latter has been controversial¹⁵⁶. The issue of whether Cav-1 exists in cardiomyocytes is one of the objectives of this thesis and is further explored in Chapters 2 and 3. Cav-2 is closely associated with Cav-1 and will often form oligomers with Cav-1, as Cav-1 is necessary for localization of Cav-2 in the plasma membrane¹⁵⁷. Cav-3 is predominantly expressed in both skeletal and cardiac striated

muscle cells and is associated with the T-tubules formed as a result of cell membrane invaginations^{158;159}.

The three human caveolin genes possess many similar characteristics. Though Cav-1 and Cav-2 are located on the same human chromosome (7q31.1) and only approximately 19 kb apart, it is Cav-1 and Cav-3 that share the highest degree of homology¹⁶⁰. Cav-1 is highly conserved between species and comparison of several mammalian species indicates that there is 94-99% identity over the protein sequence¹⁶¹, which is highly suggestive of a strong relation between structure and function.

1.8.2: Structure

The caveolins are typically found partially embedded in the inner leaflet of the cell membrane as oligomers. The cytosolic N terminal portion of both Cav-1 and Cav-3 contains a small region of amino acids (residues 82-101) termed the caveolin scaffolding domain (CSD). The CSD is not only responsible for the binding of caveolin oligomers together, but is also believed to be essential for mediating caveolin's interaction with other signaling molecules^{160;162}. Studies involving the mutation of the CSD indicate that it is both necessary and sufficient to target Cav-1 to the plasma membrane¹⁶³. Though the CSD is often considered a single functional domain, evidence now shows that the CSD can be divided into two separate functional regions. Residues 82-95 are believed to mediate signaling protein inhibition¹⁶⁴, while residues 95-101 are responsible for the binding of caveolin to cholesterol and the plasma membrane^{163;165}.

Cav-1 also possesses a hydrophobic transmembrane region (residues 102-134) which forms a hairpin within the plasma membrane, leaving both the N and C terminals of Cav-1 in the cytoplasmic domain¹⁶⁶. All three caveolin proteins have a conserved

FEDVIAEP sequence in the hydrophilic N-terminal domain which is known as the caveolin signature motif^{167;168}, though the functional significance of this motif has not yet been elucidated.

The N-terminal domain of Cav-1 appears to be relatively unstructured, with a low probability of the region possessing a known tertiary structure and no predicted coiled-coil secondary structures¹⁶¹. Secondary structure prediction of the C-terminal domain of Cav-1 indicates that this cytoplasmic region likely forms a long α -helical structure¹⁶¹.

1.8.3: Function

Caveolin, Cav-1 in particular, has been extensively examined and serves as a platform where proteins aggregate¹⁶². Sucrose gradient centrifugation to isolate lipid raft rich fractions has shown that a number of signal transduction molecules biochemically co-segregate with Cav-1. Lisanti et al¹⁶⁹ hypothesized that caveolin sequesters signal transduction molecules to the membrane and this serves to regulate signal transduction events. Since this hypothesis has been put forth, a number of different signal transduction molecules have been shown to both biochemically and morphologically localize and interact with caveolin, including G protein coupled receptors¹⁷⁰, receptor tyrosine kinases^{171;172}, growth factor receptor bound protein-2¹⁷³, and a number of protein kinases, including protein kinase A^{174;175} and various isoforms of PKC¹⁷⁶⁻¹⁷⁸. Enzymes and structural proteins such as endothelial (eNOS)¹⁷⁹ and neuronal nitric oxide synthase (nNOS)^{180;181}, actin¹⁸² and MT-1 MMP^{183;184} have also been shown to be associated with Cav-1.

Disruption of lipid rafts by chemical agents such as methyl- β -cyclodextrin can impair the function of a number of proteins that are associated with the lipid raft, including the Na⁺/H⁺ exchanger NHE3¹⁸⁵ and HCN4 channels¹⁸⁶, the pacemaker channel in the heart. Methyl- β -cyclodextrin is a cyclic oligosaccharide composed of seven sugars and removes cholesterol from membranes by sequestering the cholesterol molecule into its ring structure. Exposure of cells or tissues to methyl- β -cyclodextrin reduces or eliminates caveolae from the plasma membrane and replenishment of cholesterol restores these structures¹⁸⁷⁻¹⁸⁹. Whether methyl- β -cyclodextrin displaces Cav-1 from the plasma membrane or breaks up oligomers of caveolins so that caveolae are absent, is so far unclear.

The CSD of the Cav proteins is able to bind to proteins that contain a caveolin binding domain (CBD) which consists of $\Phi X \Phi X X X X \Phi$, $\Phi X X X X \Phi X X \Phi$ or $\Phi X \Phi X X X X \Phi X X \Phi$ where Φ is Phe, Tyr or Trp and X is any amino acid¹⁹⁰. The presence of the CBD, however, is not necessarily sufficient to induce CSD binding to a protein, as evidenced by a number of proteins that have the CBD domain, yet lack caveolin interaction.

Initially, Cav-1 was considered a scaffolding protein responsible for organization of the different molecules to which it binds. However, more recent evidence suggests that Cav-1 plays an active role in the regulation of the receptors and enzymes it associates with. For example, addition of synthetic CSD to G protein coupled receptor kinases is able to significantly inhibit GTP hydrolysis in an *in vitro* system¹⁹¹. In both biochemical and cell culture experiments, the majority of proteins that bind to the CSD have been shown to be inhibited, though the mechanism by which this acts is still largely unknown.

1.8.4: Regulation

The inhibition of eNOS is one of the most studied mechanisms of caveolin action. Targeting of eNOS to caveolae is accomplished by its acylation¹⁹². When not interacting with Cav-1, eNOS is at its most active. When interacting with Cav-1, however, the enzyme activity of eNOS is significantly reduced. This is reversed when point mutations disrupt the CBD in eNOS¹⁹².

Caveolin effect on the MMPs is less well characterized. A number of reports show the co-localization of MT1-MMP with Cav-1 and that this is a result of the direct association between the proteins. However, the effect that this association may have on either protein has not yet been determined. Examination of the MT1-MMP sequence reveals the presence of several CBD consensus sequences in its hemopexin domain¹⁸⁴. Consequently, Labrecque et al.¹⁸⁴ hypothesize that other proteins may be involved in the association between MT1-MMP and Cav-1.

1.8.5: Caveolin knockout models

The Cav-1^{-/-} mice used throughout this thesis are generated by targeted disruptions of the first two exons of Cav-1¹⁹³. These Cav-1^{-/-} mice are both viable and fertile¹⁹³, though upon closer examination, distinct abnormalities have been observed. Cav-1^{-/-} mice show ~50% reduction in life span, which appears secondary to pathologies primarily in the cardiovascular and respiratory system¹⁹⁴. Caveolae are found to be completely absent in all non-muscle tissue (reviewed in ¹⁹⁵), though caveolae are still present in muscle tissues, albeit in reduced numbers. Knockout of Cav-1 results in pulmonary hypertension, pulmonary fibrosis and cardiac hypertrophy^{194;196}. Surprisingly, Cav-1 knockout also reduces the expression of Cav-2 protein, without a

change in transcription level, and also affects Cav-2 targeting to the plasma membrane¹⁹⁷.

Like Cav-1^{-/-}, Cav-2 knockout mice are also viable and fertile. They do, however display severe structural alterations and functional deficits in their respiratory system¹⁹⁸. Additionally, these mice are exercise intolerant when subjected to a swim test¹⁹⁸. Interestingly though, these same mice have intact caveolae in both lung and adipose tissues¹⁹⁸.

A Cav-3 knockout mouse model has also been developed which demonstrates a loss of caveolae in striated muscle tissues, without perturbation of Cav-1 or Cav-2¹⁹⁹. Like Cav-1^{-/-}, Cav-3 null mice eventually develop cardiac hypertrophy²⁰⁰.

A Cav-1/Cav-3 double knockout has also proved to be both viable and fertile, with no discernable caveolae in a variety of cells, including endothelial cells, adipocytes and muscle cells, including cardiomyocytes²⁰¹. This double knockout mouse displays pulmonary, skeletal and adipose alterations similar to those found in the single knockout animals, though the Cav-1/Cav-3 null mice exhibit significantly more severe cardiac changes both in terms of gross function and at a histological level^{196;200;202}.

1.9: Working hypothesis

Cav-1 co-localizes with MMP-2 in the caveolae of cardiomyocytes and inhibits its activity tonically. In the normal heart which expresses Cav-1, scaffolding of MMP-2 to the plasma membrane by caveolin sequesters MMP-2 and inhibits its activity, thus protecting the heart from MMP-2's intracellular proteolytic actions.

MMP-2's proteolytic actions on its intracellular substrates can be inhibited by post-translational modifications, such as phosphorylation, on the substrate itself. These post-translational modifications can sterically hinder MMP-2's ability to effectively degrade the substrate.

1.10: Thesis objectives

1.10.1: Caveolin regulation of MMP-2 in the heart (Chapter 2)

MMP-2 has been localized to the caveolae of human endothelial cells¹⁸³, but whether MMP-2 and caveolae co-localize in cardiomyocytes is unknown. Similarly, the effect that Cav-1 may have on the regulation of MMP-2 activity has not yet been elucidated. The objective of Chapter 2 is to determine whether Cav-1 modulates MMP-2 activity in cardiac muscle.

1.10.2: MMP-2 and caveolin localization in the heart (Chapter 3)

Though Chapter 2 reveals the presence of Cav-1 in cardiomyocytes, the existence of Cav-1 in cardiomyocytes is controversial¹⁵⁶. The objective of Chapter 3 is to examine and characterize the relationship between the caveolins, MMP-2 in the various cells found in the heart.

1.10.3: Physiological and pharmacological challenges to caveolin-1 knockout mouse heart (Chapter 4)

Results from Chapter 2 revealed that not only do Cav-1 and MMP-2 co-localize in cardiomyocytes, but that Cav-1^{-/-} mouse hearts have increased MMP-2 gelatinolytic activity and that CSD is capable of inhibiting MMP-2 proteolysis. The purpose of Chapter

4 is to determine whether this altered MMP-2 activity in Cav-1^{-/-} hearts translates to functional alterations in a physiological situation as well as when the hearts are challenged with a β -adrenergic agonist.

***1.10.4: Ischemia/reperfusion injury in the caveolin-1 knockout mouse heart
(Chapter 5)***

As MMP-2 has been shown to play important roles in mediating I/R induced injury, and MMP-2 activity is elevated in Cav-1^{-/-} hearts, it was believed that Cav-1^{-/-} hearts would demonstrate increased myocardial injury following I/R injury. The objective of Chapter 5 is to determine whether this is indeed the case.

***1.10.5: Troponin I phosphorylation in response to ischemia/reperfusion injury
and/or β -adrenergic stimulation in the isolated working mouse heart***

TnI has been shown to be an intracellular substrate of MMP-2¹¹, though the mechanism by which MMP-2 proteolysis of TnI is regulated is largely unknown. The objective of Chapter 6 is to determine whether *in situ* phosphorylation of TnI results in protection of TnI to MMP-2 proteolysis.

1.11: Conclusion

Because of the significant role of MMP-2 in ischemic injury, the regulation of the destructive properties of this enzyme may be the key to understanding and consequently combating the debilitating effects of ischemic heart disease. The idea that intracellular MMP-2 may be regulated by caveolin is a novel concept and the following

series of experiments will attempt to not only definitively co-localize MMP-2 with caveolin in cardiac myocytes, but also show that caveolin is capable of regulating MMP activity in the heart.

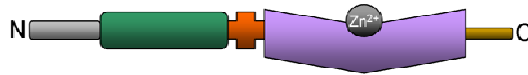
Figure 1.1: MMP structure

MMPs are typically classified according to the substrates they degrade and possess several general common structural characteristics. The N-terminal domain typically contains a signaling sequence, which allows for the extracellular export of the enzyme. All MMPs are produced in a zymogen form with a propeptide domain that contains a cysteine switch. The catalytic domain of all MMPs contain a Zn^{2+} ion. The catalytic domain of the gelatinases (MMP-2 and -9) is unique in that it contains three fibronectin repeats. Apart from the matrilysins (MMP-7 and -26), MMPs contain a flexible hinge region which also has a haemopexin domain linked to a C-terminal tail. MMP, matrix metalloproteinase; MT-MMP, membrane-type matrix metalloproteinase.

Collagenases
(MMP-1, -8 -13)
Stromelysins
(MMP-3, -10)



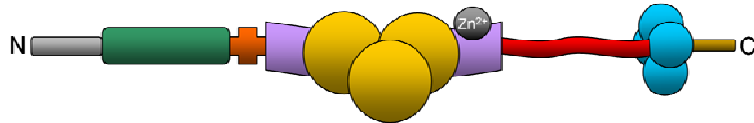
Matrilysins
(MMP-7, -26)



Membrane-type
(MT-MMPs 1-8)



Gelatinases
(MMP-2, -9)



Signal Sequence N

Propeptide

Cysteine Switch

Furin Cleavage

Catalytic Domain

Fibronectin Repeat

Hinge Region

Hemopexin Domain

Transmembrane Domain

Cytosolic Domain

Tail C

Figure 1.2: Activation mechanisms of MMP-2

The full-length MMP-2 can be activated in two ways. Proteolytic activation of MMP-2 by MT1-MMP/TIMP or by other proteases occurs by removal of the autoinhibitory propeptide domain (left arrow) resulting in an active truncated MMP-2. The presence of oxidative stress (ONOO^-) and cellular glutathione (GSH) causes the S-gluathiolation of the critical cysteine residue in the propeptide domain, disrupting its binding to the catalytic Zn^{2+} ion, resulting in an active full-length enzyme. MMP, matrix metalloproteinase; ONOO^- , peroxynitrite; TIMP, tissue inhibitor of metalloproteinase.

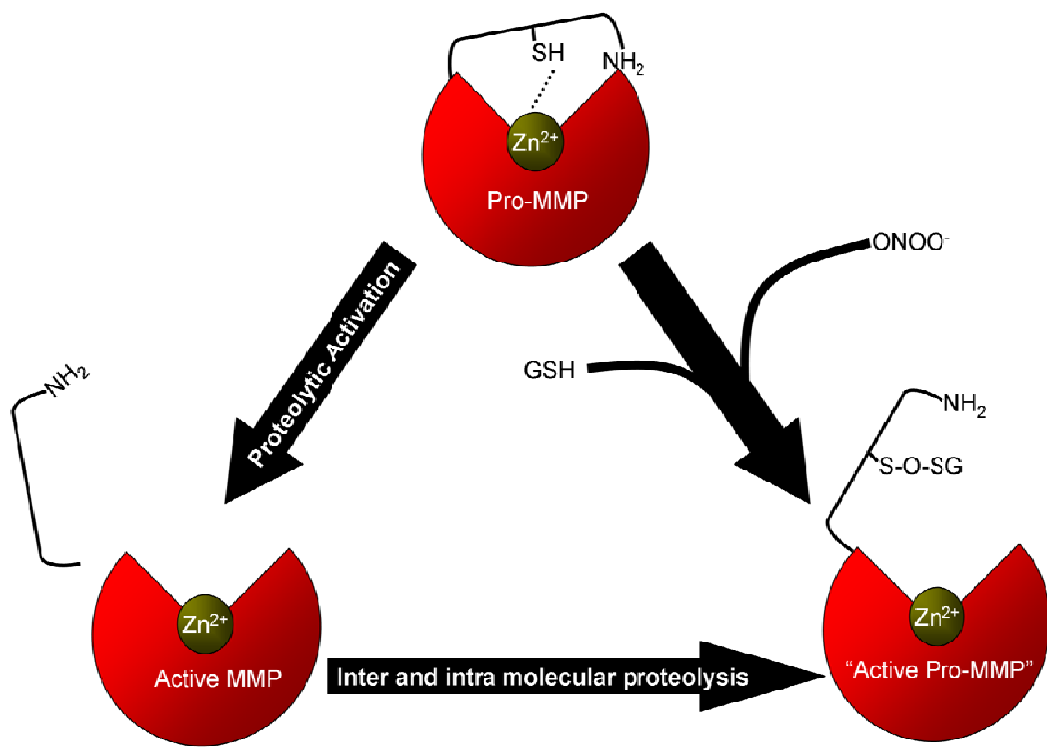


Figure 1.3: Intracellular targets and binding partners of MMP-2 in the cardiomyocyte

Sarcomeric proteins including TnI, MLC-1, and α -actinin are co-localized with and susceptible to proteolytic cleavage by MMP-2. Recent evidence suggests the presence of MMP-2 in the caveolae, mitochondria, and other intracellular organelles including the nucleus, although its precise roles in these locales are unknown.

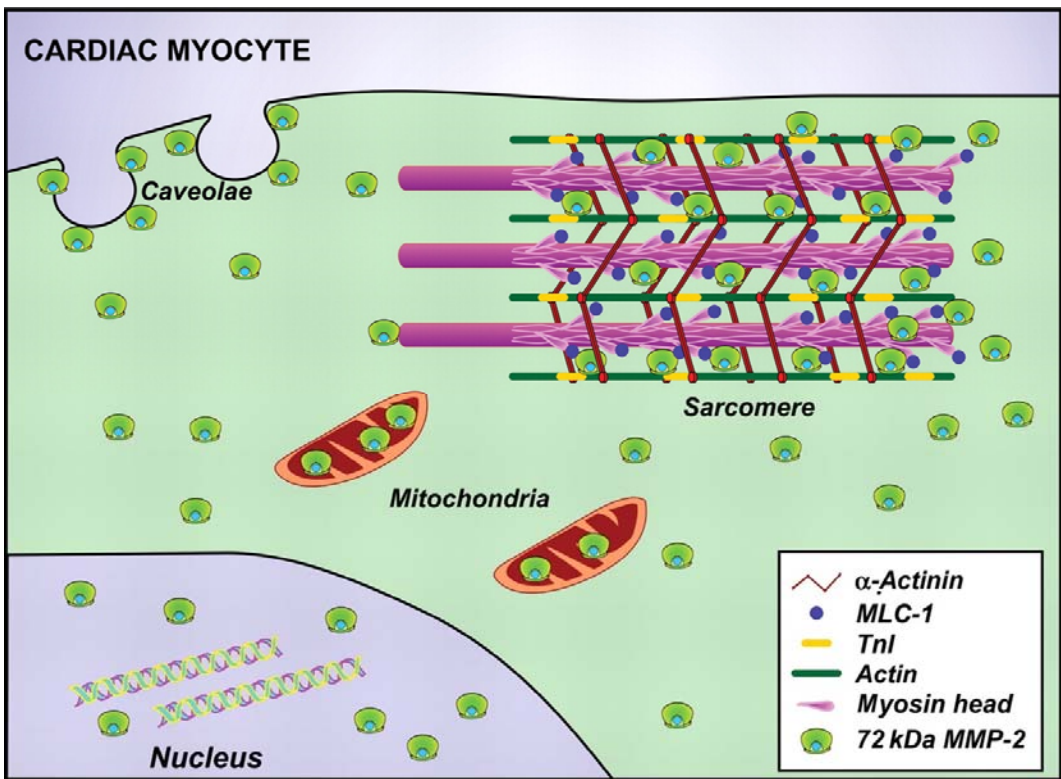


Table 1.1: Intracellular MMP-2 substrates

LOCATION	SUBSTRATE
Cytoplasm	Glycogen synthase kinase-3 β ²⁰³
Sarcomere	Troponin I ¹¹ Myosin light chain-1 ¹² Titin ²⁰⁴
Cytoskeleton	α -Actinin ¹³⁹ Desmin ¹³⁹ α -Tubulin (see Chapter 2)
Nucleus	Poly ADP-ribose polymerase ¹⁴³

1.12: References

1. Gross, J and Lapiere, CM. Collagenolytic activity in amphibian tissues: a tissue culture assay. *Proc. Natl. Acad. Sci. U. S. A* 1962; 48:1014-1022.
2. Stefanidakis, M and Koivunen, E. Cell-surface association between matrix metalloproteinases and integrins: role of the complexes in leukocyte migration and cancer progression. *Blood* 2006; 108:1441-1450.
3. Vu, TH and Werb, Z. Matrix metalloproteinases: effectors of development and normal physiology. *Genes Dev.* 2000; 14:2123-2133.
4. Roy, R, Zhang, B, and Moses, MA. Making the cut: protease-mediated regulation of angiogenesis. *Exp. Cell Res.* 2006; 312:608-622.
5. Deryugina, EI and Quigley, JP. Matrix metalloproteinases and tumor metastasis. *Cancer Metastasis Rev.* 2006; 25:9-34.
6. Mohammed, FF, Smookler, DS, and Khokha, R. Metalloproteinases, inflammation, and rheumatoid arthritis. *Ann. Rheum. Dis.* 2003; 62 Suppl 2:ii43-ii47.
7. Creemers, EE, Cleutjens, JP, Smits, JF, and Daemen, MJ. Matrix metalloproteinase inhibition after myocardial infarction: a new approach to prevent heart failure? *Circ. Res.* 2001; 89:201-210.
8. Dollery, CM, McEwan, JR, and Henney, AM. Matrix metalloproteinases and cardiovascular disease. *Circ. Res.* 1995; 77:863-868.

9. Spinale, FG, Coker, ML, Bond, BR, and Zellner, JL. Myocardial matrix degradation and metalloproteinase activation in the failing heart: a potential therapeutic target. *Cardiovasc. Res.* 2000; 46:225-238.
10. Fatar, M, Stroick, M, Griebel, M, and Hennerici, M. Matrix metalloproteinases in cerebrovascular diseases. *Cerebrovasc. Dis.* 2005; 20:141-151.
11. Wang, W, Schulze, CJ, Suarez-Pinzon, WL, Dyck, JR, Sawicki, G, and Schulz, R. Intracellular action of matrix metalloproteinase-2 accounts for acute myocardial ischemia and reperfusion injury. *Circulation* 2002; 106:1543-1549.
12. Sawicki, G, Leon, H, Sawicka, J, Sariahmetoglu, M, Schulze, CJ, Scott, PG, Szczesna-Cordary, D, and Schulz, R. Degradation of myosin light chain in isolated rat hearts subjected to ischemia-reperfusion injury: a new intracellular target for matrix metalloproteinase-2. *Circulation* 2005; 112:544-552.
13. Cheung, PY, Sawicki, G, Wozniak, M, Wang, W, Radomski, MW, and Schulz, R. Matrix metalloproteinase-2 contributes to ischemia-reperfusion injury in the heart. *Circulation* 2000; 101:1833-1839.
14. Tyagi, SC, Matsubara, L, and Weber, KT. Direct extraction and estimation of collagenase(s) activity by zymography in microquantities of rat myocardium and uterus. *Clin. Biochem.* 1993; 26:191-198.
15. Coker, ML, Doscher, MA, Thomas, CV, Galis, ZS, and Spinale, FG. Matrix metalloproteinase synthesis and expression in isolated LV myocyte preparations. *Am. J. Physiol* 1999; 277:H777-H787.

16. Galis, ZS, Sukhova, GK, Lark, MW, and Libby, P. Increased expression of matrix metalloproteinases and matrix degrading activity in vulnerable regions of human atherosclerotic plaques. *J. Clin. Invest* 1994; 94:2493-2503.
17. Hanemaaijer, R, Koolwijk, P, le, CL, de Vree, WJ, and van, H, V. Regulation of matrix metalloproteinase expression in human vein and microvascular endothelial cells. Effects of tumour necrosis factor alpha, interleukin 1 and phorbol ester. *Biochem. J.* 1993; 296 (Pt 3):803-809.
18. Heymans, S, Luttun, A, Nuyens, D, Theilmeier, G, Creemers, E, Moons, L, Dyspersin, GD, Cleutjens, JP, Shipley, M, Angellilo, A, Levi, M, Nube, O, Baker, A, Keshet, E, Lupu, F, Herbert, JM, Smits, JF, Shapiro, SD, Baes, M, Borgers, M, Collen, D, Daemen, MJ, and Carmeliet, P. Inhibition of plasminogen activators or matrix metalloproteinases prevents cardiac rupture but impairs therapeutic angiogenesis and causes cardiac failure. *Nat. Med.* 1999; 5:1135-1142.
19. Ho, FM, Liu, SH, Lin, WW, and Liau, CS. Opposite effects of high glucose on MMP-2 and TIMP-2 in human endothelial cells. *J. Cell Biochem.* 2007; 101:442-450.
20. Spallarossa, P, Altieri, P, Garibaldi, S, Ghigliotti, G, Barisione, C, Manca, V, Fabbi, P, Ballestrero, A, Brunelli, C, and Barsotti, A. Matrix metalloproteinase-2 and -9 are induced differently by doxorubicin in H9c2 cells: The role of MAP kinases and NAD(P)H oxidase. *Cardiovasc. Res.* 2006; 69:736-745.
21. Hooper, NM. Families of zinc metalloproteases. *FEBS Lett.* 1994; 354:1-6.

22. Nagase, H and Woessner, JF, Jr. Matrix metalloproteinases. *J. Biol. Chem.* 1999; 274:21491-21494.
23. Woessner, JF, Jr. Role of matrix proteases in processing enamel proteins. *Connect. Tissue Res.* 1998; 39:69-73.
24. Morgunova, E, Tuuttila, A, Bergmann, U, Isupov, M, Lindqvist, Y, Schneider, G, and Tryggvason, K. Structure of human pro-matrix metalloproteinase-2: activation mechanism revealed. *Science* 1999; 284:1667-1670.
25. Van Wart, HE and Birkedal-Hansen, H. The cysteine switch: a principle of regulation of metalloproteinase activity with potential applicability to the entire matrix metalloproteinase gene family. *Proc. Natl. Acad. Sci. U. S. A* 1990; 87:5578-5582.
26. Consolo, M, Amoroso, A, Spandidos, DA, and Mazarino, MC. Matrix metalloproteinases and their inhibitors as markers of inflammation and fibrosis in chronic liver disease (Review). *Int. J. Mol. Med.* 2009; 24:143-152.
27. Liotta, LA, Abe, S, Robey, PG, and Martin, GR. Preferential digestion of basement membrane collagen by an enzyme derived from a metastatic murine tumor. *Proc. Natl. Acad. Sci. U. S. A* 1979; 76:2268-2272.
28. Salo, T, Liotta, LA, and Tryggvason, K. Purification and characterization of a murine basement membrane collagen-degrading enzyme secreted by metastatic tumor cells. *J. Biol. Chem.* 1983; 258:3058-3063.

29. Collier, IE, Wilhelm, SM, Eisen, AZ, Marmer, BL, Grant, GA, Seltzer, JL, Kronberger, A, He, CS, Bauer, EA, and Goldberg, GI. H-ras oncogene-transformed human bronchial epithelial cells (TBE-1) secrete a single metalloprotease capable of degrading basement membrane collagen. *J. Biol. Chem.* 1988; 263:6579-6587.
30. Wilhelm, SM, Collier, IE, Marmer, BL, Eisen, AZ, Grant, GA, and Goldberg, GI. SV40-transformed human lung fibroblasts secrete a 92-kDa type IV collagenase which is identical to that secreted by normal human macrophages. *J. Biol. Chem.* 1989; 264:17213-17221.
31. Murphy, G, Reynolds, JJ, Bretz, U, and Baggiolini, M. Partial purification of collagenase and gelatinase from human polymorphonuclear leucocytes. Analysis of their actions on soluble and insoluble collagens. *Biochem. J.* 1982; 203:209-221.
32. Murphy, G, Ward, R, Hembry, RM, Reynolds, JJ, Kuhn, K, and Tryggvason, K. Characterization of gelatinase from pig polymorphonuclear leucocytes. A metalloproteinase resembling tumour type IV collagenase. *Biochem. J.* 1989; 258:463-472.
33. Eble, JA, Ries, A, Lichy, A, Mann, K, Stanton, H, Gavrilovic, J, Murphy, G, and Kuhn, K. The recognition sites of the integrins alpha1beta1 and alpha2beta1 within collagen IV are protected against gelatinase A attack in the native protein. *J. Biol. Chem.* 1996; 271:30964-30970.

34. Bergman, MR, Cheng, S, Honbo, N, Piacentini, L, Karliner, JS, and Lovett, DH. A functional activating protein 1 (AP-1) site regulates matrix metalloproteinase 2 (MMP-2) transcription by cardiac cells through interactions with JunB-Fra1 and JunB-FosB heterodimers. *Biochem. J.* 2003; 369:485-496.
35. Yan, C and Boyd, DD. Regulation of matrix metalloproteinase gene expression. *J. Cell Physiol* 2007; 211:19-26.
36. Alfonso-Jaume, MA, Bergman, MR, Mahimkar, R, Cheng, S, Jin, ZQ, Karliner, JS, and Lovett, DH. Cardiac ischemia-reperfusion injury induces matrix metalloproteinase-2 expression through the AP-1 components FosB and JunB. *Am. J. Physiol Heart Circ. Physiol* 2006; 291:H1838-H1846.
37. Ben Yosef, Y, Lahat, N, Shapiro, S, Bitterman, H, and Miller, A. Regulation of endothelial matrix metalloproteinase-2 by hypoxia/reoxygenation. *Circ. Res.* 2002; 90:784-791.
38. Mountain, DJ, Singh, M, Menon, B, and Singh, K. Interleukin-1 β Increases Expression and Activity of Matrix Metalloproteinase-2 in Cardiac Microvascular Endothelial Cells: Role of PKC α / β 1 and MAPKs. *Am. J. Physiol Cell Physiol* 2007; 292: C867-875.
39. Okamoto, T, Akaike, T, Nagano, T, Miyajima, S, Suga, M, Ando, M, Ichimori, K, and Maeda, H. Activation of human neutrophil procollagenase by nitrogen dioxide and peroxynitrite: a novel mechanism for procollagenase activation involving nitric oxide. *Arch. Biochem. Biophys.* 1997; 342:261-274.

40. Okamoto, T, Akaike, T, Sawa, T, Miyamoto, Y, van, d, V, and Maeda, H. Activation of matrix metalloproteinases by peroxynitrite-induced protein S-glutathiolation via disulfide S-oxide formation. *J. Biol. Chem.* 2001; 276:29596-29602.
41. Borges, CR, Geddes, T, Watson, JT, and Kuhn, DM. Dopamine biosynthesis is regulated by S-glutathionylation. Potential mechanism of tyrosine hydroxylase inhibition during oxidative stress. *J. Biol. Chem.* 2002; 277:48295-48302.
42. Di Simplicio, P, Franconi, F, Frosali, S, and Di Giuseppe, D. Thiolation and nitrosation of cysteines in biological fluids and cells. *Amino. Acids* 2003; 25:323-339.
43. Fratelli, M, Demol, H, Puype, M, Casagrande, S, Eberini, I, Salmons, M, Bonetto, V, Mengozzi, M, Duffieux, F, Miclet, E, Bachi, A, Vandekerckhove, J, Gianazza, E, and Ghezzi, P. Identification by redox proteomics of glutathionylated proteins in oxidatively stressed human T lymphocytes. *Proc. Natl. Acad. Sci. U. S. A* 2002; 99:3505-3510.
44. Huang, KP and Huang, FL. Glutathionylation of proteins by glutathione disulfide S-oxide. *Biochem. Pharmacol.* 2002; 64:1049-1056.
45. Owens, MW, Milligan, SA, Jourdain, D, and Grisham, MB. Effects of reactive metabolites of oxygen and nitrogen on gelatinase A activity. *Am. J. Physiol* 1997; 273:L445-L450.

46. Rajagopalan, S, Meng, XP, Ramasamy, S, Harrison, DG, and Galis, ZS. Reactive oxygen species produced by macrophage-derived foam cells regulate the activity of vascular matrix metalloproteinases in vitro. Implications for atherosclerotic plaque stability. *J. Clin. Invest* 1996; 98:2572-2579.
47. Viappiani, S and Schulz, R. Detection of specific nitrotyrosine-modified proteins as a marker of oxidative stress in cardiovascular disease. *Am. J. Physiol Heart Circ. Physiol* 2006; 290:H2167-H2168.
48. Sariahmetoglu, M, Crawford, BD, Leon, H, Sawicka, J, Li, L, Ballermann, BJ, Holmes, C, Berthiaume, LG, Holt, A, Sawicki, G, and Schulz, R. Regulation of matrix metalloproteinase-2 (MMP-2) activity by phosphorylation. *FASEB J.* 2007; 21:2486-2495.
49. Insete, J, Garcia-Dorado, D, Ruiz-Meana, M, Agullo, L, Pina, P, and Soler-Soler, J. Ischemic preconditioning attenuates calpain-mediated degradation of structural proteins through a protein kinase A-dependent mechanism. *Cardiovasc. Res.* 2004; 64:105-114.
50. Murphy, S and Frishman, WH. Protein kinase C in cardiac disease and as a potential therapeutic target. *Cardiol. Rev.* 2005; 13:3-12.
51. Juhaszova, M, Zorov, DB, Kim, SH, Pepe, S, Fu, Q, Fishbein, KW, Ziman, BD, Wang, S, Ytrehus, K, Antos, CL, Olson, EN, and Sollott, SJ. Glycogen synthase kinase-3 β mediates convergence of protection signaling to inhibit the mitochondrial permeability transition pore. *J. Clin. Invest* 2004; 113:1535-1549.

52. Wang, W, Sawicki, G, and Schulz, R. Peroxynitrite-induced myocardial injury is mediated through matrix metalloproteinase-2. *Cardiovasc. Res.* 2002; 53:165-174.
53. Ellerbroek, SM, Wu, YI, Overall, CM, and Stack, MS. Functional interplay between type I collagen and cell surface matrix metalloproteinase activity. *J. Biol. Chem.* 2001; 276:24833-24842.
54. Boger, DL, Goldberg, J, Silletti, S, Kessler, T, and Cheresh, DA. Identification of a novel class of small-molecule antiangiogenic agents through the screening of combinatorial libraries which function by inhibiting the binding and localization of proteinase MMP2 to integrin alpha(V)beta(3). *J. Am. Chem. Soc.* 2001; 123:1280-1288.
55. Silletti, S, Kessler, T, Goldberg, J, Boger, DL, and Cheresh, DA. Disruption of matrix metalloproteinase 2 binding to integrin alpha vbeta 3 by an organic molecule inhibits angiogenesis and tumor growth in vivo. *Proc. Natl. Acad. Sci. U. S. A* 2001; 98:119-124.
56. Crabbe, T, Ioannou, C, and Docherty, AJ. Human progelatinase A can be activated by autolysis at a rate that is concentration-dependent and enhanced by heparin bound to the C-terminal domain. *Eur. J. Biochem.* 1993; 218:431-438.
57. Zucker, S, Conner, C, DiMassmo, BI, Ende, H, Drews, M, Seiki, M, and Bahou, WF. Thrombin induces the activation of progelatinase A in vascular endothelial cells. Physiologic regulation of angiogenesis. *J. Biol. Chem.* 1995; 270:23730-23738.

58. Rauch, BH, Bretschneider, E, Braun, M, and Schror, K. Factor Xa releases matrix metalloproteinase-2 (MMP-2) from human vascular smooth muscle cells and stimulates the conversion of pro-MMP-2 to MMP-2: role of MMP-2 in factor Xa-induced DNA synthesis and matrix invasion. *Circ. Res.* 2002; 90:1122-1127.
59. Chow, AK, Cena, J, El-Yazbi, AF, Crawford, BD, Holt, A, Cho, WJ, Daniel, EE, and Schulz, R. Caveolin-1 inhibits matrix metalloproteinase-2 activity in the heart. *J. Mol. Cell Cardiol.* 2007; 42:896-901.
60. Brew, K, Dinakarandian, D, and Nagase, H. Tissue inhibitors of metalloproteinases: evolution, structure and function. *Biochim. Biophys. Acta* 2000; 1477:267-283.
61. Williamson, RA, Marston, FA, Angal, S, Koklitis, P, Panico, M, Morris, HR, Carne, AF, Smith, BJ, Harris, TJ, and Freedman, RB. Disulphide bond assignment in human tissue inhibitor of metalloproteinases (TIMP). *Biochem. J.* 1990; 268:267-274.
62. Goldberg, GI, Strongin, A, Collier, IE, Genrich, LT, and Marmer, BL. Interaction of 92-kDa type IV collagenase with the tissue inhibitor of metalloproteinases prevents dimerization, complex formation with interstitial collagenase, and activation of the proenzyme with stromelysin. *J. Biol. Chem.* 1992; 267:4583-4591.
63. Li, YY, McTiernan, CF, and Feldman, AM. Proinflammatory cytokines regulate tissue inhibitors of metalloproteinases and disintegrin metalloproteinase in cardiac cells. *Cardiovasc. Res.* 1999; 42:162-172.

64. Chua, CC, Hamdy, RC, and Chua, BH. Angiotensin II induces TIMP-1 production in rat heart endothelial cells. *Biochim. Biophys. Acta* 1996; 1311:175-180.
65. Fedak, PW, Altamentova, SM, Weisel, RD, Nili, N, Ohno, N, Verma, S, Lee, TY, Kiani, C, Mickle, DA, Strauss, BH, and Li, RK. Matrix remodeling in experimental and human heart failure: a possible regulatory role for TIMP-3. *Am. J. Physiol Heart Circ. Physiol* 2003; 284:H626-H634.
66. Pavloff, N, Staskus, PW, Kishnani, NS, and Hawkes, SP. A new inhibitor of metalloproteinases from chicken: ChIMP-3. A third member of the TIMP family. *J. Biol. Chem.* 1992; 267:17321-17326.
67. Leco, KJ, Apte, SS, Taniguchi, GT, Hawkes, SP, Khokha, R, Schultz, GA, and Edwards, DR. Murine tissue inhibitor of metalloproteinases-4 (Timp-4): cDNA isolation and expression in adult mouse tissues. *FEBS Lett.* 1997; 401:213-217.
68. Schulze, CJ, Wang, W, Suarez-Pinzon, WL, Sawicka, J, Sawicki, G, and Schulz, R. Imbalance between tissue inhibitor of metalloproteinase-4 and matrix metalloproteinases during acute myocardial ischemia-reperfusion injury. *Circulation* 2003; 107:2487-2492.
69. Greene, J, Wang, M, Liu, YE, Raymond, LA, Rosen, C, and Shi, YE. Molecular cloning and characterization of human tissue inhibitor of metalloproteinase 4. *J. Biol. Chem.* 1996; 271:30375-30380.

70. Cox, MJ, Hawkins, UA, Hoit, BD, and Tyagi, SC. Attenuation of oxidative stress and remodeling by cardiac inhibitor of metalloproteinase protein transfer. *Circulation* 2004; 109:2123-2128.
71. Peterson, JT. Matrix metalloproteinase inhibitor development and the remodeling of drug discovery. *Heart Fail. Rev.* 2004; 9:63-79.
72. Beaudoux, JL, Giral, P, Bruckert, E, Foglietti, MJ, and Chapman, MJ. Matrix metalloproteinases, inflammation and atherosclerosis: therapeutic perspectives. *Clin. Chem. Lab Med.* 2004; 42:121-131.
73. Koivunen, E, Arap, W, Valtanen, H, Rainisalo, A, Medina, OP, Heikkila, P, Kantor, C, Gahmberg, CG, Salo, T, Konttinen, YT, Sorsa, T, Ruoslahti, E, and Pasqualini, R. Tumor targeting with a selective gelatinase inhibitor. *Nat. Biotechnol.* 1999; 17:768-774.
74. Peterson, JT. The importance of estimating the therapeutic index in the development of matrix metalloproteinase inhibitors. *Cardiovasc. Res.* 2006; 69:677-687.
75. Koivunen, E, Arap, W, Valtanen, H, Rainisalo, A, Medina, OP, Heikkila, P, Kantor, C, Gahmberg, CG, Salo, T, Konttinen, YT, Sorsa, T, Ruoslahti, E, and Pasqualini, R. Tumor targeting with a selective gelatinase inhibitor. *Nat. Biotechnol.* 1999; 17:768-774.

76. Higashi, S and Miyazaki, K. Identification of a region of beta-amyloid precursor protein essential for its gelatinase A inhibitory activity. *J. Biol. Chem.* 2003; 278:14020-14028.
77. Gao, CQ, Sawicki, G, Suarez-Pinzon, WL, Csont, T, Wozniak, M, Ferdinandy, P, and Schulz, R. Matrix metalloproteinase-2 mediates cytokine-induced myocardial contractile dysfunction. *Cardiovasc. Res.* 2003; 57:426-433.
78. Koivunen, E, Arap, W, Valtanen, H, Rainisalo, A, Medina, OP, Heikkila, P, Kantor, C, Gahmberg, CG, Salo, T, Konttinen, YT, Sorsa, T, Ruoslahti, E, and Pasqualini, R. Tumor targeting with a selective gelatinase inhibitor. *Nat. Biotechnol.* 1999; 17:768-774.
79. Golub, LM, Lee, HM, Ryan, ME, Giannobile, WV, Payne, J, and Sorsa, T. Tetracyclines inhibit connective tissue breakdown by multiple non-antimicrobial mechanisms. *Adv. Dent. Res.* 1998; 12:12-26.
80. Golub, LM, McNamara, TF, D'Angelo, G, Greenwald, RA, and Ramamurthy, NS. A non-antibacterial chemically-modified tetracycline inhibits mammalian collagenase activity. *J. Dent. Res.* 1987; 66:1310-1314.
81. Lee, HM, Ciancio, SG, Tuter, G, Ryan, ME, Komaroff, E, and Golub, LM. Subantimicrobial dose doxycycline efficacy as a matrix metalloproteinase inhibitor in chronic periodontitis patients is enhanced when combined with a non-steroidal anti-inflammatory drug. *J. Periodontol.* 2004; 75:453-463.

82. Garcia, RA, Pantazatos, DP, Gessner, CR, Go, KV, Woods, VL, Jr., and Villarreal, FJ. Molecular interactions between matrilysin and the matrix metalloproteinase inhibitor doxycycline investigated by deuterium exchange mass spectrometry. *Mol. Pharmacol.* 2005; 67:1128-1136.
83. Golub, LM, Lee, HM, Ryan, ME, Giannobile, WV, Payne, J, and Sorsa, T. Tetracyclines inhibit connective tissue breakdown by multiple non-antimicrobial mechanisms. *Adv. Dent. Res.* 1998; 12:12-26.
84. Golub, LM, Lee, HM, Ryan, ME, Giannobile, WV, Payne, J, and Sorsa, T. Tetracyclines inhibit connective tissue breakdown by multiple non-antimicrobial mechanisms. *Adv. Dent. Res.* 1998; 12:12-26.
85. Novak, MJ, Johns, LP, Miller, RC, and Bradshaw, MH. Adjunctive benefits of subantimicrobial dose doxycycline in the management of severe, generalized, chronic periodontitis. *J. Periodontol.* 2002; 73:762-769.
86. Thompson, RW and Baxter, BT. MMP inhibition in abdominal aortic aneurysms. Rationale for a prospective randomized clinical trial. *Ann. N. Y. Acad. Sci.* 1999; 878:159-178.
87. Onoda, T, Ono, T, Dhar, DK, Yamanoi, A, Fujii, T, and Nagasue, N. Doxycycline inhibits cell proliferation and invasive potential: combination therapy with cyclooxygenase-2 inhibitor in human colorectal cancer cells. *J. Lab Clin. Med.* 2004; 143:207-216.

88. Linask, KK, Han, M, Cai, DH, Brauer, PR, and Maisastry, SM. Cardiac morphogenesis: matrix metalloproteinase coordination of cellular mechanisms underlying heart tube formation and directionality of looping. *Dev. Dyn.* 2005; 233:739-753.
89. Ratajska, A and Cleutjens, JP. Embryogenesis of the rat heart: the expression of collagenases. *Basic Res. Cardiol.* 2002; 97:189-197.
90. Linask, KK, Manisastry, S, and Han, M. Cross talk between cell-cell and cell-matrix adhesion signaling pathways during heart organogenesis: implications for cardiac birth defects. *Microsc. Microanal.* 2005; 11:200-208.
91. Cai, W, Vosschulte, R, fsah-Hedjri, A, Koltai, S, Kocsis, E, Scholz, D, Kostin, S, Schaper, W, and Schaper, J. Altered balance between extracellular proteolysis and antiproteolysis is associated with adaptive coronary arteriogenesis. *J. Mol. Cell Cardiol.* 2000; 32:997-1011.
92. Alexander, SM, Jackson, KJ, Bushnell, KM, and McGuire, PG. Spatial and temporal expression of the 72-kDa type IV collagenase (MMP-2) correlates with development and differentiation of valves in the embryonic avian heart. *Dev. Dyn.* 1997; 209:261-268.
93. Brooks, PC, Silletti, S, von Schalscha, TL, Friedlander, M, and Cheresch, DA. Disruption of angiogenesis by PEX, a noncatalytic metalloproteinase fragment with integrin binding activity. *Cell* 1998; 92:391-400.

94. Enciso, JM, Gratzinger, D, Camenisch, TD, Canosa, S, Pinter, E, and Madri, JA. Elevated glucose inhibits VEGF-A-mediated endocardial cushion formation: modulation by PECAM-1 and MMP-2. *J. Cell Biol.* 2003; 160:605-615.
95. Zhang, J, Bai, S, Zhang, X, Nagase, H, and Sarras, MP, Jr. The expression of gelatinase A (MMP-2) is required for normal development of zebrafish embryos. *Dev. Genes Evol.* 2003; 213:456-463.
96. Itoh, T, Ikeda, T, Gomi, H, Nakao, S, Suzuki, T, and Itohara, S. Unaltered secretion of beta-amyloid precursor protein in gelatinase A (matrix metalloproteinase 2)-deficient mice. *J. Biol. Chem.* 1997; 272:22389-22392.
97. Mosig, RA, Dowling, O, DiFeo, A, Ramirez, MC, Parker, IC, Abe, E, Diouri, J, Aqeel, AA, Wylie, JD, Oblander, SA, Madri, J, Bianco, P, Apte, SS, Zaidi, M, Doty, SB, Majeska, RJ, Schaffler, MB, and Martignetti, JA. Loss of MMP-2 disrupts skeletal and craniofacial development and results in decreased bone mineralization, joint erosion and defects in osteoblast and osteoclast growth. *Hum. Mol. Genet.* 2007; 16:1113-1123.
98. Esparza, J, Kruse, M, Lee, J, Michaud, M, and Madri, JA. MMP-2 null mice exhibit an early onset and severe experimental autoimmune encephalomyelitis due to an increase in MMP-9 expression and activity. *FASEB J.* 2004; 18:1682-1691.
99. Cheng, XW, Kuzuya, M, Nakamura, K, Maeda, K, Tsuzuki, M, Kim, W, Sasaki, T, Liu, Z, Inoue, N, Kondo, T, Jin, H, Numaguchi, Y, Okumura, K, Yokota, M, Iguchi, A, and Murohara, T. Mechanisms underlying the impairment of ischemia-

- induced neovascularization in matrix metalloproteinase 2-deficient mice. *Circ. Res.* 2007; 100:904-913.
100. Brenner, DA, O'Hara, M, Angel, P, Chojkier, M, and Karin, M. Prolonged activation of jun and collagenase genes by tumour necrosis factor-alpha. *Nature* 1989; 337:661-663.
 101. Mountain, DJ, Singh, M, Menon, B, and Singh, K. Interleukin-1{beta} Increases Expression and Activity of Matrix Metalloproteinase-2 in Cardiac Microvascular Endothelial Cells: Role of PKC{alpha}/{beta}1 and MAPKs. *Am. J. Physiol Cell Physiol* 2006.
 102. Siwik, DA, Chang, DL, and Colucci, WS. Interleukin-1beta and tumor necrosis factor-alpha decrease collagen synthesis and increase matrix metalloproteinase activity in cardiac fibroblasts in vitro. *Circ. Res.* 2000; 86:1259-1265.
 103. Chua, PK, Melish, ME, Yu, Q, Yanagihara, R, Yamamoto, KS, and Nerurkar, VR. Elevated levels of matrix metalloproteinase 9 and tissue inhibitor of metalloproteinase 1 during the acute phase of Kawasaki disease. *Clin. Diagn. Lab Immunol.* 2003; 10:308-314.
 104. Matsuyama, T. Tissue inhibitor of metalloproteinases-1 and matrix metalloproteinase-3 in Japanese healthy children and in Kawasaki disease and their clinical usefulness in juvenile rheumatoid arthritis. *Pediatr. Int.* 1999; 41:239-245.

105. Gavin, PJ, Crawford, SE, Shulman, ST, Garcia, FL, and Rowley, AH. Systemic arterial expression of matrix metalloproteinases 2 and 9 in acute Kawasaki disease. *Arterioscler. Thromb. Vasc. Biol.* 2003; 23:576-581.
106. Kearney, MT, Cotton, JM, Richardson, PJ, and Shah, AM. Viral myocarditis and dilated cardiomyopathy: mechanisms, manifestations, and management. *Postgrad. Med. J.* 2001; 77:4-10.
107. Heymans, S, Pauschinger, M, De, PA, Kallwellis-Opara, A, Rutschow, S, Swinnen, M, Vanhoutte, D, Gao, F, Torpai, R, Baker, AH, Padalko, E, Neyts, J, Schultheiss, HP, Van de, WF, Carmeliet, P, and Pinto, YM. Inhibition of urokinase-type plasminogen activator or matrix metalloproteinases prevents cardiac injury and dysfunction during viral myocarditis. *Circulation* 2006; 114:565-573.
108. Cheung, C, Luo, H, Yanagawa, B, Leong, HS, Samarasekera, D, Lai, JC, Suarez, A, Zhang, J, and McManus, BM. Matrix metalloproteinases and tissue inhibitors of metalloproteinases in coxsackievirus-induced myocarditis. *Cardiovasc. Pathol.* 2006; 15:63-74.
109. Kim, M and Kim, K. Elevation of cardiac troponin I in the acute stage of Kawasaki disease. *Pediatr. Cardiol.* 1999; 20:184-188.
110. Kim, M and Kim, K. Changes in cardiac troponin I in Kawasaki disease before and after treatment with intravenous gammaglobulin. *Jpn. Circ. J.* 1998; 62:479-482.
111. Checchia, PA, Borensztajn, J, and Shulman, ST. Circulating cardiac troponin I levels in Kawasaki disease. *Pediatr. Cardiol.* 2001; 22:102-106.

112. Imazio, M, Demichelis, B, Cecchi, E, Belli, R, Ghisio, A, Bobbio, M, and Trincherio, R. Cardiac troponin I in acute pericarditis. *J. Am. Coll. Cardiol.* 2003; 42:2144-2148.
113. Goser, S, Andrassy, M, Buss, SJ, Leuschner, F, Volz, CH, Ottl, R, Zittrich, S, Blaudeck, N, Hardt, SE, Pfitzer, G, Rose, NR, Katus, HA, and Kaya, Z. Cardiac troponin I but not cardiac troponin T induces severe autoimmune inflammation in the myocardium. *Circulation* 2006; 114:1693-1702.
114. Braunwald, E and Kloner, RA. The stunned myocardium: prolonged, postischemic ventricular dysfunction. *Circulation* 1982; 66:1146-1149.
115. Braunwald, E and Rutherford, JD. Reversible ischemic left ventricular dysfunction: evidence for the "hibernating myocardium". *J. Am. Coll. Cardiol.* 1986; 8:1467-1470.
116. Ausma, J, Cleutjens, J, Thone, F, Flameng, W, Ramaekers, F, and Borgers, M. Chronic hibernating myocardium: interstitial changes. *Mol. Cell Biochem.* 1995; 147:35-42.
117. Bolli, R and Marban, E. Molecular and cellular mechanisms of myocardial stunning. *Physiol Rev.* 1999; 79:609-634.
118. Yasmin, W, Strynadka, KD, and Schulz, R. Generation of peroxynitrite contributes to ischemia-reperfusion injury in isolated rat hearts. *Cardiovasc. Res.* 1997; 33:422-432.

119. Frears, ER, Zhang, Z, Blake, DR, O'Connell, JP, and Winyard, PG. Inactivation of tissue inhibitor of metalloproteinase-1 by peroxynitrite. *FEBS Lett.* 1996; 381:21-24.
120. Donnini, S, Monti, M, Roncone, R, Morbidelli, L, Rocchigiani, M, Oliviero, S, Casella, L, Giachetti, A, Schulz, R, and Ziche, M. Peroxynitrite inactivates human-tissue inhibitor of metalloproteinase-4. *FEBS Lett.* 2008; 582:1135-1140.
121. Prasan, AM, McCarron, HC, White, MY, McLennan, SV, Tchen, AS, Hambly, BD, and Jeremy, RW. Duration of ischaemia determines matrix metalloproteinase-2 activation in the reperfused rabbit heart. *Proteomics.* 2002; 2:1204-1210.
122. Inokubo, Y, Hanada, H, Ishizaka, H, Fukushi, T, Kamada, T, and Okumura, K. Plasma levels of matrix metalloproteinase-9 and tissue inhibitor of metalloproteinase-1 are increased in the coronary circulation in patients with acute coronary syndrome. *Am. Heart J.* 2001; 141:211-217.
123. Lalu, MM, Pasini, E, Schulze, CJ, Ferrari-Vivaldi, M, Ferrari-Vivaldi, G, Bachetti, T, and Schulz, R. Ischaemia-reperfusion injury activates matrix metalloproteinases in the human heart. *Eur. Heart J.* 2005; 26:27-35.
124. Lalu, MM, Csonka, C, Giricz, Z, Csont, T, Schulz, R, and Ferdinandy, P. Preconditioning decreases ischemia/reperfusion-induced release and activation of matrix metalloproteinase-2. *Biochem. Biophys. Res. Commun.* 2002; 296:937-941.

125. Giricz, Z, Lalu, MM, Csonka, C, Bencsik, P, Schulz, R, and Ferdinandy, P. Hyperlipidemia attenuates the infarct size-limiting effect of ischemic preconditioning: role of matrix metalloproteinase-2 inhibition. *J. Pharmacol. Exp. Ther.* 2006; 316:154-161.
126. Bellosa, S, Gomaschi, M, Canavesi, M, Rossoni, G, Monetti, M, Franceschini, G, and Calabresi, L. Inhibition of MMP-2 activation and release as a novel mechanism for HDL-induced cardioprotection. *FEBS Lett.* 2006; 580:5974-5978.
127. Leon, H, Baczko, I, Sawicki, G, Light, PE, and Schulz, R. Inhibition of matrix metalloproteinases prevents peroxynitrite-induced contractile dysfunction in the isolated cardiac myocyte. *Br. J. Pharmacol.* 2008; 153:676-683.
128. Chakraborti, S, Mandal, A, Das, S, and Chakraborti, T. Inhibition of Na⁺/Ca²⁺ exchanger by peroxynitrite in microsomes of pulmonary smooth muscle: role of matrix metalloproteinase-2. *Biochim. Biophys. Acta* 2004; 1671:70-78.
129. Doroshov, JH and Davies, KJ. Redox cycling of anthracyclines by cardiac mitochondria. II. Formation of superoxide anion, hydrogen peroxide, and hydroxyl radical. *J. Biol. Chem.* 1986; 261:3068-3074.
130. Bai, P, Mabley, JG, Liaudet, L, Virag, L, Szabo, C, and Pacher, P. Matrix metalloproteinase activation is an early event in doxorubicin-induced cardiotoxicity. *Oncol. Rep.* 2004; 11:505-508.
131. Kizaki, K, Ito, R, Okada, M, Yoshioka, K, Uchide, T, Temma, K, Mutoh, K, Uechi, M, and Hara, Y. Enhanced gene expression of myocardial matrix

- metalloproteinases 2 and 9 after acute treatment with doxorubicin in mice. *Pharmacol. Res.* 2006; 53:341-346.
132. Mukherjee, R, Mingoia, JT, Bruce, JA, Austin, JS, Stroud, RE, Escobar, GP, McClister, DM, Jr., Allen, CM, fonso-Jaume, MA, Fini, ME, Lovett, DH, and Spinale, FG. Selective spatiotemporal induction of matrix metalloproteinase-2 and matrix metalloproteinase-9 transcription after myocardial infarction. *Am. J. Physiol Heart Circ. Physiol* 2006; 291:H2216-H2228.
133. Bergman, MR, Teerlink, JR, Mahimkar, R, Li, L, Zhu, BQ, Nguyen, A, Dahi, S, Karliner, JS, and Lovett, DH. Cardiac matrix metalloproteinase-2 expression independently induces marked ventricular remodeling and systolic dysfunction. *Am. J. Physiol Heart Circ. Physiol* 2007; 292:H1847-H1860.
134. Zhou, HZ, Ma, X, Gray, MO, Zhu, BQ, Nguyen, AP, Baker, AJ, Simonis, U, Cecchini, G, Lovett, DH, and Karliner, JS. Transgenic MMP-2 expression induces latent cardiac mitochondrial dysfunction. *Biochem. Biophys. Res. Commun.* 2007; 358:189-195.
135. Chow, AK, Cena, J, and Schulz, R. Acute actions and novel targets of matrix metalloproteinases in the heart and vasculature. *Br. J. Pharmacol.* 2007; 152:189-205.
136. Spinale, FG, Coker, ML, Bond, BR, and Zellner, JL. Myocardial matrix degradation and metalloproteinase activation in the failing heart: a potential therapeutic target. *Cardiovasc. Res.* 2000; 46:225-238.

137. Viappiani, S, Nicolescu, AC, Holt, A, Sawicki, G, Crawford, BD, Leon, H, van, MT, and Schulz, R. Activation and modulation of 72kDa matrix metalloproteinase-2 by peroxynitrite and glutathione. *Biochem. Pharmacol.* 2009; 77:826-834.
138. Matsumura, Y, Saeki, E, Inoue, M, Hori, M, Kamada, T, and Kusuoka, H. Inhomogeneous disappearance of myofilament-related cytoskeletal proteins in stunned myocardium of guinea pig. *Circ. Res.* 1996; 79:447-454.
139. Sung, MM, Schulz, CG, Wang, W, Sawicki, G, Bautista-Lopez, NL, and Schulz, R. Matrix metalloproteinase-2 degrades the cytoskeletal protein alpha-actinin in peroxynitrite mediated myocardial injury. *J. Mol. Cell Cardiol.* 2007; 43:429-436.
140. Utz, PJ and Anderson, P. Life and death decisions: regulation of apoptosis by proteolysis of signaling molecules. *Cell Death. Differ.* 2000; 7:589-602.
141. Mazars, A, Fernandez-Vidal, A, Mondesert, O, Lorenzo, C, Prevost, G, Ducommun, B, Payrastre, B, Racaud-Sultan, C, and Manenti, S. A caspase-dependent cleavage of CDC25A generates an active fragment activating cyclin-dependent kinase 2 during apoptosis. *Cell Death. Differ.* 2009; 16:208-218.
142. Grdovic, N, Mihailovic, M, Vidakovic, M, Dinic, S, Uskokovic, A, Martinovic, V, Arambasic, J, Grigorov, I, Ivanovic-Matic, S, Bogojevic, D, Petrovic, M, and Poznanovic, G. Establishment of association of an Mg²⁺-dependent endonuclease with the rat liver nuclear matrix in cryonecrosis. *Cell Biochem. Funct.* 2007; 25:345-355.

143. Kwan, JA, Schulze, CJ, Wang, W, Leon, H, Sariahmetoglu, M, Sung, M, Sawicka, J, Sims, DE, Sawicki, G, and Schulz, R. Matrix metalloproteinase-2 (MMP-2) is present in the nucleus of cardiac myocytes and is capable of cleaving poly (ADP-ribose) polymerase (PARP) in vitro. *FASEB J.* 2004; 18:690-692.
144. Si-Tayeb, K, Monvoisin, A, Mazzocco, C, Lepreux, S, Decossas, M, Cubel, G, Taras, D, Blanc, JF, Robinson, DR, and Rosenbaum, J. Matrix metalloproteinase 3 is present in the cell nucleus and is involved in apoptosis. *Am. J. Pathol.* 2006; 169:1390-1401.
145. Munro, S. Lipid rafts: elusive or illusive? *Cell* 2003; 115:377-388.
146. Simons, K and van, MG. Lipid sorting in epithelial cells. *Biochemistry* 1988; 27:6197-6202.
147. Chang, WJ, Ying, YS, Rothberg, KG, Hooper, NM, Turner, AJ, Gambliel, HA, De, GJ, Mumby, SM, Gilman, AG, and Anderson, RG. Purification and characterization of smooth muscle cell caveolae. *J. Cell Biol.* 1994; 126:127-138.
148. Lisanti, MP, Tang, Z, Scherer, PE, and Sargiacomo, M. Caveolae purification and glycosylphosphatidylinositol-linked protein sorting in polarized epithelia. *Methods Enzymol.* 1995; 250:655-668.
149. Jacobson, K and Dietrich, C. Looking at lipid rafts? *Trends Cell Biol.* 1999; 9:87-91.
150. Heerklotz, H. Triton promotes domain formation in lipid raft mixtures. *Biophys. J.* 2002; 83:2693-2701.

151. Schlegel, A, Pestell, RG, and Lisanti, MP. Caveolins in cholesterol trafficking and signal transduction: implications for human disease. *Front Biosci.* 2000; 5:D929-D937.
152. Schroeder, F, Gallegos, AM, Atshaves, BP, Storey, SM, McIntosh, AL, Petrescu, AD, Huang, H, Starodub, O, Chao, H, Yang, H, Frolov, A, and Kier, AB. Recent advances in membrane microdomains: rafts, caveolae, and intracellular cholesterol trafficking. *Exp. Biol. Med. (Maywood.)* 2001; 226:873-890.
153. Matveev, S, Li, X, Everson, W, and Smart, EJ. The role of caveolae and caveolin in vesicle-dependent and vesicle-independent trafficking. *Adv. Drug Deliv. Rev.* 2001; 49:237-250.
154. Scherer, PE, Tang, Z, Chun, M, Sargiacomo, M, Lodish, HF, and Lisanti, MP. Caveolin isoforms differ in their N-terminal protein sequence and subcellular distribution. Identification and epitope mapping of an isoform-specific monoclonal antibody probe. *J. Biol. Chem.* 1995; 270:16395-16401.
155. Head, BP, Patel, HH, Roth, DM, Murray, F, Swaney, JS, Niesman, IR, Farquhar, MG, and Insel, PA. Microtubules and actin microfilaments regulate lipid raft/caveolae localization of adenylyl cyclase signaling components. *J. Biol. Chem.* 2006; 281:26391-26399.
156. Volonte, D, McTiernan, CF, Drab, M, Kasper, M, and Galbiati, F. Caveolin-1 and caveolin-3 form heterooligomeric complexes in atrial cardiac myocytes that are required for doxorubicin-induced apoptosis. *Am. J. Physiol Heart Circ. Physiol* 2008; 294:H392-H401.

157. Li, S, Galbiati, F, Volonte, D, Sargiacomo, M, Engelman, JA, Das, K, Scherer, PE, and Lisanti, MP. Mutational analysis of caveolin-induced vesicle formation. Expression of caveolin-1 recruits caveolin-2 to caveolae membranes. *FEBS Lett.* 1998; 434:127-134.
158. Ralston, E and Ploug, T. Caveolin-3 is associated with the T-tubules of mature skeletal muscle fibers. *Exp. Cell Res.* 1999; 246:510-515.
159. Head, BP, Patel, HH, Roth, DM, Lai, NC, Niesman, IR, Farquhar, MG, and Insel, PA. G-protein-coupled receptor signaling components localize in both sarcolemmal and intracellular caveolin-3-associated microdomains in adult cardiac myocytes. *J. Biol. Chem.* 2005; 280:31036-31044.
160. Williams, TM and Lisanti, MP. The Caveolin genes: from cell biology to medicine. *Ann. Med.* 2004; 36:584-595.
161. Spisni, E, Tomasi, V, Cestaro, A, and Tosatto, SC. Structural insights into the function of human caveolin 1. *Biochem. Biophys. Res. Commun.* 2005; 338:1383-1390.
162. Goligorsky, MS, Li, H, Brodsky, S, and Chen, J. Relationships between caveolae and eNOS: everything in proximity and the proximity of everything. *Am. J. Physiol Renal Physiol* 2002; 283:F1-10.
163. Schlegel, A, Schwab, RB, Scherer, PE, and Lisanti, MP. A role for the caveolin scaffolding domain in mediating the membrane attachment of caveolin-1. The

- caveolin scaffolding domain is both necessary and sufficient for membrane binding in vitro. *J. Biol. Chem.* 1999; 274:22660-22667.
164. Bernatchez, PN, Bauer, PM, Yu, J, Prendergast, JS, He, P, and Sessa, WC. Dissecting the molecular control of endothelial NO synthase by caveolin-1 using cell-permeable peptides. *Proc. Natl. Acad. Sci. U. S. A* 2005; 102:761-766.
165. Epand, RM, Sayer, BG, and Epand, RF. Caveolin scaffolding region and cholesterol-rich domains in membranes. *J. Mol. Biol.* 2005; 345:339-350.
166. Schlegel, A and Lisanti, MP. A molecular dissection of caveolin-1 membrane attachment and oligomerization. Two separate regions of the caveolin-1 C-terminal domain mediate membrane binding and oligomer/oligomer interactions in vivo. *J. Biol. Chem.* 2000; 275:21605-21617.
167. Scherer, PE, Okamoto, T, Chun, M, Nishimoto, I, Lodish, HF, and Lisanti, MP. Identification, sequence, and expression of caveolin-2 defines a caveolin gene family. *Proc. Natl. Acad. Sci. U. S. A* 1996; 93:131-135.
168. Tang, Z, Scherer, PE, Okamoto, T, Song, K, Chu, C, Kohtz, DS, Nishimoto, I, Lodish, HF, and Lisanti, MP. Molecular cloning of caveolin-3, a novel member of the caveolin gene family expressed predominantly in muscle. *J. Biol. Chem.* 1996; 271:2255-2261.
169. Lisanti, MP, Scherer, PE, Tang, Z, and Sargiacomo, M. Caveolae, caveolin and caveolin-rich membrane domains: a signalling hypothesis. *Trends Cell Biol.* 1994; 4:231-235.

170. Insel, PA, Head, BP, Ostrom, RS, Patel, HH, Swaney, JS, Tang, CM, and Roth, DM. Caveolae and lipid rafts: G protein-coupled receptor signaling microdomains in cardiac myocytes. *Ann. N. Y. Acad. Sci.* 2005; 1047:166-172.
171. Vihanto, MM, Vindis, C, Djonov, V, Cerretti, DP, and Huynh-Do, U. Caveolin-1 is required for signaling and membrane targeting of EphB1 receptor tyrosine kinase. *J. Cell Sci.* 2006; 119:2299-2309.
172. Xia, W, Bacus, S, Hegde, P, Husain, I, Strum, J, Liu, L, Paulazzo, G, Lyass, L, Trusk, P, Hill, J, Harris, J, and Spector, NL. A model of acquired autoresistance to a potent ErbB2 tyrosine kinase inhibitor and a therapeutic strategy to prevent its onset in breast cancer. *Proc. Natl. Acad. Sci. U. S. A* 2006; 103:7795-7800.
173. Biedi, C, Panetta, D, Segat, D, Cordera, R, and Maggi, D. Specificity of insulin-like growth factor I and insulin on Shc phosphorylation and Grb2 recruitment in caveolae. *Endocrinology* 2003; 144:5497-5503.
174. Sampson, LJ, Hayabuchi, Y, Standen, NB, and Dart, C. Caveolae localize protein kinase A signaling to arterial ATP-sensitive potassium channels. *Circ. Res.* 2004; 95:1012-1018.
175. Razani, B and Lisanti, MP. Two distinct caveolin-1 domains mediate the functional interaction of caveolin-1 with protein kinase A. *Am. J. Physiol Cell Physiol* 2001; 281:C1241-C1250.
176. Tourkina, E, Gooz, P, Pannu, J, Bonner, M, Scholz, D, Hacker, S, Silver, RM, Trojanowska, M, and Hoffman, S. Opposing effects of protein kinase Calpha and

- protein kinase Cepsilon on collagen expression by human lung fibroblasts are mediated via MEK/ERK and caveolin-1 signaling. *J. Biol. Chem.* 2005; 280:13879-13887.
177. Wu, D and Terrian, DM. Regulation of caveolin-1 expression and secretion by a protein kinase Cepsilon signaling pathway in human prostate cancer cells. *J. Biol. Chem.* 2002; 277:40449-40455.
178. Prevostel, C, Alice, V, Joubert, D, and Parker, PJ. Protein kinase C(alpha) actively downregulates through caveolae-dependent traffic to an endosomal compartment. *J. Cell Sci.* 2000; 113 (Pt 14):2575-2584.
179. Feron, O and Balligand, JL. Caveolins and the regulation of endothelial nitric oxide synthase in the heart. *Cardiovasc. Res.* 2006; 69:788-797.
180. Salapatek, AM, Wang, YF, Mao, YK, Lam, A, and Daniel, EE. Myogenic nitric oxide synthase activity in canine lower oesophageal sphincter: morphological and functional evidence. *Br. J. Pharmacol.* 1998; 123:1055-1064.
181. Salapatek, AM, Wang, YF, Mao, YK, Mori, M, and Daniel, EE. Myogenic NOS in canine lower esophageal sphincter: enzyme activation, substrate recycling, and product actions. *Am. J. Physiol* 1998; 274:C1145-C1157.
182. van Deurs, B, Roepstorff, K, Hommelgaard, AM, and Sandvig, K. Caveolae: anchored, multifunctional platforms in the lipid ocean. *Trends Cell Biol.* 2003; 13:92-100.

183. Puyraimond, A, Fridman, R, Lemesle, M, Arbeille, B, and Menashi, S. MMP-2 colocalizes with caveolae on the surface of endothelial cells. *Exp. Cell Res.* 2001; 262:28-36.
184. Labrecque, L, Nyalendo, C, Langlois, S, Durocher, Y, Roghi, C, Murphy, G, Gingras, D, and Beliveau, R. Src-mediated tyrosine phosphorylation of caveolin-1 induces its association with membrane type 1 matrix metalloproteinase. *J. Biol. Chem.* 2004; 279:52132-52140.
185. Murtazina, R, Kovbasnjuk, O, Donowitz, M, and Li, X. Na⁺/H⁺ exchanger NHE3 activity and trafficking are lipid Raft-dependent. *J. Biol. Chem.* 2006; 281:17845-17855.
186. Barbuti, A, Gravante, B, Riolfo, M, Milanesi, R, Terragni, B, and DiFrancesco, D. Localization of pacemaker channels in lipid rafts regulates channel kinetics. *Circ. Res.* 2004; 94:1325-1331.
187. Gimpl, G, Burger, K, and Fahrenholz, F. Cholesterol as modulator of receptor function. *Biochemistry* 1997; 36:10959-10974.
188. Christian, AE, Haynes, MP, Phillips, MC, and Rothblat, GH. Use of cyclodextrins for manipulating cellular cholesterol content. *J. Lipid Res.* 1997; 38:2264-2272.
189. Dreja, K, Voldstedlund, M, Vinten, J, Tranum-Jensen, J, Hellstrand, P, and Sward, K. Cholesterol depletion disrupts caveolae and differentially impairs agonist-induced arterial contraction. *Arterioscler. Thromb. Vasc. Biol.* 2002; 22:1267-1272.

190. Couet, J, Li, S, Okamoto, T, Ikezu, T, and Lisanti, MP. Identification of peptide and protein ligands for the caveolin-scaffolding domain. Implications for the interaction of caveolin with caveolae-associated proteins. *J. Biol. Chem.* 1997; 272:6525-6533.
191. Carman, CV, Lisanti, MP, and Benovic, JL. Regulation of G protein-coupled receptor kinases by caveolin. *J. Biol. Chem.* 1999; 274:8858-8864.
192. Shaul, PW, Smart, EJ, Robinson, LJ, German, Z, Yuhanna, IS, Ying, Y, Anderson, RG, and Michel, T. Acylation targets endothelial nitric-oxide synthase to plasmalemmal caveolae. *J. Biol. Chem.* 1996; 271:6518-6522.
193. Razani, B, Engelman, JA, Wang, XB, Schubert, W, Zhang, XL, Marks, CB, Macaluso, F, Russell, RG, Li, M, Pestell, RG, Di, VD, Hou, H, Jr., Kneitz, B, Lagaud, G, Christ, GJ, Edelmann, W, and Lisanti, MP. Caveolin-1 null mice are viable but show evidence of hyperproliferative and vascular abnormalities. *J. Biol. Chem.* 2001; 276:38121-38138.
194. Park, DS, Cohen, AW, Frank, PG, Razani, B, Lee, H, Williams, TM, Chandra, M, Shirani, J, De Souza, AP, Tang, B, Jelicks, LA, Factor, SM, Weiss, LM, Tanowitz, HB, and Lisanti, MP. Caveolin-1 null (-/-) mice show dramatic reductions in life span. *Biochemistry* 2003; 42:15124-15131.
195. Le, LS and Kurzchalia, TV. Getting rid of caveolins: phenotypes of caveolin-deficient animals. *Biochim. Biophys. Acta* 2005; 1746:322-333.

196. Cohen, AW, Park, DS, Woodman, SE, Williams, TM, Chandra, M, Shirani, J, Pereira de, SA, Kitsis, RN, Russell, RG, Weiss, LM, Tang, B, Jelicks, LA, Factor, SM, Shtutin, V, Tanowitz, HB, and Lisanti, MP. Caveolin-1 null mice develop cardiac hypertrophy with hyperactivation of p42/44 MAP kinase in cardiac fibroblasts. *Am. J. Physiol Cell Physiol* 2003; 284:C457-C474.
197. Parolini, I, Sargiacomo, M, Galbiati, F, Rizzo, G, Grignani, F, Engelman, JA, Okamoto, T, Ikezu, T, Scherer, PE, Mora, R, Rodriguez-Boulan, E, Peschle, C, and Lisanti, MP. Expression of caveolin-1 is required for the transport of caveolin-2 to the plasma membrane. Retention of caveolin-2 at the level of the golgi complex. *J. Biol. Chem.* 1999; 274:25718-25725.
198. Razani, B, Wang, XB, Engelman, JA, Battista, M, Lagaud, G, Zhang, XL, Kneitz, B, Hou, H, Jr., Christ, GJ, Edelmann, W, and Lisanti, MP. Caveolin-2-deficient mice show evidence of severe pulmonary dysfunction without disruption of caveolae. *Mol. Cell Biol.* 2002; 22:2329-2344.
199. Galbiati, F, Engelman, JA, Volonte, D, Zhang, XL, Minetti, C, Li, M, Hou, H, Jr., Kneitz, B, Edelmann, W, and Lisanti, MP. Caveolin-3 null mice show a loss of caveolae, changes in the microdomain distribution of the dystrophin-glycoprotein complex, and t-tubule abnormalities. *J. Biol. Chem.* 2001; 276:21425-21433.
200. Woodman, SE, Park, DS, Cohen, AW, Cheung, MW, Chandra, M, Shirani, J, Tang, B, Jelicks, LA, Kitsis, RN, Christ, GJ, Factor, SM, Tanowitz, HB, and Lisanti, MP. Caveolin-3 knock-out mice develop a progressive cardiomyopathy and show

- hyperactivation of the p42/44 MAPK cascade. *J. Biol. Chem.* 2002; 277:38988-38997.
201. Park, DS, Woodman, SE, Schubert, W, Cohen, AW, Frank, PG, Chandra, M, Shirani, J, Razani, B, Tang, B, Jelicks, LA, Factor, SM, Weiss, LM, Tanowitz, HB, and Lisanti, MP. Caveolin-1/3 double-knockout mice are viable, but lack both muscle and non-muscle caveolae, and develop a severe cardiomyopathic phenotype. *Am. J. Pathol.* 2002; 160:2207-2217.
202. Zhao, YY, Liu, Y, Stan, RV, Fan, L, Gu, Y, Dalton, N, Chu, PH, Peterson, K, Ross, J, Jr., and Chien, KR. Defects in caveolin-1 cause dilated cardiomyopathy and pulmonary hypertension in knockout mice. *Proc. Natl. Acad. Sci. U. S. A* 2002; 99:11375-11380.
203. Kandasamy, AD and Schulz, R. Glycogen synthase kinase-3beta is activated by matrix metalloproteinase-2 mediated proteolysis in cardiomyoblasts. *Cardiovasc. Res.* 2009; 83:698-706.
204. Ali, MA, Cho, WJ, Granzier, H, and Schulz, R. Matrix metalloproteinase-2 co-localizes with titin in cardiac myocytes and contributes to its proteolysis in ischemia-reperfusion injury. *FASEB J.* 2009; 23:812.11.

CHAPTER 2

CAVEOLIN REGULATION OF MMP-2 IN THE HEART

A version of this chapter has been published in:

Chow AK, Cena J, El-Yazbi AF, Crawford BD, Holt A, Cho WJ, Daniel EE, Schulz R.

Caveolin-1 inhibits matrix metalloproteinase-2 activity in the heart. *J Mol Cell Cardiol*

2007; 42:896-901.

2.1: Introduction

The MMPs are zinc-dependent endopeptidases known for their roles in the degradation of extracellular matrix components. MMPs are synthesized in a zymogen form “proMMPs” which require the proteolytic removal of the pro-peptide domain in order to trigger their enzymatic activity¹. Alternatively, proMMPs, including MMP-2², can be directly activated by oxidative stress (ONOO⁻) by the oxidation of a cysteine residue coordinated to the catalytic Zn²⁺³.

MMPs have also been shown to play significant intracellular roles. MMP-2 has been localized to the thin and thick myofilaments of the cardiac sarcomere, as well as to the nucleus⁴. The intracellular proteins TnI and MLC-1 are proteolyzed by MMP-2 in I/R injury^{5,6}. The TIMPs control MMP activities⁷, but other mechanisms of regulation are not yet elucidated.

Caveolae are small cell membrane invaginations which play important roles in regulating signaling proteins and macromolecular transport⁸. Caveolins are integral membrane proteins found within lipid rafts. Cav-1 is crucial for the formation of caveolae⁹. The CSD binds to and regulates the function of a number of caveolin-associated proteins including eNOS¹⁰.

In endothelial cells, MMP-2 has been localized to the caveolae¹¹ where its function is unknown. Disruption of caveolae activates MMP-2 in fibrosarcoma cells¹² while Cav-1 overexpression in tumor cells causes decreased MMP-2 activity¹³ suggesting that Cav-1 may participate in the regulation of MMP-2. Whether MMP-2 activity in the heart is affected by caveolin is unknown. Here we present evidence that MMP-2

localizes with Cav-1 in the mouse heart, that CSD inhibits MMP-2 activity and, that hearts of mice deficient in Cav-1 have increased MMP-2 activity.

2.2: Materials and methods

2.2.1: Animals

All experiments were performed in accordance with the Canadian Council on Animal Care *Guide to the Care and Use of Experimental Animals*. Male Cav-1^{-/-} (cav^{<tm}1 M l s>/J) and control [(B6 129 SF2/J) (Cav-1^{+/+})] mice were obtained from Jackson Laboratories.

2.2.2: Tissue collection and preparation of heart extracts

Mice were injected with 1000 IU of heparin i.p. 10 min prior to terminal anesthesia. Hearts were rapidly excised and perfused via the aorta at constant pressure (60 mmHg) with Krebs-Henseleit buffer at 37°C for 10 min to clear them of blood. Whole hearts were then freeze-clamped with liquid nitrogen and stored at -80°C. Frozen hearts were pulverized under liquid nitrogen and homogenized on ice in 150 mM Na₂CO₃ with protease inhibitor cocktail (Sigma-Aldrich, Oakville, ON) using a Polytron homogenizer and then centrifuged (12 000 g, 30 s, 4°C). An aliquot of each supernatant (heart extract) was retained for biochemical analyses and the remainder of each sample was subjected to sucrose gradient centrifugation as previously described¹⁴ in order to isolate a lipid raft enriched fraction containing caveolae. Protein content of heart extracts and lipid raft fractions were determined using the bicinchoninic assay. For immunohistochemical analysis, hearts were isolated as above except they were perfused with phosphate buffered saline (pH 7.0) for 10 min prior to perfusion with 4%

paraformaldehyde in 0.1 M sodium phosphate buffer (pH 7.6) for 10 min. Hearts for immunohistochemistry were then rinsed with 0.1 M sodium phosphate buffer eight times every hour at room temperature followed by cryoprotection with 30% sucrose in 0.1 M sodium phosphate buffer overnight at 4°C.

2.2.3: Gelatin zymography

20 µg of protein from each heart extract or lipid raft enriched fraction was subjected to gelatin zymography to determine MMP-2 activity as described¹⁵. In brief, 10 µg of protein were mixed with sodium dodecyl sulfate (SDS) non-reducing sample buffer and applied to 10% polyacrylamide separating gels copolymerized with gelatin (2 mg/mL, Sigma-Aldrich, Oakville, ON). Conditioned media from HT-1080 fibrosarcoma cells was used as a standard for MMP-2 activity. The samples were subjected to electrophoresis and then the gels were washed three times with 2% Triton X-100 and incubated in incubation buffer (50 mM Tris-HCl buffer with 0.15 M NaCl, 5 mM CaCl₂, and 0.05% NaN₃, pH 7.5) overnight at 37°C. The gels were then stained with 0.05% Coomassie Brilliant Blue G-250 (Sigma-Aldrich, Oakville, ON) in a mixture of methanol, acetic acid, and water (2.5:1:6.5, v:v) and destained in 4% methanol with 8% acetic acid. Transparent bands against a Coomassie stained background was evidence of gelatinolytic activity. Band intensities were quantitated using ImageJ software (National Institutes of Health, USA).

2.2.4: Western blot analysis

MMP-2 and Cav-1 were detected by Western blotting using a polyclonal antibody (Chemicon, Billerica, MA) against rat MMP-2 and a monoclonal Cav-1 antibody (BD Transduction Laboratories, San Jose, CA) against Rous sarcoma virus-transformed

chick fibroblast Cav-1. Antibodies against α -tubulin (ab7291 against a.a. 426-450, ab7750 against a.a. 65-97 and ab52866 against a.a. 28-41; Abcam, Cambridge, MA), β -tubulin (Abcam, Cambridge, MA), TIMP-2 (Neomarkers, Fremont, CA) and TIMP-4 (Chemicon, Billerica, MA) were also used. Briefly, 10 μ g of each sample was loaded on 10% polyacrylamide SDS-PAGE gels. They were then wet transferred (100 V, 60 min) onto polyvinylidene difluoride membranes and non-specific proteins were blocked with 5% milk in Tris-Tween buffered saline (TTBS) buffer (0.01 M Tris, pH 7.6, 0.1% Tween, 0.1 M NaCl) at room temperature for 2 h. The membranes were then incubated with primary antibody overnight at 4°C. The membranes were rinsed with TTBS buffer prior to incubation with horseradish peroxidase linked secondary antibodies at room temperature for 1 h. ECL Plus (Amersham, Baie D'Urfe, QC) was used to visualize chemiluminescence.

2.2.5: Immunohistochemistry

Confocal immunohistochemistry was performed as previously described¹⁶ using a mouse monoclonal MMP-2 antibody against human MMP-2 (Chemicon, Billerica, MA) and mouse monoclonal antibody against the N terminal of Cav-1 (82-101 a.a.) (BD Transduction Laboratories, San Jose, CA) converted to a rabbit antibody by applying Fab fragment rabbit anti-mouse IgG (Jackson ImmunoResearch Laboratories, Inc., West Grove, PA) for 17 – 18 h¹⁶. Immunohistochemistry was performed on 5 μ m thick sections. In brief, hearts were rapidly excised and retrogradely perfused through the aorta with normal saline for 10 min to flush the coronary circulation of blood. The hearts were then perfused with 4% paraformaldehyde for 10 min. The hearts were fixed with 4% paraformaldehyde at room temperature for 4 h and then cryoprotected overnight with 30% sucrose at 4°C followed by embedding in Tissue-Tek OCT. The

hearts were then sectioned into 5 μm thick longitudinal and cross-sections. The sections were placed on glass slides coated with 1.5% 3-aminopropyltriethoxysilane in acetone and dried for 2 h at room temperature. The sections were then washed in 3% Triton X-100 in phosphate buffered saline (PBS) (pH 7.0) twice for 10 min each wash. Non-specific binding was prevented by blocking the sections with 10% normal serum of the host animal of the secondary antibody for 30 min at room temperature. Antibodies to Cav-1 (Abcam, Cambridge, MA), MMP-2 (Chemicon, Billerica, MA), α -tubulin (Abcam, Cambridge, MA) and β -tubulin (Abcam, Cambridge, MA) were applied to the sections either singularly or mixed together. The sections were allowed to incubate overnight at 4°C before rinsing with 3% Triton X-100 two times for 10 min each, followed by a 10 min wash in PBS. Secondary antibodies conjugated with Alexa 488 and CY3 were placed on the sections and allowed to incubate for 60 min followed by 2x10 min rinses with 3% Triton X-100 and a 10 min rinse with PBS. The sections were then mounted in an aqueous mounting medium containing 4',6-diamidino-2-phenylindole (DAPI). Images were captured using a confocal scanning laser microscope (LSM 510, Carl Zeiss Co., Germany) and processed using LSM Image 5 software (Carl Zeiss Co., Germany). To determine the specificity of immunolabeling, the primary or secondary antibody was omitted on alternate sections. Line profile analysis was performed using Image Pro Plus software (Media Cybernetics Inc., Bethesda, MD).

2.2.6: *In vitro* MMP-2 kinetic assay

The *in vitro* inhibition of MMP-2 activity by the CSD (Cav-1₈₂₋₁₀₁, Calbiochem, San Diego, CA) was assessed by examining the hydrolysis of OmniMMP fluorogenic substrate [(Mca-Pro-Leu-Gly-Leu-Dpa-Ala-Arg-NH₂; Mca = (7-methoxycoumarin-4-yl) acetyl; Dpa=N-3-(2,4-dinitrophenyl)-L- α , β -diaminopropionyl) (Biomol, Plymouth Meeting, PA)]

with 64 kDa human recombinant MMP-2 (Chemicon, Billerica, MA). 60 μ l of 0.4 nM MMP-2 in working buffer (100 mM Tris HCl, 20 mM CaCl₂, 0.1% Brij 35, 20 mM ZnSO₄, pH 7.4), 40 μ l of 75 μ M substrate in 1.2% DMSO and 20 μ l of 0-108 nM CSD in 25.6% DMSO were added to each well in a black polystyrene half-area plate (Corning, Lowell, MA). The fluorescence associated with the breakdown of OmniMMP substrate was measured at 30 s intervals for 1 h using a Molecular Devices SPECTRAmax Gemini XPS fluorescence microplate reader (λ_{ex} 328 nm, λ_{em} 393 nm). Lag times to eliminate data prior to temperature equilibration, and end times to preclude data after the loss of linearity were entered manually. Linear regression analysis by the microplate reader software (SOFTmax Pro, v 4.8; Molecular Devices Inc., Sunnyvale, CA) was used to determine the rate of product formation. A substrate extinction coefficient of 7627 M⁻¹cm⁻¹ and a path length of 0.672 cm were used to correct for loss of signal due to substrate absorption at $\lambda=393$ nm. The rate of product formation was expressed as a ratio of the same reaction without CSD (% of control). A CSD control peptide (CSD-X, Calbiochem, San Diego, CA) which contains four rearranged amino acids from CSD (D82W, W85D, Y100R, R101Y) in 25.6% DMSO was substituted for CSD in control experiments.

2.2.7: In vitro degradation of tubulin

Human recombinant α -tubulin was purchased from Calbiochem (San Diego, CA) and incubated with human recombinant MMP-2 (Chemicon, Billerica, MA) in a 1:50 ratio in 50 mM Tris-HCl buffer (5 mM CaCl₂, 150 mM NaCl, 0.5% NaN₃) for 1 h at 37°C. A 500:1 ratio of human recombinant TnI and 64 kDa human recombinant MMP-2 in the same Tris buffer was incubated at 37°C for 40 min and used as a control to assay the activity of the MMP-2. The same amount of α -tubulin and TnI were incubated

separately without MMP-2 under the same conditions to control for degradation resulting from heating and/or contaminating proteases.

Immediately after the allotted incubation time, the samples were loaded into a 10% polyacrylamide gel, along with a visible molecular weight marker set (BioRad, Mississauga, ON) and subjected to SDS-PAGE. The gels were then stained with 0.05% Coomassie Brilliant Blue G-250 (Sigma-Aldrich, Oakville, ON) in a mixture of methanol, acetic acid, and water (2.5:1:6.5, v:v) for 2 h and destained in 4% methanol with 8% acetic acid for at least 1 h.

2.2.8: Collagen content of Cav-1^{+/+} and Cav-1^{-/-} mouse hearts

Three male Cav-1^{-/-} and three male Cav-1^{+/+} mouse hearts that were flushed and frozen, weighed, crushed and homogenized as described in 2.2.2 were used in this assay. The collagen content of the hearts was determined using the Sircol collagen assay kit (Biocolor Life Science Assays, Carrickfergus, United Kingdom). Both the salt soluble and the acid soluble assays were performed according to the directions supplied with the kit.

In brief, following homogenization in the aforementioned homogenization buffer the salt soluble collagen was extracted with 10 volumes of homogenization buffer to wet tissue weight overnight at 4°C. The samples were then centrifuged at 15 000 g for 60 min and the supernatant was saved for analysis for the salt soluble collagen. Pepsin and acetic acid were added to make a final concentration of 5 mg/mL pepsin and 0.5 M acetic acid to extract the acid soluble collagen from the samples. This was then incubated overnight with shaking at 4°C. The samples were then centrifuged at 15 000 g for 60 min at 4°C. 100 µL of the supernatant or the previously extracted salt soluble

collagen was then mixed with 1 mL of the supplied Sircol reagent and mixed at room temperature for 30 min followed by centrifugation at 15 000 g for 30 min. The resulting supernatant was drained and 1 mL of the supplied alkali reagent was added to the pellet and mixed for 10 min at room temperature. The colored solution was then read by a spectrophotometer at 540 nm. A calibration curve using the supplied collagen standard solution was used to calculate the final concentration of collagen in each sample.

2.2.9: In silico analyses

The human sequence of 72 kDa MMP-2 was obtained from UniProt and manually examined to locate the CBD. The 3D structure of MMP-2 was obtained from Protein Data Bank (<http://www.pdb.org>), generated using 3D-Mol of Vector NTI (Invitrogen) and rendered using Polyview 3D (<http://polyview.cchmc.org>) with manual insertion of the discovered CBD.

2.2.10: Statistical analysis

Results are expressed as mean \pm SEM. Statistical analysis was performed using GraphPad Prism. The Student's t-test was used to determine whether the groups were significantly different with $p \leq 0.05$ deemed statistically significant.

2.3: Results

2.3.1: Caveolin binding domains in MMP-2

Examination of the amino acid sequence of human MMP-2 revealed seven possible binding motifs for CSD ($\Phi X \Phi X X X X \Phi$ and $\Phi X X X X \Phi X X \Phi$ ¹⁷, where Φ is one of the aromatic amino acids tryptophan, phenylalanine, or tyrosine) (Fig. 2.1).

2.3.2: Confocal of MMP-2 and Cav-1

Using confocal microscopy, we first determined the co-localization of MMP-2 with Cav-1 in left ventricular sections from Cav-1^{+/+} and Cav-1^{-/-} hearts. In Cav-1^{+/+} sections, immunohistochemical analysis shows that Cav-1 is found on the plasma membrane of cardiomyocytes (Fig. 2.2-ii). MMP-2 is found both on the plasma membrane and also appears as intracellular striations as seen in longitudinal sections (Fig. 2.2-i and 2.2-v). The merged images show evidence of the co-localization of MMP-2 and Cav-1 on the plasma membrane (Fig. 2.2-iii and 2.2-vii) as evidenced by line profile analysis (Fig. 2.2-iv and 2.2-viii). In the absence of Cav-1, the membrane localization of MMP-2 is lost or severely reduced as seen in both cross (Fig. 2.2-ix) and longitudinal (Fig. 2.2-xiii) sections and verified by line analysis (Fig 2.2-xii and 2.2-xvi, respectively). Non-specific fluorescence was not observed in sections incubated with either primary or secondary antibody alone (data not shown).

2.3.3: In vitro MMP-2 kinetic assay

CSD concentration-dependently inhibited MMP-2 activity with a K_i of 668 nM (95% confidence interval 630-723 nM) (Fig. 2.3). DMSO vehicle controls had no significant effect on MMP-2 activity (data not shown). In contrast, CSD-X containing four substituted amino acids (D82W, W85D, Y100R, R101Y) has a K_i of 1217 nM (95% confidence interval 1027-1443 nM). This was significantly different in comparison to native CSD and there was no overlap between the 95% confidence intervals.

2.3.4: MMP-2 activity and protein in heart extracts

Heart extracts from Cav-1^{-/-} mice exhibited a 234% increase in MMP-2 activity with respect to controls ($p < 0.05$) (Fig. 2.4A). MMP-2 protein abundance, however, was

not significantly different between the groups (Fig. 2.4B). TIMP-2 (Fig 2.4C) and TIMP-4 (Fig. 2.4D) levels were not significantly different between Cav-1^{-/-} and Cav-1^{+/+} hearts.

2.3.5: MMP-2 activity and protein in lipid rafts of hearts

Examination of lipid raft enriched fractions from Cav-1^{-/-} and Cav-1^{+/+} mouse hearts revealed the presence of Cav-1 α and β in fractions from the latter but not the former (Fig. 2.5A). MMP-2 activity in Cav-1^{-/-} fractions showed a marked reduction to 4.6% of the activity seen in Cav-1^{+/+} fractions (p<0.05) (Fig. 5B). There was concomitantly greater MMP-2 protein levels in the lipid raft enriched fractions from Cav-1^{+/+} when compared with Cav-1^{-/-} hearts (p<0.05) (Fig. 5C).

2.3.6: Tubulin in Cav-1^{+/+} and Cav-1^{-/-} mouse hearts

It was previously shown that MMP-2 can degrade Tnl⁵ so consequently, Tnl was used in this assay to ensure that MMP-2 was enzymatically active. Incubation at a 1:50 ratio of human recombinant MMP-2 and human recombinant α -tubulin resulted in the appearance of additional possible degradation products of a lower molecular weight (~25 and 35 kDa) that were not observed with the α -tubulin alone. The experiment was repeated three times with typical results shown in Fig. 2.6A.

Western blotting reveals that there is significantly less α -tubulin detected with ab7750 in Cav-1^{-/-} heart extracts (p=0.0017), as well as with ab52866 (p=0.0311) (Fig. 2.6B and 2.6C), while no difference was observed when ab7291 was used (p=0.9911) (Fig. 2.6D). Less β -tubulin is also observed in Cav-1^{-/-} mouse heart extracts compared with controls (p=0.0497) (Fig. 2.6E).

Confocal micrographs of mouse heart sections stained using α - (ab7291 or ab7750) or β - tubulin antibodies reveal no discernible differences between Cav-1^{+/+} and Cav-1^{-/-} mouse hearts (Fig. 2.7A and 2.7B).

2.3.7: Collagen content of Cav-1^{+/+} and Cav-1^{-/-} mouse heart extracts

Using the Sircol collagen assay, no discernable difference in either acid soluble ($p=0.8238$) (Fig 2.8A) or salt soluble ($p=0.7413$) (Fig. 2.8B) collagen content was found between Cav-1^{+/+} and Cav-1^{-/-} mouse hearts. Consequently, total collagen content ($p=0.7410$) (Fig. 2.8C) was found not to be different between the hearts.

2.4: Discussion

In silico analysis showed that of the seven possible binding locations of CSD on the MMP-2 protein, four of the CSD binding motifs are in the collagen binding domain of MMP-2, while three are found in the hemopexin domain. Binding of CSD to the collagen binding domain may inhibit MMP-2 activity by preventing substrate binding while interaction of CSD with the latter may cause inhibition by preventing the binding of other proteins that would otherwise serve to enhance MMP-2 activity (e.g. heparin¹⁸ or TIMP-2¹⁹). All seven of the CSD binding motifs are on exposed outer surfaces of MMP-2 (Fig. 2.9) and are conserved between the mouse, rat, human and zebrafish MMP-2 sequences (Fig. 2.10), suggesting functional significance.

Our confocal micrographs reveal an interesting localization of MMP-2 in the two strains of mice. While the localization of MMP-2 in the Cav-1^{+/+} hearts to the plasma membrane and as intracellular striations is consistent with its reported

sarcomeric association in the heart^{5,6}, it is interesting to observe its more diffuse localization in the Cav-1^{-/-} hearts, particularly in light of the fact that total MMP-2 is not different between the two strains, as evidenced by the Western blots. This suggests that Cav-1 may play a role in maintaining MMP-2 subcellular localization, not only at the plasma membrane, but also at the sarcomeric level, though the mechanism by which this may occur is not clear.

We next determined the consequences of Cav-1 knockout in the hearts from Cav-1^{-/-} mice on myocardial MMP-2 activity. We discovered that Cav-1^{-/-} mouse hearts had significantly increased MMP-2 activity when compared to controls. As these knockout mice age, they demonstrate cardiovascular abnormalities where MMP-2 perturbation has been implicated, including dilated cardiomyopathy²⁰ and altered vascular reactivity²¹. As a result of the discovery that there is increased MMP-2 activity in these hearts without an increase in protein, we suspected that an endogenous inhibitor may be altering MMP-2 activity. Because TIMP-4 is an abundant TIMP in the heart²² and TIMP-2 is implicated in MMP-2 activation²³, we examined the abundance of these endogenous MMP inhibitors. TIMP-2 and TIMP-4 levels were not significantly different between Cav-1^{-/-} and Cav-1^{+/+} hearts suggesting that other mechanisms regulate MMP-2 activity.

Thus MMP-2 activity was increased in heart extracts from Cav-1^{-/-}, while in a lipid raft enriched fraction from the hearts, minimal MMP-2 activity was detected. This is consistent with our hypothesis that Cav-1 is responsible for maintaining MMP-2 in a membrane associated and inhibited configuration. Without Cav-1 anchoring MMP-2 to the membrane, the enzyme appears to be more diffusely distributed in the cytoplasm,

though the amount of MMP-2 protein remains unchanged. Cav-1^{-/-} hearts would thus have free and potentially active MMP-2 in areas of the myocardium whereby proteolytic damage of susceptible targets could impair contractile function.

To investigate the putative interaction of CSD with MMP-2, we measured the kinetics of MMP-2 proteolysis of an artificial substrate, OmniMMP. In its intact form, the fluorophore of OmniMMP is internally quenched whereas cleavage of the substrate by MMP-2 releases a fluorescent peptide (Mca-Pro-Leu-Gly). Though the rearrangement of four amino acids in CSD-X is sufficient to prevent CSD inhibitory activity on a number of different proteins²⁴⁻²⁶, this does not necessarily alter the ability of the CSD to bind to its targets electrostatically²⁷. CSD-X shows a significantly reduced ability to inhibit MMP-2 activity compared with CSD. Therefore the inhibition by CSD is likely a mixture of electrostatic and specific binding between CSD and the caveolin binding motifs of MMP-2.

As MMPs are best known to degrade components of the extracellular matrix, we could not overlook the fact that the altered MMP-2 activity in the Cav-1^{-/-} mouse hearts may have significant effects on the extracellular components. During handling of the hearts for tissue processing, we noted that the Cav-1^{-/-} hearts were considerably more brittle than their corresponding Cav-1^{+/+} controls (unpublished observation). Consequently, we hypothesized that the extracellular collagen components of the Cav-1^{-/-} hearts may be degraded by the elevated MMP-2 activity. However, our collagen assay results do not support this hypothesis. This is particularly surprising in light of a recent study which showed that caveolin-1 expression in COS-7 cells results in decreased MMP-2 activation and inhibited collagen degradation and cell migration²⁸. However, the

young age of the mice that we used may play a factor. Indeed, in the lungs of these Cav-1^{-/-} mice, there was increased collagen deposition in the lungs as determined by picrosirius red staining at 6 months of age, but this was not evident at 1 or 3 months of age²⁹, suggesting that the extracellular matrix changes may not be evident until the mice are older.

Interestingly, Cav-1^{-/-} mouse heart extracts have significantly less tubulin compared with Cav-1^{+/+} mice when examined by Western blot, yet these changes are not evident by immunohistochemistry. The Insel group has suggested that tubulin anchoring and the formation of the intracellular tubulin network may be responsible for the formation of the caveolar microdomain³⁰. Our results, however suggest that the reverse may also be true; that caveolae, and/or the presence of caveolin, may affect tubulin. In particular, the C-terminal domain of α -tubulin appears to be altered in some way in Cav-1^{-/-} hearts that would reduce the ability of the antibodies to recognize and/or bind to this region. Degradation or truncation of this region by MMP-2 is certainly possible, particularly since MMP-2 is indeed capable of degrading α -tubulin (Fig. 2.6A), though the MMP-2 cleavage site(s) on α -tubulin were not determined. Others have also found that the presence of Cav-1 is able to affect tubulin. Overexpression of Cav-1 in vascular smooth muscle cells actually increases tubulin polymerization while downregulation of Cav-1 does the opposite, though the authors noted that the total amount of tubulin in the cells did not change³¹. Surprisingly, immunohistochemical results using ab7750, the α -tubulin antibody that showed the greatest difference between Cav-1^{+/+} and Cav-1^{-/-} samples in Western blots, did not reveal any differences. One possible explanation for this result may be that the antibody binds differently to a reduced and denatured protein than it does to one that is fixed in its native

conformation, though the fact that the Western blot results reveal a difference between Cav-1^{+/+} and Cav-1^{-/-} hearts suggests that the difference is more than a technique limitation.

This experiments in this chapter show, for the first time, that Cav-1 is not only capable of inhibiting MMP-2 activity, but that Cav-1^{-/-} mouse hearts have increased MMP-2 activity, without a concomitant increase in protein levels. Because of the important role MMP-2 plays in heart disease, further investigation of this novel MMP-2/Cav-1 interactions and other components that may associate with it, may reveal new pharmacological targets which may ultimately reduce the impact cardiovascular diseases.

Figure 2.1: Caveolin binding domains in MMP-2

Sequence of human MMP-2 reveals the presence of seven caveolin binding motifs (bold and underlined). These sequences are conserved in the mouse, rat and zebrafish MMP-2. Colors of amino acids correspond with the same domain name in color. Experiments done by A.K. Chow.

Figure 2.2: Cav-1 localizes with MMP-2 in cardiac myocytes in left ventricular sections

MMP-2 (red) is found to be localized to the membrane of cardiac myocytes both in cross (i) and longitudinal (v) sections in Cav-1^{+/+} hearts. Cav-1 (green) is similarly localized to the membrane of cardiac myocytes in both cross (ii) and longitudinal (vi) sections. Merged images show co-localization of Cav-1 and MMP-2 in yellow (iii and vii). Magnified images of the insets of iii and vii are found in iv and viii, respectively. Line profile analyses of the line indicated in the magnified inset shows co-localization of Cav-1 and MMP-2 to the membrane in both cross (iv) and longitudinal (viii) sections. In contrast, staining for MMP-2 in Cav-1^{-/-} cross (ix) and longitudinal (xiii) sections appears to be more diffuse than in Cav-1^{+/+} hearts, with no apparent localization in the membrane. Cav-1^{-/-} hearts did not stain with Cav-1 antibody (x and xiv) and merged images (xi and xv) do not reveal areas of co-localization. Magnified images of the insets in xi and xv are shown in xii and xvi, respectively. Line profile analyses of the areas indicated by the line indicated in the magnified inset do not reveal membrane co-localization of MMP-2 and Cav-1 as seen in Cav-1^{+/+} hearts. Nuclei are stained in blue in all sections. The scale bar represents 5 μ m in panels i-iii, v-vii, ix-xi and 10 μ m in panels xii, xiv and xv. Three hearts were examined per group with similar results. Experiments done by A. K. Chow and W. J. Cho.

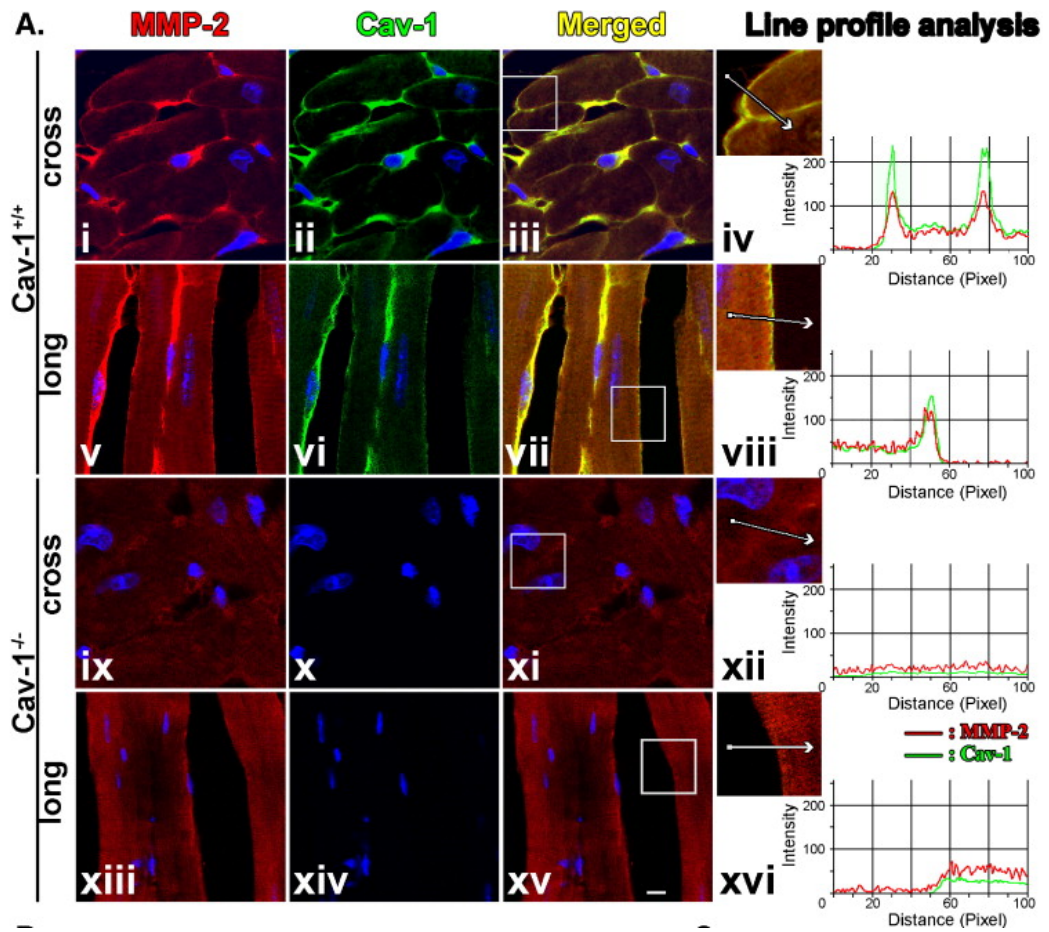


Figure 2.3: CSD inhibition of MMP-2 in a kinetic assay

Proteolysis of an internally quenched fluorescent substrate (OmniMMP) by MMP-2 is inhibited in a concentration-dependent manner by the CSD of Cav-1. The velocity of the reaction in the absence of CSD (control) was 2.34 ± 0.08 mOD/min. CSD-X inhibited MMP-2 degradation in a concentration dependent manner, though at a significantly lesser extent than CSD (N=4). Error bars indicate \pm SEM where they exceed the symbol size. Experiments done by A. K. Chow.

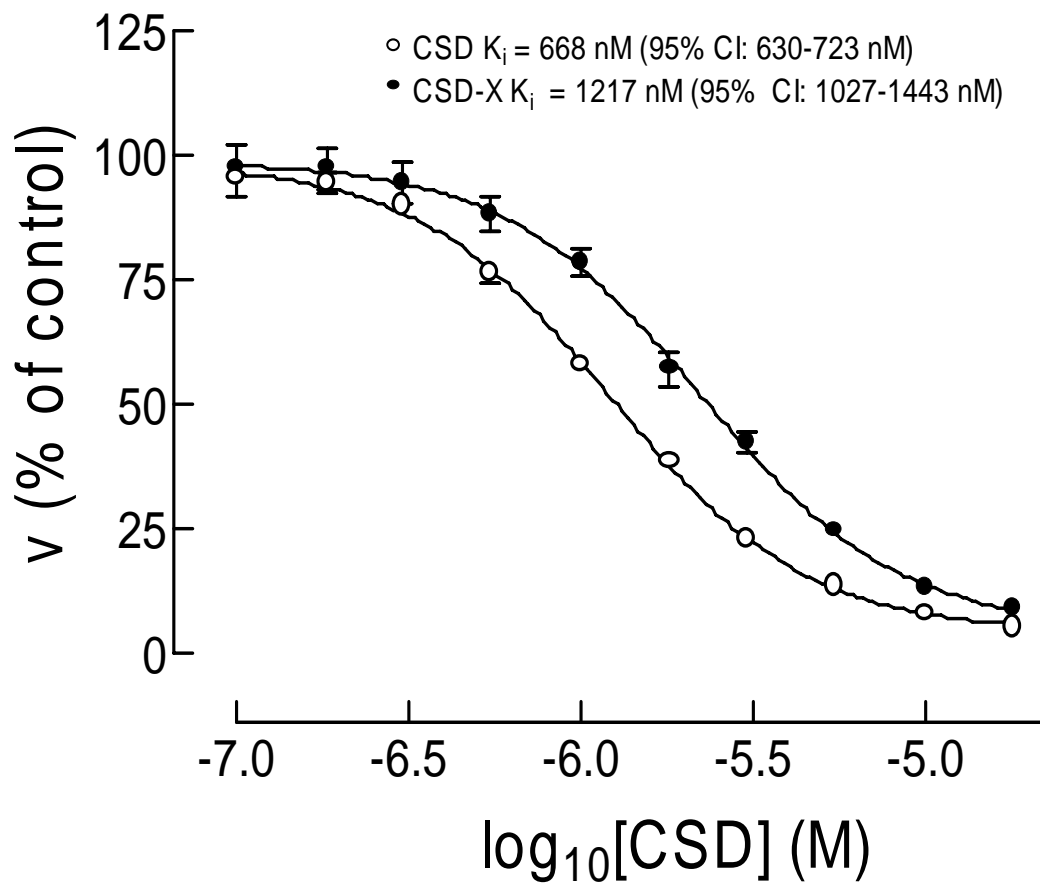


Figure 2.4: MMP-2 proteolytic activity and protein, and TIMP-2 and -4 protein in Cav-1^{+/+} and Cav-1^{-/-} hearts

(A) Whole heart extracts prepared from Cav-1^{+/+} (N=3) and Cav-1^{-/-} (N=5) mice were subjected to gelatin zymography to determine MMP-2 activity. Cav-1^{-/-} hearts exhibit significantly more MMP-2 gelatinolytic activity than Cav-1^{+/+} hearts (p<0.05). (B) The protein levels of MMP-2 in these hearts are not significantly different (p>0.05). The protein levels of TIMP-2 (C) and TIMP-4 (D) were not significantly different between Cav-1^{+/+} and Cav-1^{-/-} mouse hearts. Experiments done by A. K. Chow.

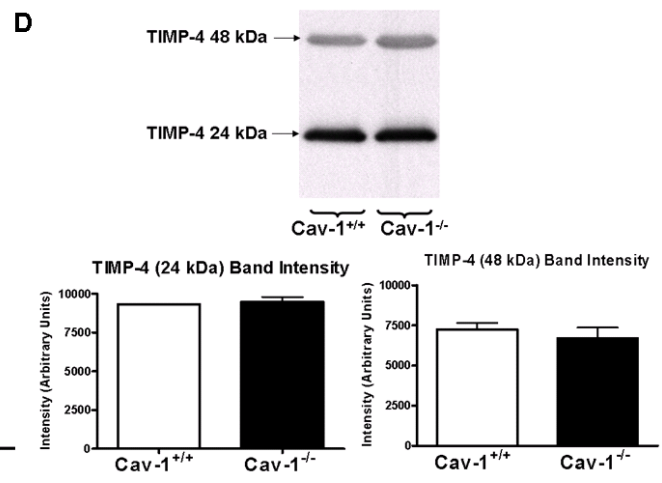
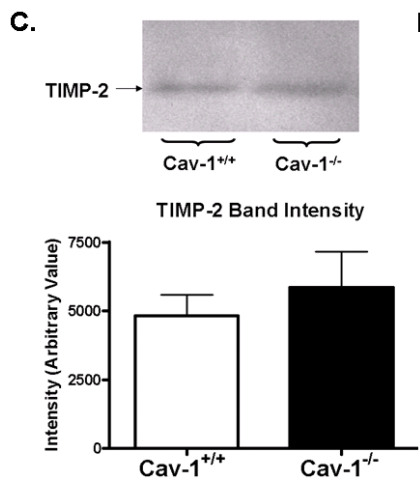
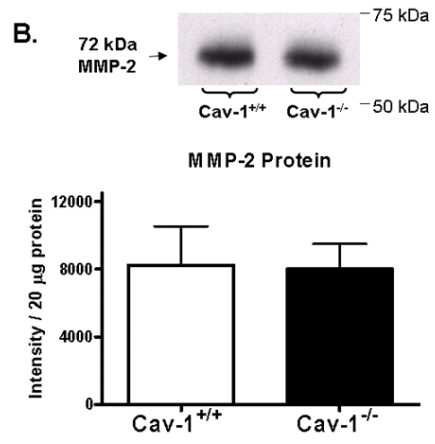
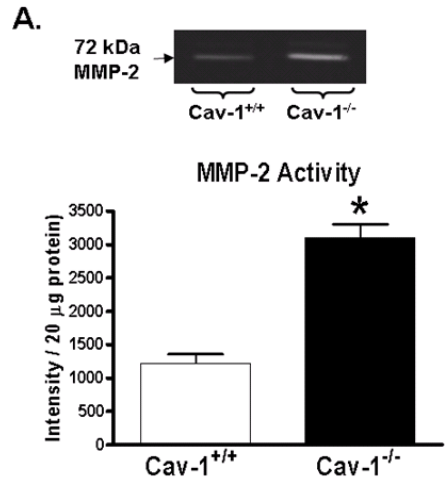


Figure 2.5: Characteristics of lipid raft enriched fractions from Cav-1^{+/+} and Cav-1^{-/-} hearts

(A) Lipid raft enriched fractions from Cav-1^{-/-} mouse hearts lacked both isoforms of Cav-1, but contained levels of Cav-3 comparable to those found in Cav-1^{+/+} lipid raft enriched fractions. Cav-1^{+/+} lipid raft enriched fractions contained significantly more MMP-2 gelatinolytic activity (B) and MMP-2 protein (C) than that from Cav-1^{-/-} hearts. N=3 per group. Experiments done by A. K. Chow, J. Cena and A. F. El-Yazbi.

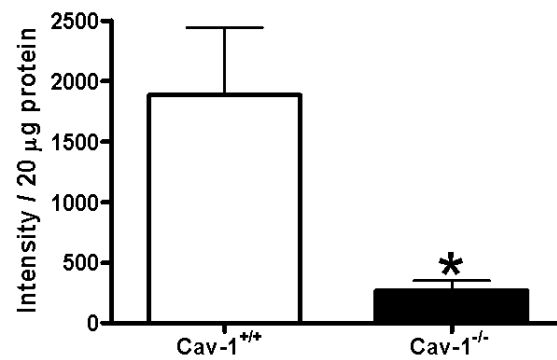
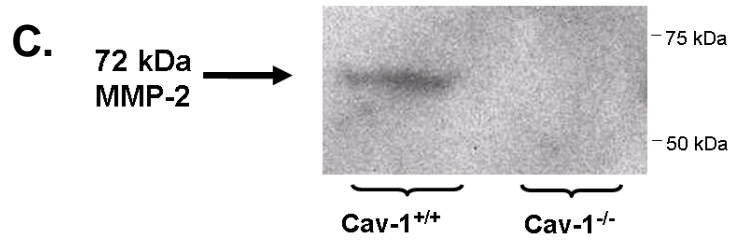
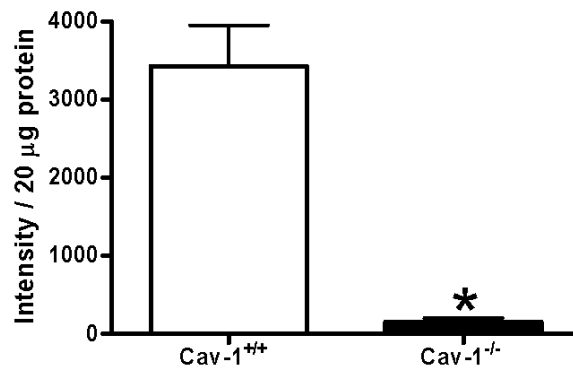
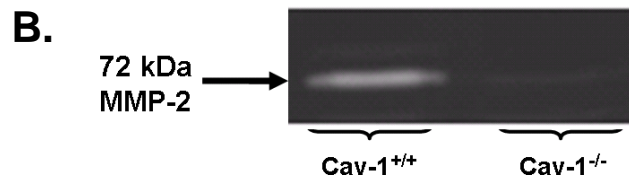
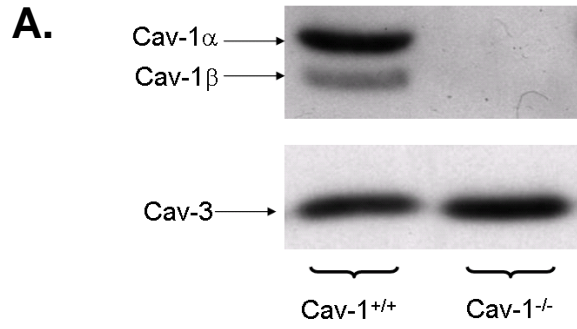


Figure 2.6: α -tubulin degradation and content in Cav-1^{-/-} mouse hearts

(A) Human recombinant MMP-2 degrades human recombinant α -tubulin when incubated at 37°C for one hour in a 1:50 ratio prior to being run on SDS PAGE and Coomassie stained. Possible degradation products are indicated by arrows. Two antibodies to α -tubulin show differences in tubulin content between Cav-1^{+/+} (N=3) and Cav-1^{-/-} (N=3) mouse hearts [(B) ab7750, p=0.0017; (C) ab52866, p=0.0311)] while one does not [(D) ab7291, p=0.9911]. Less β -tubulin was also observed in Cav-1^{-/-} hearts (E). Experiments done by A. K. Chow.

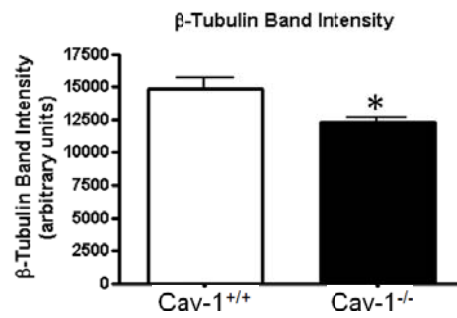
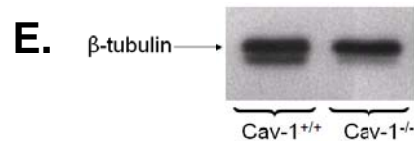
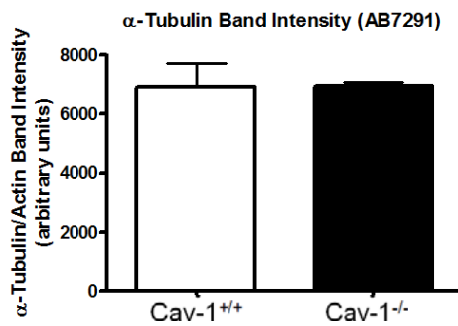
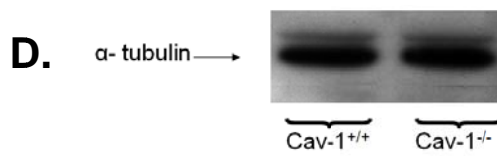
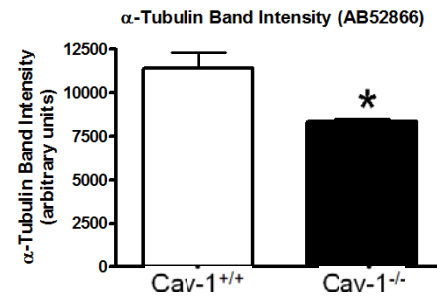
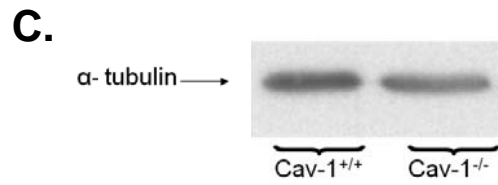
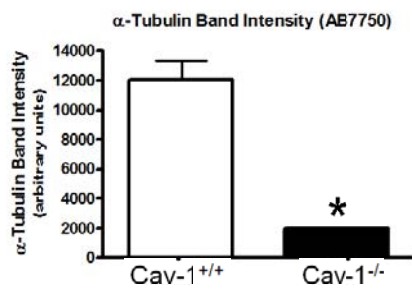
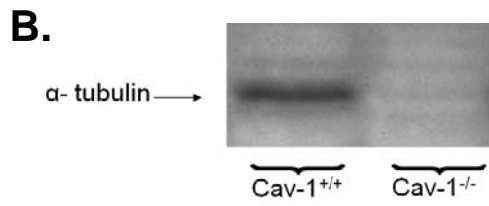
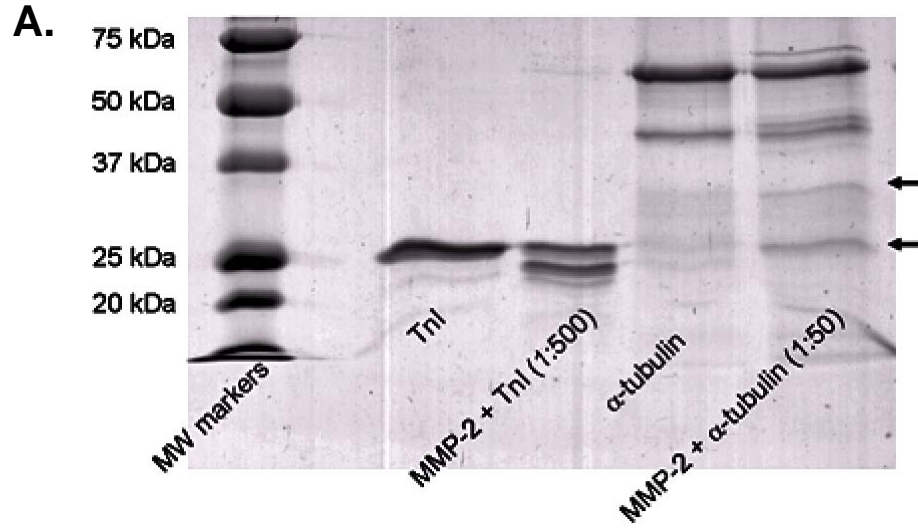
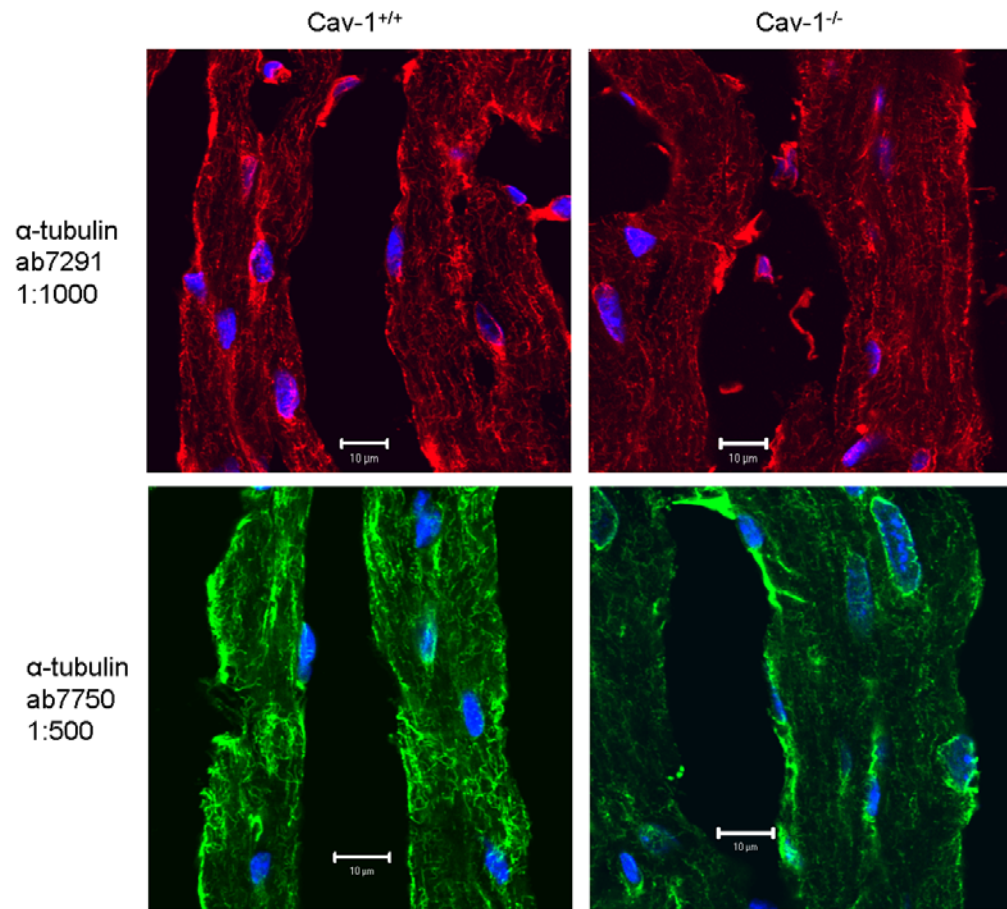


Figure 2.7: Immunohistochemical staining for tubulin in Cav-1^{+/+} and Cav-1^{-/-} mouse ventricle

(A) Cav-1^{+/+} and Cav-1^{-/-} mouse heart ventricular sections stained with α -tubulin antibodies (ab7291 and ab7750). No differences between Cav-1^{+/+} and Cav-1^{-/-} ventricular sections were observed when stained with ab7291 (red), raised against a.a. 426-450 at the C-terminal end of α -tubulin. Likewise, no differences were observed when stained with ab7750, which is raised against a.a 65-97 on the N terminal of α -tubulin. Similarly, no differences were observed when Cav-1^{+/+} and Cav-1^{-/-} ventricles were stained for β -tubulin (B). Nuclei are stained with DAPI and appear blue in the micrographs. Scale bar represents 10 μ m. N=3 per group with typical results shown. Experiments done by W.J Cho.

A.



B.

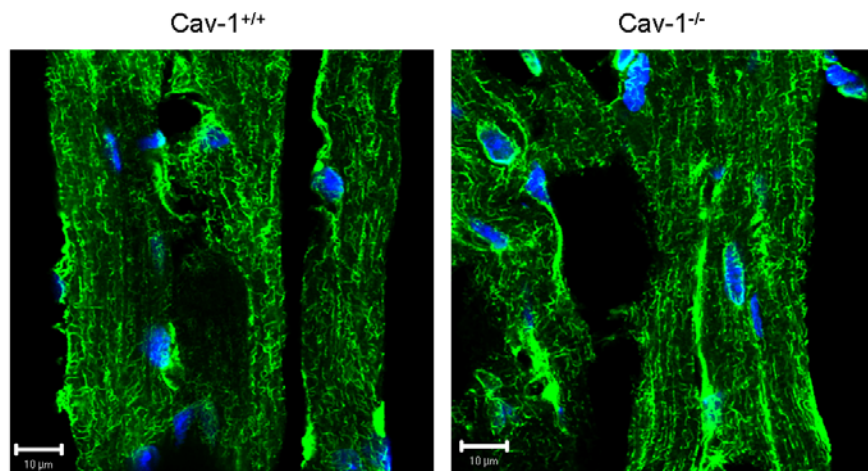
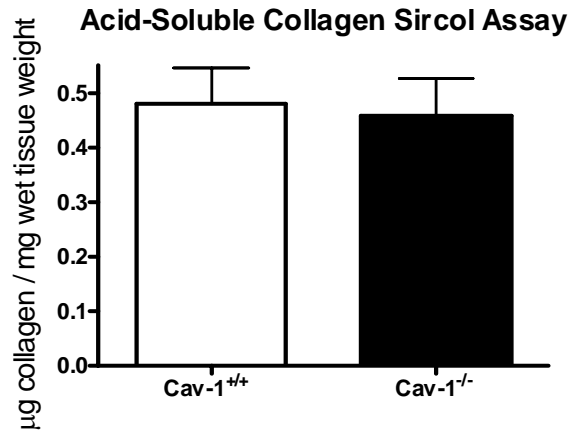


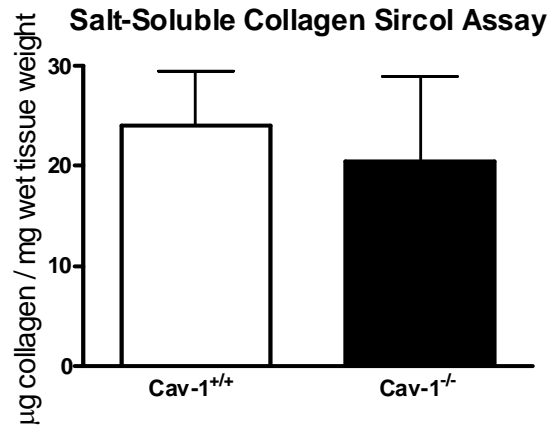
Figure 2.8: Collagen content Cav-1^{+/+} and Cav-1^{-/-} mouse heart as determined by Sircol assay.

The acid soluble collagen content (A) and the salt soluble collagen content (B) were not different between Cav-1^{+/+} (N=3) and Cav-1^{-/-} (N=3) mouse hearts (p=0.8238 and p=0.7413, respectively). Consequently, the total collagen content (C) was not different between these hearts (p=0.7410), as determined by the colorimetric Sircol assay. Experiments done by A. K. Chow.

A.



B.



C.

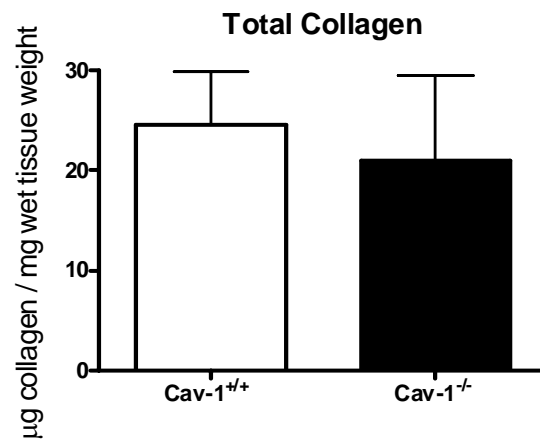
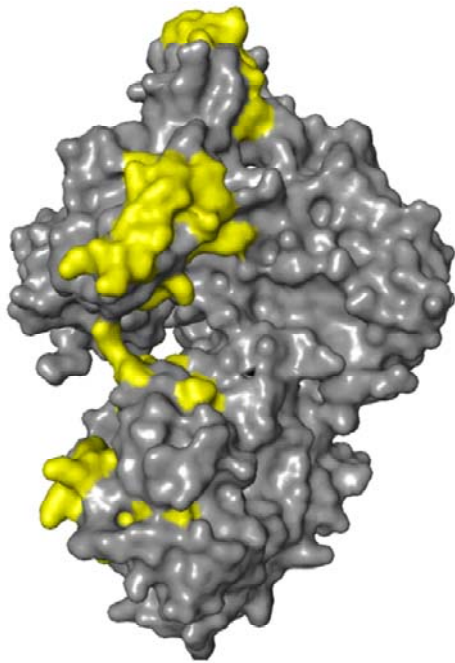
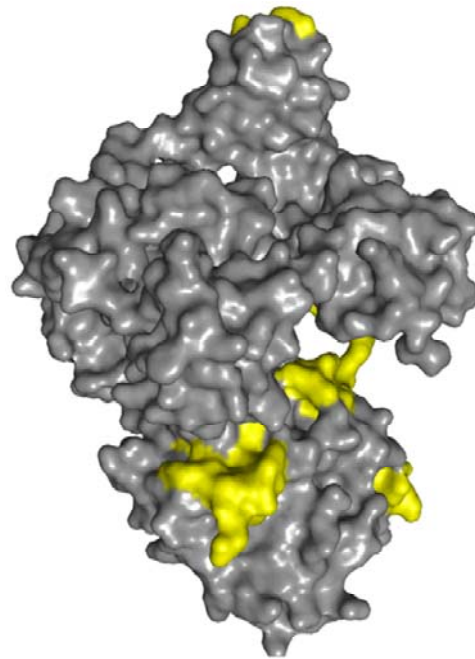


Figure 2.9: CSD binding motifs on MMP-2

The CSD binding motifs (yellow) are illustrated on surface renderings and ribbon structures of MMP-2. Experiments done by A. K. Chow.



Front



Back

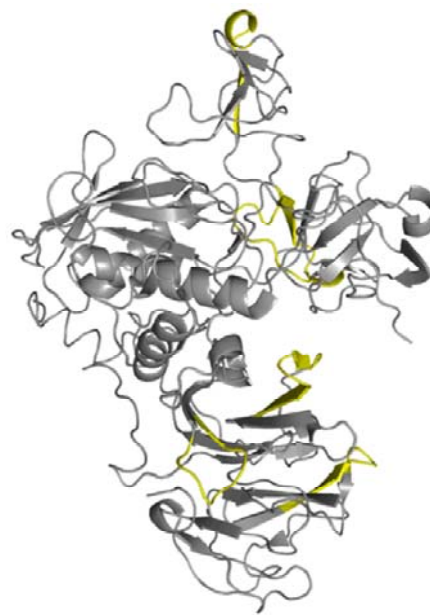


Figure 2.10: Sequence alignment of rat, mouse, human, pig, turkey medaka and zebrafish MMP-2 proteins

The sequence alignment of MMP-2 proteins between different species shows that the CBD (shown highlighted in yellow) is highly conserved between species. Amino acids in red are poorly conserved between species while those in blue are highly conserved. Black amino acids are moderately conserved. Experiments done by B. D. Crawford.

Rat	m-ea---rlvw	gvlvgplrvl	cvlccllgha	iaapspiikf	pgdvspkttdk	elavqylntf	ygcpkescnl	fvldkdlkkm	
Mouse	m-ea---rvaw	galagplrvl	cvlccllgra	iaapspiikf	pgdvapkttdk	elavqylntf	ygcpkescnl	fvldkdlkkm	
Human	m-ea---lmar	galatgplral	cllglcllsha	aaapspiikf	pgdvapkttdk	elavqylntf	ygcpkescnl	fvldkdlkkm	
Pig	mtea---rgar	galagplral	cvlglcllgra	aaapspiikf	pgdvapkttdk	elavqylntf	ygcpkescnl	fvldkdlkkm	
Turkey	m-kt---hsvf	gfv---fklv	llqvyllfntk	laapspiikf	pgdstpkttdk	elavqylnty	ygcpkdcncl	fvldkdlkkm	
Medaka	mtptlvrscr	gfv---lkvf	vllflvflqls	narpspirf	pgdstpkttdk	evaldylnkf	ygcpqdcncl	mvldkdlkkm	
Zebrafish	mlsvkffrcr	hiv---lkvf	lvqlflaslqt	faapspiikf	pgddtahtdk	evalhylnkf	ygcpkdcncl	mvldkdlkkm	
Conservation									
Rat	qkffglpatg	dldqntietm	rkprcgnpdv	anydffprkp	kwdknqityr	liigytpdlip	etvddafara	lkwsvdvtpl	
Mouse	qkffglpatg	dldqntietm	rkprcgnpdv	anydffprkp	kwdknqityr	liigytpdlip	etvddafara	lkwsvdvtpl	
Human	qkffglpatg	dldqntietm	rkprcgnpdv	anydffprkp	kwdknqityr	liigytpdlip	etvddafara	lkwsvdvtpl	
Pig	qkffglpatg	dldqntietm	rkprcgnpdv	anydffprkp	kwdkntityr	liigytpdlip	etvddafara	lkwsvdvtpl	
Turkey	qkffglpetg	dldqntietm	kkprcgnpdv	anydffprkp	kweknhityr	liigytpdlip	etvddafara	fkwsvdvtpl	
Medaka	qkfftlpetg	eidaqvaam	kkprcgvpdv	anydffhnkp	kwgkddityr	liigytpdlip	etvddafara	fkwsvdvtpl	
Zebrafish	qkffalpetg	eidaqveim	kkprcgvpdv	anydffhrkp	kwgkntityr	liigytpdlip	etvddafara	fkwsvdvtpl	
Conservation									
Rat	rfsrihdgea	diminfrwe	hgdgyppfdgk	dglahafap	gtvggdsdhf	dddelwtlge	gqvrvkygn	adgcyckfpf	
Mouse	rfsrihdgea	diminfrwe	hgdgyppfdgk	dglahafap	gtvggdsdhf	dddelwtlge	gqvrvkygn	adgcyckfpf	
Human	rfsrihdgea	diminfrwe	hgdgyppfdgk	dglahafap	gtvggdsdhf	dddelwtlge	gqvrvkygn	adgcyckfpf	
Pig	rfsrihdgea	diminfrwe	hgdgyppfdgk	dglahafap	gtvggdsdhf	dddelwtlge	gqvrvkygn	adgcyckfpf	
Turkey	rfrnindgea	diminfrwe	hgdgyppfdgk	dglahafap	gpgiggdsdhf	dddelwtlge	gqvrvkygn	adgcyckfpf	
Medaka	qftrimdgea	diminfrne	hgdgyppfdgk	dglahafap	gpgiggdsdhf	dddeqwtlge	gqvrvkygn	adgcyckfpf	
Zebrafish	kftrimdgea	diminfrne	hgdgyppfdgk	dglahafap	gpgiggdsdhf	dddeqwtlge	gqvrvkygn	aegefckfpf	
Conservation									
Rat	lfnGREYSSC	tdtgrsdg	WCSSTTYNfEK	dgykfcphe	alftmgngd	gpcckfprff	qqtsynscctt	egrtddyrcw	
Mouse	lfnGREYSSC	tdtgrsdg	WCSSTTYNfEK	dgykfcphe	alftmgngd	gpcckfprff	qqtsynscctt	egrtddyrcw	
Human	lfnGREYSSC	tdtgrsdg	WCSSTTYNfEK	dgykfcphe	alftmgngd	gpcckfprff	qqtsynscctt	egrtddyrcw	
Pig	wfnGKEYNSC	tdtgrsdg	WCSSTTYNfEK	dgykfcphe	alftmgngd	gpcckfprff	qqtsynscctt	egrtddyrcw	
Turkey	sfnGKEYNSC	tdagrndg	WCSSTTYNfEK	dgykfcph-	slftmgngd	gpcckfprff	qqtsynscctt	egrtddyrcw	
Medaka	lfnGREYSSC	tdtgrsdg	WCSSTTYNfEK	dgykfcphe	lftlgngd	gpcckfprff	qqtsynscctt	egrtddyrcw	
Zebrafish	lfnGREYSSC	tdtgrsdg	WCSSTTYNfEK	dgykfcphe	lftlgngd	gpcckfprff	qqtsynscctt	egrtddyrcw	
Conservation									
Rat	gttedydrdk	kygfcpetam	stvggnsega	pcvfp	tlflg nky	escttsag	rsdgkwcat	ttnyddrrkw	gfcpdqgysl
Mouse	gttedydrdk	kygfcpetam	stvggnsega	pcvfp	tlflg nky	escttsag	rsdgkwcat	ttnyddrrkw	gfcpdqgysl
Human	gttedydrdk	kygfcpetam	stvggnsega	pcvfp	tlflg nky	escttsag	rsdgkwcat	ttnyddrrkw	gfcpdqgysl
Pig	gttedydrdk	kygfcpetam	stvggnsega	pcvfp	tlflg nky	escttsag	rsdgkwcat	ttnyddrrkw	gfcpdqgysl
Turkey	gttedydrdk	kygfcpetam	stvggnsega	pcvfp	tlflg nky	escttsag	rsdgkwcat	ttnyddrrkw	gfcpdqgysl
Medaka	attdydrdk	kygfcpetam	stvggnsega	pcvfp	tlflg nky	escttsag	rsdgkwcat	ttnyddrrkw	gfcpdqgysl
Zebrafish	attdydrdk	kygfcpetam	stvggnsega	pcvfp	tlflg nky	escttsag	rsdgkwcat	ttnyddrrkw	gfcpdqgysl
Conservation									
Rat	flvaahefgh	amglehsqdp	galmapiyty	tknfrlsdd	ikgiqelygp	spdadtdtgt	gp-----tptl	gpvtp-eick	
Mouse	flvaahefgh	amglehsqdp	galmapiyty	tknfrlsdd	ikgiqelygp	spdadtdtgt	gp-----tptl	gpvtp-eick	
Human	flvaahefgh	amglehsqdp	galmapiyty	tknfrlsdd	ikgiqelygp	spdadtdtgt	gp-----tptl	gpvtp-eick	
Pig	flvaahefgh	amglehsqdp	galmapiyty	tknfrlsdd	ikgiqelygp	spdadtdtgt	gp-----tptl	gpvtp-eick	
Turkey	flvaahefgh	amglehsqdp	galmapiyty	tknfrlsdd	ikgiqelygp	spdadtdtgt	gp-----tptl	gpvtp-eick	
Medaka	flvaahefgh	amglehsqdp	galmapiyty	tknfrlsdd	ikgiqelygp	spdadtdtgt	gp-----tptl	gpvtp-eick	
Zebrafish	flvaahefgh	amglehsqdp	galmapiyty	tknfrlsdd	ikgiqelygp	spdadtdtgt	gp-----tptl	gpvtp-eick	
Conservation									
Rat	adivfdgiag	irgeiffkdk	rfiwrvtvpr	dkptgpllva	tfwpeipeki	davyeapqee	kavf	fagney wvy	sastler
Mouse	adivfdgiag	irgeiffkdk	rfiwrvtvpr	dkptgpllva	tfwpeipeki	davyeapqee	kavf	fagney wvy	sastler
Human	adivfdgiag	irgeiffkdk	rfiwrvtvpr	dkptgpllva	tfwpeipeki	davyeapqee	kavf	fagney wvy	sastler
Pig	adivfdgiag	irgeiffkdk	rfiwrvtvpr	dkptgpllva	tfwpeipeki	davyeapqee	kavf	fagney wvy	sastler
Turkey	adivfdgiag	irgeiffkdk	rfiwrvtvpr	dkptgpllva	tfwpeipeki	davyeapqee	kavf	fagney wvy	sastler
Medaka	adivfdgiag	irgeiffkdk	rfiwrvtvpr	dkptgpllva	tfwpeipeki	davyeapqee	kavf	fagney wvy	sastler
Zebrafish	adivfdgiag	irgeiffkdk	rfiwrvtvpr	dkptgpllva	tfwpeipeki	davyeapqee	kavf	fagney wvy	sastler
Conservation									
Rat	gypkltslg	lppdvqavda	afnwsknkkt	yflsagdkfwr	y	nevkkkmdp	gfpkliadsw	naipdnldav	vd qggghs
Mouse	gypkltslg	lppdvqavda	afnwsknkkt	yflsagdkfwr	y	nevkkkmdp	gfpkliadsw	naipdnldav	vd qggghs
Human	gypkltslg	lppdvqavda	afnwsknkkt	yflsagdkfwr	y	nevkkkmdp	gfpkliadsw	naipdnldav	vd qggghs
Pig	gypkltslg	lppdvqavda	afnwsknkkt	yflsagdkfwr	y	nevkkkmdp	gfpkliadsw	naipdnldav	vd qggghs
Turkey	gypkltslg	lppdvqavda	afnwsknkkt	yflsagdkfwr	y	nevkkkmdp	gfpkliadsw	naipdnldav	vd qggghs
Medaka	gypkltslg	lppdvqavda	afnwsknkkt	yflsagdkfwr	y	nevkkkmdp	gfpkliadsw	naipdnldav	vd qggghs
Zebrafish	gypkltslg	lppdvqavda	afnwsknkkt	yflsagdkfwr	y	nevkkkmdp	gfpkliadsw	naipdnldav	vd qggghs
Conservation									
Rat	ffkgaayy	kl	enqslksvkf	gsiksdwlgc					
Mouse	ffkgaayy	kl	enqslksvkf	gsiksdwlgc					
Human	ffkgaayy	kl	enqslksvkf	gsiksdwlgc					
Pig	ffkgaayy	kl	enqslksvkf	gsiksdwlgc					
Turkey	ffkgaayy	kl	enqslksvkf	gsiksdwlgc					
Medaka	ffkgaayy	kl	enqslksvkf	gsiksdwlgc					
Zebrafish	ffkgaayy	kl	enqslksvkf	gsiksdwlgc					
Conservation									

2.5: References

1. Strongin, AY, Collier, I, Bannikov, G, Marmer, BL, Grant, GA, and Goldberg, GI. Mechanism of cell surface activation of 72-kDa type IV collagenase. Isolation of the activated form of the membrane metalloprotease. *J. Biol. Chem.* 1995; 270:5331-5338.
2. Viappiani, S, Nicolescu, AC, Holt, A, Sawicki, G, Crawford, BD, Leon, H, van, MT, and Schulz, R. Activation and modulation of 72kDa matrix metalloproteinase-2 by peroxynitrite and glutathione. *Biochem. Pharmacol.* 2009; 77:826-834.
3. Okamoto, T, Akaike, T, Sawa, T, Miyamoto, Y, van, d, V, and Maeda, H. Activation of matrix metalloproteinases by peroxynitrite-induced protein S-glutathiolation via disulfide S-oxide formation. *J. Biol. Chem.* 2001; 276:29596-29602.
4. Kwan, JA, Schulze, CJ, Wang, W, Leon, H, Sariahmetoglu, M, Sung, M, Sawicka, J, Sims, DE, Sawicki, G, and Schulz, R. Matrix metalloproteinase-2 (MMP-2) is present in the nucleus of cardiac myocytes and is capable of cleaving poly (ADP-ribose) polymerase (PARP) in vitro. *FASEB J.* 2004; 18:690-692.
5. Wang, W, Schulze, CJ, Suarez-Pinzon, WL, Dyck, JR, Sawicki, G, and Schulz, R. Intracellular action of matrix metalloproteinase-2 accounts for acute myocardial ischemia and reperfusion injury. *Circulation* 2002; 106:1543-1549.
6. Sawicki, G, Leon, H, Sawicka, J, Sariahmetoglu, M, Schulze, CJ, Scott, PG, Szczesna-Cordary, D, and Schulz, R. Degradation of myosin light chain in isolated

- rat hearts subjected to ischemia-reperfusion injury: a new intracellular target for matrix metalloproteinase-2. *Circulation* 2005; 112:544-552.
7. Nagase, H, Visse, R, and Murphy, G. Structure and function of matrix metalloproteinases and TIMPs. *Cardiovasc. Res.* 2006; 69:562-573.
 8. Gratton, JP, Bernatchez, P, and Sessa, WC. Caveolae and caveolins in the cardiovascular system. *Circ. Res.* 2004; 94:1408-1417.
 9. Fra, AM, Williamson, E, Simons, K, and Parton, RG. De novo formation of caveolae in lymphocytes by expression of VIP21-caveolin. *Proc. Natl. Acad. Sci. U. S. A* 1995; 92:8655-8659.
 10. Feron, O and Balligand, JL. Caveolins and the regulation of endothelial nitric oxide synthase in the heart. *Cardiovasc. Res.* 2006; 69:788-797.
 11. Puyraimond, A, Fridman, R, Lemesle, M, Arbeille, B, and Menashi, S. MMP-2 colocalizes with caveolae on the surface of endothelial cells. *Exp. Cell Res.* 2001; 262:28-36.
 12. Atkinson, SJ, English, JL, Holway, N, and Murphy, G. Cellular cholesterol regulates MT1 MMP dependent activation of MMP 2 via MEK-1 in HT1080 fibrosarcoma cells. *FEBS Lett.* 2004; 566:65-70.
 13. Fiucci, G, Ravid, D, Reich, R, and Liscovitch, M. Caveolin-1 inhibits anchorage-independent growth, anoikis and invasiveness in MCF-7 human breast cancer cells. *Oncogene* 2002; 21:2365-2375.

14. Song, KS, Li, S, Okamoto, T, Quilliam, LA, Sargiacomo, M, and Lisanti, MP. Co-purification and direct interaction of Ras with caveolin, an integral membrane protein of caveolae microdomains. Detergent-free purification of caveolae microdomains. *J. Biol. Chem.* 1996; 271:9690-9697.
15. Cheung, PY, Sawicki, G, Wozniak, M, Wang, W, Radomski, MW, and Schulz, R. Matrix metalloproteinase-2 contributes to ischemia-reperfusion injury in the heart. *Circulation* 2000; 101:1833-1839.
16. Cho, WJ and Daniel, EE. Colocalization between caveolin isoforms in the intestinal smooth muscle and interstitial cells of Cajal of the Cav1(+/+) and Cav1(-/-) mouse. *Histochem. Cell Biol.* 2006; 126:9-16.
17. Couet, J, Li, S, Okamoto, T, Ikezu, T, and Lisanti, MP. Identification of peptide and protein ligands for the caveolin-scaffolding domain. Implications for the interaction of caveolin with caveolae-associated proteins. *J. Biol. Chem.* 1997; 272:6525-6533.
18. Wallon, UM and Overall, CM. The hemopexin-like domain (C domain) of human gelatinase A (matrix metalloproteinase-2) requires Ca²⁺ for fibronectin and heparin binding. Binding properties of recombinant gelatinase A C domain to extracellular matrix and basement membrane components. *J. Biol. Chem.* 1997; 272:7473-7481.
19. Fridman, R, Fuerst, TR, Bird, RE, Hoyhtya, M, Oelkuct, M, Kraus, S, Komarek, D, Liotta, LA, Berman, ML, and Stetler-Stevenson, WG. Domain structure of human 72-kDa gelatinase/type IV collagenase. Characterization of proteolytic activity

- and identification of the tissue inhibitor of metalloproteinase-2 (TIMP-2) binding regions. *J. Biol. Chem.* 1992; 267:15398-15405.
20. Wunderlich, C, Schober, K, Lange, SA, Drab, M, Braun-Dullaeus, RC, Kasper, M, Schwencke, C, Schmeisser, A, and Strasser, RH. Disruption of caveolin-1 leads to enhanced nitrosative stress and severe systolic and diastolic heart failure. *Biochem. Biophys. Res. Commun.* 2006; 340:702-708.
 21. Drab, M, Verkade, P, Elger, M, Kasper, M, Lohn, M, Lauterbach, B, Menne, J, Lindschau, C, Mende, F, Luft, FC, Schedl, A, Haller, H, and Kurzchalia, TV. Loss of caveolae, vascular dysfunction, and pulmonary defects in caveolin-1 gene-disrupted mice. *Science* 2001; 293:2449-2452.
 22. Leco, KJ, Apte, SS, Taniguchi, GT, Hawkes, SP, Khokha, R, Schultz, GA, and Edwards, DR. Murine tissue inhibitor of metalloproteinases-4 (Timp-4): cDNA isolation and expression in adult mouse tissues. *FEBS Lett.* 1997; 401:213-217.
 23. Wang, Z, Juttermann, R, and Soloway, PD. TIMP-2 is required for efficient activation of proMMP-2 in vivo. *J. Biol. Chem.* 2000; 275:26411-26415.
 24. Gratton, JP, Lin, MI, Yu, J, Weiss, ED, Jiang, ZL, Fairchild, TA, Iwakiri, Y, Groszmann, R, Claffey, KP, Cheng, YC, and Sessa, WC. Selective inhibition of tumor microvascular permeability by cavtratin blocks tumor progression in mice. *Cancer Cell* 2003; 4:31-39.
 25. Sukumaran, SK, Quon, MJ, and Prasadarao, NV. Escherichia coli K1 internalization via caveolae requires caveolin-1 and protein kinase Calpha

- interaction in human brain microvascular endothelial cells. *J. Biol. Chem.* 2002; 277:50716-50724.
26. Bucci, M, Gratton, JP, Rudic, RD, Acevedo, L, Roviezzo, F, Cirino, G, and Sessa, WC. In vivo delivery of the caveolin-1 scaffolding domain inhibits nitric oxide synthesis and reduces inflammation. *Nat. Med.* 2000; 6:1362-1367.
 27. Arbuzova, A, Wang, L, Wang, J, Hangyas-Mihalyne, G, Murray, D, Honig, B, and McLaughlin, S. Membrane binding of peptides containing both basic and aromatic residues. Experimental studies with peptides corresponding to the scaffolding region of caveolin and the effector region of MARCKS. *Biochemistry* 2000; 39:10330-10339.
 28. Kim, HN and Chung, HS. Caveolin-1 inhibits membrane-type 1 matrix metalloproteinase activity. *BMB. Rep.* 2008; 41:858-862.
 29. Le, SO, Teeters, K, Miyasato, S, Choi, J, Nakamatsu, G, Richardson, JA, Starcher, B, Davis, EC, Tam, EK, and Jourdan-Le, SC. The role of caveolin-1 in pulmonary matrix remodeling and mechanical properties. *Am. J. Physiol Lung Cell Mol. Physiol* 2008; 295:L1007-L1017.
 30. Head, BP, Patel, HH, Roth, DM, Murray, F, Swaney, JS, Niesman, IR, Farquhar, MG, and Insel, PA. Microtubules and actin microfilaments regulate lipid raft/caveolae localization of adenylyl cyclase signaling components. *J. Biol. Chem.* 2006; 281:26391-26399.

31. Kawabe, J, Okumura, S, Nathanson, MA, Hasebe, N, and Ishikawa, Y. Caveolin regulates microtubule polymerization in the vascular smooth muscle cells. *Biochem. Biophys. Res. Commun.* 2006; 342:164-169.

CHAPTER 3

MMP-2 AND CAVEOLIN LOCALIZATION IN THE HEART

A version of this chapter has been published in:

Cho WJ, Chow AK, Schulz R, Daniel EE. Matrix metalloproteinase-2, caveolins, focal adhesion kinase and c-Kit in cells of the mouse myocardium. *J Cell Mol Med* 2007; 11:1069-1086.

3.1: Introduction

Though biochemical and molecular biology advances have allowed us to examine the possible relationships between proteins by using techniques such as Western blotting, yeast two hybrid systems and immunoprecipitation, examination of proteins via immunohistochemistry is one of the few methods by which proteins can be examined *in situ*. Immunohistochemistry is primarily used to determine the localization of specific antigens or proteins in tissue sections by exploiting the antigen-antibody interaction. Antibodies labeled with a fluorescent dye, horseradish peroxidase, colloidal gold or radioactivity are bound to the antigen/protein of interest and then visualized. Previous immunohistochemical studies of the myocardium have revealed that cardiomyocytes were closely apposed to fibroblasts, capillary endothelial cells and other components in the interstitial space in heart tissue¹⁻⁵.

Researchers have used specific proteins as markers for particular structures within the myocardium. Both myomesin and caveolin-3 can be found in cardiomyocytes^{1,6,7}. Myomesin is a prominent protein found at the sarcomeric M-line, while caveolin-3 has thus far only been observed in striated and smooth muscle. Prominent fibroblast markers include vimentin, discoidin domain receptor-2, α -smooth muscle actin and focal adhesion kinase (FAK)^{6,8-10}. Vimentin is a major protein component of intermediate filaments in mesenchymal cells while discoidin domain receptor-2 is a receptor tyrosine kinase whose expression is restricted to cardiac fibroblasts in the adult heart⁸. α -smooth muscle actin has been shown to be important in the regulation of fibroblast contractility¹¹. FAK is a protein tyrosine kinase that is required by cardiac fibroblasts for proliferation and migration¹². von Willebrand factor

(vWF) is used as a marker of capillary endothelial cells^{13;14}. It is a large glycoprotein that is stored in the Weibel-Palade bodies of endothelial cells¹⁵. Despite the use of these protein markers, identification of cell types and protein localization and co-localization in the myocardium *in situ* remains difficult as cardiomyocytes, fibroblasts and capillary endothelial cells are closely interposed.

Transmission electron microscopy, combined with immunolabeling is one method by which it is possible to more accurately elucidate the localization of proteins in cells when they are closely apposed. Transmission electron microscopy is a powerful technique which can be used to visualize particles as small as 50 pm¹⁶, thus allowing for more accurate examination of protein localization at cellular and especially subcellular levels.

Matrix metalloproteinase-2 (MMP-2) (gelatinase A, type II collagenase) is a tightly regulated enzyme that is in multiple cells of the heart, including cardiomyocytes, fibroblasts and the endothelium. MMP-2 has been shown to play important roles in wound healing and heart failure. Both intracellular and extracellular matrix action of MMP-2 have been described in the heart during ischemia/reperfusion injury¹⁷⁻¹⁹. More recently, MMP-2 has been found at the cardiomyocyte plasma membrane, Z-line and myofilaments^{18;20} and is co-localized with Cav-1 at the surface of human endothelial cells²¹. Its localization with other proteins in other cardiac cells such as fibroblasts or capillary endothelial cells is yet unknown.

Caveolins are structural proteins that insert in the plasma membrane to form caveolae, major components of lipid rafts, along with cholesterol, sphingolipids and G-proteins in a number of cells²², including smooth muscle cells²³⁻²⁹. The caveolin gene

family consists of three members which encode for the caveolin-1, -2 and -3 proteins. All members of the caveolin family contain a CSD that can bind to signaling molecules and play crucial roles in cell signal transduction²³. The CSD (residues 82-101 in Cav-1, 54-73 in Cav-2 and 55-74 in Cav-3) is able to bind to exposed sequences of $\Phi X \Phi X X X X \Phi X X \Phi$ (where Φ is Phe, Tyr or Trp and X is any amino acid) when at least three Φ are present. Once bound to the CSD, protein function is generally inhibited by caveolin. In Chapter 2, it was previously reported that Cav-1 localized to the cardiomyocyte plasma membrane and co-localizes with MMP-2, using confocal microscopy and immunofluorescent analysis, and further showed that a synthetic CSD domain is able to significantly inhibit the proteolytic activity of MMP-2²⁰.

The objectives of this study are to expand on our previous observations and show the localization and co-localization of MMP-2 with all three caveolins in cardiomyocytes, fibroblasts and capillary endothelial cells in the left ventricular myocardium of Cav-1^{+/+} and Cav-1^{-/-} mouse hearts. Studies of the distributions of focal adhesion kinase, discoidin domain receptor-2, von Willebrand factor and tyrosine kinase receptor were used to identify fibroblasts, endothelial cells and interstitial Cajal-like cells (ICLC). In this study, we used 5 μ m heart cryosections for 2D confocal microscopy and 20 μ m cryosections for a 3D study with two-photon confocal microscopy.

3.2: Materials and methods

3.2.1: Animals

All experiments were performed in accordance with the Canadian Council on Animal Care *Guide to the Care and Use of Experimental Animals*. 6-8 week old male Cav-

1^{-/-} (cav<tm 1 M ls>/J) and control [(B6 129 SF2/J) (Cav-1^{+/+})] mice were obtained from Jackson Laboratories.

3.2.2: Tissue preparation

All mice were sacrificed by intraperitoneal injection of 12 mg i.p. sodium pentobarbital 10 min after administration of 1000 IU i.p. heparin according to a protocol approved by the University of Alberta Animal Care Committee and following the guidelines of the Canada Council on Animal Care. The hearts were rapidly excised and Langendorff perfused at constant pressure (60 mm Hg) via the aorta with Krebs-Henseleit buffer²⁰ for 10 min, followed by perfusion fixation in 4% paraformaldehyde in 0.1 M sodium phosphate buffer (pH 7.2–7.4) for 4 h at 4°C. The left ventricles were then dissected out and rinsed and cryoprotected in 30% sucrose in 0.1 M phosphate buffer overnight at 4°C and then stored at -80°C.

3.2.3: Cryosectioning

The cryoprotected left ventricles were frozen in Tissue-Tek® O.C.T. compound in disposable embedding molds in the pre-cooler of the cryostat for 1 h. 5 µm thick cryosections for 2D imaging and 20 µm sections for 3D imaging were attached to glass slides coated with 1.5% 3-amino-propyltriethoxysilane (Sigma) in acetone. The cryosections were allowed to dry at room temperature for 15 min.

3.2.4: Double immunofluorescent labeling

The dried cryosections were first rinsed in Triton-X 100 (0.3% for 5 µm sections and 0.5% for the for 20 µm sections) in PBS (137 mM NaCl, 2.7 mM KCl, 10 mM Na₂HPO₄, 1.76 mM KH₂PO₄) (pH 7.2–7.4) 2 x 10 min at room temperature to remove the O.C.T. compound and accelerate antibody penetration to the target antigen followed by

a rinse in PBS. To reduce artificial staining of non-specific proteins, 10% normal donkey serum in PBS was applied for 1 h before applying primary antibody. For co-localization studies of two different proteins, double immunolabeling was accomplished by one of two different methods, either: (1) double labeling of primary antibodies from different host species or, (2) double labeling of primary antibodies from the same host species, as previously described²⁹. Sequential staining of each primary antibody provided the best results and was performed in both methods. Endogenous mouse IgG in the mouse heart tissue was blocked by using the mouse IgG blocking reagent from M.O.M.[™] kits (Vector Laboratories Inc.).

All antibodies and sera used are summarized in Table 3.1. During the incubation with antibodies, 2% normal donkey serum of total incubation volume was added. All experimental procedures were performed at room temperature (22±1°C) unless otherwise specified. To determine the specificity of immunolabeling, the primary antibody was omitted, or when the antigen was available (Cav-2, Cav-3), it was used to saturate the primary antibody by incubating 1 µg/mL of the blocking peptide with 1 µg of the antibody for 30 min at room temperature prior to applying the saturated antibody to the cryosections.

3.2.5: Confocal microscopy

The immunolabeled cryosections were observed using a two photon confocal microscope (LSM 510, Carl Zeiss Co.) and saved using LSM 5 Image software (Carl Zeiss Co.). Cy3 (red) was scanned by a helium / neon laser (wavelength 543 nm laser line) with a long path 590 filter (560–700 nm excitation). Alexa488 (green) was captured by an argon laser (wavelength 488 nm laser line) with a band path 500–550 infrared filter

(500–550 nm excitation). DAPI (blue) for nuclear staining in all cells was acquired in the range of 400–470 nm excitation. All images obtained from the confocal microscope were enhanced in brightness, contrast and with the γ functions with the tools in LSM 5 Image software. Some images were de-convoluted using AutoDeblur and AutoVisualize (Media Cybernetics Inc).

3.2.6: Electron microscopy

Two Cav-1^{+/+} and 2 Cav-1^{-/-} (6–8 week old male) mouse hearts were examined ultrastructurally. The mouse was deeply anaesthetized with halothane and the thorax opened. The heart was freed from the pericardium and a 26G1/2 needle (Becton Dickinson & Co.) was inserted into the left ventricle. The right auricular appendage was cut and the mouse was exsanguinated by flushing its circulatory system with 30 mL of 0.1 M phosphate buffer, followed by 30 mL of a mixture of 0.1% glutaraldehyde and 2% paraformaldehyde in 0.1 M phosphate buffer. The partially fixed heart was removed and cut into 1 mm³ pieces and placed in a mixture of 2.5% glutaraldehyde and 4% paraformaldehyde in 0.075 M sodium cacodylate buffer for a further 2 h at 4°C. The fixed heart samples were briefly rinsed in 0.075 M cacodylate buffer, followed by post-fixation in 1% OsO₄ (Electron Microscopic Sciences) in 0.05 M cacodylate buffer for 2 h at 4°C. The pre- and post-fixed heart samples were dehydrated using ethyl-alcohol substitution with propylene oxide, and infiltrated using a mixture of Araldite512-Embed812. The samples were heat polymerized with an epoxy accelerator, 1.5% DMP-30 (2,4,6-tri-(dimethylaminomethyl) phenol) (Electron Microscopic Sciences) for 48 h at 60°C. 1 μ m thick sections were cut, stained with 1% toluidine blue and evaluated for ultra-thin sectioning. Ultra-thin sections of 50 nm were cut and loaded using Perfect Loop (Electron Microscopic Sciences) onto a 300-mesh copper grid or a 100-mesh

copper grid coated with 0.25% Formvar solution in ethylene dichloride (Electron Microscopy Sciences). Sections were stained with 4% uranyl acetate (Canemco & Marivac Inc.) in 50% ethanol and Reynold's lead citrate, lead nitrate (TAAB Laboratories Equipment Ltd.) and sodium citrate (J.T. Baker Inc.). The grids were examined using a Philips 410 electron microscope equipped with a charge-coupled device camera (MegView III) at 80 kV.

3.3: Results

3.3.1: General distribution of MMP-2

The cell types of the heart were identified based on morphological characteristics. Cardiomyocytes are striated, multi-nucleated cells with intercalated disks. Fibroblasts lack a basement membrane, have an oval nucleus with one or two nucleoli and have multiple extensions. Capillary endothelial cells are long, narrow, frequently branching structures with a smaller nucleus than fibroblasts and rest on a basement membrane. In the Cav-1^{+/+} mouse left ventricular myocardium, MMP-2 was widely and prominently distributed at cardiomyocyte plasma membranes and Z-lines and the plasma membrane and cytoplasm of fibroblasts and capillary endothelial cells (Fig. 3.1). In Cav-1^{-/-} samples however, MMP-2 immunostaining was significantly reduced or absent in all three cell types examined (Fig. 3.1).

3.3.2: MMP-2 and Cav-1 co-localization in cardiomyocytes

MMP-2 co-localized well with Cav-1 at the plasma membrane of cardiomyocytes, fibroblasts and capillary endothelial cells in the Cav-1^{+/+} ventricular samples. Partial co-localization between MMP-2 and Cav-1 was observed in the Cav-1^{+/+}

ventricles at the Z-lines (Fig. 3.2A–C). In contrast, the Cav-1^{-/-} heart showed that MMP-2 was significantly reduced or absent in all these cell types (Fig. 3.2D).

3.3.3: Localization of MMP-2 and Cav-2 in cardiomyocytes

The distribution of Cav-2 is markedly different from that of Cav-1. In Cav-1^{+/+} myocardial samples, Cav-2 was present only in capillary endothelial cells, seen as long narrow tubular and anastomotic structures shown optimally in longitudinal sections. However, no Cav-2 was observed in cardiomyocytes at the plasma membranes or Z-lines. MMP-2 co-localized well with Cav-2 in the capillary endothelial cells. A few cells adjacent to the cardiomyocyte plasma membrane in the interstitial space were MMP-2-positive, but Cav-2-negative and it was unclear whether these cells were fibroblasts or another cell type (Fig. 3.2E–G).

The distribution of Cav-2 in Cav-1^{-/-} ventricular samples is similar to that found in Cav-1^{+/+} myocardium, despite the absence of Cav-1. Cav-2 was present in capillary endothelial cells and absent in cardiomyocyte plasmalemma and Z-lines in Cav-1^{-/-} left ventricular myocardium (Fig. 3.2H).

3.3.4: Localization of MMP-2 and Cav-3 in cardiomyocytes

In the Cav-1^{+/+} myocardial samples, Cav-3 was prominent and co-localized well with MMP-2 at cardiomyocyte plasma membranes and Z-lines (Fig. 3.2I–K). In addition to the cardiomyocyte plasma membrane and Z-lines, Cav-3 localization in Cav-1^{-/-} myocardium was observed in capillary endothelial cells and fibroblasts. Fibroblasts were identified by comparatively larger nuclei and narrower cytoplasm than endothelial cells (Fig. 3.2L).

3.3.5: Localization of MMP-2 in FAK positive fibroblasts

In Cav-1^{+/+} myocardium, fibroblasts which run alongside cardiomyocytes and endothelial cells were FAK positive. In Fig. 3.3A–C, one FAK-positive fibroblast was connected to another FAK-positive fibroblast by a thin, elongated tail. MMP-2 also appeared in the FAK-positive fibroblast and co-localized with FAK in Cav-1^{+/+} samples (Fig. 3.3A–C). Interestingly, Cav-1^{-/-} myocardial fibroblasts show no evidence of FAK immunoreactivity (Fig. 3.3D).

3.3.6: Localization of MMP-2 in DDR-2 positive fibroblasts

Discoidin domain receptor-2 (DDR-2) was used as an additional fibroblast marker to further elucidate the relationships between proteins. DDR-2 immunoreactivity was observed in fibroblasts found in the interstitial space. It also appeared faintly in cardiomyocytes, though this is likely a result of non-specific staining (Fig. 3.3F).

DDR-2 positive fibroblasts in Cav-1^{+/+} myocardium contained MMP-2 which was partially co-localized with DDR-2 (Fig. 3.3E–G). Fibroblasts in the interstitial space of Cav-1^{-/-} myocardium were also positive for DDR-2 immunohistochemical staining (Fig. 3.3H).

3.3.7: MMP-2 in capillary endothelial cells

Capillary endothelial cells of both Cav-1^{+/+} and Cav-1^{-/-} ventricles showed similar positive staining for von Willebrand factor. In Cav-1^{+/+} sections, von Willebrand factor co-localized with MMP-2, while this was not seen in the Cav-1^{-/-} section (Fig. 3.3I–L).

3.3.8: MMP-2 in interstitial Cajal-like cells

Interstitial Cajal-like cells (ICLC) appeared as c-Kit positive groups in the interstitial space near cardiomyocytes and capillary endothelial cells. The c-Kit positive ICLC run parallel to or are intertwined with capillary endothelial cells. MMP-2 appeared co-localized with c-Kit in these ICLCs in Cav-1^{+/+} myocardium (Fig. 3.3M–O). In Cav-1^{-/-} ventricular sections, MMP-2 and c-Kit immunoreactivity were significantly reduced or absent, respectively (Fig. 3.3P).

3.3.9: Co-localization of Cav-1 and Cav-2

Though Cav-1 appears in fibroblasts, capillary endothelial cells and the plasma membrane and Z-lines of cardiomyocytes in Cav-1^{+/+} sections, Cav-1 immunoreactivity co-localized with Cav-2 only in capillary endothelial cells. 3D structural analysis of Cav-1 positive fibroblasts and Cav-2 positive capillary endothelial cells showed that these cells are intertwined and are closely apposed (Fig. 3.4A–C). Cav-2 staining was observed in capillary endothelial cells in Cav-1^{-/-} sections, similar to that observed in Cav-1^{+/+} sections (Fig. 3.4D).

3.3.10: Co-localization of Cav-1 and Cav-3

Cav-1 shows strong co-localization with Cav-3 on the plasma membranes of Cav-1^{+/+} cardiomyocytes, fibroblasts and capillary endothelial cells. However, Z-line staining shows differences between Cav-1 and Cav-3. Cav-3 appears strongly at the Z-lines while Cav-1 appears as distinct, punctate sites at or near the Z-lines (Fig. 3.4E–G). In Cav-1^{-/-} sections, Cav-3 distribution is similar to that in Cav-1^{+/+} samples with immunostaining clearly present at cardiomyocyte plasma membranes and Z-lines, and also appearing in some fibroblasts and capillary endothelial cells (Fig. 3.4H).

3.3.11: Co-localization of Cav-2 and Cav-3

In both Cav-1^{+/+} and Cav-1^{-/-} hearts, Cav-2 staining appears in capillary endothelial cells identified by their tubular, anastomotic shapes. Cav-2 partially co-localizes with Cav-3 in both strains of mice (Fig. 3.4I–L).

3.3.12: FAK-positive fibroblasts and co-localization with Cav-1

In Cav-1^{+/+} myocardium, FAK immunoreactivity was evident throughout the cytoplasm of fibroblasts, including their elongated cytoplasmic tails, and co-localizes with Cav-1. Some FAK-positive fibroblasts also appeared interconnected (Fig. 3.5A–C). In contrast, Cav-1^{-/-} myocardium, FAK was completely absent in the cytoplasm of fibroblasts and only appeared in some nuclei of various cell types (Fig. 3.5D).

3.3.13: vWF-positive capillary endothelial cell and its co-localization with Cav-1

Cav-1 immunoreactivity was observed in the plasma membrane and cytoplasm of capillary endothelial cells of Cav-1^{+/+} myocardium, while vWF was seen in the cytoplasm and co-localized well with Cav-1 where present. Cav-1 and vWF co-localization show that Cav-1 is present in the capillary endothelial cells of Cav-1^{+/+} myocardium (Fig. 3.5E–G). vWF was also present in the endothelial cells of Cav-1^{-/-} hearts, despite the absence of Cav-1 (Fig. 3.5H).

3.3.14: DDR-2-positive fibroblast and its co-localization with Cav-1

Several DDR-2 positive fibroblasts were in the interstitial space when observed in cross sections of mouse myocardium. DDR-2 also partially co-localized with Cav-1 in Cav-1^{+/+} sections (Fig. 3.5I–K). DDR-2 positive fibroblasts were also evident in the interstitial space of Cav-1^{-/-} cross sections (Fig. 3.5L).

3.3.15: *c-Kit-positive ICLCs and its co-localization with Cav-1*

ICLCs in Cav-1^{+/+} sections showed c-Kit-positive staining which revealed multiple processes. This immunoreactivity co-localized well with Cav-1 in Cav-1^{+/+} ventricle (Fig. 3.5M–O). Interestingly, c-Kit was completely absent in Cav-1^{-/-} ventricular sections (Fig. 3.5P).

3.3.16: *FAK-positive fibroblast and its relationship with Cav-2*

3D reconstructed images showed that in Cav-1^{+/+} sections, FAK positive fibroblasts were in close proximity to Cav-2 positive capillary endothelial cells, though the two proteins did not co-localize (Fig. 3.6A–C). In Cav-1^{-/-} 3D images, Cav-2 appears in non-nuclear components (Fig. 3.6D).

3.3.17: *c-Kit-positive interstitial Cajal-like cell and its relationship with Cav-2*

Cav-1^{+/+} sections showed that c-Kit positive ICLCs appeared in the interstitial space in close proximity to cardiomyocytes and was not found with Cav-2 in capillary endothelial cells (Fig. 3.6E–G). Again, c-Kit was completely absent in Cav-1^{-/-} mouse myocardium (Fig. 3.6H).

3.3.18: *FAK-positive fibroblasts and its co-localization with Cav-3*

Both FAK positive fibroblasts and FAK negative cells were observed in the interstitial space of Cav-1^{+/+} myocardium. Some of the FAK positive fibroblasts also showed Cav-3 immunoreactivity and this was co-localized with FAK. All FAK-negative cells showed evidence of Cav-3 staining (Fig. 3.7A–C). In Cav-1^{-/-} sections, FAK was not observed in non-nuclear areas of cells but did appear in fibroblasts in the interstitial space (Fig. 3.7D).

3.3.19: DDR-2-positive fibroblasts and its co-localization with Cav-3

Examination of Cav-1^{+/+} myocardium revealed the presence of DDR-2 positive fibroblasts in the interstitial space. DDR-2 was occasionally found to be co-localized with Cav-3 (Fig. 3.7E–G). Several weakly DDR-2 positive processes were present near cardiomyocytes in the interstitial space, though no co-localization with Cav-3 was observed. Non-specific staining of DDR-2 was observed in Cav-1^{-/-} cardiomyocytes (Fig. 3.7H).

3.3.20: vWF-positive capillary endothelial cells and its relationship with Cav-3

In both Cav-1^{+/+} and Cav-1^{-/-} myocardium, vWF was present in capillary endothelial cells, without co-localization with Cav-3. Thus, it appears that vWF is closely associated with Cav-1 but not with Cav-3 in both Cav-1^{+/+} and Cav-1^{-/-} myocardium (Fig. 3.7I–L).

3.3.21: c-Kit-positive ICLCs and its co-localization with Cav-3

ICLCs in Cav-1^{+/+} sections revealed the presence of both Cav-3 and c-kit, though they were only partially co-localized at ICLC processes. The ICLC processes were in close proximity to cardiomyocytes making it hard to distinguish between Cav-3 positive ICLC processes and Cav-3 positive cardiomyocyte plasma membranes (Fig. 3.7M–O). Examination of Cav-1^{-/-} sections revealed a complete absence of c-Kit but Cav-3 appeared at the plasma membranes and Z-lines of cardiomyocytes, as well as in fibroblasts (Fig. 3.7P).

3.3.22: FAK and vWF are not associated

In order to determine whether FAK and vWF are markers of fibroblasts and capillary endothelial cells, respectively, it was necessary to determine whether these

two markers are ever present in the same cell. FAK was found to be present specifically in the cytosol of fibroblasts and non-specifically in nuclei of all cell types in Cav-1^{+/+} myocardium (Fig. 3.8A–C). vWF was found specifically in the endothelial cells of both Cav-1^{+/+} (Fig. 3.8B) and Cav-1^{-/-} heart samples (Fig. 3.8D).

3.3.23: Association between DDR-2 and c-Kit

Both DDR-2 positive fibroblasts and c-Kit positive ICLC appeared in the interstitial space in distinct cells, however, a few fibroblasts possessed both DDR-2 and c-Kit and the two proteins partially co-localized in the Cav-1^{+/+} heart (Fig. 3.8E–G). Although c-Kit was completely absent in Cav-1^{-/-} samples, DDR-2 positive fibroblasts were present (Fig. 3.8H).

3.3.24: Cardiomyocyte electron microscopy

Examination of longitudinal sections of Cav-1^{+/+} cardiomyocytes by electron microscopy revealed caveolae that present as flask-shaped invaginations at the sarcolemma. A number of large mitochondria were also observed interrupting myofilaments. Spherical lipid droplets were frequently found at the ends of the mitochondria. The sarcoplasmic reticulum was present along the sarcolemma and found between masses of myofilaments. Dense glycogen granules were found near the mitochondria and nearby Z-lines (Fig. 3.9A and B).

In contrast, Cav-1^{-/-} longitudinal cardiomyocyte sections revealed fewer open caveolae along the sarcolemma and the sarcoplasmic reticulum is discontinuous. Similar to Cav-1^{+/+} sections, Cav-1^{-/-} sections revealed abundant mitochondria and myofilaments (Fig. 3.9D and E).

3.3.25: Capillary endothelial cell electron microscopy

Capillary endothelial cells were typically located near or in-between cardiomyocytes. Open caveolae were present at the capillary endothelial cell membrane while closed caveolae were found in the cytoplasm of Cav-1^{+/+} samples (Fig. 3.9A and B).

Capillary endothelial cell localization in Cav-1^{-/-} sections was similar to that found in Cav-1^{+/+} myocardium. Interestingly, some open caveolae also appeared at the membranes of capillary endothelial cells and pericytes also occasionally appeared (Fig. 3.9D and E).

3.3.26: Fibroblast electron microscopy

Fibroblasts were typically found either between cardiomyocytes and cardiomyocytes and capillary endothelial cells, or in the interstitial space near cardiomyocytes. Electron microscopy revealed that fibroblasts had a large, centrally located nucleus and a well developed rough endoplasmic reticulum, though mitochondria were rare. Open caveolae were not observed in the Cav-1^{+/+} section (Fig. 3.9B and C).

Fibroblast localization in Cav-1^{-/-} samples was similar to that found in Cav-1^{+/+} sections with similar organelle distribution. Interestingly, open caveolae were also observed in the membranes of Cav-1^{-/-} fibroblasts (Fig. 3.9E and F).

A complete summary of the findings of this study are also summarized in Tables 2 and 3.

3.4: Discussion

Using two-photon confocal microscopy, we found that: 1) MMP-2 protein expression and localization is perturbed in Cav-1^{-/-} cardiomyocytes, fibroblasts and capillary endothelial cells; 2) Cav-2 is found independent of Cav-1 in capillary endothelial cells; 3) Cav-3 is independent of Cav-1 in cardiomyocytes and fibroblasts; 4) FAK is dependent on Cav-1 in fibroblasts and 5) c-Kit is dependent on Cav-1 in ICLC.

The finding that MMP-2 protein is found in cardiomyocyte membrane and Z-lines has been previously reported¹⁹. The fact that MMP-2 is closely linked with Cav-1 in cardiomyocyte membranes is consistent with our previous observations²⁰. Our current results clearly show that MMP-2 expression is dramatically diminished in Cav-1^{-/-} myocardium when compared with Cav-1^{+/+} samples. Though it is not yet clear why exactly the absence of Cav-1 affects the presence of MMP-2 protein, we hypothesize that Cav-1 may be responsible for scaffolding MMP-2 at sites where it is in close proximity to both upstream and downstream effectors of MMP-2 action. As a result of Cav-1 knockout, the MMP-2 is more diffusely localized within the cardiomyocyte and less obvious with immunohistochemical staining, though the total amount of MMP-2 remains unchanged, as we have previously reported²⁰.

In Cav-1^{+/+} cardiomyocytes, Cav-1 appeared as a continuous stain along the cardiomyocyte membrane, which is significantly different from the staining pattern observed in intestinal smooth muscle cells and interstitial cells of Cajal where a distinct punctate stain was reported^{24;29}. In smooth muscle cells, caveolae, the formation of which are solely dependent on Cav-1, tend to form along the long axis of the smooth muscle cell. Consequently, when the cells are cut in cross section, the staining appears

as a speckled pattern. In contrast, caveolae in cardiomyocytes appear at irregular intervals and may be formed by either Cav-1 or Cav-3. It is also possible that in cardiomyocytes, Cav-1 may appear in lipid rafts that are independent of caveolae.

Interestingly, in this study we found that Cav-2 appears only in capillary endothelial cells, independent of the presence of Cav-1. This also differs from the previous observation in the intestine, where the presence of Cav-2 was entirely dependent on the existence of Cav-1 in both intestinal smooth muscle cells and interstitial cells of Cajal²⁹, suggesting that Cav-2 expression may be differentially regulated depending on the tissue type. The observation that Cav-2 appears in myocardium, regardless of Cav-1 status is particularly intriguing, especially since it has been observed that Cav-2 targeting to the membrane is dependent on its phosphorylation status, which in turn is influenced by Cav-1 in human umbilical vein endothelial cells³⁰.

Another difference between the observations in the intestine and those in the myocardium is the appearance of Cav-3. In intestinal smooth muscle cells and interstitial cells of Cajal, Cav-1 knockout abolished the presence of Cav-3 and greatly diminished its presence in the outer circular muscle when compared with Cav-1^{+/+} intestine²⁹. In the myocardium, however, Cav-3 appears similarly in both Cav-1^{+/+} and Cav-1^{-/-} with punctuate staining at the Z-lines and a more diffuse pattern in fibroblasts. This is of particular interest, especially in light of the fact that the Lisanti group has found that though all three members of the caveolin family can interact to form hetero-oligomers in skeletal muscle and L6 myoblasts, but not in mouse embryonic fibroblasts,

and they have thus concluded that the hetero-oligomer formation occurs only in muscle cells³¹.

Electron microscopy revealed the presence of caveolae in cardiomyocytes of Cav-1^{-/-} myocardium and this is consistent with reports that indicate the presence of Cav-3 is sufficient to induce the formation of caveolae in muscle cells^{22;32}. What is not yet known, however, is whether the absence of Cav-1 in the heart can cause functional perturbations when caveolae are still present. For example, disruption of lipid rafts, and thus caveolae, using methyl- β -cyclodextrin can severely disrupt β -adrenergic signaling in cardiac myocytes³³ and Cav-1 knockout disrupts β -adrenergic function in the small intestine³⁴, but whether this adrenergic perturbation is also present in the Cav-1^{-/-} heart is examined in Chapter 4 of this thesis.

Apart from the cardiomyocytes in Cav-1^{-/-} mouse hearts, immunohistochemical analysis of fibroblasts from these same hearts revealed interesting results. Fibroblasts in the heart are involved in wound healing following myocardial infarction^{35;36} and one factor which may play an important role in mediating this healing is FAK, which is involved in cell adhesion and migration³⁷. We found that FAK co-localizes with both MMP-2 and Cav-1 in Cav-1^{+/+} fibroblasts while Cav-1^{-/-} fibroblasts show a distinct absence of FAK. This result is not particularly surprising, given that the phosphorylated form of Cav-1 has been found to associate with FAK, independent of caveolae. This may have significant consequences as this may regulate actin stress fiber formation, altering fibroblast/myofibroblast transformation and result in extracellular matrix deposition which is essential for wound healing¹⁰. It has also been noted that FAK signaling may be responsible for Cav-3 expression. Indeed, FAK inhibition suppressed normal increases in

Cav-3 expression during normal myoblast fusion and the authors postulate that this may result in impaired myoblast fusion³⁸, though whether Cav-1 is also involved has yet to be examined.

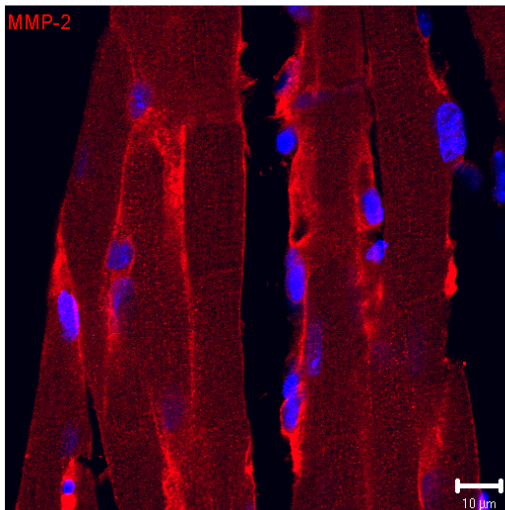
c-Kit, a receptor tyrosine kinase, has been implicated in playing roles in cell differentiation, cell survival and proliferation. Our finding that c-Kit protein expression is notably absent in Cav-1^{-/-} heart ICLC is also interesting, given the fact that c-Kit protein expression appears to be independent of Cav-1 in interstitial cells of Cajal in Cav-1^{-/-} small intestine²⁹. Others who have examined Cav-1^{-/-} ICLC using electron microscopy found that caveolae were completely absent³⁹, though they also report an absence of caveolae in capillary endothelial cells, which is not the case in our samples. Though the pacemaker activity of the interstitial cells of Cajal in the gut is well characterized (reviewed in ⁴⁰), much less is known about the function of ICLCs in the heart, though there is speculation that ICLCs may also be responsible for pacemaker activity and intercellular communication⁴.

In conclusion, our immunohistochemical and electron microscopic findings suggest that Cav-1 knockout in the heart may have consequences beyond the absence of the Cav-1 protein. A variety of different proteins, such as MMP-2, FAK and c-Kit are also notably perturbed in Cav-1^{-/-} cardiomyocytes, fibroblasts, ICLC and capillary endothelial cells. Whether these alterations result in altered function, either physiologically or pathophysiologically, remains to be seen.

Figure 3.1: MMP-2 in Cav-1^{+/+} and Cav-1^{-/-} left ventricular myocardium

MMP-2 (red) is found at the plasma membrane and the Z-lines of Cav-1^{+/+} left ventricular myocardium, while it is notably reduced in the Cav-1^{-/-} myocardium. Nuclei are stained with DAPI and appear blue. The scale bar represents 10 μm.

Cav-1^{+/+}



Cav-1^{-/-}

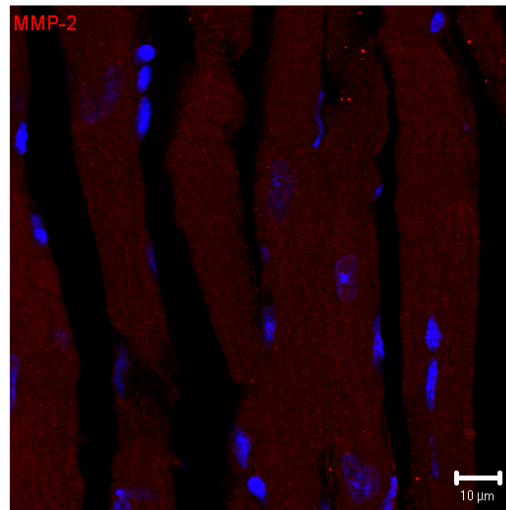


Figure 3.2: MMP-2 localization with caveolins in Cav-1^{+/+} and Cav-1^{-/-} left ventricular myocardium

(A-C) MMP-2 (red) appeared to have good co-localization (yellow) with Cav-1 (green) at cardiomyocyte plasma membranes (large black arrows), capillary endothelial cells (white arrows) and fibroblasts (small black arrows) in Cav-1^{+/+} sections. Partial co-localization between Cav-1 and MMP-2 is also observed at the Z-lines (arrowheads). (D) Cav-1 is absent and MMP-2 is markedly reduced at cardiomyocyte plasma membranes (black arrow), capillary endothelial cells and fibroblasts. (E-G) MMP-2 (red) co-localization with Cav-2 (green) appears only at capillary endothelial cells (black arrows). MMP-2 is also present in fibroblasts (white arrows). (H) Cav-2 (green) is present in capillary endothelial cells of Cav-1^{-/-} myocardium. (I-K) MMP-2 (red) and Cav-3 (green) are co-localized (yellow) at cardiomyocyte plasma membranes (black arrows), Z-lines (arrowheads) and partially at fibroblasts (white arrows). (L) In Cav-1^{-/-} myocardium, Cav-3 (green) appears in a similar pattern as seen in Cav-1^{+/+} myocardium. CM, cardiomyocyte; IS, interstitial space. The scale bar represents 10 μ m for A-H, and L and 20 μ m for I-K.

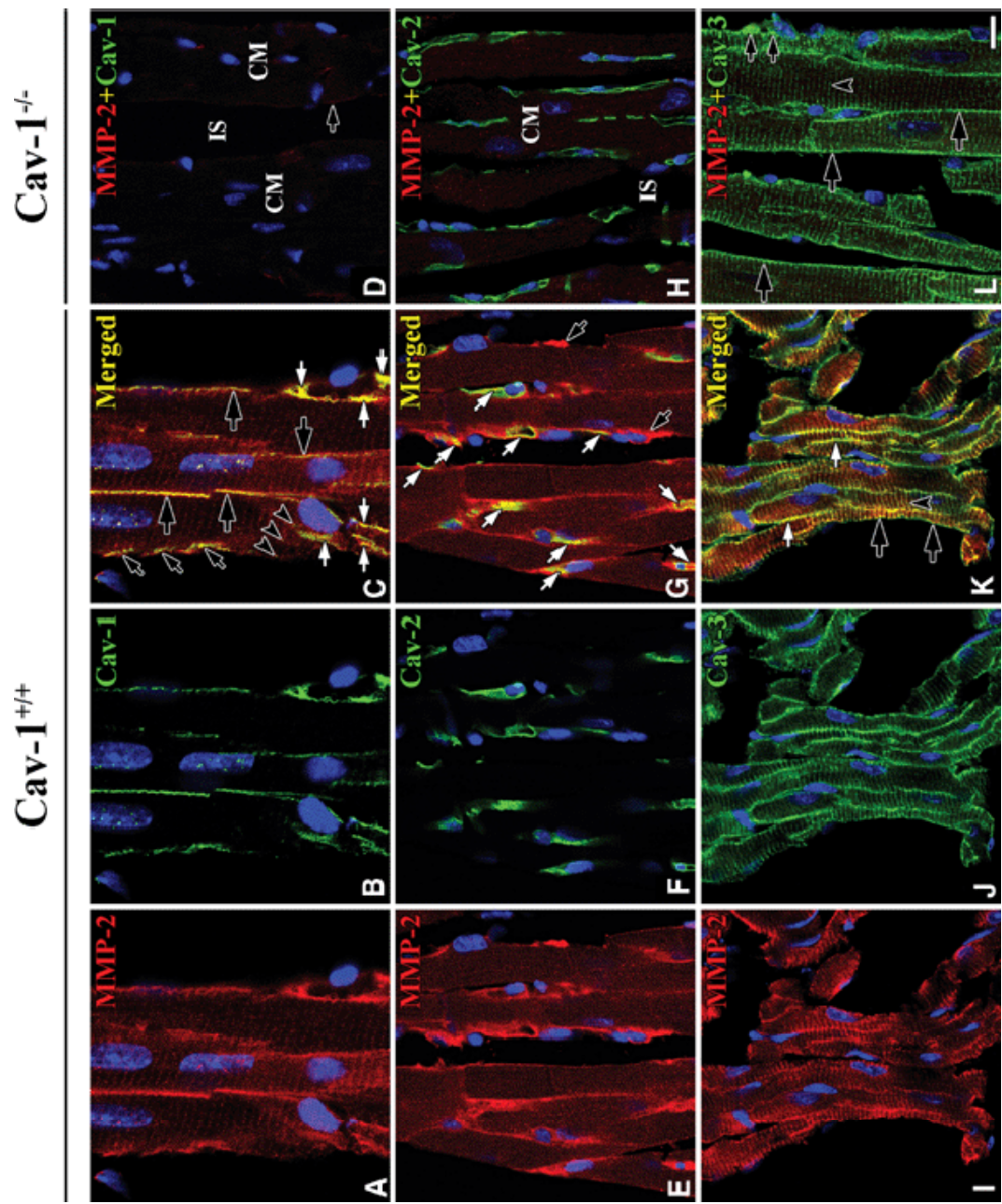


Figure 3.3: MMP-2 co-localization with FAK, DDR-2, vWF and c-Kit in Cav-1^{+/+} and Cav-1^{-/-} myocardium

(A-C) MMP-2 (green) and FAK (red) co-localize (black arrow) in Cav-1^{+/+} myocardium. (E-G) MMP-2 (green) and DDR-2 (red) also co-localize in Cav-1^{+/+} myocardium at fibroblasts (nucleus: large asterisk). (I-K) MMP-2 (red) and vWF (green) are co-localized at Cav-1^{+/+} capillary endothelial cells (nucleus: small asterisks). (M-O) MMP-2 (green) also co-localizes (arrows) with c-Kit (red) in Cav-1^{+/+} myocardial ICLC adjacent to cardiomyocytes. In Cav-1^{-/-}, FAK (red) (D) and c-Kit (red) (P) are completely absent in fibroblasts and ICLC, respectively, though FAK is present in the nuclei of all cells. vWF, however, is still present in capillary endothelial cells of Cav-1^{-/-} myocardium (L). Cell borders are outlined in white in (L). CM, cardiomyocyte; IS, interstitial space. Scale bar is 10 μ m for all images.

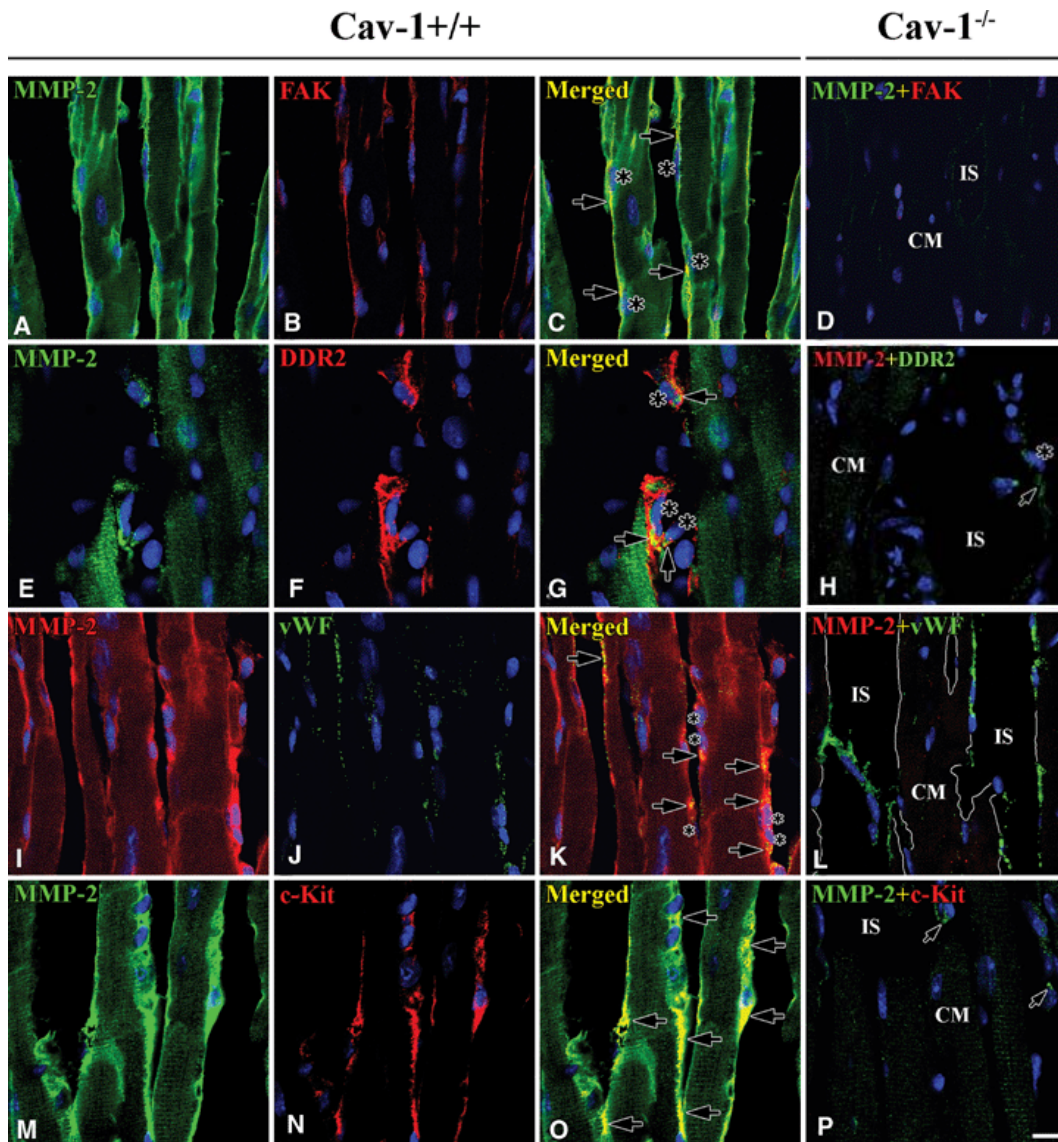


Figure 3.4: Co-localizations of caveolins in Cav-1^{+/+} and Cav-1^{-/-} myocardium

(A-C) Cav-1^{+/+} 3D reconstructed images (-45° rotation of y-axis) shows Cav-1 (red) in both fibroblasts (nucleus: large asterisks) and capillary endothelial cells (nucleus: small asterisks) while Cav-2 (green) is found only in capillary endothelial cells. Cav-1 and Cav-2 partially co-localize at capillary endothelial cells (black arrows), though Cav-1 also appears independently of Cav-2 in these (white arrows). (E-G) Cav-1 (red) co-localizes with Cav-3 (green) at cardiomyocyte membranes (large black arrow), fibroblasts (nucleus: large asterisks) and their interconnecting tails (small open arrow) and capillary endothelial cells (nucleus: small asterisks). Cav-1 is also found at cardiomyocyte Z-lines, partially co-localized with Cav-3. (I-K) Cav-2 (green) and Cav-3 (red) also co-localize at anastomotic (asterisk) capillary endothelial cells (arrows). (D) Cav-2 (green) is present in capillary endothelial cells of Cav-1^{-/-} myocardium. (H) Cav-3 (green) is found in cardiomyocyte plasma membranes, Z-lines and fibroblasts (asterisks) of Cav-1^{-/-} myocardium. (I) Cav-2 (green) and Cav-3 (red) co-localization (black arrows) in Cav-1^{-/-} myocardium in capillary endothelial cells is similar to that found in Cav-1^{+/+} myocardium. Co-localization (open arrows) of Cav-2 (green) and Cav-3 (red) at CEC is similar to that in Cav-1^{+/+}. CM, cardiomyocyte; IS, interstitial space. Scale bar is 10 μm for all images.

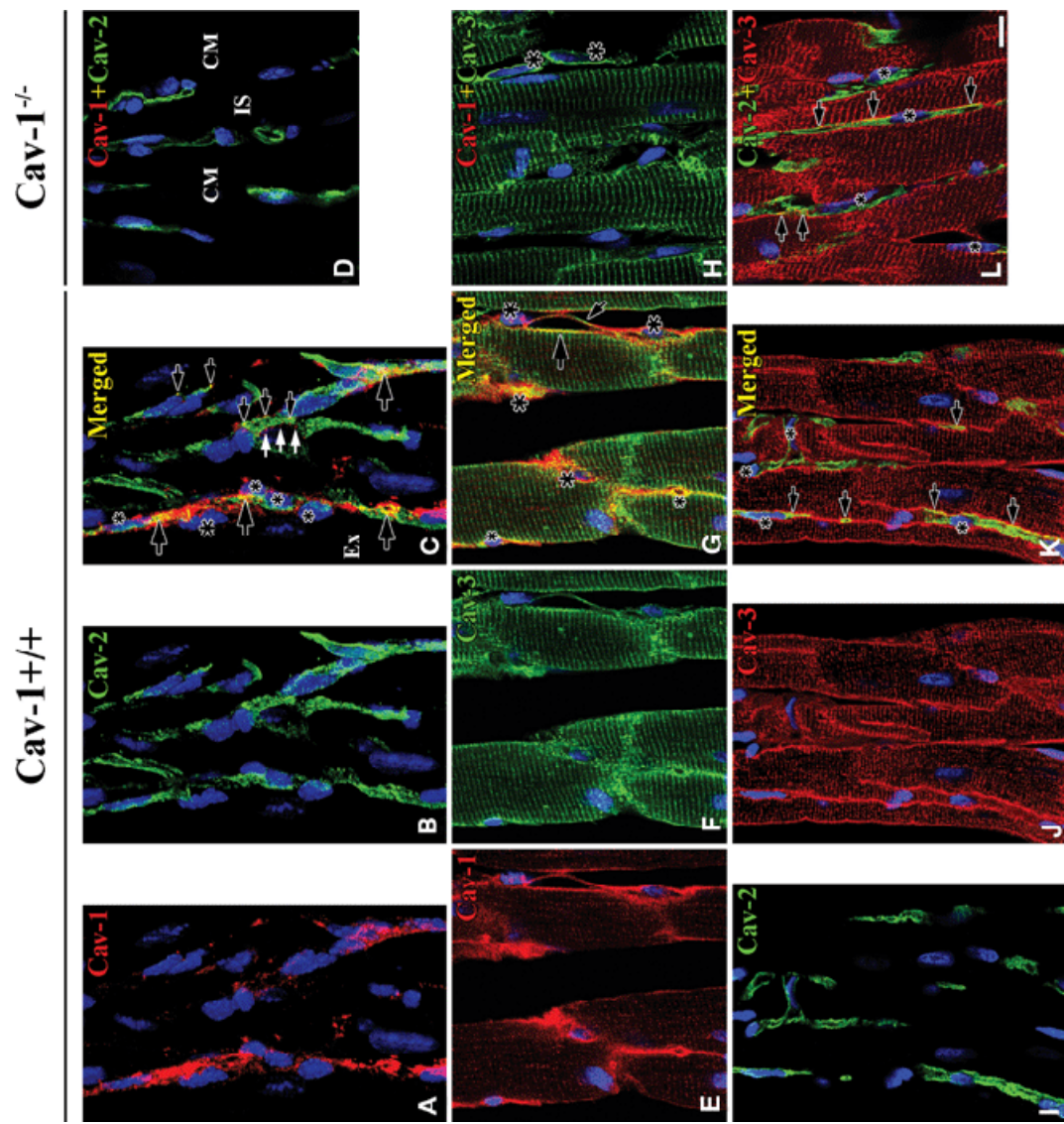


Figure 3.5: Cav-1 localization with FAK, DDR-2, vWF and c-Kit in Cav-1^{+/+} and Cav-1^{-/-} myocardium

(A-C) Cav-1 (green) co-localized with FAK (red) in fibroblasts with long tails (nucleus: asterisks) in Cav-1^{+/+} myocardium. (E-G) Cav-1 (red) co-localized (arrows) with vWF (green) at capillary endothelial cells (nucleus: asterisks) in Cav-1^{+/+} myocardium. (I-K) Cav-1 (red) co-localized (arrows) with DDR-2 (green) at some fibroblasts around a venule, but not others (asterisks) in Cav-1^{+/+} myocardium. (M-O) Cav-1 (green) co-localized with c-Kit (red) in Cav-1^{+/+} myocardium. (D, P) FAK and c-Kit are absent in Cav-1^{-/-} fibroblasts and ICLC, respectively. (H, I) vWF (green) and DDR-2 (green) appear in Cav-1^{-/-} capillary endothelial cells and fibroblasts, respectively. Borders of cells are outlined in white. CM, cardiomyocyte; IS, interstitial space. Scale bar is 10 μm for all images.

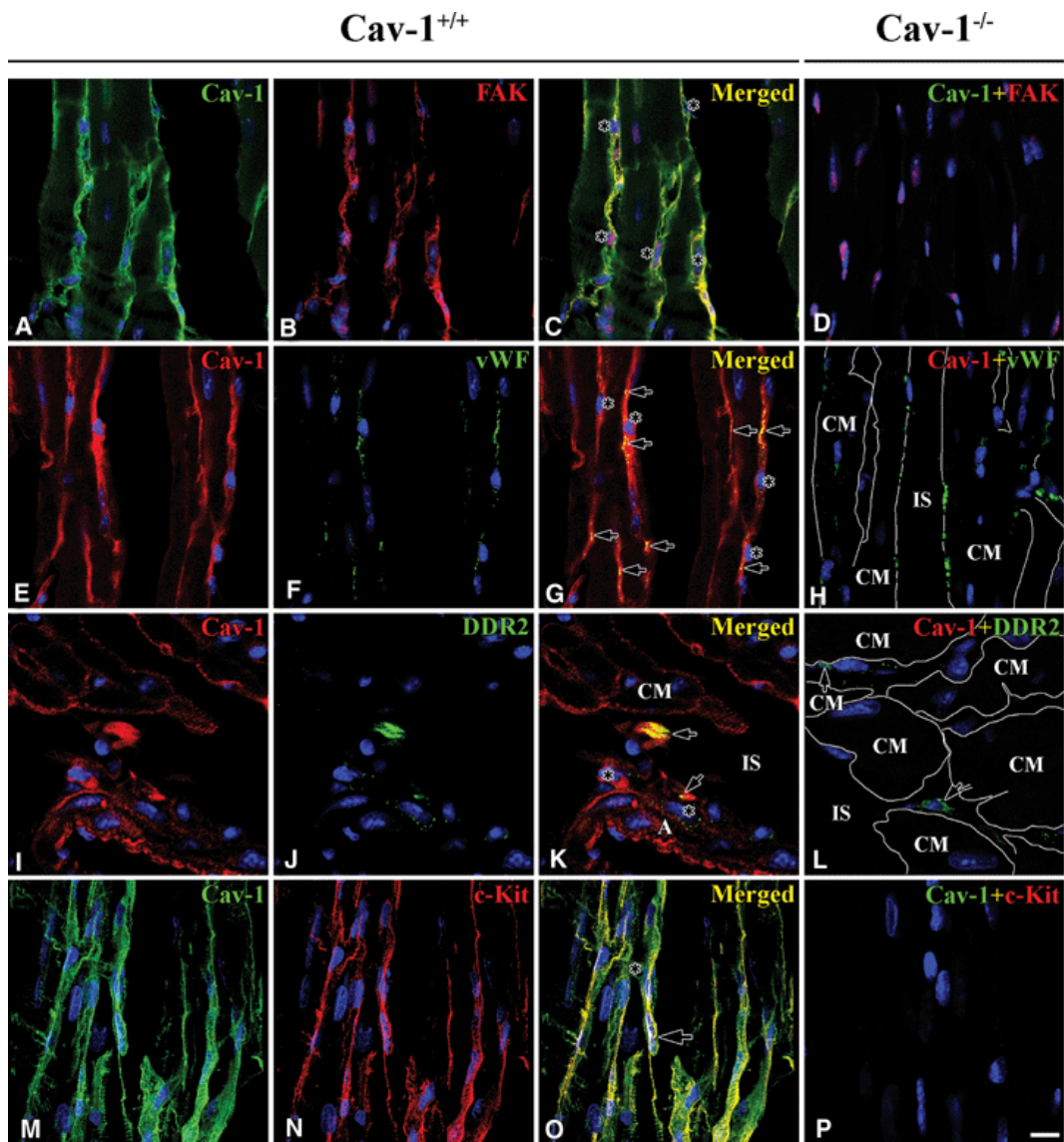
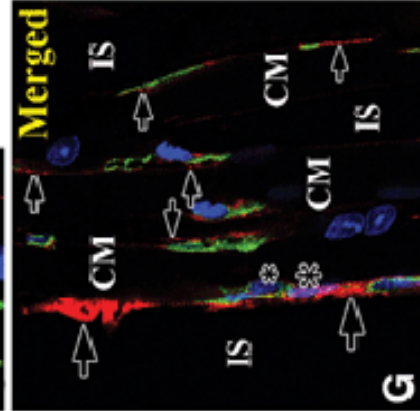
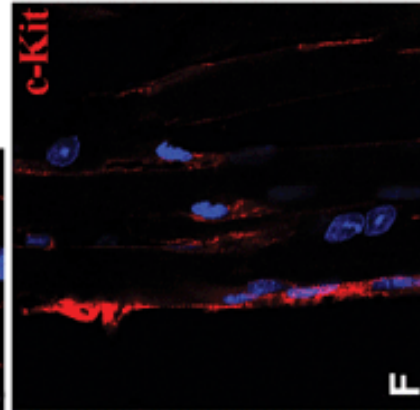
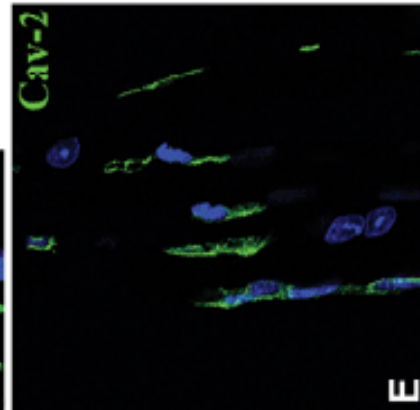
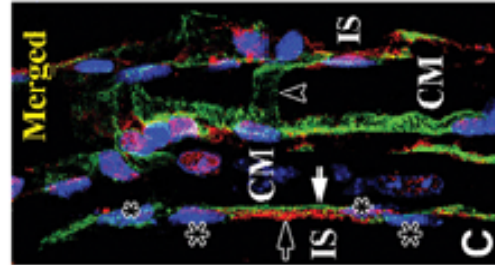
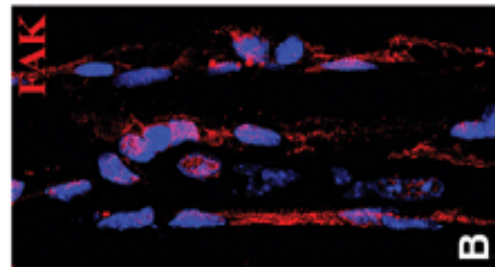
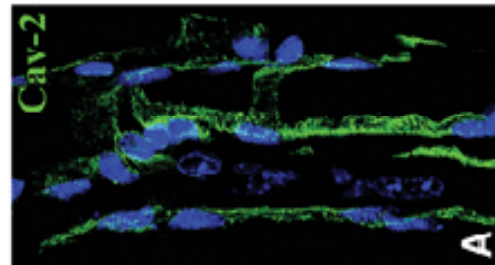


Figure 3.6: Co-localization of Cav-2 with FAK and c-Kit in Cav-1^{+/+} and Cav-1^{-/-} myocardium

(A-C) Cav-2 (green) (white arrow) appears only in capillary endothelial cells (nucleus: small asterisks) and FAK (red) (black arrow) only in fibroblasts (nucleus: large asterisks) of Cav-1^{+/+} myocardium. An anastomotic structure is also present (open arrowhead). (E-G) Cav-2 (green) does not co-localize with c-Kit (red). Black arrows indicate fibroblasts, large asterisk fibroblast nucleus and small asterisk capillary endothelial cell nucleus. (D, H) FAK, c-Kit and Cav-1 are all absent in Cav-1^{-/-} myocardium. Borders of cells are outlined in white. Cell borders are outlined in white. CM, cardiomyocyte; IS, interstitial space. Scale bar is 10 μm for all images.

Cav-1^{+/+}



Cav-1^{-/-}

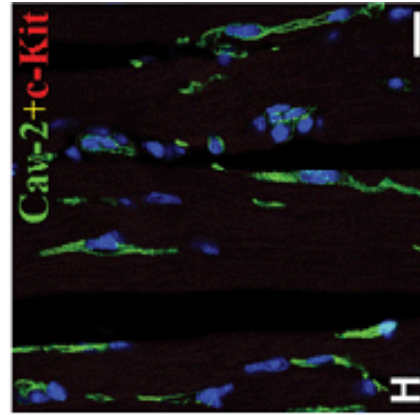
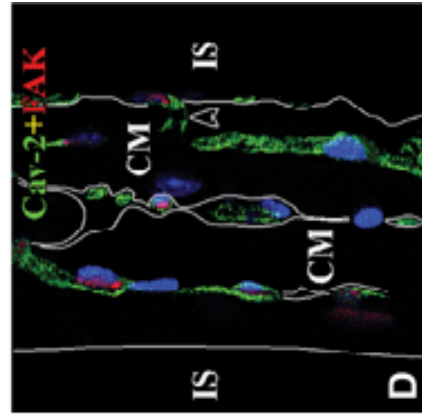


Figure 3.7: Co-localization of Cav-3 with FAK, DDR-2, vWF and c-Kit in Cav-1^{+/+} and Cav-1^{-/-} myocardium

(A-C) Cav-3 (green) and FAK (red) are partially co-localized (yellow) (large arrows) in Cav-1^{+/+} fibroblasts. Other fibroblasts are Cav-3-positive but FAK-negative (small arrows). (E-G) Cav-3-positive (red) fibroblasts are DDR-2-positive (green) and the two proteins are partially co-localized in fibroblast tails (arrows). (I-K) vWF-positive capillary endothelial cells (arrows) lack Cav-3. (M-O) ICLC are both Cav-3- (green) and c-Kit-positive (red) and the two proteins are partially co-localized (yellow) in Cav-1^{+/+} myocardium. (D, P) Cav-3 is present in cardiomyocyte plasma membranes, Z-lines and fibroblasts (arrows), but FAK and c-Kit are completely absent in Cav-1^{-/-} myocardium. (H, I) DDR-2 and vWF appear in Cav-1^{-/-} fibroblasts and capillary endothelial cells, respectively. FB and CEC, respectively. Scale bar is 10 μm for (A-D, I-P) and 7 μm for (E-G).

Cav-1^{+/+}

Cav-1^{-/-}

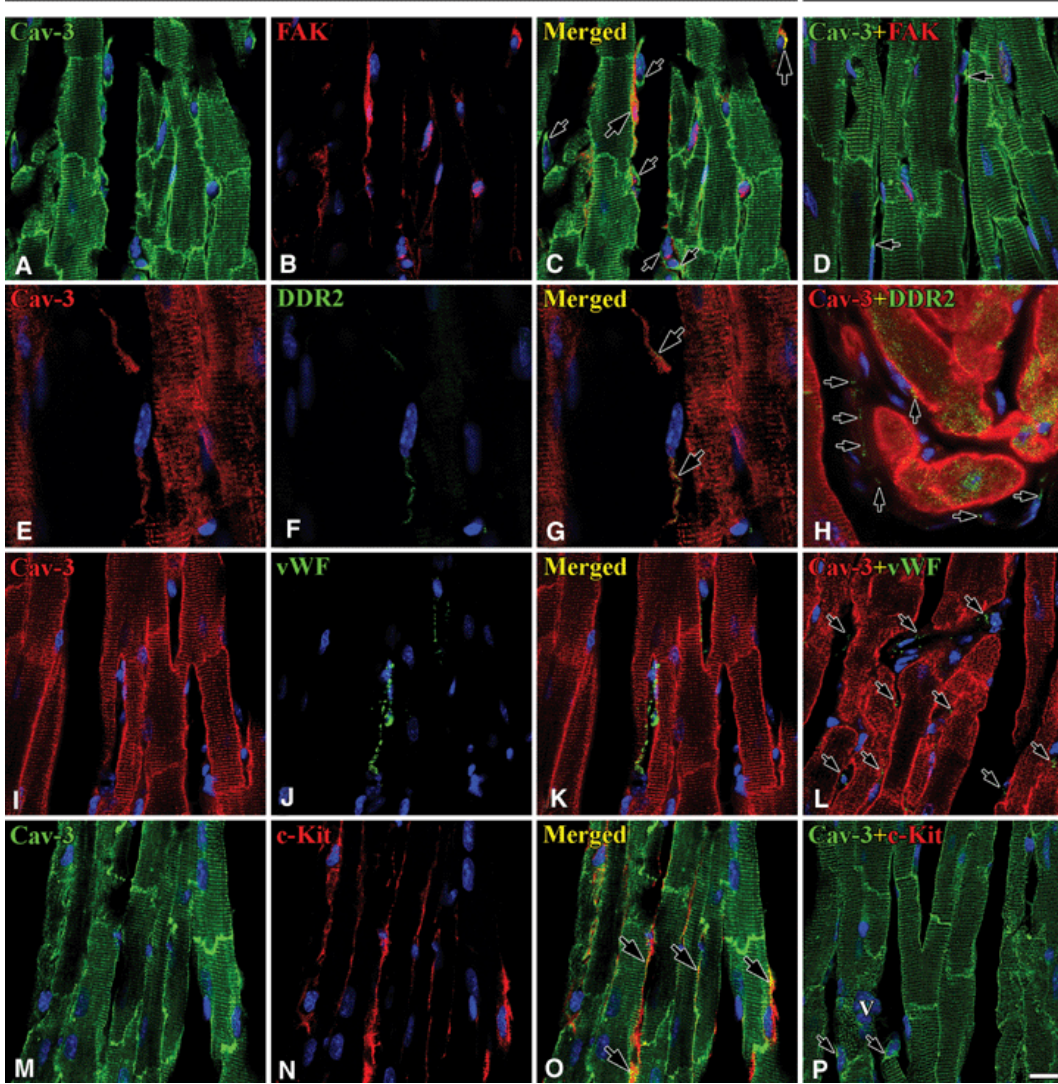


Figure 3.8: FAK, vWF, DDR-2 and c-Kit in Cav-1^{+/+} and Cav-1^{-/-} myocardium

(A-C) FAK (red, black arrows) appear in fibroblasts and vWF (green, white arrows) appear in capillary endothelial cells and do not co-localize in Cav-1^{+/+} myocardium. (E-G) Some DDR-2-positive fibroblasts (green, small open arrow) and are partially co-localized with c-Kit (red, small closed arrows). (D) vWF (green, arrows) is present in Cav-1^{-/-} capillary endothelial cells, but FAK is absent. (H) c-Kit is absent but DDR-2 (green, arrows) appears in fibroblasts of Cav-1^{-/-} myocardium. CM, cardiomyocyte; IS, interstitial space. Scale bar is 10 μ m for all images.

Cav-1^{-/-}

Cav-1^{+/+}

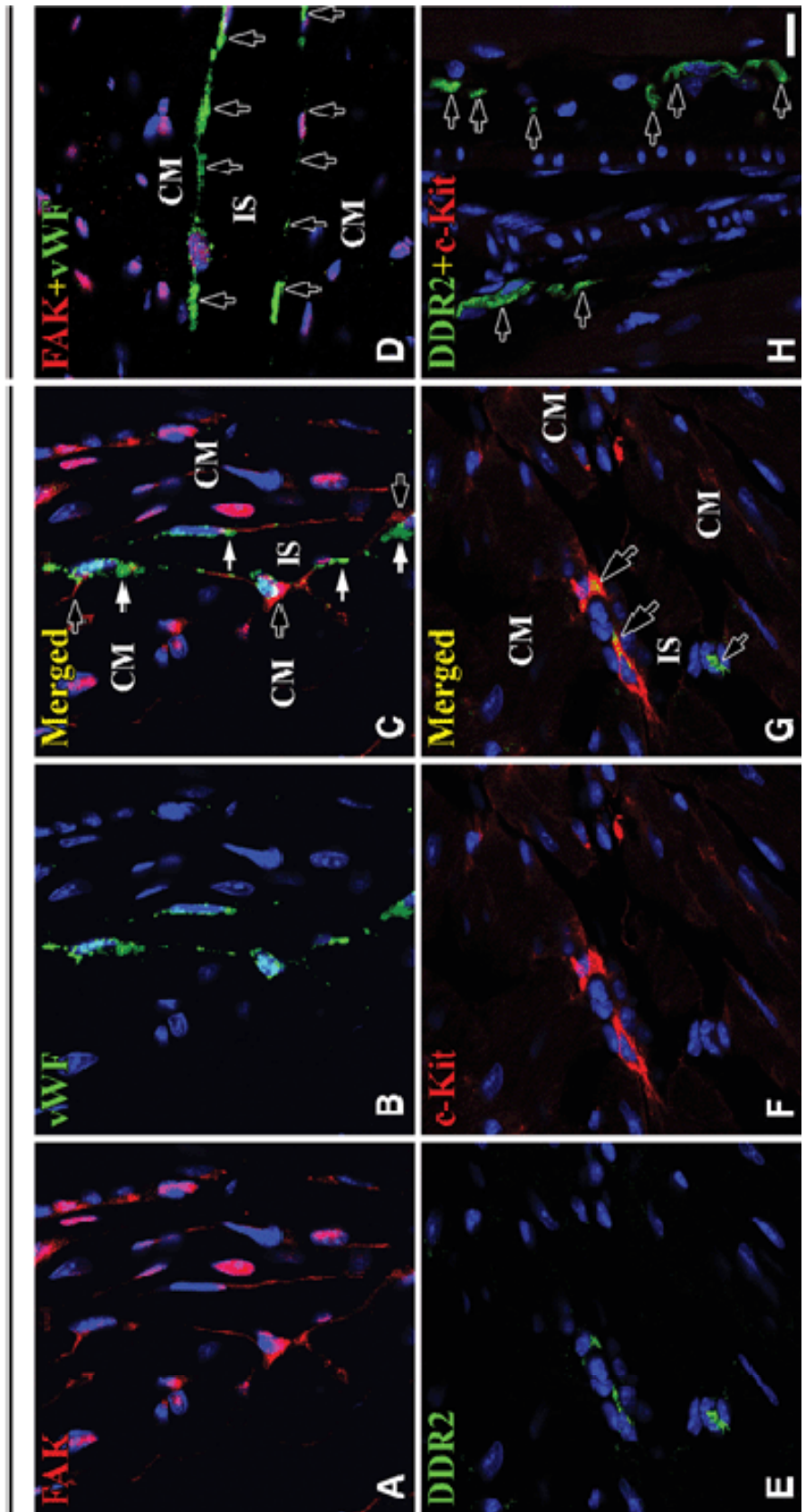


Figure 3.9: Electron micrographs of cardiomyocytes, fibroblasts and capillary endothelial cells in Cav-1^{+/+} and Cav-1^{-/-} myocardium

(A–C) Cardiomyocytes, fibroblasts and capillary endothelial cells are closely apposed in Cav-1^{+/+} myocardium. Caveolae (Cav, arrows) are present in cardiomyocyte sarcolemma and at capillary endothelial cell membrane. The sarcoplasmic reticulum (SR, closed thin arrows) is continuously arranged between myofilaments in cardiomyocytes. The endoplasmic reticulum (ER, open thin arrows) are in close proximity to Cav at capillary endothelial cell membranes. T-tubules (arrowheads) are adjacent to Cav and SR in cardiomyocytes and large mitochondria (m) are adjacent to the sarcolemma. Fibroblasts do not have Cav but have well-developed rough ER. (D-F) As in Cav-1^{+/+} myocardium, Cav-1^{-/-} myocardium shows that cardiomyocytes, fibroblasts and capillary endothelial cells are closely apposed. Some Cav (arrow) are present at the sarcolemma and the flat-shaped SR (closed thin arrows) found along the sarcolemma is discontinuous in Cav-1^{-/-} cardiomyocytes. T-tubules (arrowheads) are adjacent to SR. Capillary endothelial cells and fibroblasts have few Cav (FB-p, fibroblastic process).

Cav-1^{+/+}

Cav-1^{-/-}

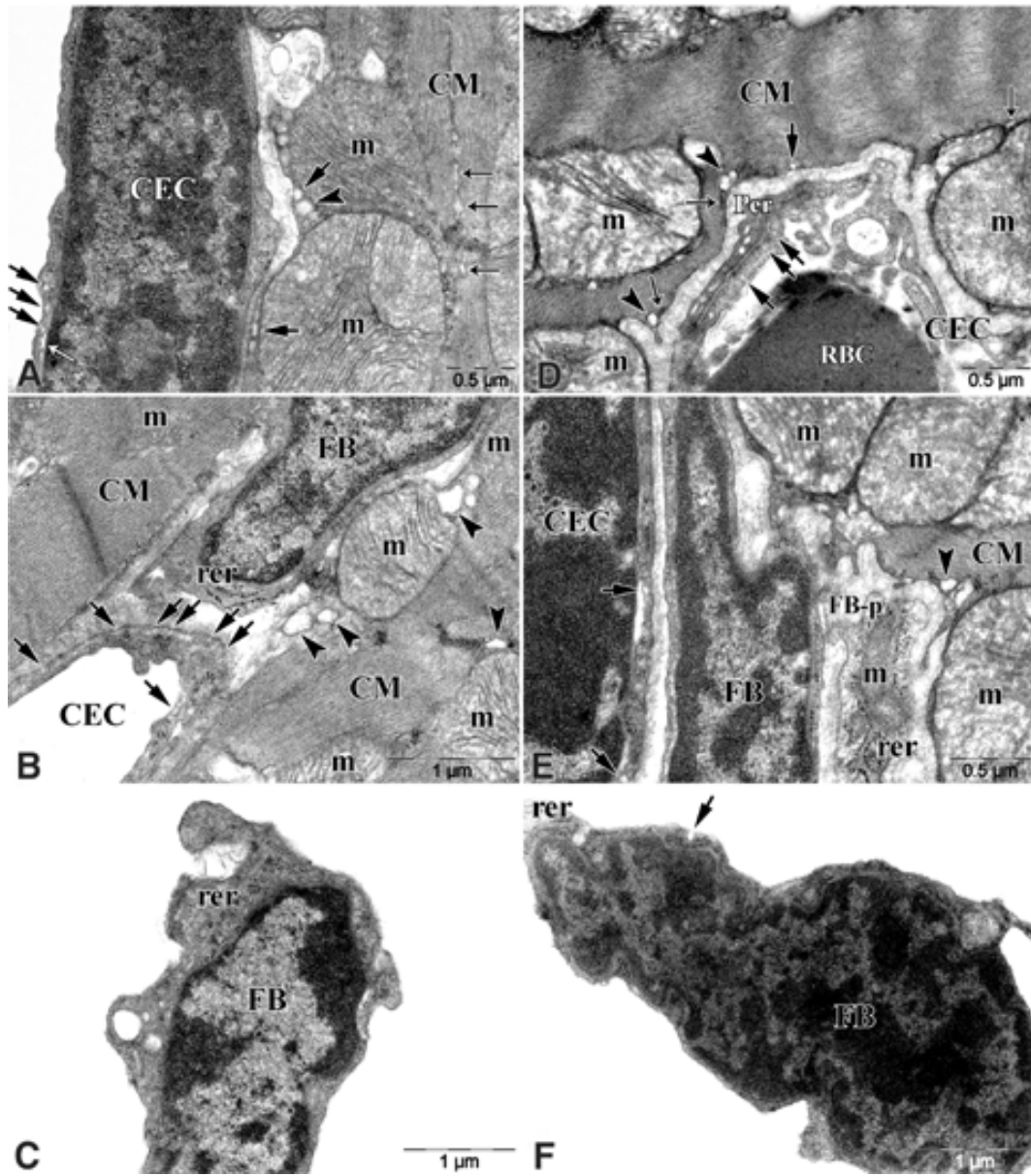


Table 3.1: Antibodies and sera used in experiments

Primary antibodies

Antibody	Host	Dilution	Cat. No.	Source
MMP-2	Mouse (monoclonal)	1:400	MAB3308	Chemicon International
Cav-1	Mouse (monoclonal)	1:50	610406	BD Transduction
Cav-2	Rabbit (polyclonal)	1:400	Ab2911	AbCam
Cav-3	Mouse (monoclonal)	1:200	610420	BD Transduction
Cav-3	Rabbit (polyclonal)	1:200	Ab2912	AbCam
FAK	Mouse (monoclonal)	1:100	MAB1144	Chemicon International
DDR2	Rabbit (polyclonal)	1:10	Ab5520	AbCam
vWF	Rabbit (polyclonal)	1:200	Ab7356	AbCam
c-Kit	Mouse (monoclonal)	1:20	32-9000	Invitrogen

Secondary antibodies

Fab fragment rabbit anti-mouse IgG	325-007-003	Jackson ImmunoResearch
Cy3 donkey anti-mouse IgG	715-165-151	Jackson ImmunoResearch
Alexa488 donkey anti-rabbit IgG	A-21206	Invitrogen

Sera

Mouse IgG blocking reagent	BMK-2202	Vector
Normal donkey serum	566460	Calbiochem

MMP-2, matrix metalloproteinase-2; Cav-1, caveolin-1; Cav-2, caveolin-2; Cav-3, caveolin-3; FAK, focal adhesion kinase; DDR2, discoidin domain receptor-2; vWF, von Willebrand factor; c-2kit, receptor tyrosine kinase

Table 3.2: Protein co-localization in Cav-1^{+/-} myocardium

Proteins	CM			CEC	FB	ICLC
	PM	Z-line	MF			
MMP-2 + Cav-1	+++	+	+	+++	+++	n/a
MMP-2 + Cav-2	-	-	-	+++	-	n/a
MMP-2 + Cav-3	+++	+++	+++	++	+	n/a
MMP-2 + FAK	-	-	-	-	+++	n/a
MMP-2 + DDR2	-	-	-	-	+++	-
MMP-2 + vWF	-	-	-	+++	-	-
MMP-2 + c-Kit	-	-	-	-	+/-	+++
Cav-1 + Cav-2	-	-	-	+	-	n/a
Cav-1 + Cav-3	++	+	+	++	+	n/a
Cav-2 + Cav-3	-	-	-	++	-	n/a
Cav-1 + FAK	-	-	-	-	+++	n/a
Cav-1 + vWF	-	-	-	+++	-	-
Cav-1 + DDR-2	-	-	-	-	+++	-
Cav-1 + c-Kit	-	-	-	-	+/-	+++
Cav-2 + FAK	-	-	-	-	-	n/a
Cav-2 + c-Kit	-	-	-	-	-	-
Cav-3 + FAK	-	-	-	-	++	n/a
Cav-3 + DDR2	-	-	-	-	+	-
Cav-3 + vWF	-	-	-	-	-	-
Cav-3 + c-Kit	-	-	-	-	+/-	++
FAK + vWF	-	-	-	-	-	-
DDR2 + c-Kit	-	-	-	-	+/-	+/-

CM, cardiomyocytes; FB, fibroblasts; CEC, capillary endothelial cells; ICLC, interstitial Cajal-like cells; PM, plasma membrane; MF, myofilaments; MMP-2, matrix metalloproteinase-2; Cav-1, caveolin-1; Cav-2, caveolin-2; Cav-3, caveolin-3; FAK, focal adhesion kinase; DDR2, discoidin domain receptor-2; vWF, von Willebrand factor; c-2kit, receptor tyrosine kinase; +, ++ and +++ indicate immunoreactive intensity; - means absent or inconspicuous; +/- means present occasionally; n/a means not applicable.

Table 3.3: Protein co-localization in Cav-1^{-/-} myocardium

Proteins	CM			CEC	FB	ICLC
	PM	Z-line	MF			
MMP-2 + Cav-1	-	-	-	-	-	n/a
MMP-2 + Cav-2	-	-	-	-	-	n/a
MMP-2 + Cav-3	-	+/-	+/-	+/-	-	n/a
MMP-2 + FAK	-	-	-	-	-	n/a
MMP-2 + DDR2	-	-	-	-	-	-
MMP-2 + vWF	-	-	-	-	-	-
MMP-2 + c-Kit	-	-	-	-	-	-
Cav-1 + Cav-2	-	-	-	-	-	n/a
Cav-1 + Cav-3	-	-	-	-	-	n/a
Cav-2+ Cav-3	-	-	-	+	+	n/a
Cav-1 + FAK	-	-	-	-	-	n/a
Cav-1 + vWF	-	-	-	-	-	-
Cav-1 + DDR-2	-	-	-	-	-	-
Cav-1 + c-Kit	-	-	-	-	-	-
Cav-2 + FAK	-	-	-	-	-	n/a
Cav-2 + c-Kit	-	-	-	-	-	-
Cav-3 + FAK	-	-	-	-	-	n/a
Cav-3 + DDR2	-	-	-	-	+	-
Cav-3 + vWF	-	-	-	-	-	-
Cav-3 + c-Kit	-	-	-	-	-	-
FAK + vWF	-	-	-	-	-	-
DDR2 + c-Kit	-	-	-	-	-	-

CM, cardiomyocytes; FB, fibroblasts; CEC, capillary endothelial cells; ICLC, interstitial Cajal-like cells; PM, plasma membrane; MF, myofilaments; MMP-2, matrix metalloproteinase-2; Cav-1, caveolin-1; Cav-2, caveolin-2; Cav-3, caveolin-3; FAK, focal adhesion kinase; DDR2, discoidin domain receptor-2; vWF, von Willebrand factor; c-2kit, receptor tyrosine kinase; +, ++ and +++ indicate immunoreactive intensity; - means absent or inconspicuous; +/- means present occasionally; n/a means not applicable.

3.5: References

1. Camelliti, P, McCulloch, AD, and Kohl, P. Microstructured cocultures of cardiac myocytes and fibroblasts: a two-dimensional in vitro model of cardiac tissue. *Microsc. Microanal.* 2005; 11:249-259.
2. Camelliti, P, Borg, TK, and Kohl, P. Structural and functional characterisation of cardiac fibroblasts. *Cardiovasc. Res.* 2005; 65:40-51.
3. Voldstedlund, M, Vinten, J, and Trandum-Jensen, J. cav-p60 expression in rat muscle tissues. Distribution of caveolar proteins. *Cell Tissue Res.* 2001; 306:265-276.
4. Hinescu, ME, Gherghiceanu, M, Mandache, E, Ciontea, SM, and Popescu, LM. Interstitial Cajal-like cells (ICLC) in atrial myocardium: ultrastructural and immunohistochemical characterization. *J. Cell Mol. Med.* 2006; 10:243-257.
5. Popescu, LM, Gherghiceanu, M, Hinescu, ME, Cretoiu, D, Ceafalan, L, Regalia, T, Popescu, AC, Ardeleanu, C, and Mandache, E. Insights into the interstitium of ventricular myocardium: interstitial Cajal-like cells (ICLC). *J. Cell Mol. Med.* 2006; 10:429-458.
6. Chen, Y, Li, Y, Zhang, P, Traverse, JH, Hou, M, Xu, X, Kimoto, M, and Bache, RJ. Dimethylarginine dimethylaminohydrolase and endothelial dysfunction in failing hearts. *Am. J. Physiol Heart Circ. Physiol* 2005; 289:H2212-H2219.
7. Feron, O, Belhassen, L, Kobzik, L, Smith, TW, Kelly, RA, and Michel, T. Endothelial nitric oxide synthase targeting to caveolae. Specific interactions with caveolin

- isoforms in cardiac myocytes and endothelial cells. *J. Biol. Chem.* 1996; 271:22810-22814.
8. Goldsmith, EC, Hoffman, A, Morales, MO, Potts, JD, Price, RL, McFadden, A, Rice, M, and Borg, TK. Organization of fibroblasts in the heart. *Dev. Dyn.* 2004; 230:787-794.
 9. LaFramboise, WA, Scalise, D, Stoodley, P, Graner, SR, Guthrie, RD, Magovern, JA, and Becich, MJ. Cardiac fibroblasts influence cardiomyocyte phenotype in vitro. *Am. J. Physiol Cell Physiol* 2007; 292:C1799-C1808.
 10. Swaney, JS, Patel, HH, Yokoyama, U, Head, BP, Roth, DM, and Insel, PA. Focal adhesions in (myo)fibroblasts scaffold adenylyl cyclase with phosphorylated caveolin. *J. Biol. Chem.* 2006; 281:17173-17179.
 11. Hinz, B, Celetta, G, Tomasek, JJ, Gabbiani, G, and Chaponnier, C. Alpha-smooth muscle actin expression upregulates fibroblast contractile activity. *Mol. Biol. Cell* 2001; 12:2730-2741.
 12. Manso, AM, Kang, SM, Plotnikov, SV, Thievessen, I, Oh, J, Beggs, HE, and Ross, RS. Cardiac fibroblasts require focal adhesion kinase for normal proliferation and migration. *Am. J. Physiol Heart Circ. Physiol* 2009; 296:H627-H638.
 13. Preissner ,KT and Potzsch, B. Vessel wall-dependent metabolic pathways of the adhesive proteins, von-Willebrand-factor and vitronectin. *Histol. Histopathol.* 1995; 10:239-251.

14. Makkar, RR, Price, MJ, Lill, M, Frantzen, M, Takizawa, K, Kleisli, T, Zheng, J, Kar, S, McClellan, R, Miyamota, T, Bick-Forrester, J, Fishbein, MC, Shah, PK, Forrester, JS, Sharifi, B, Chen, PS, and Qayyum, M. Intramyocardial injection of allogenic bone marrow-derived mesenchymal stem cells without immunosuppression preserves cardiac function in a porcine model of myocardial infarction. *J. Cardiovasc. Pharmacol. Ther.* 2005; 10:225-233.
15. Wagner, DD. The Weibel-Palade body: the storage granule for von Willebrand factor and P-selectin. *Thromb. Haemost.* 1993; 70:105-110.
16. Erni, R, Rossell, MD, Kisielowski, C, and Dahmen, U. Atomic-resolution imaging with a sub-50-pm electron probe. *Phys. Rev. Lett.* 2009; 102:096101.
17. Lalu, MM, Wang, W, and Schulz, R. Peroxynitrite in myocardial ischemia-reperfusion injury. In: Role of nitric oxide in heart failure. Heart Failure Reviews. Ed. Jugdutt BI. 2004; 7:359-369. Kluwer Academic Publishers, Hingham, MA, USA.
18. Wang, W, Schulze, CJ, Suarez-Pinzon, WL, Dyck, JR, Sawicki, G, and Schulz, R. Intracellular action of matrix metalloproteinase-2 accounts for acute myocardial ischemia and reperfusion injury. *Circulation* 2002; 106:1543-1549.
19. Sawicki, G, Leon, H, Sawicka, J, Sariahmetoglu, M, Schulze, CJ, Scott, PG, Szczesna-Cordary, D, and Schulz, R. Degradation of myosin light chain in isolated rat hearts subjected to ischemia-reperfusion injury: a new intracellular target for matrix metalloproteinase-2. *Circulation* 2005; 112:544-552.

20. Chow, AK, Cena, J, El-Yazbi, AF, Crawford, BD, Holt, A, Cho, WJ, Daniel, EE, and Schulz, R. Caveolin-1 inhibits matrix metalloproteinase-2 activity in the heart. *J. Mol. Cell Cardiol.* 2007; 42:896-901.
21. Puyraimond, A, Fridman, R, Lemesle, M, Arbeille, B, and Menashi, S. MMP-2 colocalizes with caveolae on the surface of endothelial cells. *Exp. Cell Res.* 2001; 262:28-36.
22. Park, DS, Woodman, SE, Schubert, W, Cohen, AW, Frank, PG, Chandra, M, Shirani, J, Razani, B, Tang, B, Jelicks, LA, Factor, SM, Weiss, LM, Tanowitz, HB, and Lisanti, MP. Caveolin-1/3 double-knockout mice are viable, but lack both muscle and non-muscle caveolae, and develop a severe cardiomyopathic phenotype. *Am. J. Pathol.* 2002; 160:2207-2217.
23. Head, BP and Insel, PA. Do caveolins regulate cells by actions outside of caveolae? *Trends Cell Biol.* 2007; 17:51-57.
24. Daniel, EE, Bodie, G, Mannarino, M, Boddy, G, and Cho, WJ. Changes in membrane cholesterol affect caveolin-1 localization and ICC-pacing in mouse jejunum. *Am. J. Physiol Gastrointest. Liver Physiol* 2004; 287:G202-G210.
25. El-Yazbi, AF, Cho, WJ, Boddy, G, and Daniel, EE. Caveolin-1 gene knockout impairs nitrergic function in mouse small intestine. *Br. J. Pharmacol.* 2005; 145:1017-1026.
26. El-Yazbi, AF, Cho, WJ, Boddy, G, Schulz, R, and Daniel, EE. Impact of caveolin-1 knockout on NANC relaxation in circular muscles of the mouse small intestine

- compared with longitudinal muscles. *Am. J. Physiol Gastrointest. Liver Physiol* 2006; 290:G394-G403.
27. Darby, PJ, Kwan, CY, and Daniel, EE. Caveolae from canine airway smooth muscle contain the necessary components for a role in Ca²⁺ handling. *Am. J. Physiol Lung Cell Mol. Physiol* 2000; 279:L1226-L1235.
 28. Daniel, EE, Jury, J, and Wang, YF. nNOS in canine lower esophageal sphincter: colocalized with Cav-1 and Ca²⁺-handling proteins? *Am. J. Physiol Gastrointest. Liver Physiol* 2001; 281:G1101-G1114.
 29. Cho, WJ and Daniel, EE. Colocalization between caveolin isoforms in the intestinal smooth muscle and interstitial cells of Cajal of the Cav1(+/-) and Cav1(-/-) mouse. *Histochem. Cell Biol.* 2006; 126:9-16.
 30. Sowa, G, Xie, L, Xu, L, and Sessa, WC. Serine 23 and 36 phosphorylation of caveolin-2 is differentially regulated by targeting to lipid raft/caveolae and in mitotic endothelial cells. *Biochemistry* 2008; 47:101-111.
 31. Capozza, F, Cohen, AW, Cheung, MW, Sotgia, F, Schubert, W, Battista, M, Lee, H, Frank, PG, and Lisanti, MP. Muscle-specific interaction of caveolin isoforms: differential complex formation between caveolins in fibroblastic vs. muscle cells. *Am. J. Physiol Cell Physiol* 2005; 288:C677-C691.
 32. Zhao, YY, Liu, Y, Stan, RV, Fan, L, Gu, Y, Dalton, N, Chu, PH, Peterson, K, Ross, J, Jr., and Chien, KR. Defects in caveolin-1 cause dilated cardiomyopathy and

- pulmonary hypertension in knockout mice. *Proc. Natl. Acad. Sci. U. S. A* 2002; 99:11375-11380.
33. Balijepalli, RC, Foell, JD, Hall, DD, Hell, JW, and Kamp, TJ. Localization of cardiac L-type Ca(2+) channels to a caveolar macromolecular signaling complex is required for beta(2)-adrenergic regulation. *Proc. Natl. Acad. Sci. U. S. A* 2006; 103:7500-7505.
34. El-Yazbi, AF, Cho, WJ, Schulz, R, and Daniel, EE. Caveolin-1 knockout alters beta-adrenoceptors function in mouse small intestine. *Am. J. Physiol Gastrointest. Liver Physiol* 2006; 291:G1020-G1030.
35. Squires, CE, Escobar, GP, Payne, JF, Leonardi, RA, Goshorn, DK, Sheats, NJ, Mains, IM, Mingoia, JT, Flack, EC, and Lindsey, ML. Altered fibroblast function following myocardial infarction. *J. Mol. Cell Cardiol.* 2005; 39:699-707.
36. Mollmann, H, Nef, HM, Kostin, S, von, KC, Pilz, I, Weber, M, Schaper, J, Hamm, CW, and Elsasser, A. Bone marrow-derived cells contribute to infarct remodelling. *Cardiovasc. Res.* 2006; 71:661-671.
37. Hakuno, D, Takahashi, T, Lammerding, J, and Lee, RT. Focal adhesion kinase signaling regulates cardiogenesis of embryonic stem cells. *J. Biol. Chem.* 2005; 280:39534-39544.
38. Quach, NL, Biressi, S, Reichardt, LF, Keller, C, and Rando, TA. Focal adhesion kinase signaling regulates the expression of caveolin 3 and beta1 integrin, genes essential for normal myoblast fusion. *Mol. Biol. Cell* 2009; 20:3422-3435.

39. Gherghiceanu, M, Hinescu, ME, and Popescu, LM. Myocardial interstitial Cajal-like cells (ICLC) in caveolin-1 KO mice. *J. Cell Mol. Med.* 2009; 13:202-206.
40. Sanders, KM. A case for interstitial cells of Cajal as pacemakers and mediators of neurotransmission in the gastrointestinal tract. *Gastroenterology* 1996; 111:492-515.

CHAPTER 4

PHYSIOLOGICAL AND PHARMACOLOGICAL CHALLENGES TO CAVEOLIN-1 KNOCKOUT MOUSE HEART

A version of this chapter is in press:

Chow AK, Daniel EE, Schulz R. Cardiac function is not significantly diminished in hearts isolated from young caveolin-1 knockout mice. *Am J Physiol Heart Circ Physiol*.

4.1: Introduction

Matrix metalloproteinases (MMPs) are a large family of zinc-dependent endopeptidases best known for their proteolysis of extracellular matrix proteins to effect remodeling of tissues in both physiological and pathological processes. MMPs have recently been shown to play a role in targeting non-matrix proteins such as cytokines and cell surface receptors^{1;2}. In contrast, MMP-2 has been shown to have biological actions within cardiac myocytes where it degrades susceptible sarcomeric and cytoskeletal proteins such as troponin I (TnI)³, myosin light chain-1 (MLC-1)⁴ and α -actinin⁵ under conditions of enhanced oxidative stress.

Because of the significant physiological and pathological actions of MMPs, it is essential that MMP activation and activity is tightly regulated. MMPs can be activated in a number of ways. MMPs are produced in a full length zymogen form and proteolytic removal of the N-terminal propeptide domain results in a truncated and active MMP. Alternatively, full length MMP can also be activated by peroxynitrite which oxidizes a cysteine residue in the propeptide domain that is coordinated with the catalytic zinc ion^{6;7}. We have also recently shown that MMP-2 is a phosphoprotein and its activity can be regulated via phosphorylation⁸.

The study of the regulation of extracellular MMP activity has traditionally centered on the examination of the tissue inhibitors of metalloproteinases (TIMPs), of which there are four⁹. The role of TIMPs in regulating MMP activity has been explored almost exclusively in the extracellular milieu and little is known about the regulation of intracellular MMPs.

One candidate protein that may be involved in the regulation of intracellular MMP activity is caveolin-1 (Cav-1). The caveolin family of proteins is made up of three integral membrane proteins that are found embedded in the inner leaflet of the plasma membrane. Cav-1 is the best characterized of the three and contains a domain known as the caveolin scaffolding domain which has been demonstrated to be responsible for the binding and inhibition of a number of intracellular proteins, including endothelial nitric oxide synthase¹⁰. MMP-2 has been shown to localize to the caveolae of both endothelial cells¹¹ and cardiomyocytes^{12;13} and evidence suggests that Cav-1 may play a role in the regulation of this enzyme. We showed that Cav-1 knockout mouse hearts have increased MMP-2 activity. MMP-2 proteolysis of an internally quenched, artificial fluorogenic substrate is inhibited by the caveolin scaffolding domain¹³.

The isolated working mouse heart model is a modification of the Langendorff isolated heart model and was developed by Neely et al. in 1973¹⁴. It is now often used to investigate the effects of pharmacological agents and/or I/R injury on heart function. The isolated working heart is a better approximation of physiological heart function than the Langendorff model. In the Langendorff model, the perfusate solution is retrogradely perfused through the aorta and enters the coronary circulation through the ostia at the base of the aorta. Consequently, the ventricles are not actually filled with perfusate and do not perform work to eject it. In the isolated working heart model, the perfusate enters the heart through a cannula inserted into the left atrium, where it then enters into the left ventricle and is ejected by the ventricle through the aorta, the same path as blood in the left side of the *in vivo* heart. The isolated working heart model offers an additional benefit over the Langendorff model as differing preload and afterload perfusion pressures can be used.

Isoproterenol is a commonly used β -adrenergic agonist that has positive inotropic and chronotropic effects on the heart. Isoproterenol stimulates both β_1 and β_2 -adrenoreceptors and capable of initiating a number of downstream effects, including activation of protein kinase A¹⁵, protein kinase C and phosphorylation of troponin I¹⁵ (see Chapter 6).

In this study, we used an isolated working mouse heart model to elucidate whether increased MMP-2 activity found in Cav-1 knockout hearts affects cardiac function during physiological or pharmacological challenges. We used in Cav-1 knockout mouse hearts at an age (6-8 weeks old) when they show no obvious signs of pathology as older Cav-1^{-/-} mice show signs of cardiac hypertrophy¹⁶ and structural changes¹⁷.

4.2: Materials and methods

All experiments were performed in accordance with the Canadian Council on Animal Care *Guide to the Care and Use of Experimental Animals*.

4.2.1: Animals

Male 6- to 8-wk-old Cav-1^{-/-} (cav < tm 1 M Is > /J) and control [(B6 129 SF2/J) (Cav-1^{+/+})] mice were obtained from Jackson Laboratories (Bar Harbor, ME, USA).

4.2.2: Isolated working mouse heart

Mice were injected with 100 IU of heparin (i.p) 10 minutes prior to euthanasia by intraperitoneal pentobarbital injection. Hearts were rapidly excised from deeply anesthetized mice and placed immediately into an ice-cold Krebs-Henseleit bicarbonate

solution (118 mM NaCl, 25 mM NaHCO₃, 4.7 mM KCl, 1.2 mM MgSO₄, 1.2 mM KH₂PO₄, 2.25 mM CaCl₂, 0.5 mM EDTA, and 11.1 mM glucose, oxygenated with 95% O₂ - 5% CO₂ (pH 7.4)). The aorta was then cannulated with a 20 gauge cannula and perfused in Langendorff mode at 60 mmHg constant hydrostatic pressure at 37°C with the aforementioned Krebs-Henseleit solution. The left atrium was then cannulated through the pulmonary opening and the heart is switched from the Langendorff mode to the working mode whereby the heart is perfused with a recirculating Krebs-Henseleit bicarbonate solution (total volume: 125 mL) at 37°C supplemented with 0.2% bovine serum albumin, 5 mM pyruvate, and 100 mU/L human insulin and continuously gassed with 95% O₂ - 5% CO₂ (pH 7.4) at a left atrial preload pressure of 11.5 mmHg and an aortic afterload pressure of 50 mmHg. Spontaneously beating hearts were allowed to equilibrate aerobically for 30 min. Following this the hearts were physiologically challenged by step-wise adjustment of the preload pressure to 7, 10, 15, 20 and 22.5 mmHg, for 2 min at each pressure. The preload was then returned to 11.5 mmHg for 20 min to allow hearts to recover from the preload challenge. The hearts were then pharmacologically challenged by sequential administration of 0.1, 1, 10 and 100 nM DL-isoproterenol (Calbiochem) for 2 min at each concentration. Functional measurements were continuously recorded with the MP100 system from AcqKnowledge (BioPac Systems, Santa Barbara, CA, USA) for a total of 90 min. Cardiac output was measured via a Doppler flow probe (Transonic Systems, Ithaca, NY, USA) placed in the left atrial line while aortic flow was measured using a probe in the aortic afterload line. Heart rate and peak systolic and developed (systolic – diastolic) pressures were measured with a pressure transducer (Harvard Apparatus, South Natick, MA), placed at the level of the heart, in the aortic line. Cardiac work was calculated as the product of peak systolic

pressure and cardiac output. Coronary flow was calculated as the difference between cardiac output and aortic flows. The rate pressure product is the product of the heart rate and the peak systolic pressure. At the end of the perfusion whole hearts were then clamped with Wollenberger tongs pre-cooled in liquid nitrogen and stored at -80°C until used.

4.2.3: Langendorff mouse hearts

To control for the effects of *in vitro* heart perfusion, hearts were isolated from an additional series of heparin-treated mice as above and perfused with Krebs-Henseleit solution only in Langendorff mode at 60 mmHg constant hydrostatic pressure for 10 or 90 min at 37°C with the aforementioned Krebs-Henseleit bicarbonate solution and frozen as above.

4.2.4: Tissue preparation

Frozen whole heart tissues were crushed and powdered in liquid nitrogen and weighed. Four volumes (weight/volume) of ice-cold homogenization buffer (pH 7.4; 50 mM Tris, 31 mM sucrose, 1 mM DL-dithiothreitol, 0.1% Triton X-100, 10 µg/L soybean trypsin inhibitor, 10 mg/L leupeptin, 2 g/L aprotinin, and 100 mg/L phenylmethylsulfonyl fluoride) was added to the tissue. The powdered tissues were then homogenized with a Polytron, 3x30 s with 30 s of cooling in ice between each cycle. The samples were then centrifuged (4°C, 1000 × *g*, 5 min) and the supernatants were used for determination of enzyme activities and Western blot analysis. Protein concentration was assessed by the bicinchoninic acid method using bovine serum albumin as a reference standard.

4.2.5: Western blotting

40 µg protein of each whole heart sample was run in 10% SDS-PAGE under reducing conditions. Human recombinant MMP-2 and troponin I were loaded as controls. Following electrophoresis, samples were electroblotted onto polyvinylidene difluoride membranes. The membranes were then blocked at room temperature for 1 hour with 5% milk, followed by an overnight incubation at 4°C with primary antibodies (1:1000 monoclonal mouse anti-human troponin I (Novogen), 1:1000 monoclonal mouse anti human α -actinin (Chemicon), 1:1000 monoclonal mouse anti- human MMP-2 (Chemicon)). These membranes were then probed with 1:5000 anti mouse horseradish peroxidase conjugated secondary antibody and incubated with ECL or ECL Plus (Amersham) for 5 minutes before being exposed to film. Membranes were Ponceau stained to ensure equal loading of proteins¹⁸.

4.2.6: Gelatin zymography

40 µg protein of each sample was run in an 8% polyacrylamide gel containing 2 mg/mL gelatin. Conditioned media from HT-1080 human fibrosarcoma cells were used as a standard for MMP-2 activity. Following electrophoresis, the gel was washed 3x20 min in 2.5% Triton X-100. The gel was then incubated in 50 mM Tris HCl, 150 mM NaCl, 5 mM CaCl₂, pH. 7.6 for 30 h at 37°C prior to being stained with 0.05% Coomassie Brilliant Blue in 25% methanol: 10% acetic acid for 1 h and destained with 4% methanol: 8% acetic acid for 30 min.

4.2.7: Data analysis

Western blots and zymograms were analyzed using Image J software (NIH). Statistics and graphs were compiled using GraphPad Prism 4.03.

4.2.8: Statistics

Data are expressed as mean \pm SEM. Functional differences between groups were analyzed by two-way repeated measures analysis of variance and if significant, followed by Bonferroni post-hoc tests. Differences in protein levels were analyzed using Student's t-test. Gelatinolytic activity was measured by Student's t-test or two-way analysis of variance, as appropriate. P values of less than 0.05 were considered statistically significant.

4.3: Results

4.3.1: Response of caveolin-1 knockout mouse hearts to preload challenge

Following the equilibration period, there were no differences between Cav-1^{-/-} (N=6) and Cav-1^{+/+} (N=9) in any of the measured or calculated functional parameters (heart rate, cardiac output, aortic flow, cardiac work, coronary flow, developed pressure, peak systolic pressure, rate pressure product. During the preload challenge, the Cav-1^{+/+} and Cav-1^{-/-} mouse hearts did not significantly differ from each other at 7, 10 or 15 mmHg (Fig. 4.1). At preload pressures of 15, 20 and 22.5 mmHg, Cav-1^{-/-} hearts demonstrated a significantly increased coronary flow when compared with Cav-1^{+/+} hearts (P<0.05 at 15 mmHg, P<0.01 at 20 mmHg, P<0.001 at 22.5 mmHg) (Fig. 4.1). Also, at 20 and 22.5 mmHg of left atrial preload pressure, Cav-1^{-/-} hearts demonstrated an increased cardiac output when compared with controls (P<0.05 at 20 mmHg, P<0.001 at 22.5 mmHg). Consequently, cardiac work is also increased at these pressures in Cav-1^{-/-} hearts (P<0.05 at 20 mmHg, P<0.01 at 22.5 mmHg). An interaction effect of preload and strain are observed in cardiac output (P=0.001), cardiac work (P=0.0034), heart rate

($P=0.0373$), and coronary flow ($P<0.0001$) (Fig. 4.1) were also observed. No differences were observed in aortic flow, peak systolic pressure, developed pressure or rate pressure product measures.

4.3.2: Response of caveolin-1 knockout mouse hearts to isoproterenol challenge

Administration of isoproterenol caused a concentration-dependent increase in heart rate and developed pressure, and consequently, rate-pressure product in the hearts from both strains of mice (Fig. 4.2). An interaction effect of isoproterenol concentration and mouse strain was observed in heart rate ($P=0.0389$), aortic flow ($P=0.0156$) and rate pressure product ($P=0.0458$) measures. 100 nM of isoproterenol resulted in a significantly higher heart rate ($P<0.05$) and rate pressure product ($P<0.05$) in Cav-1^{-/-} hearts compared with controls. Coronary flow was increased in Cav-1^{-/-} hearts at all concentrations of isoproterenol ($P<0.05$) (Fig 4.2).

4.3.3: MMP-2 activity and protein content in Cav-1^{-/-} mouse hearts following preload and adrenergic challenges

Gelatin zymography did not reveal any differences in MMP-2 activity between Cav-1^{+/+} and Cav-1^{-/-} mouse hearts (Fig. 4.3A). Additionally, MMP-2 protein content is not different between the Cav-1^{+/+} and Cav-1^{-/-} hearts (Fig. 4.3B). Fig. 3C illustrates the amount of MMP-2 activity per unit of MMP-2 protein.

4.3.4: Sarcomeric and cytoskeletal protein levels in Cav-1^{-/-} mouse hearts following preload and isoproterenol challenges

Examination of the levels of sarcomeric and cytoskeletal proteins known to be proteolyzed by MMP-2 in the Cav-1^{+/+} and Cav-1^{-/-} hearts did not reveal any differences between the two strains. No differences in the levels of troponin I (Fig. 4.4A) or α -actinin (Fig. 4.4B) were apparent in the hearts from either Cav-1^{+/+} or Cav-1^{-/-} mice.

4.3.5: MMP-2 activity in Cav-1^{-/-} mouse hearts Langendorff perfused for 10 or 90 minutes

The 72 kDa gelatinolytic activity of both the Cav-1^{+/+} and Cav-1^{-/-} mouse hearts is significantly greater in hearts that were flushed for 10 min when compared with hearts flushed for 90 min ($P < 0.0001$) (Fig. 4.5). Cav-1^{-/-} hearts also demonstrate higher gelatinolytic activity when compared with Cav-1^{+/+} hearts after 10 min of perfusion ($P = 0.0332$).

4.4: Discussion

The purpose of this study was to evaluate whether the Cav-1^{-/-} mouse hearts, which have previously been shown to have higher basal levels of MMP-2 activity¹³, are functionally different from their wild-type controls when exposed to stimuli similar to what may be experienced physiologically. Interestingly, following the physiological and pharmacological challenges, no difference in MMP-2 activity was observed between Cav-1^{+/+} and Cav-1^{-/-} hearts (90 min total perfusion time). This is in contrast to hearts that were perfused for 10 min before freezing, where Cav-1^{-/-} hearts show significantly

increased MMP-2 activity¹³ (Fig. 5). As a result of the challenges and/or longer perfusion times in this study, the MMP-2 in hearts may have been released into the perfusate consistent with the observation that myocardial MMP-2 activity is lost over extended perfusion time due to the mild oxidative stress inherent in isolated heart perfusions¹⁹.

Perhaps as a result of differential losses of MMP-2, Cav-1^{-/-} mouse hearts fared better during preload challenges than Cav-1^{+/+} hearts. This may also be the result of reduced membrane binding of MMP-2 by Cav-1 in Cav-1^{-/-} hearts. As a result, MMP-2 would be more readily removed from the heart during perfusion and thus, would not have the opportunity to cause damage. The improved function of the Cav-1^{-/-} hearts during the preload challenge is particularly evident in the coronary flow measurements. We hypothesize that as a result of the absence of Cav-1, eNOS activity might be increased²⁰ and thus results in vasodilatation which is reflected as an increased cardiac output and consequently cardiac work. Echocardiographic data obtained by other groups demonstrate a lack of functional difference between Cav-1^{-/-} and Cav-1^{+/+} hearts from 8-10 week old mice²¹, though these mice were not exposed to changing preloads or adrenergic stimulation.

The β -adrenergic receptor has been previously found to be localized to caveolae in the cardiac myocyte²² and co-localized with caveolin-3²³. It has been proposed that caveolin is responsible for scaffolding the components of the β -adrenergic signaling cascade²⁴, which would result in a rapid and effective conveyance of signal propagation. Thus we hypothesized that this signal transduction would be perturbed in hearts that lack Cav-1. The lack of difference between Cav-1^{-/-} and Cav-1^{+/+} heart function in response to an adrenergic agonist was unexpected, given that Cav-1^{-/-} mice have altered

adrenergic receptor function in the gut²⁵. This altered function in the gut did not appear to reflect altered β -adrenergic receptor location, but was likely a result of perturbed protein kinase A activity that is downstream of the β -adrenergic receptor²⁶. Perturbed adrenergic response in Cav-1^{-/-} hearts has not yet been reported. In fact, another group using a dog model of heart failure hypothesized that a relative increase in the amount of caveolin protein would augment the NO synthase pathway response to β -adrenergic agonists as a result of compartmentalization of the pathway elements to plasma membrane agonist receptors, while at the same time inhibiting basal NOS activity, since caveolin acts as a NOS inhibitor²⁷.

Age related changes have also been observed in these Cav-1^{-/-} mouse hearts and may play a significant role in the similar biochemical results between the knockout and wild-type mouse strains. In this study, the mice were between 6 and 8 weeks of age, which is younger than many studies which report changes in heart function and morphology^{16,17,28}. Further confounding this issue is the fact that many studies that use Cav-1^{-/-} mouse hearts do not indicate the age at which these mice were used, which may further explain literature discrepancies regarding the heart function of these mice. This issue is of particular importance, since changes in the structure of these hearts is evident as early as 10 weeks of age¹⁷. By 5 months of age, hypertrophic changes are apparent in the Cav-1^{-/-} mice and functional changes are measurable by echocardiography¹⁶. We chose to use mice between 6 and 8 weeks of age to elucidate whether the alterations in MMP-2 previously described¹³ would lead to functional changes independent of the structural changes observed by others. Whether these changes occur subsequently as a result of the observed pulmonary hypertension, or concurrently, are not yet fully elucidated. It is also possible that the structural and

functional changes observed in these hearts are a result of prolonged exposure to increased MMP-2 activity, particularly as it has been shown that MMP-2 can play a role in the mechanisms leading to hypertrophic changes²⁹⁻³¹.

Following I/R injury, MMP-2 was shown to cause degradation of important sarcomeric and cytoskeletal proteins²⁻⁵. Also, a decrease in myocardial Cav-1 content has been observed following ischemia and reperfusion injury³². Both of these observations, as well as the fact that the caveolin scaffolding domain has been shown to inhibit MMP-2 activity¹³, supports the hypothesis that Cav-1 may play a role in regulating the potentially destructive properties of this intracellular enzyme. The experimental design of this study may have obscured any potential changes observed in MMP-2 substrates. The administration of isoproterenol could lead to activation of numerous protein kinases, including PKA and PKC, both of which have been shown to be phosphorylated and diminish the activity of MMP-2 *in vitro*⁸. Though the data from this study does not indicate a role of Cav-1 regulation of MMP-2 during aerobic perfusion of young mouse hearts, this does not exclude a role of this protein during periods of more intense oxidative stress or later in life.

Figure 4.1: Functional measurements of isolated working hearts in response to step-wise increase in preload pressure from Cav-1^{+/+} and Cav-1^{-/-} mice

Cav-1^{+/+} (○) (N=9) and Cav-1^{-/-} (●) (N=6). * P<0.05 within group differences. † P<0.05 between group differences. P values are listed where interaction effects of preload and strain effects are significant. Error bars indicate ± SEM where they exceed the symbol size.

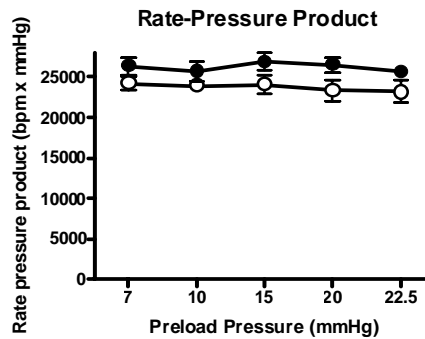
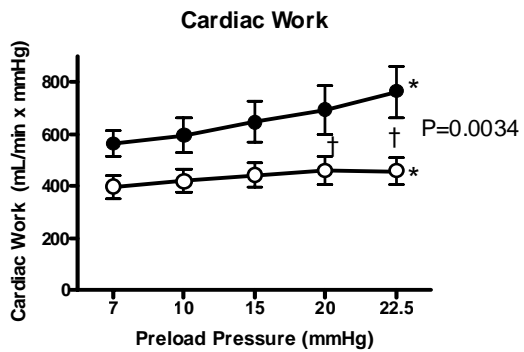
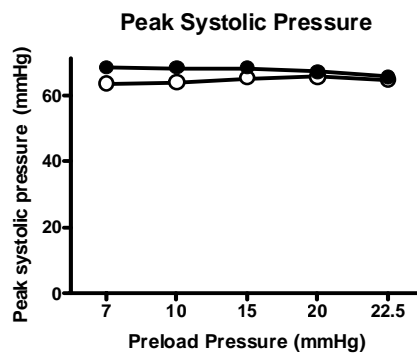
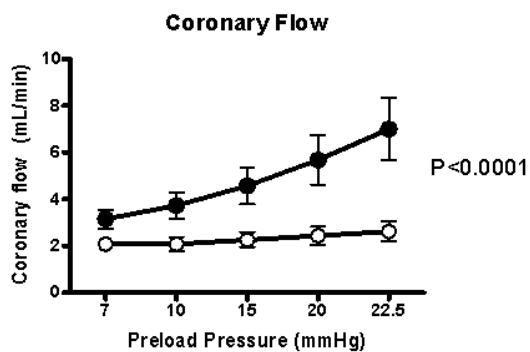
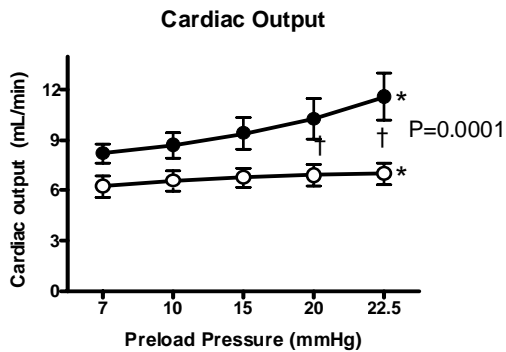
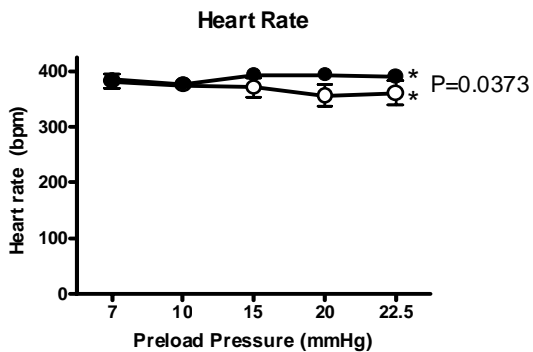


Figure 4.2: Functional measurements of isolated working hearts from Cav-1^{+/+} and Cav-1^{-/-} mice challenged with varying concentrations of DL-isoproterenol (Iso)

Cav-1^{+/+} (o) (N=9) and Cav-1^{-/-} (●) (N=6). * P<0.05 within group differences. † P<0.05 between group differences. P values are listed where interaction effects of isoproterenol concentration and strain effects are significant. Error bars indicate ± SEM where they exceed the symbol size.

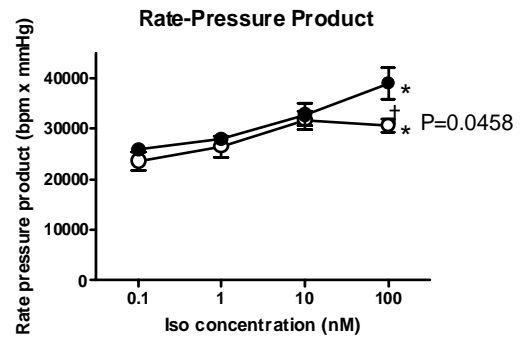
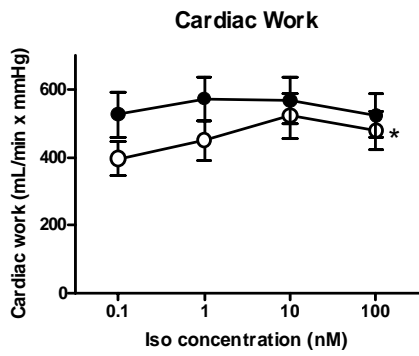
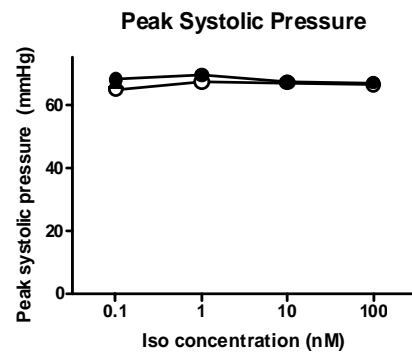
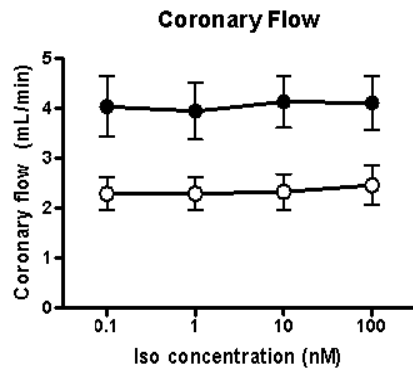
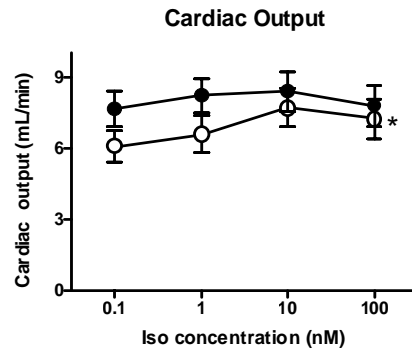
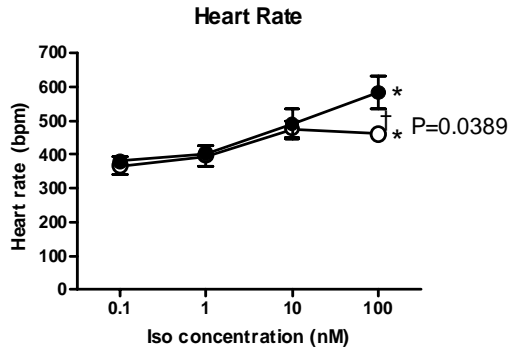


Figure 4.3: MMP-2 activity and protein from Cav-1^{+/+} and Cav-1^{-/-} mouse hearts following preload and isoproterenol challenges

MMP-2 activity and protein in Cav-1^{+/+} (N=9) and Cav-1^{-/-} (N=6) mouse hearts following preload and isoproterenol challenges. A) Upper panel: representative gelatin zymogram showing 72 kDa MMP-2 activity in three Cav-1^{+/+} and three Cav-1^{-/-} hearts. The position of the 75 kDa molecular weight marker is shown on the right side of the panel. Lower panel: quantitative analysis of MMP-2 activity in all hearts. MMP-2 zymographic activity is not different between Cav-1^{+/+} and Cav-1^{-/-} hearts. B) Upper panel: representative Western blot showing 72 kDa MMP-2 protein levels in three Cav-1^{+/+} and three Cav-1^{-/-} hearts. The loading control (Ponceau stain of the PVDF membrane following antibody probing) is also shown. A 72 kDa human recombinant MMP-2 standard is shown on the left and the location of the 75 kDa molecular weight marker is shown on the right side of the panel. Lower panel: quantitative analysis of MMP-2 protein level in all hearts. Protein levels of MMP-2 in Cav-1^{+/+} and Cav-1^{-/-} mouse hearts are not different following preload and isoproterenol challenge. C) Ratio of 72 kDa MMP-2 activity / 72 kDa MMP-2 protein level shows that there is no significant difference in MMP-2 activity per unit of MMP-2 protein between Cav-1^{+/+} and Cav-1^{-/-} hearts.

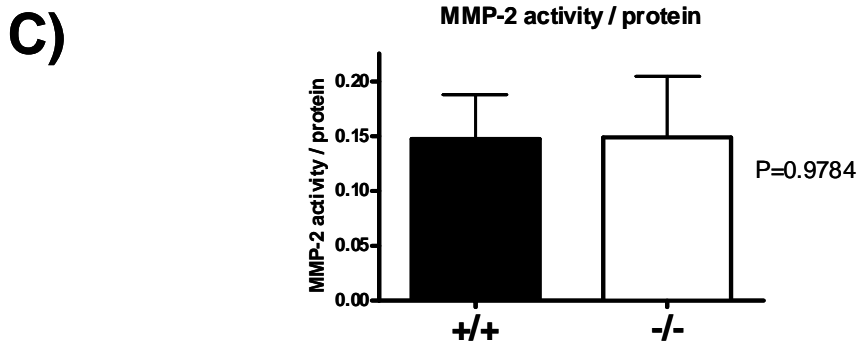
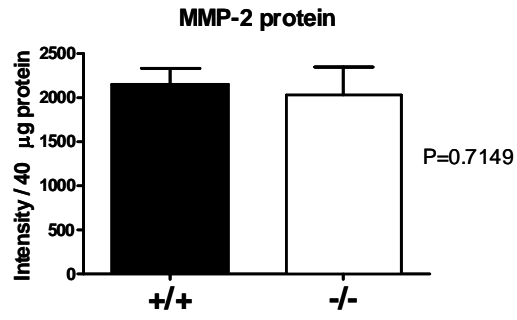
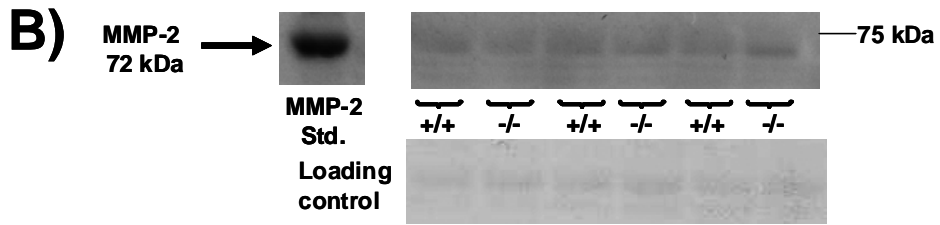
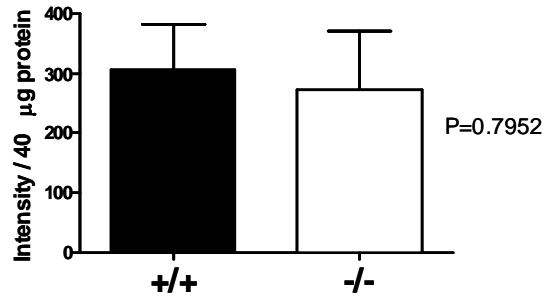
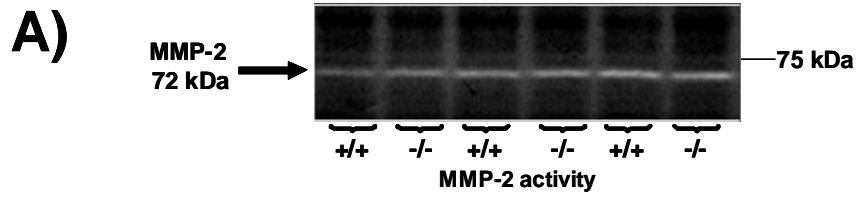


Figure 4.4: Levels of sarcomeric and cytoskeletal proteins in Cav-1^{+/+} and Cav-1^{-/-} following preload and isoproterenol challenges

Cav-1^{-/-} (N=6) and Cav-1^{+/+} (N=9) hearts exposed to varying preloads and concentrations of isoproterenol have similar levels of troponin I (A) and α -actinin (B). The upper panels show representative Western blots of troponin I (A) and α -actinin (B) with the molecular weight markers shown on the right side of the panel. The loading control is a Ponceau stain of the PVDF membrane following antibody probing. The lower panels show the quantitative analysis of troponin I (A) and α -actinin (B) of all hearts. No significant difference is seen in either troponin I or α -actinin between Cav-1^{+/+} and Cav-1^{-/-} hearts.

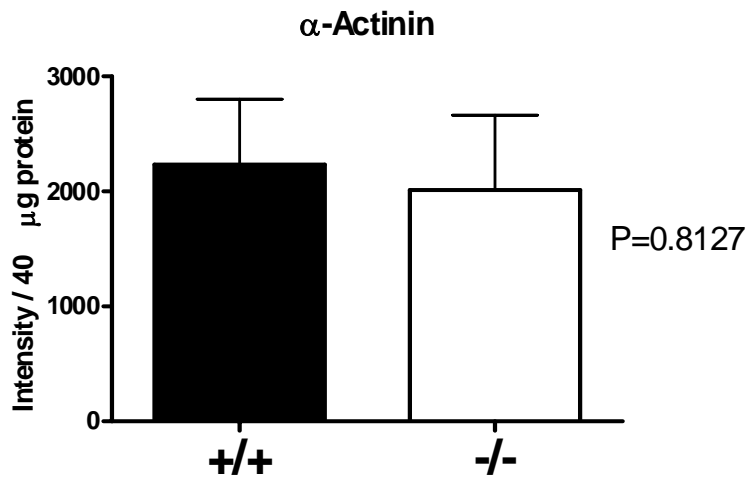
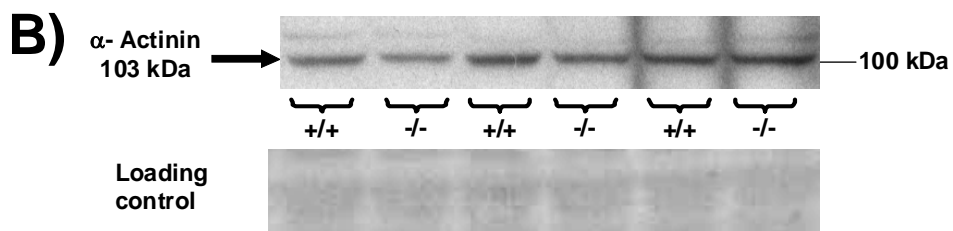
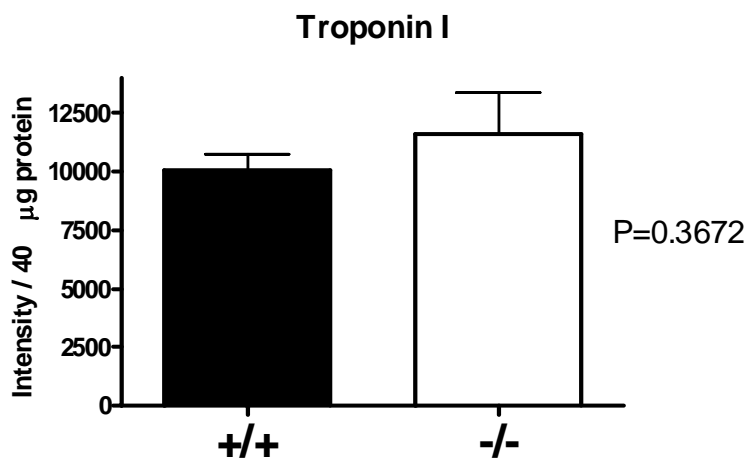
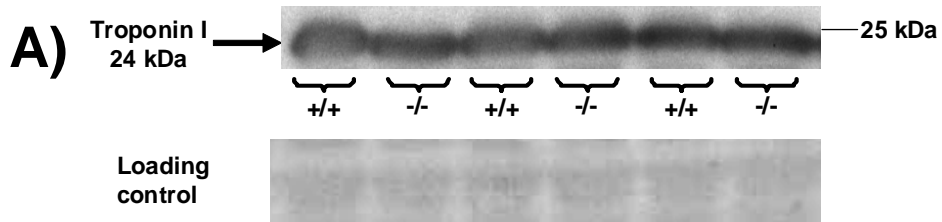
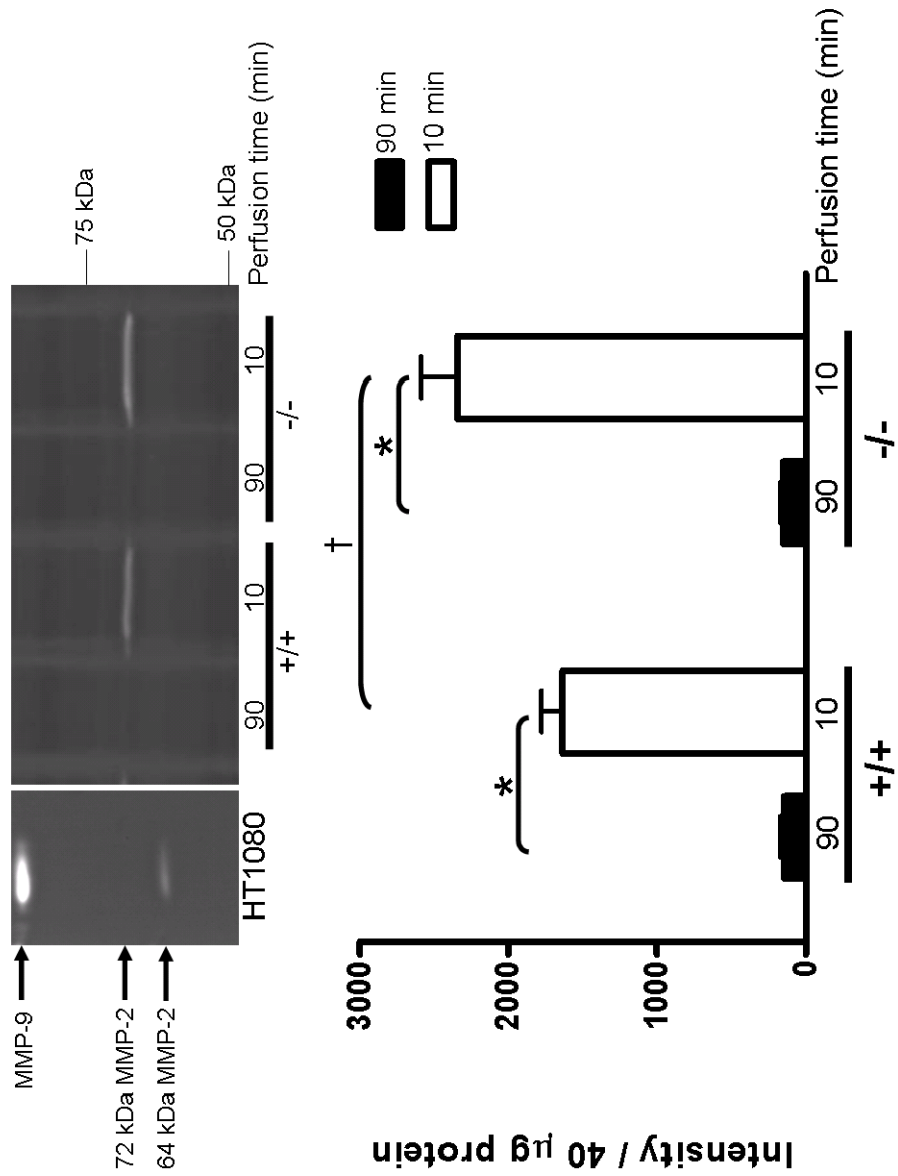


Figure 4.5: MMP-2 activity in Cav-1^{+/+} and Cav-1^{-/-} mouse hearts perfused for 10 min or 90 min

Upper panel: Representative zymogram demonstrating gelatinolytic activity in Cav-1^{+/+} and Cav-1^{-/-} hearts following 10 or 90 min perfusion in Langendorff mode. Lower panel: Quantitative analysis of all hearts (N=3 per group). Hearts perfused for 10 min showed significantly more MMP-2 gelatinolytic activity than hearts perfused for 90 min (*P<0.0001) and Cav-1^{-/-} hearts perfused for 10 min showed more gelatinolytic activity than Cav-1^{+/+} hearts perfused for the same amount of time (†P=0.0332).



4.5: References

1. McCawley, LJ and Matrisian, LM. Matrix metalloproteinases: they're not just for matrix anymore! *Curr. Opin. Cell Biol.* 2001; 13:534-540.
2. Schulz, R. Intracellular targets of matrix metalloproteinase-2 in cardiac disease: rationale and therapeutic approaches. *Annu. Rev. Pharmacol. Toxicol.* 2007; 47:211-242.
3. Wang, W, Schulze, CJ, Suarez-Pinzon, WL, Dyck, JR, Sawicki, G, and Schulz, R. Intracellular action of matrix metalloproteinase-2 accounts for acute myocardial ischemia and reperfusion injury. *Circulation* 2002; 106:1543-1549.
4. Sawicki, G, Leon, H, Sawicka, J, Sariahmetoglu, M, Schulze, CJ, Scott, PG, Szczesna-Cordary, D, and Schulz, R. Degradation of myosin light chain in isolated rat hearts subjected to ischemia-reperfusion injury: a new intracellular target for matrix metalloproteinase-2. *Circulation* 2005; 112:544-552.
5. Sung, MM, Schulz, CG, Wang, W, Sawicki, G, Bautista-Lopez, NL, and Schulz, R. Matrix metalloproteinase-2 degrades the cytoskeletal protein alpha-actinin in peroxynitrite mediated myocardial injury. *J. Mol. Cell Cardiol.* 2007; 43:429-436.
6. Okamoto, T, Akaike, T, Nagano, T, Miyajima, S, Suga, M, Ando, M, Ichimori, K, and Maeda, H. Activation of human neutrophil procollagenase by nitrogen dioxide and peroxynitrite: a novel mechanism for procollagenase activation involving nitric oxide. *Arch. Biochem. Biophys.* 1997; 342:261-274.
7. Okamoto, T, Akaike, T, Sawa, T, Miyamoto, Y, van der Vliet, A, and Maeda, H. Activation of matrix metalloproteinases by peroxynitrite-induced protein S-

- glutathiolation via disulfide S-oxide formation. *J. Biol. Chem.* 2001; 276:29596-29602.
8. Sariahmetoglu, M, Crawford, BD, Leon, H, Sawicka, J, Li, L, Ballermann, BJ, Holmes, C, Berthiaume, LG, Holt, A, Sawicki, G, and Schulz, R. Regulation of matrix metalloproteinase-2 (MMP-2) activity by phosphorylation. *FASEB J.* 2007; 21:2486-2495.
 9. Nagase, H, Visse, R, and Murphy, G. Structure and function of matrix metalloproteinases and TIMPs. *Cardiovasc. Res.* 2006; 69:562-573.
 10. Feron, O and Balligand, JL. Caveolins and the regulation of endothelial nitric oxide synthase in the heart. *Cardiovasc. Res.* 2006; 69:788-797.
 11. Puyraimond, A, Fridman, R, Lemesle, M, Arbeille, B, and Menashi, S. MMP-2 colocalizes with caveolae on the surface of endothelial cells. *Exp. Cell Res.* 2001; 262:28-36.
 12. Cho, WJ, Chow, AK, Schulz, R, and Daniel, EE. Matrix metalloproteinase-2, caveolins, focal adhesion kinase and c-Kit in cells of the mouse myocardium. *J. Cell Mol. Med.* 2007; 11:1069-1086.
 13. Chow, AK, Cena, J, El-Yazbi, AF, Crawford, BD, Holt, A, Cho, WJ, Daniel, EE, and Schulz, R. Caveolin-1 inhibits matrix metalloproteinase-2 activity in the heart. *J. Mol. Cell Cardiol.* 2007; 42:896-901.

14. Neely, JR, Rovetto, MJ, Whitmer, JT, and Morgan, HE. Effects of ischemia on function and metabolism of the isolated working rat heart. *Am. J. Physiol* 1973; 225:651-658.
15. Sulakhe, PV and Vo, XT. Regulation of phospholamban and troponin-I phosphorylation in the intact rat cardiomyocytes by adrenergic and cholinergic stimuli: roles of cyclic nucleotides, calcium, protein kinases and phosphatases and depolarization. *Mol. Cell Biochem.* 1995; 149-150:103-126.
16. Zhao, YY, Liu, Y, Stan, RV, Fan, L, Gu, Y, Dalton, N, Chu, PH, Peterson, K, Ross, J, Jr., and Chien, KR. Defects in caveolin-1 cause dilated cardiomyopathy and pulmonary hypertension in knockout mice. *Proc. Natl. Acad. Sci. U. S. A* 2002; 99:11375-11380.
17. Murata, T, Lin, MI, Huang, Y, Yu, J, Bauer, PM, Giordano, FJ, and Sessa, WC. Reexpression of caveolin-1 in endothelium rescues the vascular, cardiac, and pulmonary defects in global caveolin-1 knockout mice. *J. Exp. Med.* 2007; 204:2373-2382.
18. Sasse, J and Gallagher, SR. Detection of proteins on blot transfer membranes. *Curr. Protoc. Immunol.* 2008; Chapter 8:Unit.
19. Wang, W, Viappiani, S, Sawicka, J, and Schulz, R. Inhibition of endogenous nitric oxide in the heart enhances matrix metalloproteinase-2 release. *Br. J. Pharmacol.* 2005; 145:43-49.

20. Bernatchez, PN, Bauer, PM, Yu, J, Prendergast, JS, He, P, and Sessa, WC. Dissecting the molecular control of endothelial NO synthase by caveolin-1 using cell-permeable peptides. *Proc. Natl. Acad. Sci. U. S. A* 2005; 102:761-766.
21. Patel, HH, Tsutsumi, YM, Head, BP, Niesman, IR, Jennings, M, Horikawa, Y, Huang, D, Moreno, AL, Patel, PM, Insel, PA, and Roth, DM. Mechanisms of cardiac protection from ischemia/reperfusion injury: a role for caveolae and caveolin-1. *FASEB J.* 2007; 21:1565-1574.
22. Rybin, VO, Xu, X, Lisanti, MP, and Steinberg, SF. Differential targeting of beta -adrenergic receptor subtypes and adenylyl cyclase to cardiomyocyte caveolae. A mechanism to functionally regulate the cAMP signaling pathway. *J. Biol. Chem.* 2000; 275:41447-41457.
23. Head, BP, Patel, HH, Roth, DM, Lai, NC, Niesman, IR, Farquhar, MG, and Insel, PA. G-protein-coupled receptor signaling components localize in both sarcolemmal and intracellular caveolin-3-associated microdomains in adult cardiac myocytes. *J. Biol. Chem.* 2005; 280:31036-31044.
24. Schwencke, C, Okumura, S, Yamamoto, M, Geng, YJ, and Ishikawa, Y. Colocalization of beta-adrenergic receptors and caveolin within the plasma membrane. *J. Cell Biochem.* 1999; 75:64-72.
25. El Yazbi, AF, Cho, WJ, Schulz, R, and Daniel, EE. Caveolin-1 knockout alters beta-adrenoceptors function in mouse small intestine. *Am. J. Physiol Gastrointest. Liver Physiol* 2006; 291:G1020-G1030.

26. El Yazbi, AF, Cho, WJ, Schulz, R, and Daniel, EE. Caveolin-1 knockout alters beta-adrenoceptors function in mouse small intestine. *Am. J. Physiol Gastrointest. Liver Physiol* 2006; 291:G1020-G1030.
27. Hare, JM, Lofthouse, RA, Juang, GJ, Colman, L, Ricker, KM, Kim, B, Senzaki, H, Cao, S, Tunin, RS, and Kass, DA. Contribution of caveolin protein abundance to augmented nitric oxide signaling in conscious dogs with pacing-induced heart failure. *Circ. Res.* 2000; 86:1085-1092.
28. Cohen, AW, Park, DS, Woodman, SE, Williams, TM, Chandra, M, Shirani, J, Pereira de, SA, Kitsis, RN, Russell, RG, Weiss, LM, Tang, B, Jelicks, LA, Factor, SM, Shtutin, V, Tanowitz, HB, and Lisanti, MP. Caveolin-1 null mice develop cardiac hypertrophy with hyperactivation of p42/44 MAP kinase in cardiac fibroblasts. *Am. J. Physiol Cell Physiol* 2003; 284:C457-C474.
29. Errami, M, Galindo, CL, Tassa, AT, Dimaio, JM, Hill, JA, and Garner, HR. Doxycycline attenuates isoproterenol- and transverse aortic banding-induced cardiac hypertrophy in mice. *J. Pharmacol. Exp. Ther.* 2008; 324:1196-1203.
30. Sivakumar, P, Gupta, S, Sarkar, S, and Sen, S. Upregulation of lysyl oxidase and MMPs during cardiac remodeling in human dilated cardiomyopathy. *Mol. Cell Biochem.* 2008; 307:159-167.
31. Bergman, MR, Teerlink, JR, Mahimkar, R, Li, L, Zhu, BQ, Nguyen, A, Dahi, S, Karliner, JS, and Lovett, DH. Cardiac matrix metalloproteinase-2 expression independently induces marked ventricular remodeling and systolic dysfunction. *Am. J. Physiol Heart Circ. Physiol* 2007; 292:H1847-H1860.

32. Ballard-Croft, C, Locklar, AC, Kristo, G, and Lasley, RD. Regional myocardial ischemia-induced activation of MAPKs is associated with subcellular redistribution of caveolin and cholesterol. *Am. J. Physiol Heart Circ. Physiol* 2006; 291:H658-H667.

CHAPTER 5

ISCHEMIA/REPERFUSION INJURY IN THE CAVEOLIN-1 KNOCKOUT MOUSE HEART

5.1: Introduction

Myocardial stunning is induced by an acute, sublethal ischemic insult, followed by reperfusion. This results in transient contractile dysfunction which may persist for hours, but is eventually followed by a complete functional recovery^{1,2}. Coronary artery bypass graft surgery is a clinically induced form of myocardial stunning³. The mechanisms that underlie cardiac stunning are being extensively explored, as this is a period during which clinical intervention could lead to substantial decreases in morbidity and mortality.

One element that may play a significant role in the initiation of I/R damage is MMP-2. MMP-2 has been shown to co-localize with and proteolyze sarcomeric and cytoskeletal elements such as Tnl⁴, MLC-1⁵ and α -actinin⁶ following I/R injury^{4,5} or by subjecting the heart to other means to increase oxidative stress⁶. MMP-2 activity is enhanced during the reperfusion period following global, no-flow ischemia in isolated rat hearts⁷. In fact, the detection of circulating levels of α -actinin and Tnl and their fragments can be used as a measure of the severity of myocardial ischemia⁸. The perturbation between MMP-2 and its endogenous inhibitor, TIMP-4, has been proposed to be one mechanism which can lead to the enhanced proteolytic activity of MMPs observed following I/R⁹. In addition, the production of reactive oxygen species such as peroxynitrite during I/R injury¹⁰ can activate MMPs^{11,12}, including MMP-2¹³.

Though much of the research investigating myocardial I/R injury has centered around the notion that oxidative stress is responsible for mediating the sarcomeric damage in the heart, this does not preclude the fact that other agents may be involved. One potential mediator of MMP-2 activity in the heart may be caveolin. We previously

found that hearts from Cav-1 null mice have increased MMP-2 activity and that the CSD of Cav-1 is capable of inhibiting MMP-2 activity in an *in vitro* assay¹⁴. Indeed, others have also found evidence that Cav-1 may have a role in mediating ischemic injury. Mice whose brains were subjected to I/R injury by middle cerebral artery occlusion showed reduced levels of Cav-1 protein when compared with controls¹⁵. Brains from Cav-1^{-/-} mice exposed to I/R have both an increased number of TUNEL positive cells and increased infarction size¹⁶ when compared with brains from Cav-1^{+/+} mice. Cell permeable Cav-1 CSD peptide, administered 1 h prior to experimentation, protected against I/R injury in isolated rat hearts¹⁷. All of this supports the notion that Cav-1 may protect against I/R injury. Consequently, we hypothesize that as a result of both the lack of Cav-1 and the increased MMP-2 activity in Cav-1^{-/-} myocardium, Cav-1^{-/-} hearts would be more susceptible to I/R injury, manifested as compromised contractile function and greater degree of proteolysis of both sarcomeric and cytoskeletal MMP-2 substrates in the heart.

5.2: Materials and methods

All experiments were performed in accordance with the Canadian Council on Animal Care *Guide to the Care and Use of Experimental Animals*.

5.2.1: Animals

Male 6- to 8-wk-old Cav-1^{-/-} (cav < tm 1 M Is > /J) and control [(B6 129 SF2/J) (Cav-1^{+/+})] mice were obtained from Jackson Laboratories (Bar Harbor, ME, USA).

5.2.2: Isolated working mouse heart

Ten min prior to euthanasia by intraperitoneal pentobarbital injection, mice were injected with 100 IU of heparin (i.p) to prevent blood clotting in the coronary vessels. Hearts were rapidly excised from deeply anesthetized mice and placed immediately into an ice-cold Krebs-Henseleit bicarbonate solution (118 mM NaCl, 25 mM NaHCO₃, 4.7 mM KCl, 1.2 mM MgSO₄, 1.2 mM KH₂PO₄, 2.25 mM CaCl₂, 0.5 mM EDTA, and 11.1 mM glucose, oxygenated with 95% O₂ - 5% CO₂ (pH 7.4)) to arrest beating. The aorta was then cannulated with a 20 gauge cannula and the heart was perfused in Langendorff mode at 60 mmHg constant hydrostatic pressure with the aforementioned Krebs-Henseleit solution at 37°C. The left atrium was then cannulated through the pulmonary vein opening and the heart was switched from the Langendorff mode to the working mode whereby the heart is perfused with a recirculating Krebs-Henseleit bicarbonate solution at 37°C supplemented with 0.2% bovine serum albumin, 5 mM pyruvate, and 100 mU/L human insulin and continuously gassed with 95% O₂ - 5% CO₂ (pH 7.4) at a left atrial preload pressure of 11.5 mmHg and an aortic afterload pressure of 50 mmHg.

Spontaneously beating hearts were allowed to equilibrate aerobically for 10 min prior to 20 min of aerobic perfusion. Following this, the hearts were subjected to 15 or 17 min of global, no-flow ischemia by clamping both the atrial in-flow and the aortic out-flow lines. While optimizing ischemia times, other hearts were exposed to 12 (N=3) and 20 min (N=3) of global, no-flow ischemia. Twelve min of ischemia followed by reperfusion led to no appreciable decline in cardiac function, while 20 min of ischemia resulted in no functional recovery. Thus it was decided that 15 and 17 min of ischemia was optimal to observe changes in cardiac function. After the elapsed ischemia times,

the atrial in-flow and aortic out-flow clamps were released to initiate 35 min of reperfusion for hearts subjected to 15 min of ischemia and 33 min of reperfusion for hearts subjected to 17 min of ischemia for a total perfusion time of 80 min (Fig. 5.1). Functional measurements were continuously recorded with the MP100 system from AcqKnowledge (BioPac Systems, Santa Barbara, CA) for a total of 80 min. Cardiac output was measured via a Doppler flow probe (Transonic Systems, Ithaca, NY) placed in the left atrial line while aortic flow was measured using a probe in the aortic afterload line. Heart rate and peak systolic and pulse (systolic – diastolic) pressures were measured with a pressure transducer (Harvard Apparatus, South Natick, MA), placed at the level of the heart, in the aortic line. Cardiac work was calculated as the product of peak systolic pressure and cardiac output. Coronary flow was calculated as the difference between cardiac output and aortic flows. The rate pressure product is the product of the heart rate and the peak systolic pressure. At the end of the perfusion whole hearts were then clamped with Wollenberger tongs pre-cooled in liquid nitrogen and stored at -80°C until used.

5.2.3: Tissue preparation

Frozen whole hearts were crushed and powdered in liquid nitrogen and weighed. Four volumes (weight/volume) of ice-cold homogenization buffer (pH 7.4; 50 mM Tris, 31 mM sucrose, 1 mM DL-dithiothreitol, 0.1% Triton X-100, 10 µg/L soybean trypsin inhibitor, 10 mg/L leupeptin, 2 g/L aprotinin, and 100 mg/L phenylmethylsulfonyl fluoride) was added to the tissue. The powdered tissues were then homogenized with a Polytron (3x30 s) with 30 s of cooling in ice between each cycle. The samples were then centrifuged (4°C, 1000 × *g*, 5 min) and the supernatants were used for determination of

enzyme activities and Western blot analysis. Protein concentration was assessed by the bicinchoninic acid method using bovine serum albumin as a reference standard.

5.2.4: Western blotting

40 µg of each whole heart sample was run in 10% SDS-PAGE under reducing conditions. Human recombinant MMP-2 and TnI were loaded as controls. Following electrophoresis, samples were electroblotted onto polyvinylidene difluoride membranes. The membranes were then blocked at room temperature for 1 h with 5% milk, followed by an overnight incubation at 4°C with primary antibodies (1:1000 monoclonal mouse anti-human troponin I (Novogen, Oakville, ON), 1:1000 monoclonal mouse anti human α-actinin (Chemicon, Billerica, MA), 1:1000 monoclonal mouse anti-human MMP-2 (Chemicon, Billerica, MA). These membranes were then probed with 1:5000 anti mouse horseradish peroxidase conjugated secondary antibody and incubated with ECL Plus (Amersham, Baie d'Urfe, QC) for 5 min before being exposed to film. Membranes were Ponceau stained to ensure equal loading¹⁸.

5.2.5: Gelatin zymography

40 µg of each sample was run in an 8% polyacrylamide gel containing 2 mg/mL gelatin. Conditioned media from HT-1080 human fibrosarcoma cells were used as a standard for MMP-2 activity. Following electrophoresis, the gel was washed 3x20 min in 2.5% Triton X-100. The gel was then incubated in 50 mM Tris HCl, 150 mM NaCl, 5 mM CaCl₂, pH. 7.6 for 48 hr at 37°C prior to being stained with 0.05% Coomassie Brilliant Blue in 25% methanol: 10% acetic acid for 1 h and destained with 4% methanol: 8% acetic acid for 30 min.

5.2.6: Data analysis

Western blots and zymograms were analyzed using Image J software (NIH). Statistics and graphs were compiled using GraphPad Prism 4.03.

5.2.7: Statistics

Data are expressed as mean \pm SEM. Functional differences between groups were analyzed by two-way repeated measures analysis of variance and, if significant, followed by Bonferroni post-hoc tests. Differences in protein levels and gelatinolytic activity were analyzed using Student's t-test. P values of less than 0.05 were considered statistically significant.

5.3: Results

5.3.1: Cav-1^{-/-} hearts are not functionally different from Cav-1^{+/+} hearts following 15 min of ischemia and reperfusion

Both Cav-1^{+/+} and Cav-1^{-/-} hearts experienced a significant reduction in aortic flow following 15 min of I/R when compared to their aerobic values (P=0.025 and 0.034 respectively). No other function differences were observed when comparing the aerobic function to the function at the end of the reperfusion period (Table 5.1).

No differences between Cav-1^{-/-} (N=6) and Cav-1^{+/+} (N=8) hearts were observed during the initial aerobic perfusion period in any of the measured or calculated functional parameters (heart rate, cardiac output, peak systolic pressure, pulse pressure, coronary flow, rate pressure product, cardiac work, aortic flow). During the reperfusion period, no significant interactions were observed between the strain of

mouse over time (i.e. whether the mouse was Cav-1^{+/+} or Cav-1^{-/-} did not affect recovery during reperfusion) on any measured or calculated functional parameter (heart rate, P=0.9265; cardiac output, P=0.9862; peak systolic pressure, P=0.4166; pulse pressure, P=0.8697; coronary flow, P=0.7017; aortic flow, P=0.9086; cardiac work, P=0.9742; rate pressure product, P=0.9545). There were also no significant differences between Cav-1^{+/+} and Cav-1^{-/-} hearts during reperfusion in any of the measured or calculated functional parameters (heart rate, P=0.2420; cardiac output, P=0.8261; peak systolic pressure, P=0.2142; pulse pressure, P=0.4389; coronary flow, P=0.9728; aortic flow, P=0.7562; cardiac work, P=0.8594; rate pressure product, P=0.1094;) (Fig 5.2).

5.3.2: MMP-2 activity and protein content in Cav-1^{-/-} and Cav-1^{+/+} mouse hearts after 15 min of ischemia followed by reperfusion

Cav-1^{-/-} hearts subjected to 15 min of I/R demonstrate significantly decreased MMP-2 activity by gelatin zymography when compared with Cav-1^{+/+} hearts (P=0.0438) (Fig 5.3A). Interestingly, MMP-2 protein content is not different between Cav-1^{+/+} and Cav-1^{-/-} hearts in hearts subjected to 15 min of ischemia (P=0.9229) (Fig 5.3B). The ratio of MMP-2 activity per unit protein is illustrated in Fig. 5.3C (P=0.0899).

5.3.3: Sarcomeric and cytoskeletal protein levels in Cav-1^{-/-} mouse hearts is greater than that in Cav-1^{+/+} hearts after 15 min of ischemia followed by reperfusion

Following 15 min of ischemia, both TnI (Fig. 5.4A) content and α -actinin (Fig. 5.4B) content were significantly higher in Cav-1^{-/-} hearts when compared with Cav-1^{+/+} hearts (P=0.0498 and P=0.0404 respectively).

5.3.4: Cav-1^{-/-} hearts are not functionally different from Cav-1^{+/+} hearts following 17 min of ischemia

17 min of I/R significantly reduced the cardiac output, aortic flow and cardiac work of both Cav-1^{+/+} and Cav-1^{-/-} mouse hearts when compared to their initial aerobic function. Additionally, Cav-1^{+/+} hearts also had significantly lower peak systolic pressures and rate pressure products during their reperfusion period when compared to their aerobic values (Table 5.2).

During the initial aerobic period, there were no differences between Cav-1^{-/-} (N=9) and Cav-1^{+/+} (N=10) in any of the measured or calculated functional parameters (heart rate, cardiac output, peak systolic pressure, pulse pressure, coronary flow, rate pressure product, cardiac work, aortic flow). During the reperfusion period, no significant interactions were observed between the strain of mouse over time (i.e. whether the mouse was Cav-1^{+/+} or Cav-1^{-/-} did not affect recovery during reperfusion) on any measured or calculated functional parameter (heart rate, P=0.4738; cardiac output, P=0.2909; peak systolic pressure, P=0.9027; pulse pressure, P=0.7056; coronary flow, P=0.9252; aortic flow, P=0.1178; cardiac work, P=0.3981; rate pressure product, P=0.4486). There were also no significant differences between Cav-1^{+/+} and Cav-1^{-/-} hearts during reperfusion in any of the measured or calculated functional parameters (heart rate, P=0.2494; cardiac output, P=0.9246; peak systolic pressure, P=0.5850; pulse pressure, P=0.5847; coronary flow, P=0.2481; aortic flow, P=0.3639; cardiac work, P=0.9943; rate pressure product, P=0.8534) (Fig 5.5).

5.3.5 MMP-2 activity and protein content in Cav-1^{-/-} and Cav-1^{+/+} mouse hearts after 17 min of ischemia followed by reperfusion

No differences in MMP-2 activity were observed between Cav-1^{+/+} and Cav-1^{-/-} hearts subjected to 17 min (Fig. 5.6A) of ischemia by gelatin zymography. Interestingly, MMP-2 protein content was significantly higher in the Cav-1^{-/-} hearts when compared with the Cav-1^{+/+} hearts (P=0.0004) (Fig. 5.6B). The ratio of MMP-2 activity per unit protein is illustrated in Fig. 5.6C (P=0.0710).

5.3.6: Sarcomeric and cytoskeletal protein levels in Cav-1^{-/-} mouse hearts is greater than that in Cav-1^{+/+} hearts after 17 min of ischemia followed by reperfusion

In the group of hearts subjected to 17 min of ischemia, the Cav-1^{+/+} hearts showed significantly lower levels of both Tnl (Fig. 5.7A) and α -actinin (Fig 5.7B) (P=0.0059 and P=0.0095 respectively) when compared with Cav-1^{-/-} hearts.

5.4: Discussion

Because of the fact that 12 min of I/R did not produce any significant functional deficits, and because 20 min I/R produced no appreciable recovery, it was decided that 15 and 17 min of I/R would provide the optimal window to observe functional differences between Cav-1^{+/+} and Cav-1^{-/-} mouse hearts. Though 15 min of I/R produced only functional changes in aortic flow, 17 min of I/R produced significantly more functional deficits in both Cav-1^{+/+} and Cav-1^{-/-} mouse hearts when compared with 15 min of I/R.

The functional results do not reveal any significant differences between Cav-1^{+/+} and Cav-1^{-/-} mouse heart recovery after I/R, which is particularly surprising given that there is evidence to suggest that the presence of Cav-1 may indeed be protective^{16;17;19;20}. However, one other group has found, using an *in vivo* model of I/R, that Cav-1^{-/-} hearts have the same infarct size as Cav-1^{+/+} mice after 5 min of left coronary artery occlusion, followed by 5 min of reperfusion, though they did find that Cav-1 null hearts were resistant to isoflurane preconditioning²⁰.

The Cav-1^{-/-} hearts in the 15 min ischemia group show reduced MMP-2 activity levels while protein levels remain unchanged, though there is a reduced amount of TnI and α -actinin in the Cav-1^{+/+} group when compared with the Cav-1^{-/-} hearts. The mild 15 min ischemic insult may cause the MMP-2 that is scaffolded to Cav-1 in the Cav-1^{+/+} hearts to be activated and degrade TnI and α -actinin, though the insult may have been insufficient to cause MMP-2 release. In the Cav-1^{-/-} hearts, the MMP-2 is not scaffolded in close proximity to its substrates, and as a result, TnI and α -actinin integrity may be preserved.

Interestingly, the Cav-1^{-/-} hearts in the 17 min ischemia group demonstrate significantly higher levels of MMP-2 protein, unlike that observed in the hearts subjected to 15 minutes of ischemia. This may be a result of the stronger oxidative insult in the 17 min group that would consequently result in more scaffolded MMP-2 release from the Cav-1^{+/+} hearts into the perfusate. 15 min of ischemia may not have generated sufficient reactive oxygen species to trigger the activation and release of MMP-2. This is supported by the fact that the 17 min ischemia group demonstrated significantly more functional impairment than the group exposed to 15 min of ischemia.

Cav-1^{-/-} hearts may be spared this release of MMP-2 because the MMP-2 is not scaffolded to caveolae, where release may be facilitated.

Surprisingly, in both the 15 min ischemia group, as well as in the 17 min ischemia group, Cav-1^{-/-} hearts appear to have better preserved Tnl and α -actinin than Cav-1^{+/+} hearts, despite having MMP-2 activity levels that are not different. Thus far, the majority of evidence has suggested that the presence of Cav-1 in the cell serves as a protective mechanism against ischemia^{16;17;19;20}, however, the results presented above suggest that the absence of Cav-1 preserves the integrity of the sarcomeric and cytoskeletal elements that have been shown to be proteolytically degraded by MMP-2 during I/R injury^{4;5}. We believe that the Cav-1 protein may be involved in holding MMP-2 and its intracellular substrates in close proximity to each other, where it is more likely they will interact. In the absence of the Cav-1 protein, MMP-2 would be less likely to degrade these intracellular substrates, as they are not nearby.

We have previously shown that Cav-1 and MMP-2 co-localize in cardiomyocytes^{14;21} and there is also evidence demonstrating that MMP-2 substrates such as Tnl and α -actinin may also be in close proximity. In fact, α -actinin is believed to be involved in the regulation of the formation of caveolae as one of the components that anchors caveolae to the cytoskeletal network, and may indeed be partially responsible for the formation of caveolae²². Cav-3 has been found to be associated with α -actinin at the T-tubules of cardiomyocytes where they co-immunoprecipitate²³. Interestingly, Cav-3 and α -actinin co-immunoprecipitation occurs only in cardiac muscle and is not observed in skeletal muscle²³. Whether Cav-1 is also associated or interacts with α -actinin is not yet known, though given the structural similarities between Cav-1

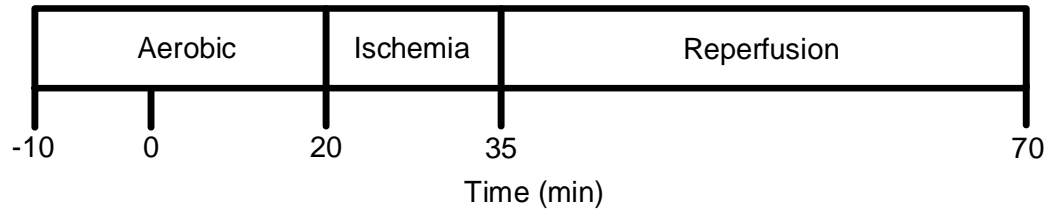
and Cav-3, this is certainly a possibility. Indeed, α -actinin has been found to occupy the same lipid microenvironment in whole heart lysates as Cav-1²⁴ and both Cav-1 and α -actinin have been shown to play important, distinct roles in the regulation of eNOS targeting and release²⁵.

The presence or absence of Cav-1 may affect TnI more indirectly. Compartmentalization of second messengers such as cAMP in caveolae serves to ensure efficient and rapid response to exogenous stimuli. Disruption of caveolae using methyl- β -cyclodextrin is able to perturb cAMP signaling initiated by β -adrenergic stimulation²⁶. Indeed, β -adrenergic activation of cAMP dependent protein kinase (PKA) can lead to the phosphorylation of TnI²⁷. As one of the phosphorylation sites in TnI is located near an MMP-2 cleavage site (Schulz lab, unpublished observations), it is possible that altering the phosphorylation status of TnI may serve to protect it from MMP-2 proteolysis as it may block access to the cleavage site itself (see Chapter 6).

Figure 5.1: Experimental design for Cav-1^{+/+} and Cav-1^{-/-} hearts exposed to I/R injury

Cav-1^{+/+} and Cav-1^{-/-} isolated mouse hearts were subjected to either 15 or 17 min of ischemia, preceded by an aerobic perfusion period and followed by reperfusion.

15 min I/R



17 min I/R



Figure 5.2: Functional measurements of isolated hearts from Cav-1^{+/+} and Cav-1^{-/-} subjected to 15 min of global, no-flow ischemia

Cav-1^{+/+} (●) (N=8) and Cav-1^{-/-} (○) (N=6). No significant differences were observed during the reperfusion period between the strains, nor was there an interaction effect between the strain and time. Error bars indicate \pm SEM where they exceed the symbol size.

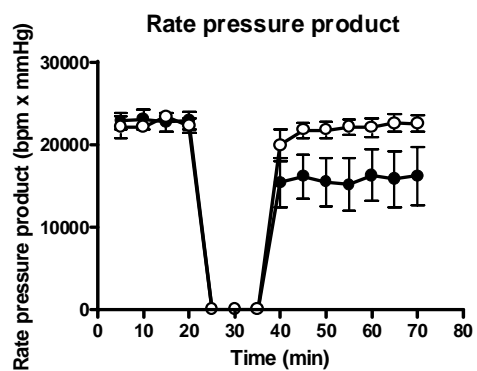
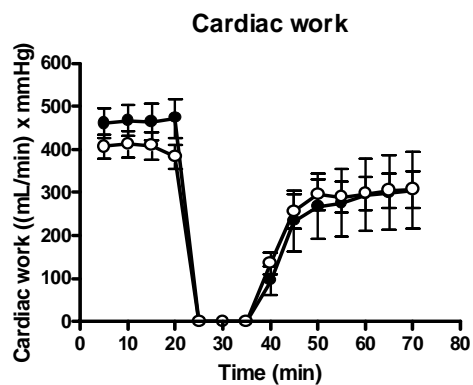
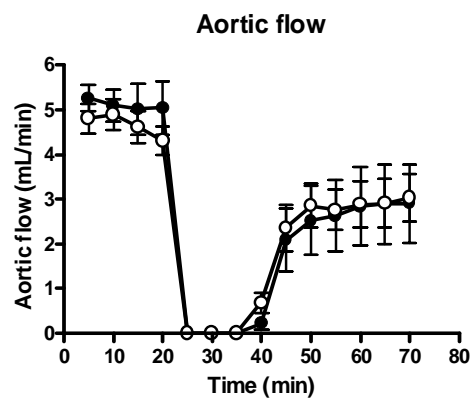
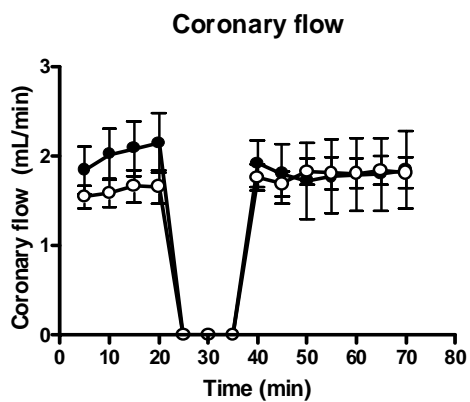
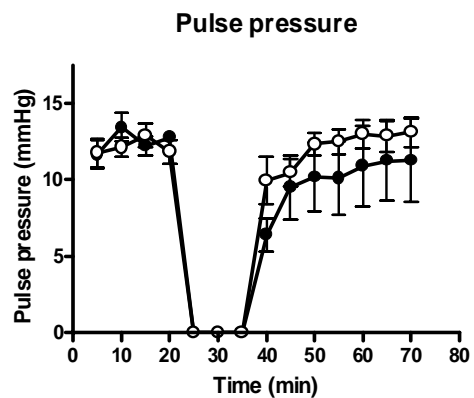
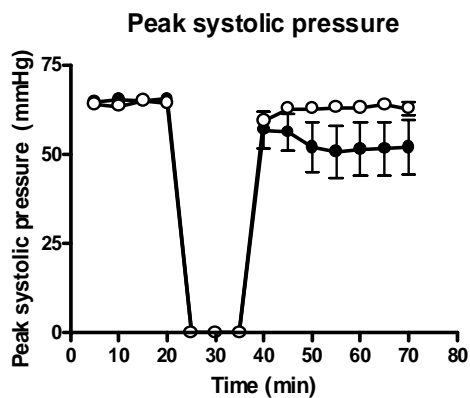
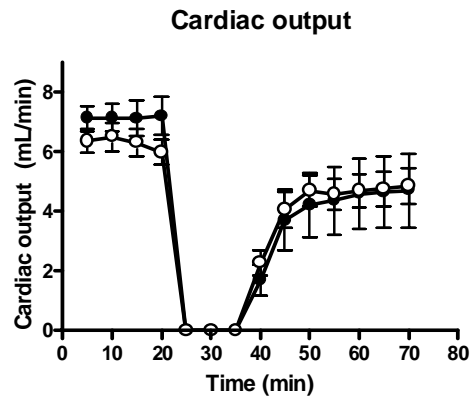
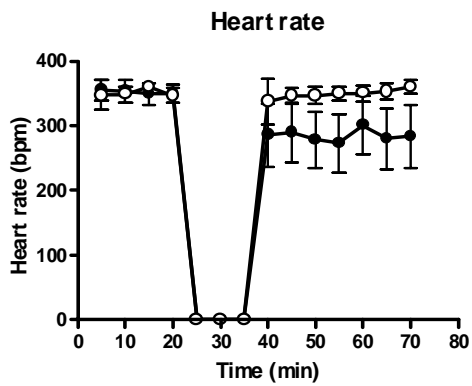


Figure 5.3: MMP-2 protein and activity in Cav-1^{+/+} and Cav-1^{-/-} subjected to 15 min I/R

A) Upper panel: representative gelatin zymogram showing 72 kDa MMP-2 activity in three Cav-1^{+/+} and three Cav-1^{-/-} hearts. The position of the 75 kDa molecular weight marker is shown on the right side of the panel. Lower panel: quantitative analysis of MMP-2 activity in all hearts following 15 min I/R. MMP-2 zymographic activity is higher in Cav-1^{+/+} than in Cav-1^{-/-} hearts (P=0.0438). B) Upper panel: representative Western blot showing 72 kDa MMP-2 protein levels in three Cav-1^{+/+} and three Cav-1^{-/-} hearts. The loading control (Ponceau stain of the PVDF membrane following antibody probing) is also shown. A 72 kDa human recombinant MMP-2 standard is shown on the left and the location of the 75 kDa molecular weight marker is shown on the right side of the panel. Lower panel: quantitative analysis of MMP-2 protein level in all hearts. Protein levels of MMP-2 in Cav-1^{+/+} and Cav-1^{-/-} mouse hearts are not different following 15 min I/R (P=0.9229). C) The ratio of MMP-2 activity per unit protein (P=0.0899).

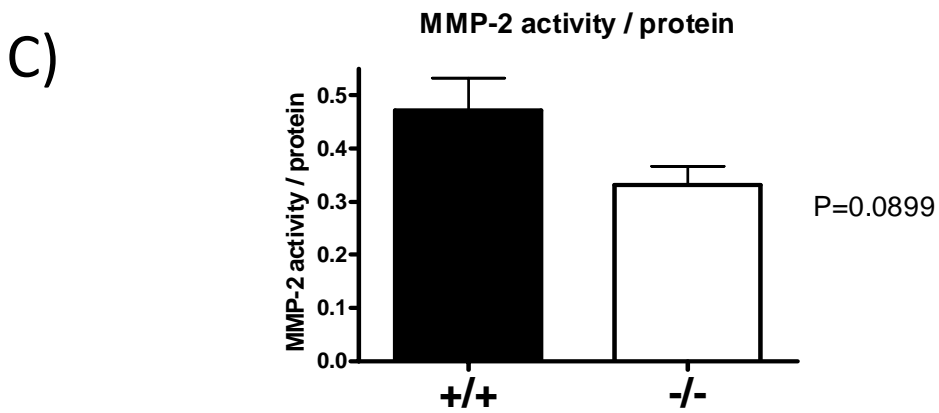
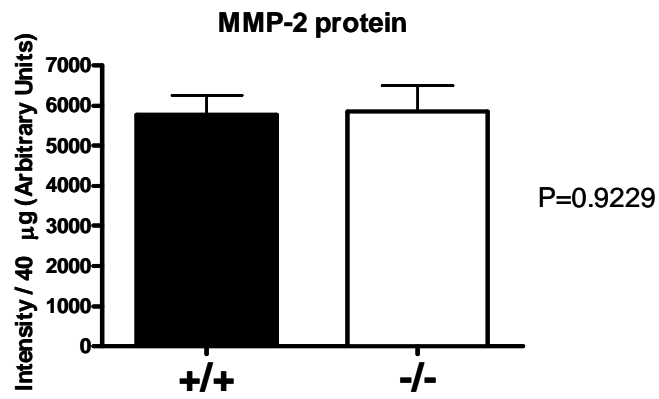
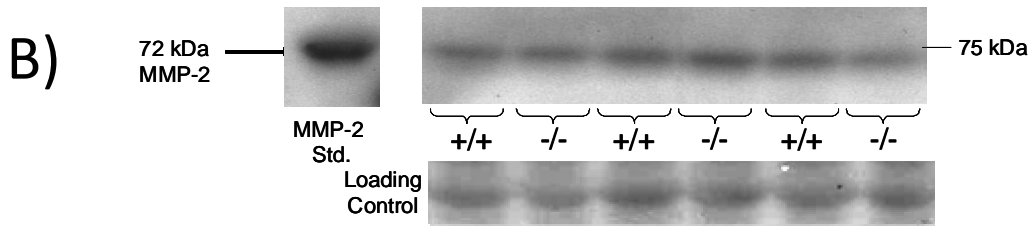
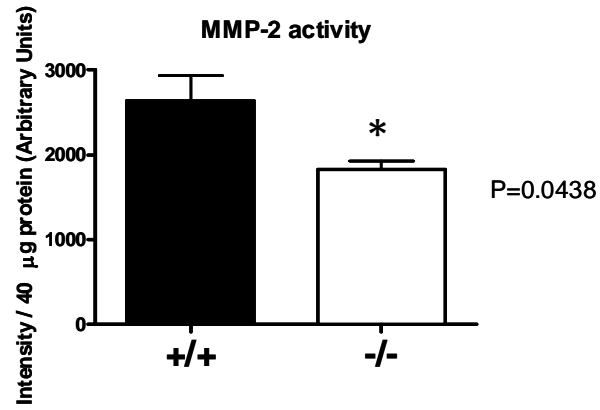
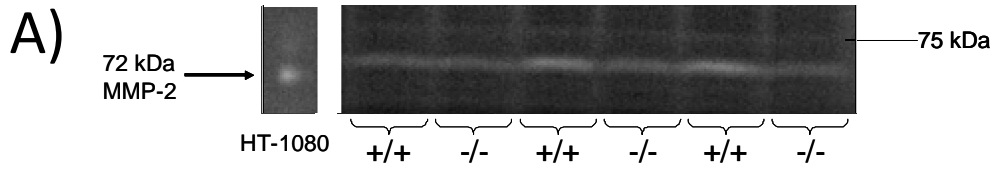


Figure 5.4: Levels of sarcomeric and cytoskeletal proteins Cav-1^{+/+} and Cav-1^{-/-} subjected to 15 min I/R

Levels of sarcomeric and cytoskeletal proteins in Cav-1^{+/+} (N=8) and Cav-1^{-/-} (N=6) mouse hearts subjected to 15 min I/R. Cav-1^{-/-} hearts subjected to 15 min I/R have significantly higher levels of troponin I (A) and α -actinin (B) than Cav-1^{+/+} hearts (P=0.029 and P=0.0404 respectively). The upper panels show representative Western blots of troponin I (A) and α -actinin (B) with the molecular weight markers shown on the right side of the panel. The loading control is a Ponceau stain of the PVDF membrane following antibody probing. The lower panels show the quantitative analysis of troponin I (A) and α -actinin (B) of all hearts.

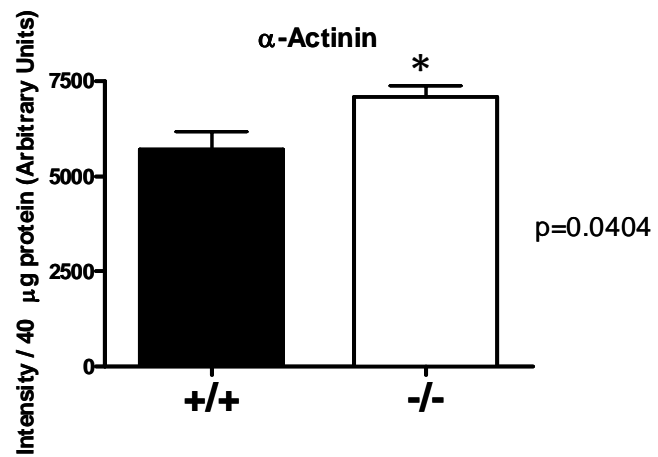
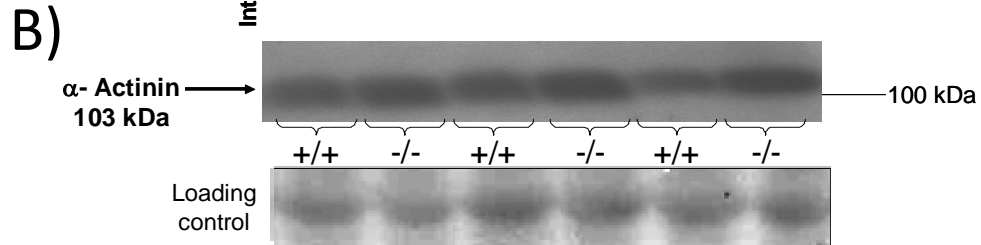
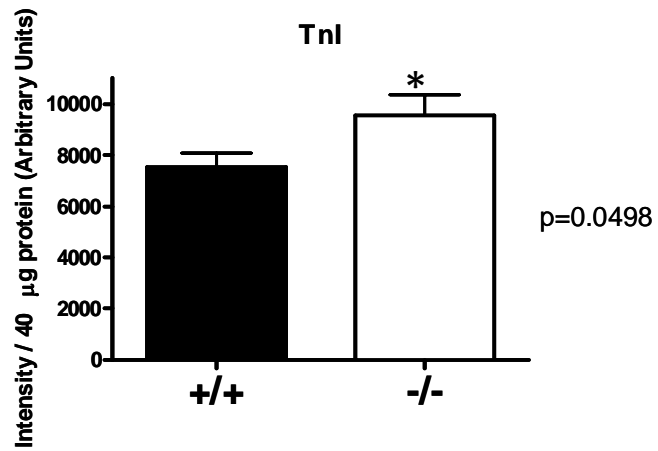
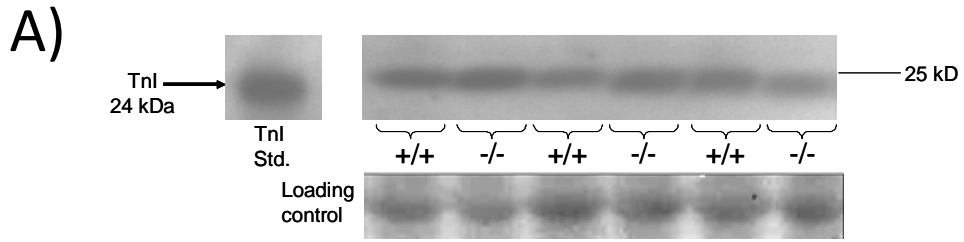


Figure 5.5: Functional measurements of isolated hearts from Cav-1^{+/+} and Cav-1^{-/-} subjected to 17 min of global no-flow ischemia

Cav-1^{+/+} (●) (N=10) and Cav-1^{-/-}(○) (N=9). No significant differences were observed during the reperfusion period between the strains, nor was there an interaction effect between the strain and time. Error bars indicate \pm SEM where they exceed the symbol size.

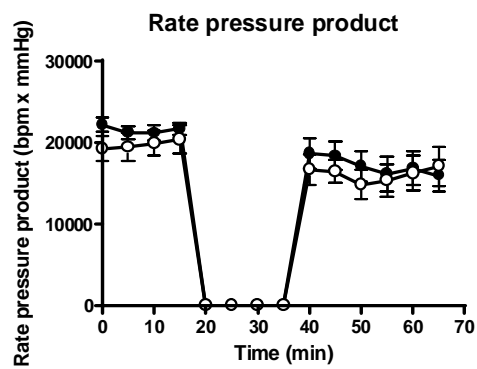
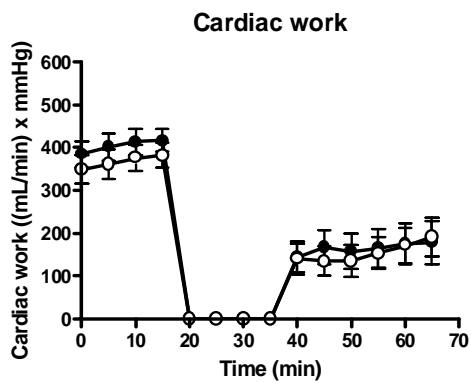
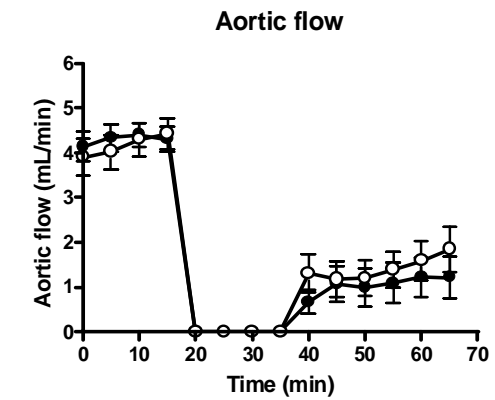
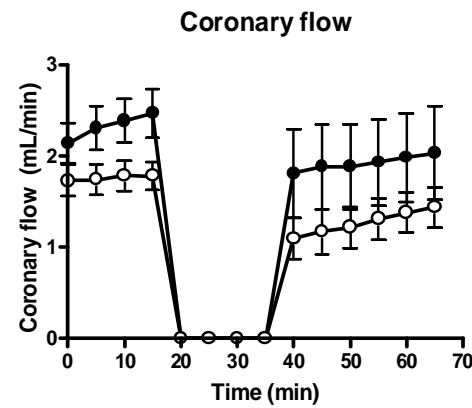
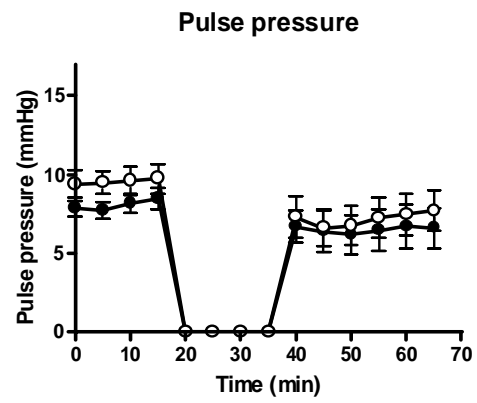
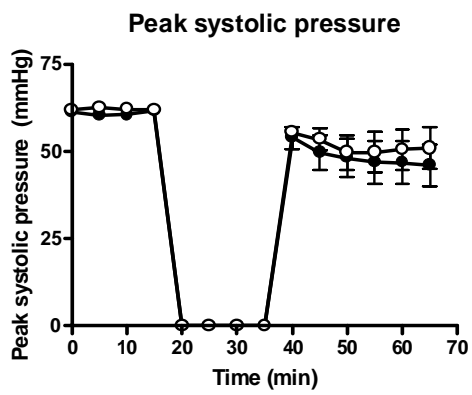
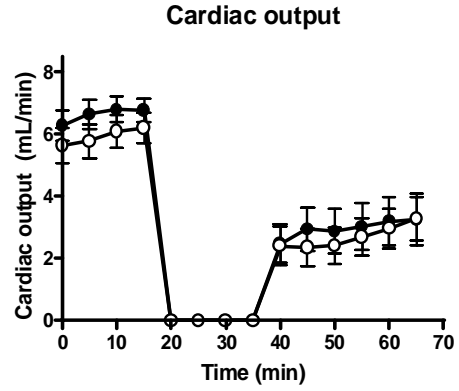
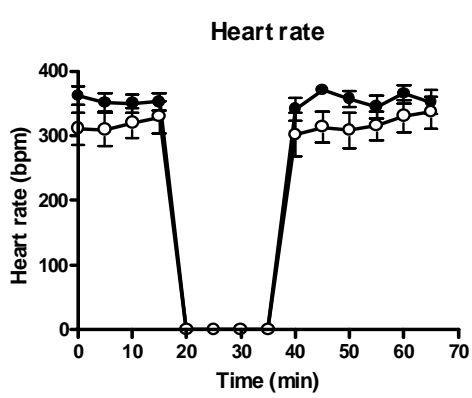


Figure 5.6: MMP-2 protein and activity in Cav-1^{+/+} and Cav-1^{-/-} subjected to 17 min I/R

A) Upper panel: representative gelatin zymogram showing 72 kDa MMP-2 activity in three Cav-1^{+/+} and three Cav-1^{-/-} hearts. The position of the 75 kDa molecular weight marker is shown on the right side of the panel. Lower panel: quantitative analysis of MMP-2 activity in all hearts following 17 min I/R. MMP-2 zymographic activity is not different between Cav-1^{+/+} and Cav-1^{-/-} hearts following 17 min I/R (P=0.9827). B) Upper panel: representative Western blot showing 72 kDa MMP-2 protein levels in three Cav-1^{+/+} and three Cav-1^{-/-} hearts. The loading control (Ponceau stain of the PVDF membrane following antibody probing) is also shown. A 72 kDa human recombinant MMP-2 standard is shown on the left and the location of the 75 kDa molecular weight marker is shown on the right side of the panel. Lower panel: quantitative analysis of MMP-2 protein level in all hearts. Protein levels of MMP-2 in Cav-1^{+/+} are significantly lower than those from Cav-1^{-/-} mouse hearts following 17 min I/R (P=0.0004). C) The ratio of MMP-2 activity per unit protein (P=0.0710).

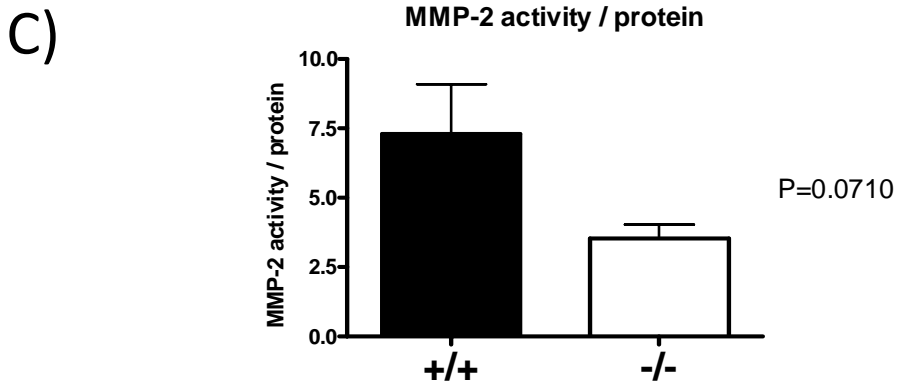
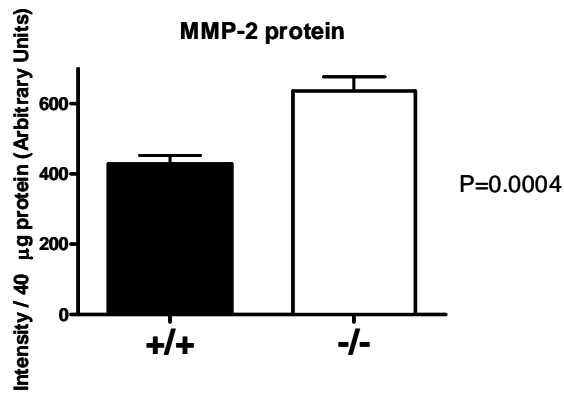
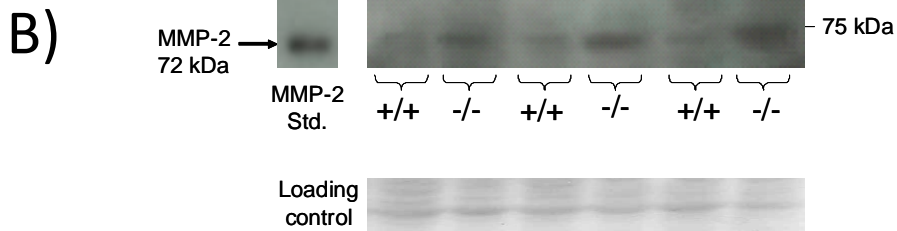
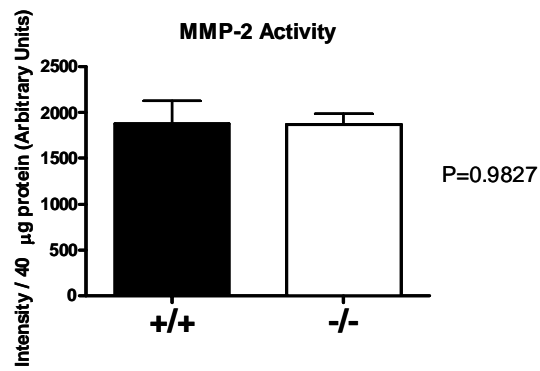
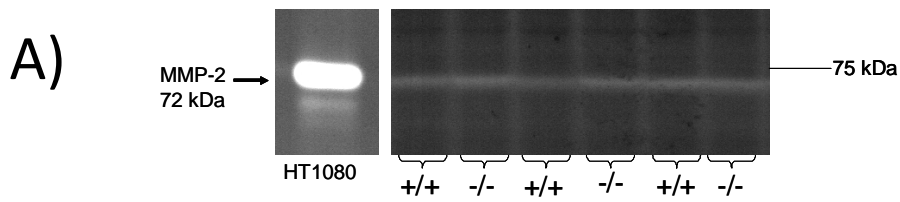
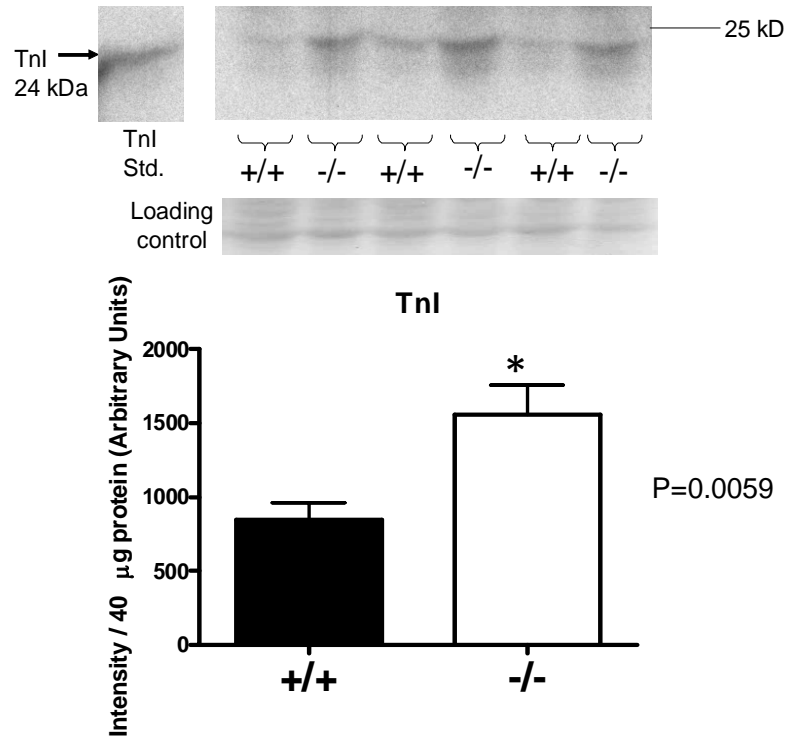


Figure 5.7: Levels of sarcomeric and cytoskeletal proteins Cav-1^{+/+} and Cav-1^{-/-} subjected to 17 min I/R

Levels of sarcomeric and cytoskeletal proteins in Cav-1^{+/+} (N=10) and Cav-1^{-/-} (N=9) mouse hearts subjected to 17 min I/R. Cav-1^{-/-} hearts subjected to 17 min I/R have significantly higher levels of troponin I (A) and α -actinin (B) than Cav-1^{+/+} hearts (P=0.0059 and P=0.0095 respectively). The upper panels show representative Western blots of troponin I (A) and α -actinin (B) with the molecular weight markers shown on the right side of the panel. The loading control is a Ponceau stain of the PVDF membrane following antibody probing. The lower panels show the quantitative analysis of troponin I (A) and α -actinin (B) of all hearts.

A)



B)

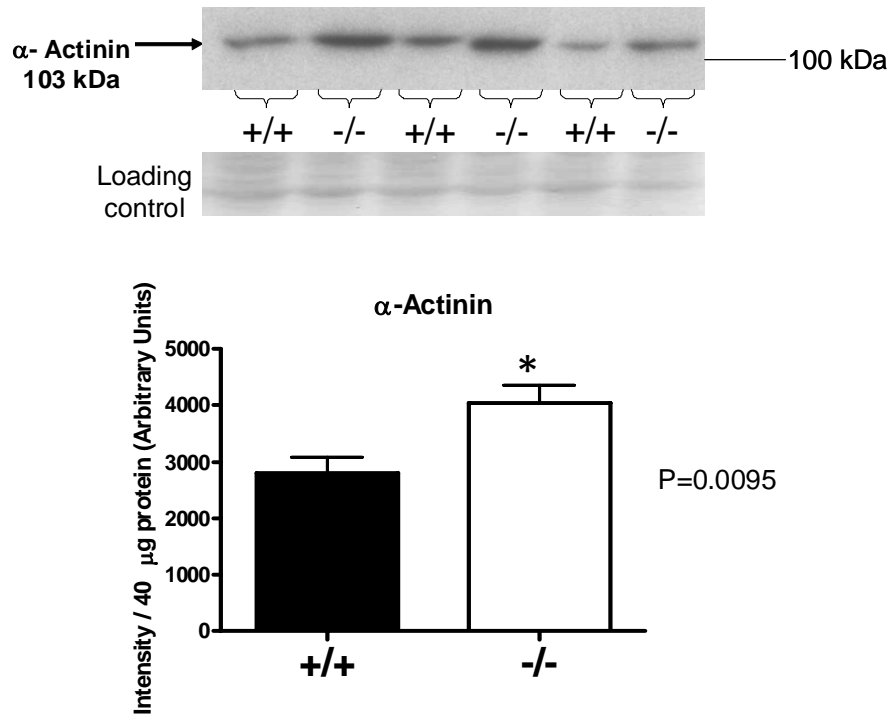


Table 5.1: Differences in functional parameters between the final aerobic measurement and the final measurement obtained during reperfusion, within each group for hearts exposed to 15 min ischemia

Cav-1^{+/+}

	Aerobic	Reperfusion	P
Heart rate (bpm)	350 ± 15	283 ± 48	0.188
Cardiac output (mL/min)	7.18 ± 0.64	4.69 ± 1.23	0.102
Peak systolic pressure (mmHg)	65.48 ± 0.90	51.94 ± 7.52	0.253
Pulse pressure (mmHg)	12.76 ± 0.29	11.25 ± 2.72	0.218
Coronary flow (mL/min)	2.14 ± 0.33	1.84 ± 0.43	0.379
Aortic flow (mL/min)	5.04 ± 0.60	2.90 ± 0.88	0.025*
Cardiac work ((mL/min) X mmHg)	472 ± 45	305 ± 88	0.138
Rate pressure product (bpm X mmHg)	22913 ± 1074	16214 ± 3499	0.237

Cav-1^{-/-}

	Aerobic	Reperfusion	P
Heart rate (bpm)	347 ± 11	360 ± 11	0.21
Cardiac output (mL/min)	5.96 ± 0.42	4.84 ± 0.59	0.077
Peak systolic pressure (mmHg)	64.27 ± 0.76	62.25 ± 1.89	0.223
Pulse pressure (mmHg)	11.83 ± 0.79	13.11 ± 0.99	0.169
Coronary flow (mL/min)	1.65 ± 0.19	1.81 ± 0.17	0.273
Aortic flow (mL/min)	4.31 ± 0.31	3.03 ± 0.54	0.034*
Cardiac work ((mL/min) X mmHg)	383 ± 27	306 ± 42	0.077
Rate pressure product (bpm X mmHg)	22286 ± 816	22543 ± 996	0.423

P values were determined using Student's t-test comparing the last aerobic value obtained to the final reperfusion value.

Table 5.2: Differences in functional parameters between the final aerobic measurement and the final measurement obtained during reperfusion, within each group for hearts exposed to 17 min ischemia

Cav-1^{+/+}

	Aerobic	Reperfusion	P
Heart rate (bpm)	352 ± 14	352 ± 19	0.491
Cardiac output (mL/min)	6.76 ± 0.38	3.25 ± 0.83	<0.001*
Peak systolic pressure (mmHg)	61.56 ± 1.21	45.97 ± 6.06	0.029*
Pulse pressure (mmHg)	8.49 ± 0.66	6.61 ± 1.29	0.256
Coronary flow (mL/min)	2.46 ± 0.26	2.03 ± 0.51	0.277
Aortic flow (mL/min)	4.30 ± 0.28	1.22 ± 0.45	<0.001*
Cardiac work ((mL/min) X mmHg)	417 ± 26	179 ± 51	0.001*
Rate pressure product (bpm X mmHg)	21636 ± 749	15906 ± 1938	0.025*

Cav-1^{-/-}

	Aerobic	Reperfusion	P
Heart rate (bpm)	329 ± 25	336 ± 25	0.416
Cardiac output (mL/min)	6.20 ± 0.48	3.28 ± 0.69	0.003*
Peak systolic pressure (mmHg)	61.84 ± 1.44	50.93 ± 5.93	0.104
Pulse pressure (mmHg)	9.74 ± 0.93	7.69 ± 1.29	0.091
Coronary flow (mL/min)	1.78 ± 0.16	1.43 ± 0.22	0.145
Aortic flow (mL/min)	4.42 ± 0.35	1.85 ± 0.50	0.001*
Cardiac work ((mL/min) X mmHg)	382 ± 29	192 ± 44	0.005*
Rate pressure product (bpm X mmHg)	20386 ± 1689	17049 ± 2374	0.22

P values were determined using Student's t-test comparing the last aerobic value obtained to the final reperfusion value.

5.5: References

1. Braunwald, E and Kloner, RA. The stunned myocardium: prolonged, postischemic ventricular dysfunction. *Circulation* 1982; 66:1146-1149.
2. Ambrosio, G, Betocchi, S, Pace, L, Losi, MA, Perrone-Filardi, P, Soricelli, A, Piscione, F, Taube, J, Squame, F, Salvatore, M, Weiss, JL, and Chiariello, M. Prolonged impairment of regional contractile function after resolution of exercise-induced angina. Evidence of myocardial stunning in patients with coronary artery disease. *Circulation* 1996; 94:2455-2464.
3. Breisblatt, WM, Stein, KL, Wolfe, CJ, Follansbee, WP, Capozzi, J, Armitage, JM, and Hardesty, RL. Acute myocardial dysfunction and recovery: a common occurrence after coronary bypass surgery. *J. Am. Coll. Cardiol.* 1990; 15:1261-1269.
4. Wang, W, Schulze, CJ, Suarez-Pinzon, WL, Dyck, JR, Sawicki, G, and Schulz, R. Intracellular action of matrix metalloproteinase-2 accounts for acute myocardial ischemia and reperfusion injury. *Circulation* 2002; 106:1543-1549.
5. Sawicki, G, Leon, H, Sawicka, J, Sariahmetoglu, M, Schulze, CJ, Scott, PG, Szczesna-Cordary, D, and Schulz, R. Degradation of myosin light chain in isolated rat hearts subjected to ischemia-reperfusion injury: a new intracellular target for matrix metalloproteinase-2. *Circulation* 2005; 112:544-552.
6. Sung, MM, Schulz, CG, Wang, W, Sawicki, G, Bautista-Lopez, NL, and Schulz, R. Matrix metalloproteinase-2 degrades the cytoskeletal protein alpha-actinin in peroxynitrite mediated myocardial injury. *J. Mol. Cell Cardiol.* 2007; 43:429-436.

7. Cheung, PY, Sawicki, G, Wozniak, M, Wang, W, Radomski, MW, and Schulz, R. Matrix metalloproteinase-2 contributes to ischemia-reperfusion injury in the heart. *Circulation* 2000; 101:1833-1839.
8. Van Eyk, JE, Powers, F, Law, W, Larue, C, Hodges, RS, and Solaro, RJ. Breakdown and release of myofilament proteins during ischemia and ischemia/reperfusion in rat hearts: identification of degradation products and effects on the pCa-force relation. *Circ. Res.* 1998; 82:261-271.
9. Schulze, CJ, Wang, W, Suarez-Pinzon, WL, Sawicka, J, Sawicki, G, and Schulz, R. Imbalance between tissue inhibitor of metalloproteinase-4 and matrix metalloproteinases during acute myocardial [correction of myoectardial] ischemia-reperfusion injury. *Circulation* 2003; 107:2487-2492.
10. Yasmin, W, Strynadka, KD, and Schulz, R. Generation of peroxynitrite contributes to ischemia-reperfusion injury in isolated rat hearts. *Cardiovasc. Res.* 1997; 33:422-432.
11. Okamoto, T, Akaike, T, Nagano, T, Miyajima, S, Suga, M, Ando, M, Ichimori, K, and Maeda, H. Activation of human neutrophil procollagenase by nitrogen dioxide and peroxynitrite: a novel mechanism for procollagenase activation involving nitric oxide. *Arch. Biochem. Biophys.* 1997; 342:261-274.
12. Okamoto, T, Akaike, T, Sawa, T, Miyamoto, Y, van, d, V, and Maeda, H. Activation of matrix metalloproteinases by peroxynitrite-induced protein S-glutathiolation via disulfide S-oxide formation. *J. Biol. Chem.* 2001; 276:29596-29602.

13. Viappiani, S, Nicolescu, AC, Holt, A, Sawicki, G, Crawford, BD, Leon, H, van, MT, and Schulz, R. Activation and modulation of 72kDa matrix metalloproteinase-2 by peroxynitrite and glutathione. *Biochem. Pharmacol.* 2009; 77:826-834.
14. Chow, AK, Cena, J, El-Yazbi, AF, Crawford, BD, Holt, A, Cho, WJ, Daniel, EE, and Schulz, R. Caveolin-1 inhibits matrix metalloproteinase-2 activity in the heart. *J. Mol. Cell Cardiol.* 2007; 42:896-901.
15. Shen, J, Ma, S, Chan, P, Lee, W, Fung, PC, Cheung, RT, Tong, Y, and Liu, KJ. Nitric oxide down-regulates caveolin-1 expression in rat brains during focal cerebral ischemia and reperfusion injury. *J. Neurochem.* 2006; 96:1078-1089.
16. Jasmin, JF, Malhotra, S, Singh, DM, Mercier, I, Rosenbaum, DM, and Lisanti, MP. Caveolin-1 deficiency increases cerebral ischemic injury. *Circ. Res.* 2007; 100:721-729.
17. Young, LH, Ikeda, Y, and Lefer, AM. Caveolin-1 peptide exerts cardioprotective effects in myocardial ischemia-reperfusion via nitric oxide mechanism. *Am. J. Physiol Heart Circ. Physiol* 2001; 280:H2489-H2495.
18. Sasse, J and Gallagher, SR. Detection of proteins on blot transfer membranes. *Curr. Protoc. Immunol.* 2008; Chapter 8:Unit.
19. Head, BP, Patel, HH, Tsutsumi, YM, Hu, Y, Mejia, T, Mora, RC, Insel, PA, Roth, DM, Drummond, JC, and Patel, PM. Caveolin-1 expression is essential for N-methyl-D-aspartate receptor-mediated Src and extracellular signal-regulated

- kinase 1/2 activation and protection of primary neurons from ischemic cell death. *FASEB J.* 2008; 22:828-840.
20. Patel, HH, Tsutsumi, YM, Head, BP, Niesman, IR, Jennings, M, Horikawa, Y, Huang, D, Moreno, AL, Patel, PM, Insel, PA, and Roth, DM. Mechanisms of cardiac protection from ischemia/reperfusion injury: a role for caveolae and caveolin-1. *FASEB J.* 2007; 21:1565-1574.
 21. Cho, WJ, Chow, AK, Schulz, R, and Daniel, EE. Matrix metalloproteinase-2, caveolins, focal adhesion kinase and c-Kit in cells of the mouse myocardium. *J. Cell Mol. Med.* 2007; 11:1069-1086.
 22. Maguy, A, Hebert, TE, and Nattel, S. Involvement of lipid rafts and caveolae in cardiac ion channel function. *Cardiovasc. Res.* 2006; 69:798-807.
 23. Ueda, H, Kawagishi, K, Terasawa, F, Nakamura, A, and Moriizumi, T. Caveolin-3 at the t-tubule colocalizes with alpha-actinin in the adult murine cardiac muscle. *Acta Histochem Cytochem* 2004; 37:373-378.
 24. Fishfader, P, Kirkpatrick, V, Eghbali, M, Minosyan, TY, and Stefani, E. Estrogen receptor alpha, caveolin and alpha-actinin form a macromolectular complex in the hearts. *Anesthesiology* 2006; 105:A659.
 25. Hiroi, Y, Guo, Z, Li, Y, Beggs, AH, and Liao, JK. Dynamic regulation of endothelial NOS mediated by competitive interaction with alpha-actinin-4 and calmodulin. *FASEB J.* 2008; 22:1450-1457.

26. Calaghan, S, Kozera, L, and White, E. Compartmentalisation of cAMP-dependent signalling by caveolae in the adult cardiac myocyte. *J. Mol. Cell Cardiol.* 2008; 45:88-92.
27. Li, L, Desantiago, J, Chu, G, Kranias, EG, and Bers, DM. Phosphorylation of phospholamban and troponin I in beta-adrenergic-induced acceleration of cardiac relaxation. *Am. J. Physiol Heart Circ. Physiol* 2000; 278:H769-H779.

CHAPTER 6

TROPONIN I PHOSPHORYLATION IN RESPONSE TO ISCHEMIA / REPERFUSION INJURY AND/OR β -ADRENERGIC STIMULATION IN THE ISOLATED WORKING MOUSE HEART

6.1: Introduction

Serum troponin is one of the primary biomarkers used for the detection of cardiac injury¹, though the mechanisms by which troponin and its degradation products are released into the circulation are still relatively unknown. The troponin complex is composed of three units: troponins C, I and T. Cardiac troponin I (cTnI) is a heart specific isoform² that is complexed to tropomyosin on actin filaments and prevents the binding of myosin to the actin filament. The presence of circulating cTnI is considered to be the “gold standard” marker for cardiac injury, as it has been shown to be more sensitive than creatine kinase-MB, myoglobin and lactate dehydrogenase assays for detecting myocardial damage³.

Though serum cTnI is a specific indicator of acute myocardial infarction⁴⁻⁶, it is still not known how this cTnI enters the circulation. One theory suggests that the proteolysis of cTnI may allow it to enter the blood stream. Indeed, an isolated working rat heart model of the stunned myocardium revealed that cTnI is degraded⁷. More specifically, myocardial stunning can remove the 17 C-terminal amino acids of cTnI⁷ and mice expressing this truncated cTnI have compromised function⁸. In fact, this C-terminal degradation of cTnI was also observed in patients undergoing coronary artery bypass graft surgery, a form of myocardial stunning⁹.

Post-translational modifications may play an important role in determining the susceptibility of TnI to degradation and/or release. Both degraded cTnI and extensively phosphorylated cTnI were detected in the serum of patients with acute myocardial infarction¹⁰. A number of phosphorylation sites in cTnI have been found and have been shown to have functional significance, particularly S23 and S24^{11;12}, though the

significance of the numerous other cTnI phosphorylation sites is still a matter of debate¹³. Both protein kinase A (PKA)^{14;15} and protein kinase C (PKC)^{14;16} have been shown to be able to phosphorylate cTnI at S23 and S24. PKC- δ can also phosphorylate S43, S45 and T144 while PKC- β more specifically phosphorylates T144¹⁷. Additionally, adrenergic stimulation has been shown to phosphorylate S77 and S150¹⁸, and *in vitro* studies examining the phosphorylation of these two sites induces a structural change in cTnI that alters its interaction with TnC, resulting in an exacerbated response to calcium¹⁹. Studies using cTnI mutant mice also adds support to the role of cTnI in mediating cardiac function. Transgenic mice expressing C-terminally truncated cTnI also demonstrated characteristics of myocardial stunning, including altered calcium responsiveness, reduced contractility and ventricular dilatation⁸. In mutant mice with the cTnI phosphorylation sites S23/S24/S43/S45/T144 all replaced with alanine to prevent phosphorylation from occurring, β -adrenergic stimulation caused a reduction of myocyte twitch relaxation that was observed in controls^{20;21}. Another study using mutated cTnI (S23/S24 mutated to aspartate) to mimic phosphorylated cTnI showed that this mutation altered cTnI's interaction with cTnC²², resulting in a decreased affinity to calcium. It also provided an explanation of why enhanced relaxation is observed with β -adrenergic induced PKA phosphorylation of cTnI²³. As well, ischemic heart muscle showed a decline in S23/24 cTnI phosphorylation when compared with aerobically perfused hearts²⁴, which is consistent with other observations²⁵⁻²⁸.

One enzyme that plays a role in the proteolysis and also possibly the release of TnI is MMP-2. MMP-2 was shown to degrade TnI in an *in vitro* assay and this degradation was prevented by pharmacological inhibition of MMP-2^{29;30}. MMP-2 may

be activated during I/R as a result of the rapid increase in oxidative stress via the biosynthesis of ONOO⁻, especially at the onset of reperfusion³¹. ONOO⁻ has been shown to activate MMP-2³², resulting in increased proteolysis of intracellular MMP-2 targets such as TnI^{29;33}. MMP-2 has been shown to play an important role in mediating I/R injury^{34;35}. Inhibition of MMP-2 during I/R by the administration of an oral MMP-2 inhibitor (TISAM) prior to I/R reduced the mortality rate of mice by cardiac rupture³⁶. Additionally, inhibition of MMP-2 in isolated rat hearts using a neutralizing antibody or the MMP inhibitors doxycycline or o-phenanthroline resulted in improved cardiac function during reperfusion³⁷ and prevented TnI proteolysis²⁹. MMP-2 knockout mice demonstrated similar results to TISAM treated mice³⁶. Of note is the fact that one of the potential MMP-2 cleavage sites in cTnI is located near a phosphorylation site (Schulz lab, unpublished observations). Indeed, phosphorylation of PKA sites on cTnI reduces the susceptibility of cTnI to proteolysis by MMP-2 and the protective effect is increased when a PKC site in the inhibitory domain of cTnI is blocked by mutation³⁸.

β -adrenergic agonists can activate MMPs in cardiomyocytes³⁹⁻⁴¹. Indeed, in studies using adult rat ventricular myocytes, β -adrenergic stimulation using isoproterenol resulted in both increased MMP-2 activity, mRNA and protein expression, as well as subsequent cell death via apoptosis⁴¹. Inhibition of MMPs using GM-6001 or SB-3CT reduced the isoproterenol-induced apoptosis while treatment with MMP-2 exacerbated cell death⁴¹, though the mechanism by which this may occur is yet undefined.

Because adrenergic stimulation results in the phosphorylation of cTnI via PKC or PKA, and one of the phosphorylation sites is near an MMP-2 cleavage site, we

hypothesize that this phosphorylation may sterically hinder the proteolysis of cTnI by MMP-2. Thus, the purpose of this study is to examine whether *in situ* phosphorylation of cTnI using isoproterenol in the isolated heart results in the protection of cTnI from MMP-2 cleavage.

6.2: Materials and methods

All experiments were performed in accordance with the Canadian Council on Animal Care *Guide to the Care and Use of Experimental Animals*

6.2.1: Animals

Male 6- to 8-wk-old C57Bl/6J mice were obtained from Jackson Laboratories (Bar Harbor, ME, USA).

6.2.2: Isolated working mouse heart

Ten min prior to euthanasia by intraperitoneal pentobarbital injection, mice were injected with 100 IU of heparin (i.p.) to prevent blood clotting in the coronary vessels. Hearts were rapidly excised from deeply anesthetized mice and placed immediately into an ice-cold Krebs-Henseleit bicarbonate solution (118 mM NaCl, 25 mM NaHCO₃, 4.7 mM KCl, 1.2 mM MgSO₄, 1.2 mM KH₂PO₄, 2.25 mM CaCl₂, 0.5 mM EDTA, and 11.1 mM glucose, oxygenated with 95% O₂ - 5% CO₂ (pH 7.4)) to arrest beating. The aorta was then cannulated with a 20 gauge cannula and perfused in Langendorff mode at 60 mmHg constant hydrostatic pressure at 37°C with the aforementioned Krebs-Henseleit solution. The left atrium was then cannulated through the pulmonary opening and the heart is switched from the Langendorff mode to the working mode whereby the heart is

perfused with a recirculating Krebs-Henseleit bicarbonate solution at 37°C supplemented with 0.2% bovine serum albumin, 5 mM pyruvate, and 100 mU/L human insulin and continuously gassed with 95% O₂ - 5% CO₂ (pH 7.4) at a left atrial preload pressure of 11.5 mmHg and an aortic afterload pressure of 50 mmHg.

Spontaneously beating hearts were allowed to equilibrate aerobically for 10 min prior to 20 min of aerobic perfusion. The heart groups were administered 100 nM DL-isoproterenol added to the recirculating perfusate 10 min into the aerobic perfusion period. Ten min later, the hearts in the ischemia groups were subjected to 17 min of global, no-flow ischemia by clamping both the atrial in-flow and the aortic out-flow lines. After the elapsed ischemia time, the atrial in-flow and aortic out-flow clamps were released to initiate 15 min of reperfusion for a total perfusion time of 57 min.

There were a total of four different treatment groups: Control, aerobically perfused for 57 min; Control + Iso, isoproterenol treated and aerobically perfused; I/R, 17 min of ischemia followed by 10 min of reperfusion; I/R + Iso, treated with isoproterenol prior to 17 min of ischemia followed by 10 min of reperfusion (Fig. 6.1).

Functional measurements were continuously recorded with the MP100 system from AcqKnowledge (BioPac Systems, Santa Barbara, CA, USA) for a total of 57 min. Cardiac output was measured via a Doppler flow probe (Transonic Systems, Ithaca, NY, USA) placed in the left atrial line while aortic flow was measured using a probe in the aortic afterload line. Heart rate and peak systolic and pulse (systolic – diastolic) pressures were measured with a pressure transducer (Harvard Apparatus, South Natick, MA), placed at the level of the heart, in the aortic line. Cardiac work was calculated as the product of peak systolic pressure and cardiac output. Coronary flow was calculated

as the difference between cardiac output and aortic flows. The rate pressure product is the product of the heart rate and the peak systolic pressure. At the end of the perfusion whole hearts were then clamped with Wollenberger tongs pre-cooled in liquid nitrogen and stored at -80°C until used.

6.2.3: Heart extracts

Frozen whole hearts were crushed and powdered using a mortar and pestle in liquid nitrogen and weighed. Four volumes (in mL) of ice-cold homogenization buffer (pH 7.4; 50 mM Tris, 31 mM sucrose, 1 mM DL-dithiothreitol, 0.1% Triton X-100, 10 µg/L soybean trypsin inhibitor, 10 mg/L leupeptin, 2 g/L aprotinin, and 100 mg/L phenylmethylsulfonyl fluoride) was added per gram frozen heart powder. The mixture was then homogenized with a Polytron, 3x30 s with 30 s of cooling in ice between each cycle. The samples were then centrifuged (4°C, 1000 × *g*, 5 min) and the supernatants were used for determination of protein content, enzyme activities and for Western blot analysis. Protein concentration was assessed by the bicinchoninic acid method using bovine serum albumin as a reference standard.

6.2.4: Western blotting

40 µg of total protein in each heart extract was run in 10% SDS-PAGE under reducing conditions. Separate gels used for the separation of phosphorylated proteins also contained 3 µM of Phos-tag™ acrylamide (NARD Institute Ltd., Amagasaki, Japan) and 20 µM MnCl₂. Human recombinant MMP-2 and troponin I were loaded as controls. Following electrophoresis, samples were electroblotted onto polyvinylidene difluoride membranes. The membranes were then blocked at room temperature for 1 hour with 5% milk, followed by an overnight incubation at 4°C with primary antibodies (1:10 000

monoclonal mouse anti-human troponin I (Novogen), 1:1000 polyclonal rabbit anti-phospho Tnl (Cell Signaling), 1:1000 monoclonal mouse anti-human MMP-2 (Chemicon)). These membranes were then probed with 1:5000 anti-mouse or anti-rabbit horseradish peroxidase conjugated secondary antibody and incubated with ECL Plus (Amersham) for 5 minutes before being exposed to film. Membranes were Ponceau stained to ensure equal loading⁴².

Using $MnCl_2$ as a binding agent for Phos-tagTM, Phos-tagTM was immobilized in the acrylamide gel. As protein samples move through the acrylamide gel, phosphate groups were reversibly captured by Phos-tagTM, resulting in a mobility shift. Samples with a higher phosphorylation status were more delayed while running through the gel and would thus have a higher apparent molecular weight than less phosphorylated samples. Thus, in combination with an antibody that is capable of detecting all phosphorylation states of a protein, Phos-tagTM was capable of separating the multiple phosphorylation states of a single protein in a sample.

6.2.5: Gelatin zymography

40 μ g total protein in each heart extract was run in an 8% polyacrylamide gel containing 2 mg/mL porcine gelatin (Sigma-Aldrich, Oakville, ON). Conditioned media from HT-1080 human fibrosarcoma cells were used as a standard for MMP-2 activity. Following electrophoresis, the gel was washed 3x20 min in 2.5% Triton X-100. The gel was then incubated in 50 mM Tris HCl, 150 mM NaCl, 5 mM $CaCl_2$, pH. 7.6 for 48 hr at 37°C prior to being stained with 0.05% Coomassie Brilliant Blue in 25% methanol: 10% acetic acid for 1 hr and destained with 4% methanol: 8% acetic acid for 30 minutes.

6.2.6: Data analysis

Western blots and zymograms were analyzed using Image J software (NIH). Statistics and graphs were compiled using GraphPad Prism 4.03.

6.2.7: Statistics

Data are expressed as mean \pm SEM. Functional differences between groups were analyzed by two-way repeated measures analysis of variance and if significant, followed by Bonferroni post-hoc tests. Within group functional measures recorded immediately prior to the initiation of ischemia were compared to the final reperfusion values by Student's t-test. Differences in protein levels and gelatinolytic activity were analyzed by one-way analysis of variance and if significant, followed by Bonferroni post-hoc tests to compare differences between groups. P values of less than 0.05 were considered statistically significant.

6.3: Results

6.3.1: Functional measures

During the initial aerobic perfusion period, no significant differences were seen between the four groups in any of the functional parameters measured. Following injection of isoproterenol, the Control + Iso and the I/R + Iso groups showed significant increases in pulse pressure (Fig. 6.2B), heart rate (Fig. 6.4A) and rate pressure product (Fig. 6.4B) while aortic output (Fig 6.3B), cardiac output (Fig 6.5A) and cardiac work (Fig 6.5B) decreased significantly when compared with Control or I/R groups ($P < 0.05$ for 16 min time point). Coronary flow remained unchanged following isoproterenol administration (Fig. 6.3A).

Control hearts fared significantly better than both I/R groups as well as the Control + Iso group during the reperfusion period in terms of cardiac work, cardiac output and aortic output (Control vs Control + Iso, $P < 0.001$; Control vs I/R, $P < 0.001$; Control vs I/R + Iso, $P < 0.001$ at all reperfusion time points) (Fig. 6.3B, 6.5A, B).

Groups that were exposed to I/R alone fared better during the reperfusion period in terms of cardiac output ($P < 0.05$ at 44 min) (Fig. 6.5A) and aortic output ($P < 0.05$ at 44min) (Fig 6.3B) when compared with the I/R + Iso group.

The I/R group experienced significant reductions in aortic output, cardiac output and cardiac work during the reperfusion period when compared with the initial aerobic perfusion immediately prior to the initiation of ischemia. The I/R + Iso group had significant reductions in all of the measured functional parameters during the reperfusion period when compared to the aerobic period immediately prior to the initiation of ischemia, but following the administration of isoproterenol. These results are summarized in Table 6.1.

6.3.2: MMP-2 activity and protein content

No differences in MMP-2 protein content was observed between the four groups ($P = 0.4312$) (Fig. 6.6A). Likewise, gelatin zymography did not reveal any significant differences in 72kDa MMP-2 activity between the four groups ($P = 0.4391$) (Fig. 6.6B).

6.3.3: Troponin I levels

Western blotting did not reveal any significant differences in total cTnI levels between any of the four groups ($P = 0.6651$) (Fig. 6.7A).

6.3.4: Phospho Troponin I levels

Western blotting of the samples using a phospho-cTnI antibody revealed that there are differences between the treatment groups ($P=0.0004$). The Bonferroni post-hoc tests showed that the Control + Iso group had significantly increased levels of phospho-cTnI when compared with the Control ($P<0.01$) and the I/R ($P<0.001$) groups (Fig. 6.7B).

Western blotting of samples run on gels containing Phos-tagTM showed that three different phosphorylation states of cTnI were present in the samples (Fig 6.8A), while the total cTnI (the sum of all three phosphorylation states) was not different between the groups ($P=0.5713$) (Fig. 6.8B). There were significant differences between groups in the cTnI with the lowest apparent molecular weight (unphosphorylated cTnI) ($P<0.0001$) with Control having significantly higher levels of unphosphorylated cTnI than Control + Iso ($P<0.001$), I/R ($P<0.05$) and I/R + Iso ($P<0.001$). The I/R group also had higher levels of unphosphorylated cTnI than the Control + Iso group ($P<0.05$) (Fig. 6.8C). There were no apparent significant differences between groups of the cTnI of intermediate apparent molecular weight (phosphorylated cTnI) ($P=0.6615$) (Fig. 6.8D). Analysis of variance of the multi-phosphorylated cTnI with the highest apparent molecular weight (multiply phosphorylated cTnI) also revealed significant differences between groups ($P=0.0049$) with the Control + Iso group having higher levels than Control ($P<0.01$) and I/R ($P<0.05$), and the I/R + Iso group having higher levels than Control ($P<0.05$) (Fig. 6.8E).

6.4: Discussion

These data show that administration of isoproterenol prior to I/R leads to greater functional impairment than hearts subjected to I/R in the absence of isoproterenol. Additionally, it was also found that isoproterenol administration and I/R both result in the phosphorylation of cTnI, however, results from our Phos-tagTM gel electrophoresis revealed that β -adrenergic stimulation also leads to a more highly phosphorylated form of cTnI than that observed in hearts exposed I/R alone.

Isoproterenol increased the amount of phosphorylated cTnI in aerobically perfused hearts and ischemia reduced the amount of phosphorylation⁴³. In our hands, although β -adrenergic stimulation was sufficient to cause phosphorylation of cTnI, protection against I/R injury was not observed. This may be due to a limitation of the isolated working heart model. At higher heart rates, the heart may not be receiving sufficient oxygen to maintain its ideal cardiac output. Additionally, isoproterenol has a multitude of effects on the heart in addition to those which would result in the downstream phosphorylation of cTnI. For instance, β -adrenergic activation of PKC and/or PKA could result in the activation of multiple protein kinases which would have further downstream effects besides the phosphorylation of cTnI. Consequently, the exacerbated injury in hearts administered isoproterenol was not unexpected and confirms previous observations by other groups^{44;45}. An alternate strategy may be to administer more specific agents that would result in the phosphorylation of cTnI without some of the non-specific effects of isoproterenol.

The lack of change in the MMP-2 levels in these mice following I/R is surprising given that previous studies in rats have indicated that MMP-2 levels in hearts are decreased following ischemia^{29;37;46}. The similar MMP-2 levels between the groups may be a result of a “wash-out” effect where the MMP-2 may be rinsed into the perfusate as a result of the long perfusion time³³. As MMP-2 is activated by ONOO⁻ during I/R, it is also released into the effluent, resulting in decreased MMP-2 content in the tissue.

The results of this study did not reveal any appreciable difference in the levels of intact cTnI, which had been previously demonstrated in rat heart models of I/R^{7;29}. This may be due to a species difference, differences in lengths of ischemia, or a result of inter-operator variability. Alternatively, the short reperfusion time which was necessary to detect the transient nature of phosphorylation, may not have been sufficient to observe MMP-2 induced cleavage of cTnI.

Interestingly, our results from the Phos-tagTM gel indicate that isoproterenol is able to phosphorylate cTnI at sites that I/R alone does not, though we were not able to distinguish which particular site this may be. Adrenergic stimulation has been shown to phosphorylate S77 and S150 of cTnI¹⁸, while ischemia is most often associated with PKC-induced phosphorylation of S43/S45⁴⁷. It is likely that the more phosphorylated form of cTnI we observed in this current study is a result of adrenergic stimulation of multiple pathways, including PKC and PKA, which would lead to phosphorylation of multiple cTnI sites. Additionally, though the short reperfusion time was chosen to ensure that the transient cTnI phosphorylation could be observed, even this brief period may have resulted in the phosphorylation/dephosphorylation of multiple sites, which would not have been detectable using our current methods. Other groups have found that

isoproterenol treatment, which activates PKA, protects against TnI degradation⁴⁸. The fact that the phosphorylation of specific sites of a protein can alter its susceptibility to degradation is not novel. In fact, cTnI phosphorylation by PKC increases its susceptibility to calpain degradation while phosphorylation with PKA decreases the likelihood it is proteolyzed⁴⁹. Consistent with this notion is the fact that human failing hearts have significantly lower levels of PKA phosphorylated cTnI than non-failing hearts, though the authors did not find evidence of cTnI proteolysis²⁸.

Consistent with our results, one group reported that low-flow ischemia in perfused rat hearts does not alter the phosphorylation status of cTnI⁴³, though increased phosphorylation of both TnI and TnI was observed in dogs following myocardial infarction⁵⁰. Interestingly, 2D electrophoresis showed that phosphorylation of cTnI prevents I/R-induced degradation, though it was not shown which sites on cTnI were phosphorylated⁴⁸. However, this same study showed that phosphorylation of cTnI is able to protect against both N- and C- terminal degradation and that the I/R induced degradation products of cTnI are unphosphorylated⁴⁸ which is in line with our hypothesis that phosphorylation may protect the cTnI from degradation.

Though previous studies have shown that altering the phosphorylation status of cTnI can modify its susceptibility to proteolysis by MMP-2³⁸, the results from this study are equivocal. Though we were able to show that isoproterenol administration to the isolated working mouse heart is able to phosphorylate cTnI, this did not translate into improvement of function. This may be a result of the more complex *ex vivo* model that was used, when compared with the *in vitro* experiments. Additionally, in an attempt to capture the transient nature of cTnI phosphorylation, we limited the reperfusion period

to 10 min, which may have restricted our ability to detect functional changes. Finally, isoproterenol administration is a rather non-specific, though physiologically relevant, method of stimulating PKC and/or PKA to phosphorylate cTnI, and may indeed have a number of other actions which would confound our results. Nevertheless, whether cTnI phosphorylation is able to protect it from MMP-2 induced degradation is worthy of further study, though perhaps in a more simplified model.

Figure 6.1: Experimental design for mouse hearts exposed to isoproterenol and/or I/R

Functional parameters for four groups of C57Bl/6J isolated mouse hearts were measured for 20 min during aerobic perfusion. Isoproterenol treated groups (Control + Iso and I/R + Iso) were given 100 nM of DL-isoproterenol 10 min after the initiation of aerobic measurements. I/R groups (I/R and I/R + Iso) were subjected to 17 min of global, no-flow ischemia prior to 10 min of reperfusion.

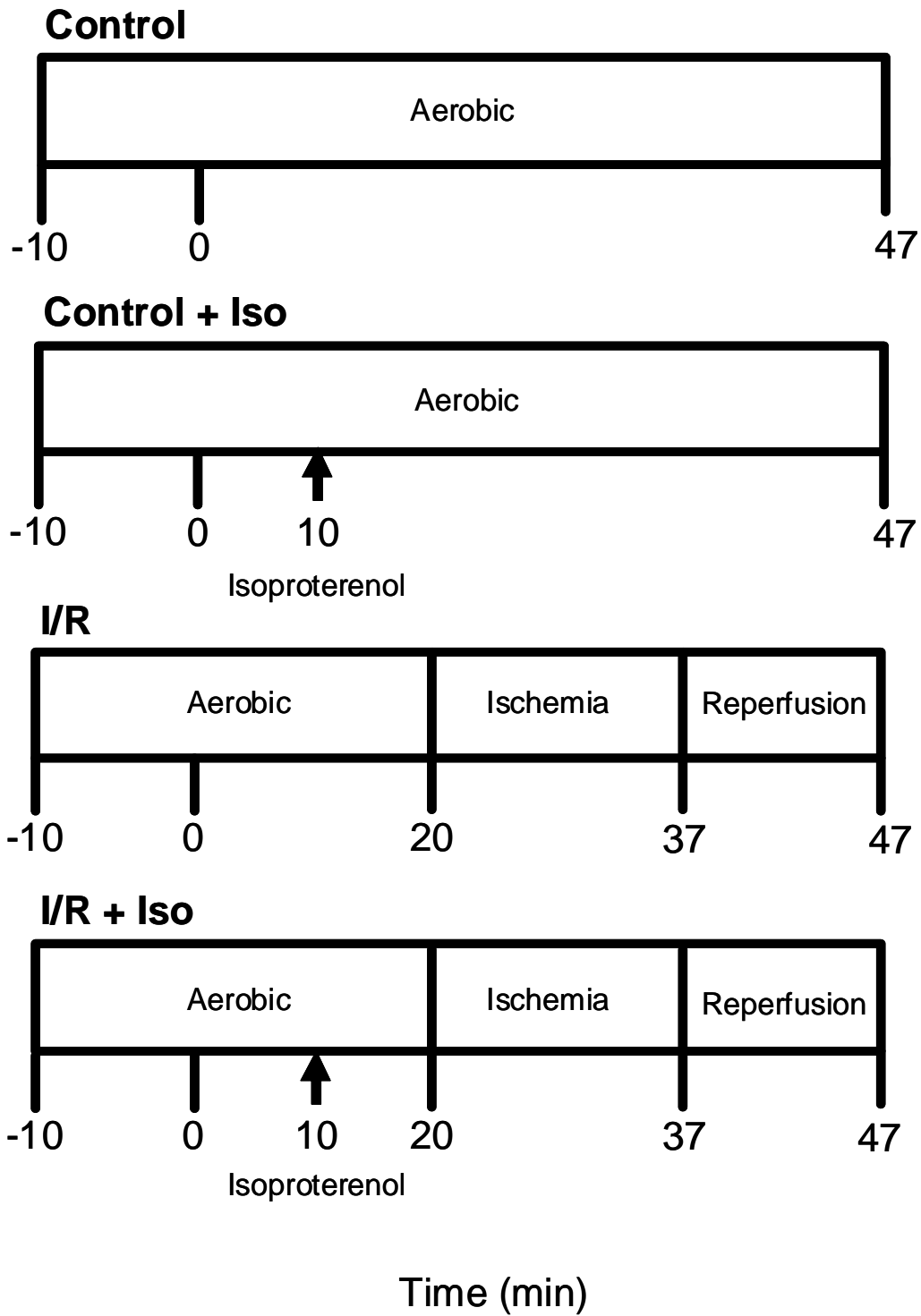
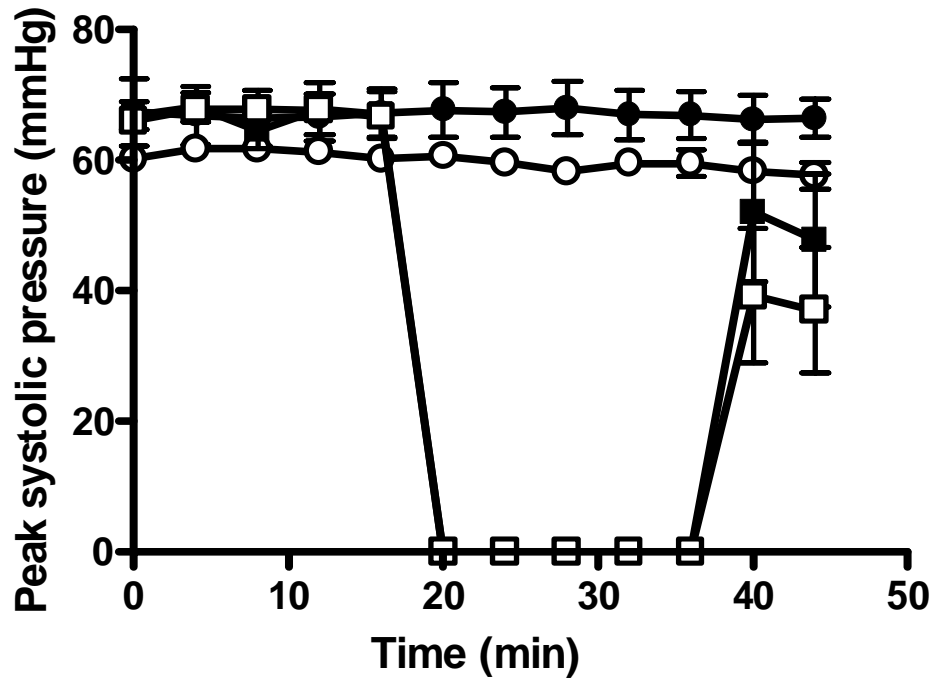


Figure 6.2: Peak systolic pressure and pulse pressure of isolated mouse hearts exposed to isoproterenol and/or I/R

Control (●) (N=4), Control + Iso (○) (N=4), I/R (■) (N=6) and I/R + Iso (□) (N=7). Error bars indicate \pm SEM where they exceed the symbol size.

A)

Peak systolic pressure



B)

Pulse Pressure

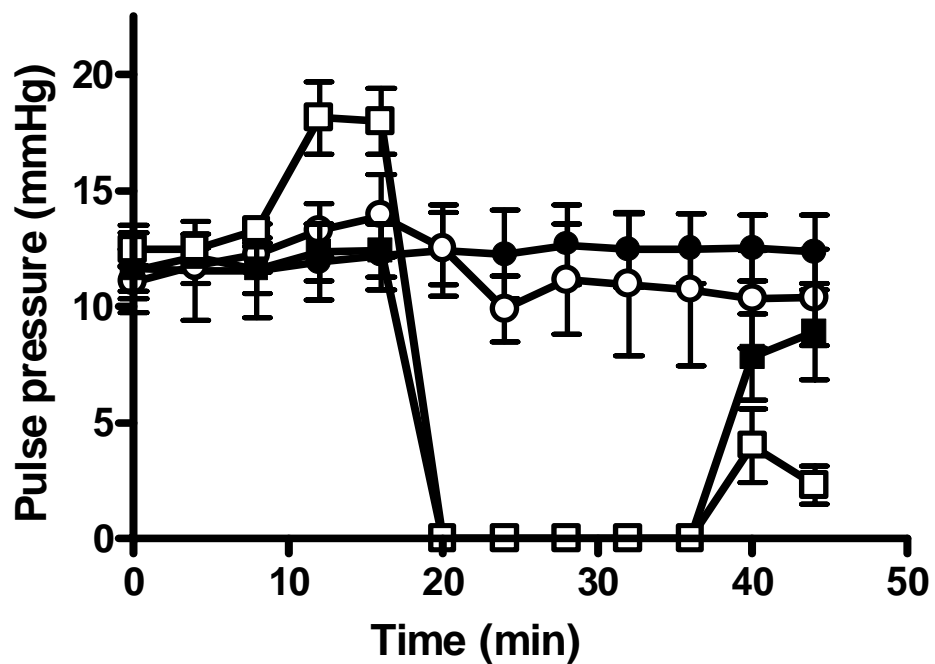
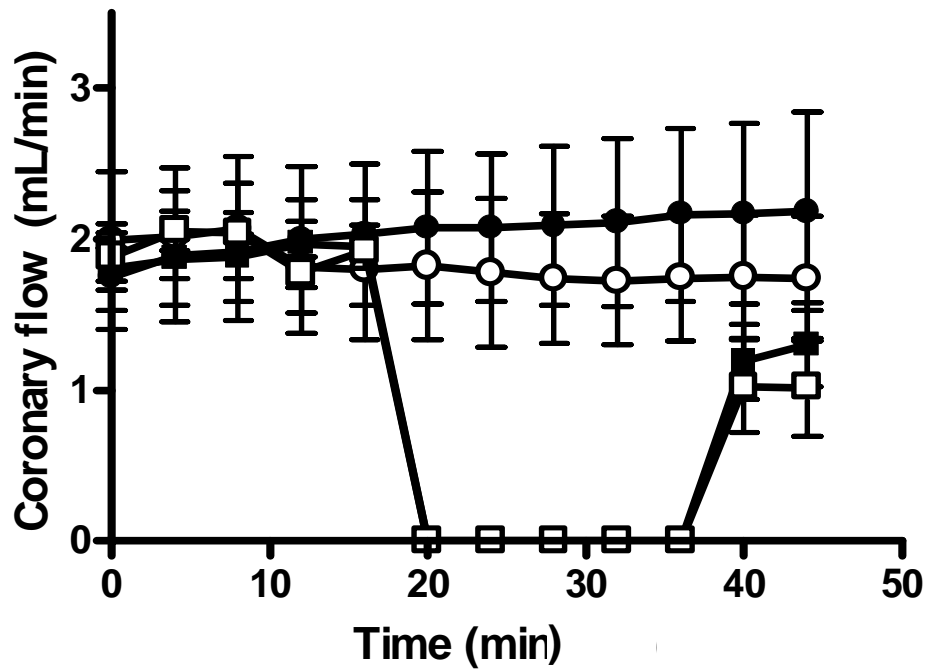


Figure 6.3: Coronary flow and aortic output of isolated mouse hearts exposed to isoproterenol and/or I/R

Control (●) (N=4), Control + Iso (○) (N=4), I/R (■) (N=6) and I/R + Iso (□) (N=7). Error bars indicate \pm SEM where they exceed the symbol size.

A) Coronary Flow



B) Aortic Output

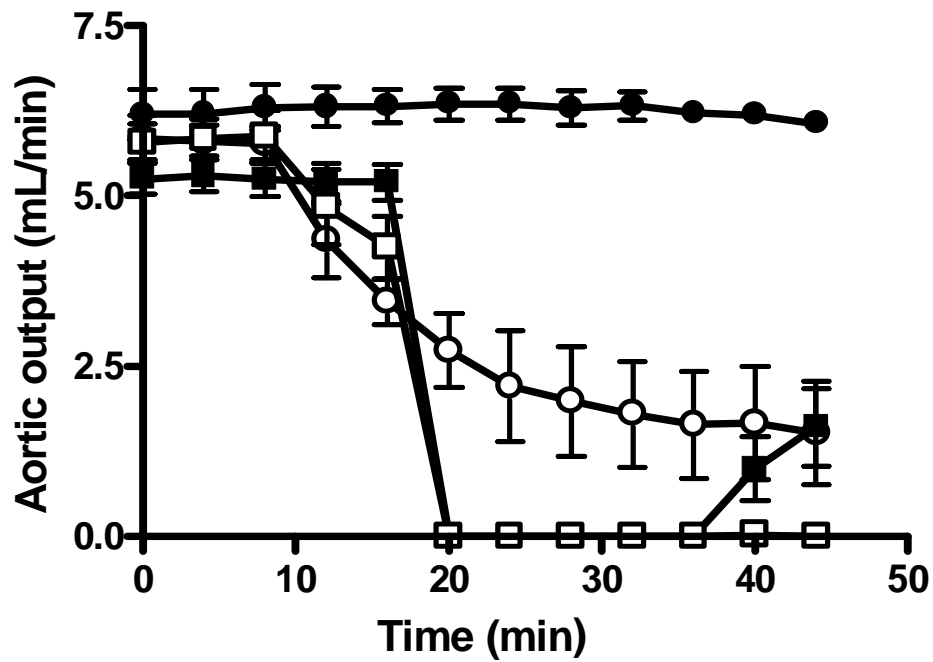
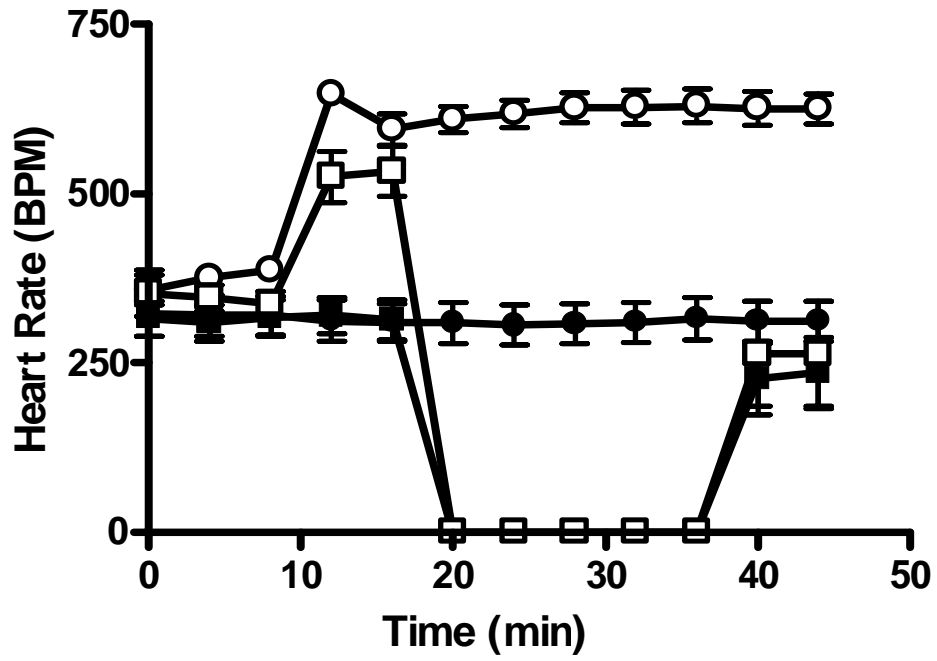


Figure 6.4: Heart rate and rate pressure product of isolated mouse hearts exposed to isoproterenol and/or I/R

Control (●) (N=4), Control + Iso (○) (N=4), I/R (■) (N=6) and I/R + Iso (□) (N=7). Error bars indicate \pm SEM where they exceed the symbol size.

A)

Heart Rate



B)

Rate pressure product

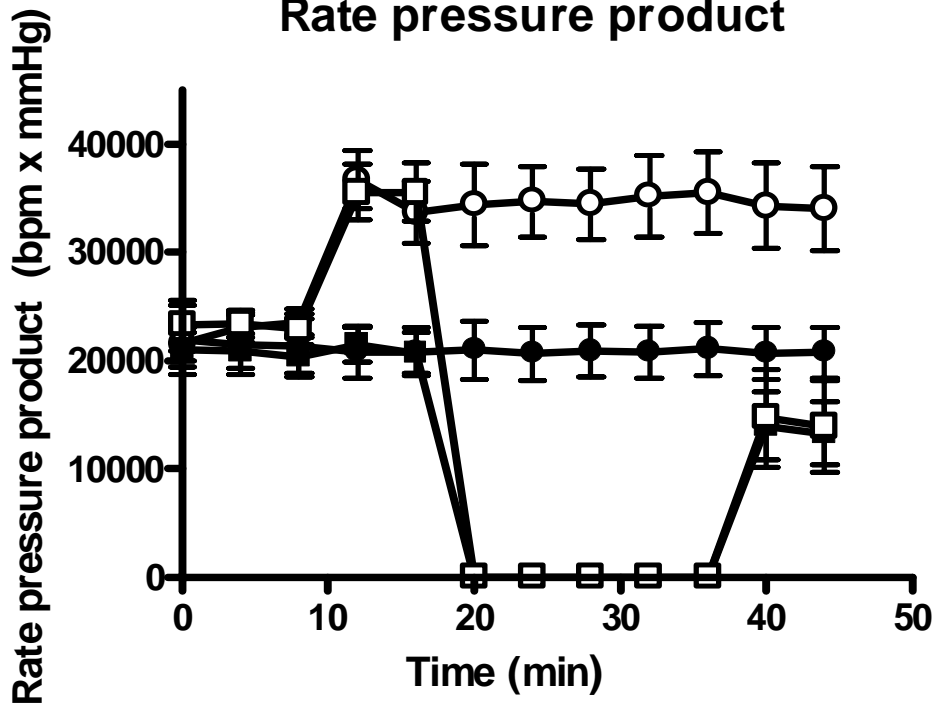


Figure 6.5: Cardiac output and cardiac work of isolated mouse hearts exposed to isoproterenol and/or I/R

Control (●) (N=4), Control + Iso (○) (N=4), I/R (■) (N=6) and I/R + Iso (□) (N=7). Error bars indicate \pm SEM where they exceed the symbol size.

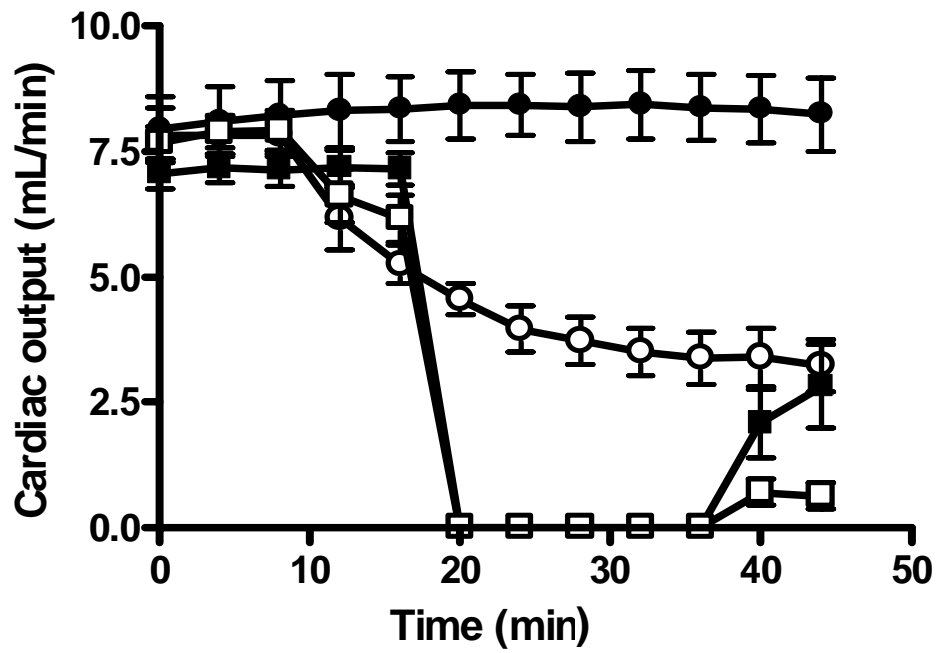
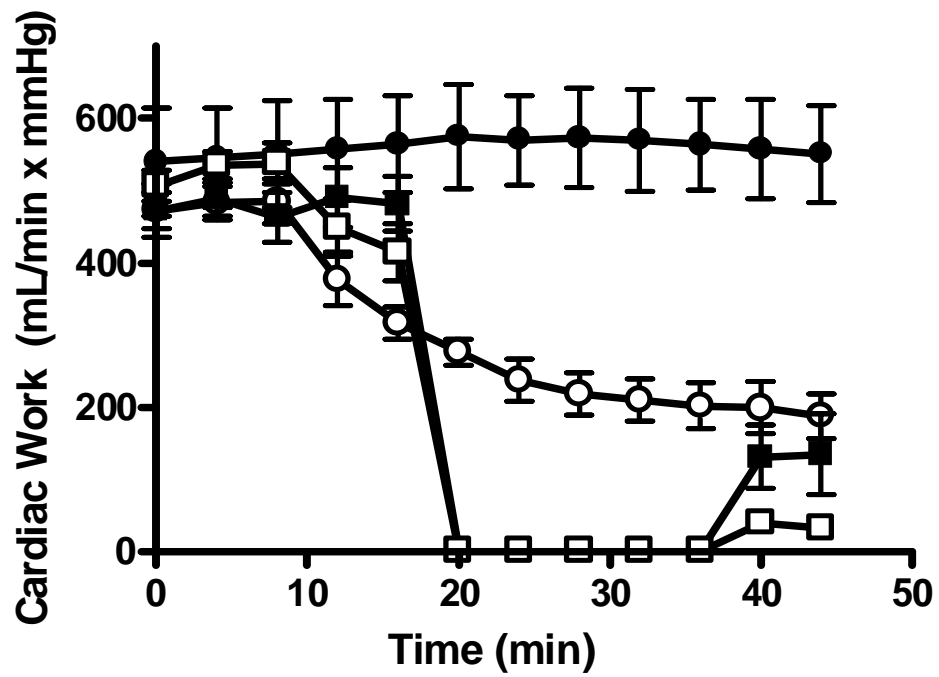
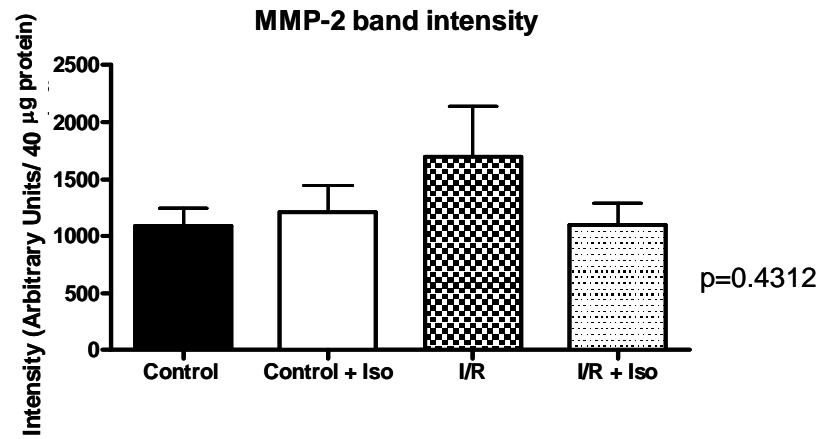
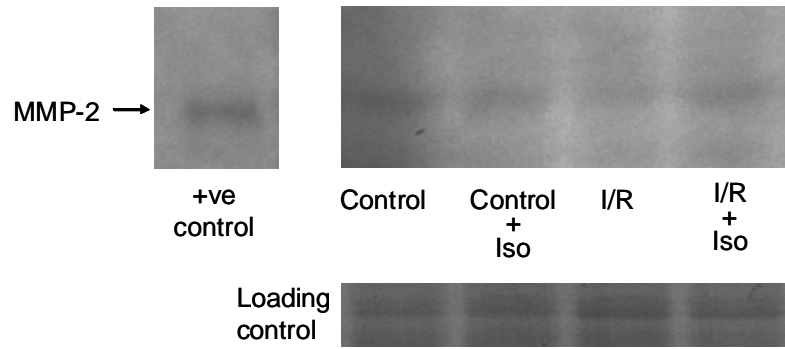
A)**Cardiac Output****B)****Cardiac Work**

Figure 6.6: MMP-2 protein and activity in isolated mouse hearts exposed to isoproterenol and/or I/R

A) Upper panel: representative Western blot showing 72 kDa MMP-2 protein levels in Control (N=4), Control + Iso (N=4), I/R (N=6) and I/R + Iso (N=7) hearts. A 72 kDa human recombinant MMP-2 standard is shown on the left. Lower panel: quantitative analysis of MMP-2 protein level in all hearts. Protein levels of MMP-2 are not different between the four groups (P=0.4312). Ponceau stained membranes are used as loading controls.

B) Upper panel: representative gelatin zymogram showing 72 kDa MMP-2 activity in Control, Control + Iso, I/R and I/R + Iso groups. To the left is a HT1080 MMP-2 standard showing both the 72 and 64 kDa isoforms of MMP-2. Lower panel: quantitative analysis of MMP-2 activity in all hearts MMP-2 zymographic activity is not different between the four groups (P=0.4391).

A)



B)

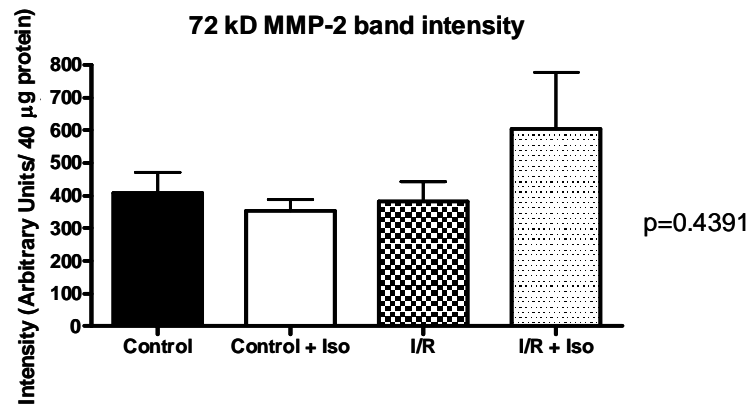
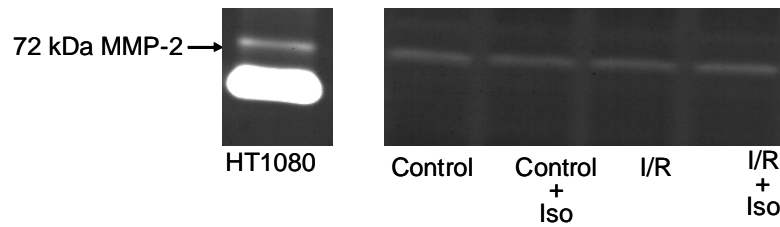
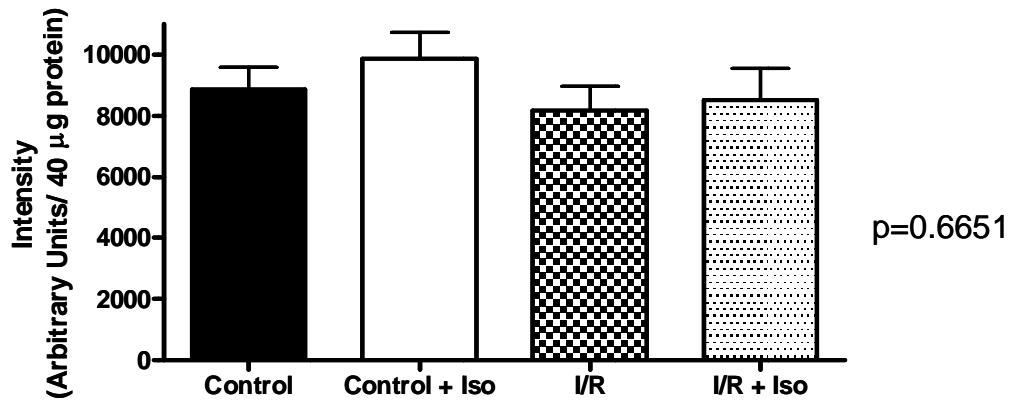
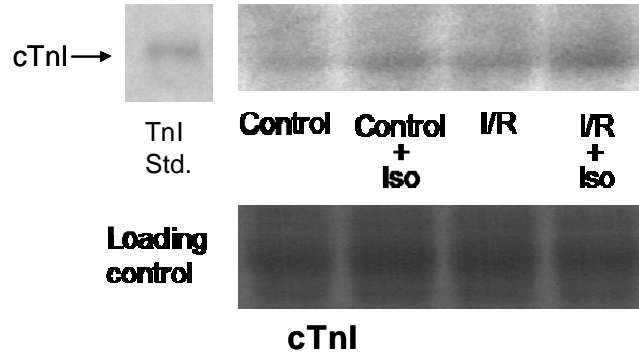


Figure 6.7: Levels of total and phosphorylated cTnI in isolated mouse hearts exposed to isoproterenol and/or I/R

Levels of cTnI in Control (N=4), Control + Iso (N=4), I/R (N=6) and I/R + Iso (N=7) hearts

Total cTnI levels did not vary between the four groups (P=0.6772). Differences were observed between groups for phosphorylated cTnI (P=0.0004) with Bonferroni post-hoc tests showing differences between the Control and Control + Iso and the I/R (P<0.001) groups. The upper panels show representative Western blots of cTnI (A) and phosphorylated cTnI (B). The lower panels show the quantitative analysis of cTnI (A) and phosphorylated cTnI (B) of all hearts. Ponceau stained membranes are used as loading controls.

A)



B)

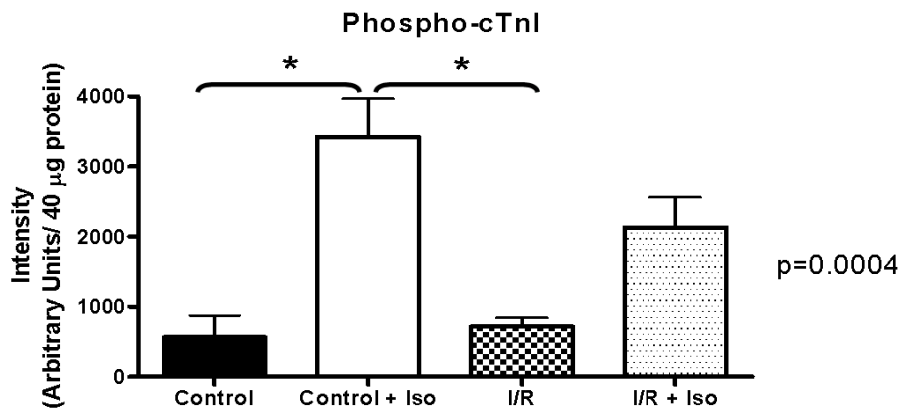
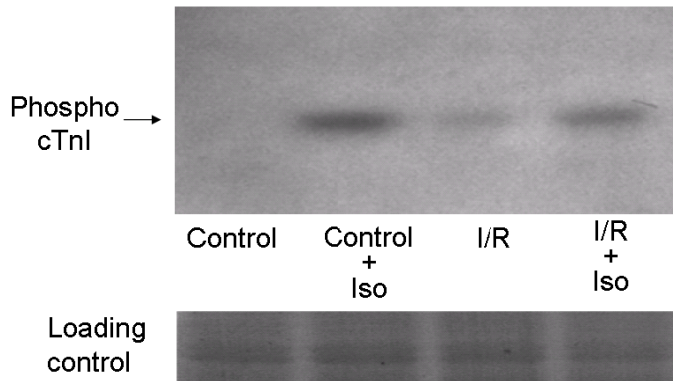


Figure 6.8: Levels of phosphorylated cTnI in isolated mouse hearts exposed to isoproterenol and/or I/R using a Phos-tagTM acrylamide gel

Levels of phosphorylated cTnI in Control (N=4), Control + Iso (N=4), I/R (N=6) and I/R + Iso (N=7) hearts run on a Phos-tagTM acrylamide gel. A) Heart samples run on Phos-tagTM acrylamide gels revealed three different phosphorylation states of cTnI. Ponceau stained membrane was used as a loading control. B) Quantification of the sum of all cTnI phosphorylation states (P=0.5713). C) Quantification of the lowest apparent molecular weight of cTnI (cTnI) (P<0.0001). The Control group has significantly higher levels of unphosphorylated cTnI than Control + Iso (***P<0.001), I/R (*P<0.05) and I/R + Iso (***P<0.001). The I/R group also had higher levels of unphosphorylated cTnI than the Control + Iso group (*P<0.05). D) Quantification of the intermediate molecular weight of cTnI (phospho cTnI) (P=0.6615). E) Quantification of the highest apparent molecular weight of cTnI (multiply phosphorylated cTnI). (P=0.0049). The Control + Iso group has higher levels than Control (**P<0.01) and I/R (*P<0.05), and the I/R + Iso group having higher levels than Control (*P<0.05).

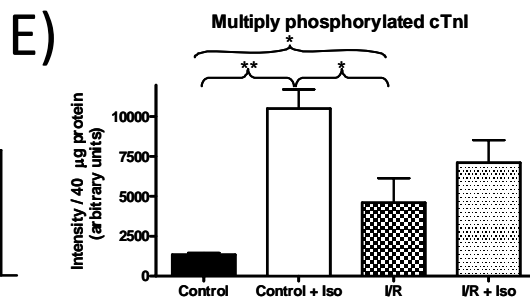
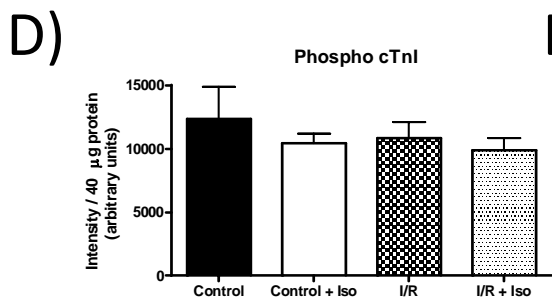
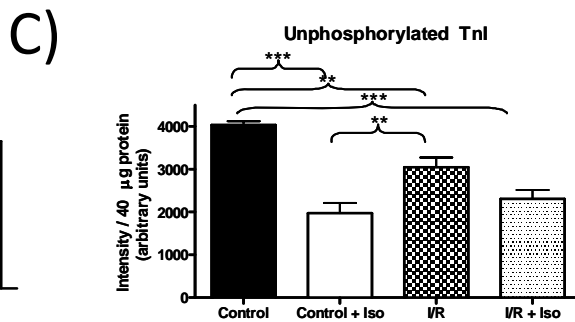
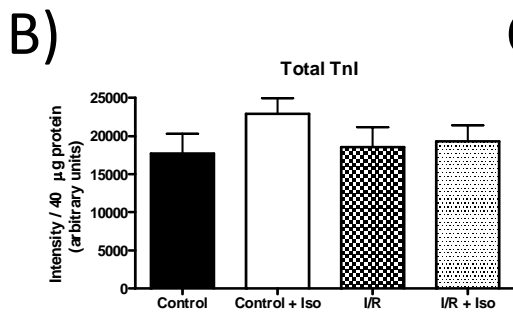
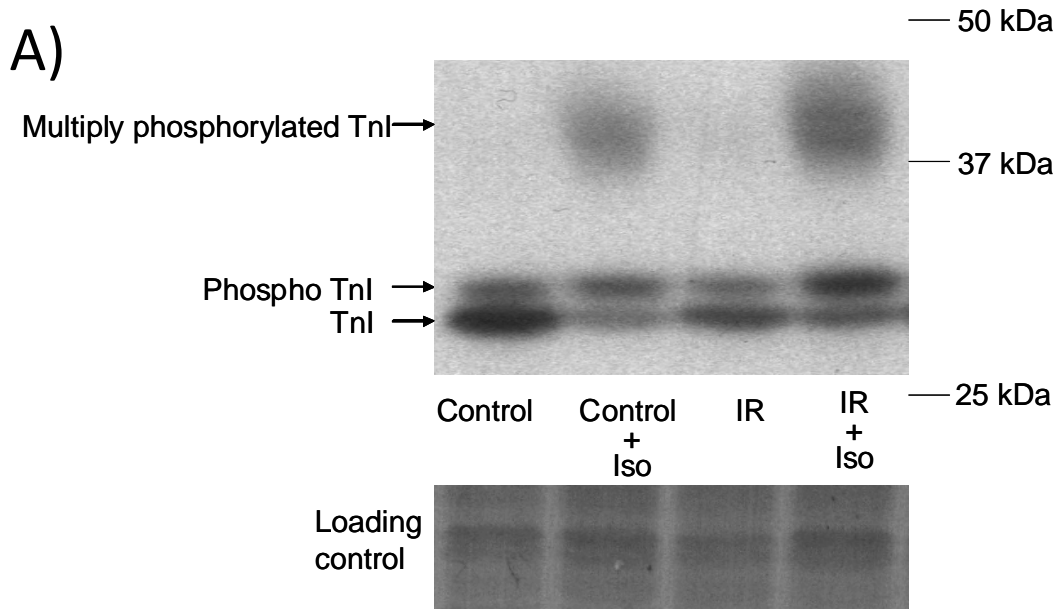


Table 6.1: Difference in functional parameters between the final aerobic measurement and the final measurement obtained during reperfusion, within each group

	Treatment	Pre-Ischemia Mean ± SEM	Post-Ischemia Mean ± SEM	P
Peak systolic pressure (mmHg)	I/R	67.02 ± 3.55	47.83 ± 10.17	0.105
	I/R + Iso	66.71 ± 1.67	37.06 ± 9.65	0.010 *
Pulse pressure (mmHg)	I/R	12.43 ± 1.13	8.91 ± 2.07	0.166
	I/R + Iso	17.99 ± 1.42	2.32 ± 0.81	< 0.001 *
Coronary flow (mL/min)	I/R	1.95 ± 0.14	1.30 ± 0.28	0.064
	I/R + Iso	1.92 ± 0.07	1.02 ± 0.32	0.018 *
Aortic output (mL/min)	I/R	5.20 ± 0.26	1.61 ± 0.57	< 0.001 *
	I/R + Iso	4.25 ± 0.46	0.00 ± 0.00	< 0.001 *
Heart Rate (bpm)	I/R	313.00 ± 29.30	235.17 ± 53.39	0.230
	I/R + Iso	532.71 ± 37.63	263.57 ± 77.67	0.009 *
Rate pressure product (bpm x mmHg)	I/R	20720.86 ± 1860.07	13262.57 ± 2911.13	0.056
	I/R + Iso	35533.90 ± 2651.60	13884.32 ± 4241.80	0.001 *
Cardiac output (mL/min)	I/R	7.15 ± 0.33	2.81 ± 0.83	0.001 *
	I/R + Iso	6.17 ± 0.47	0.64 ± 0.26	< 0.001 *
Cardiac work (mL/min x mmHg)	I/R	481.56 ± 37.58	134.62 ± 55.42	< 0.001 *
	I/R + Iso	414.30 ± 39.77	32.41 ± 13.01	< 0.001 *

6.5: References

1. Babuin, L and Jaffe, AS. Troponin: the biomarker of choice for the detection of cardiac injury. *CMAJ*. 2005; 173:1191-1202.
2. Cummins, P and Perry, SV. Troponin I from human skeletal and cardiac muscles. *Biochem. J*. 1978; 171:251-259.
3. del Rey, JM, Madrid, AH, Valino, JM, Rubi, J, Mercader, J, Moro, C, and Ripoll, E. Cardiac troponin I and minor cardiac damage: biochemical markers in a clinical model of myocardial lesions. *Clin. Chem*. 1998; 44:2270-2276.
4. Larue, C, Calzolari, C, Bertinchant, JP, Leclercq, F, Grolleau, R, and Pau, B. Cardiac-specific immunoenzymometric assay of troponin I in the early phase of acute myocardial infarction. *Clin. Chem*. 1993; 39:972-979.
5. Mair, J, Wagner, I, Puschendorf, B, Mair, P, Lechleitner, P, Dienstl, F, Calzolari, C, and Larue, C. Cardiac troponin I to diagnose myocardial injury. *Lancet* 1993; 341:838-839.
6. Adams, JE, III, Bodor, GS, vila-Roman, VG, Delmez, JA, Apple, FS, Ladenson, JH, and Jaffe, AS. Cardiac troponin I. A marker with high specificity for cardiac injury. *Circulation* 1993; 88:101-106.
7. Gao, WD, Atar, D, Liu, Y, Perez, NG, Murphy, AM, and Marban, E. Role of troponin I proteolysis in the pathogenesis of stunned myocardium. *Circ. Res*. 1997; 80:393-399.

8. Murphy, AM, Kogler, H, Georgakopoulos, D, McDonough, JL, Kass, DA, Van Eyk, JE, and Marban, E. Transgenic mouse model of stunned myocardium. *Science* 2000; 287:488-491.
9. McDonough, JL, Labugger, R, Pickett, W, Tse, MY, MacKenzie, S, Pang, SC, Atar, D, Ropchan, G, and Van Eyk, JE. Cardiac troponin I is modified in the myocardium of bypass patients. *Circulation* 2001; 103:58-64.
10. Labugger, R, Organ, L, Collier, C, Atar, D, and Van Eyk, JE. Extensive troponin I and T modification detected in serum from patients with acute myocardial infarction. *Circulation* 2000; 102:1221-1226.
11. Metzger, JM and Westfall, MV. Covalent and noncovalent modification of thin filament action: the essential role of troponin in cardiac muscle regulation. *Circ. Res.* 2004; 94:146-158.
12. Kobayashi, T and Solaro, RJ. Calcium, thin filaments, and the integrative biology of cardiac contractility. *Annu. Rev. Physiol* 2005; 67:39-67.
13. Solaro, RJ and van, d, V. Why does troponin I have so many phosphorylation sites? Fact and Fancy. *J. Mol. Cell Cardiol.* 2010.
14. Noland, TA, Jr., Guo, X, Raynor, RL, Jideama, NM, veryhart-Fullard, V, Solaro, RJ, and Kuo, JF. Cardiac troponin I mutants. Phosphorylation by protein kinases C and A and regulation of Ca(2+)-stimulated MgATPase of reconstituted actomyosin S-1. *J. Biol. Chem.* 1995; 270:25445-25454.

15. Stull, JT, Brostrom, CO, and Krebs, EG. Phosphorylation of the inhibitor component of troponin by phosphorylase kinase. *J. Biol. Chem.* 1972; 247:5272-5274.
16. Noland, TA, Jr., Raynor, RL, and Kuo, JF. Identification of sites phosphorylated in bovine cardiac troponin I and troponin T by protein kinase C and comparative substrate activity of synthetic peptides containing the phosphorylation sites. *J. Biol. Chem.* 1989; 264:20778-20785.
17. Sumandea, MP, Rybin, VO, Hinken, AC, Wang, C, Kobayashi, T, Harleton, E, Sievert, G, Balke, CW, Feinmark, SJ, Solaro, RJ, and Steinberg, SF. Tyrosine phosphorylation modifies protein kinase C delta-dependent phosphorylation of cardiac troponin I. *J. Biol. Chem.* 2008; 283:22680-22689.
18. Moir, AJ and Perry, SV. Phosphorylation of rabbit cardiac-muscle troponin I by phosphorylase kinase. The effect of adrenaline. *Biochem. J.* 1980; 191:547-554.
19. Li, MX, Wang, X, Lindhout, DA, Buscemi, N, Van Eyk, JE, and Sykes, BD. Phosphorylation and mutation of human cardiac troponin I differentially destabilize the interaction of the functional regions of troponin I with troponin C. *Biochemistry* 2003; 42:14460-14468.
20. Pi, Y, Zhang, D, Kemnitz, KR, Wang, H, and Walker, JW. Protein kinase C and A sites on troponin I regulate myofilament Ca²⁺ sensitivity and ATPase activity in the mouse myocardium. *J. Physiol* 2003; 552:845-857.

21. Pi, Y, Kemnitz, KR, Zhang, D, Kranias, EG, and Walker, JW. Phosphorylation of troponin I controls cardiac twitch dynamics: evidence from phosphorylation site mutants expressed on a troponin I-null background in mice. *Circ. Res.* 2002; 90:649-656.
22. Gaponenko, V, Abusamhadneh, E, Abbott, MB, Finley, N, Gasmi-Seabrook, G, Solaro, RJ, Rance, M, and Rosevear, PR. Effects of troponin I phosphorylation on conformational exchange in the regulatory domain of cardiac troponin C. *J. Biol. Chem.* 1999; 274:16681-16684.
23. Solaro, RJ and Rarick, HM. Troponin and tropomyosin: proteins that switch on and tune in the activity of cardiac myofilaments. *Circ. Res.* 1998; 83:471-480.
24. Han, YS and Ogut, O. Regulation of Fibre Contraction in a Rat Model of Myocardial Ischemia. *PLoS. One.* 2010; 5:e9528.
25. Christopher, B, Pizarro, GO, Nicholson, B, Yuen, S, Hoit, BD, and Ogut, O. Reduced force production during low blood flow to the heart correlates with altered troponin I phosphorylation. *J. Muscle Res. Cell Motil.* 2009; 30:111-123.
26. Zakhary, DR, Moravec, CS, Stewart, RW, and Bond, M. Protein kinase A (PKA)-dependent troponin-I phosphorylation and PKA regulatory subunits are decreased in human dilated cardiomyopathy. *Circulation* 1999; 99:505-510.
27. Bodor, GS, Oakeley, AE, Allen, PD, Crimmins, DL, Ladenson, JH, and Anderson, PA. Troponin I phosphorylation in the normal and failing adult human heart. *Circulation* 1997; 96:1495-1500.

28. Messer, AE, Jacques, AM, and Marston, SB. Troponin phosphorylation and regulatory function in human heart muscle: dephosphorylation of Ser23/24 on troponin I could account for the contractile defect in end-stage heart failure. *J. Mol. Cell Cardiol.* 2007; 42:247-259.
29. Wang, W, Schulze, CJ, Suarez-Pinzon, WL, Dyck, JR, Sawicki, G, and Schulz, R. Intracellular action of matrix metalloproteinase-2 accounts for acute myocardial ischemia and reperfusion injury. *Circulation* 2002; 106:1543-1549.
30. Rork, TH, Hadzimichalis, NM, Kappil, MA, and Merrill, GF. Acetaminophen attenuates peroxynitrite-activated matrix metalloproteinase-2-mediated troponin I cleavage in the isolated guinea pig myocardium. *J. Mol. Cell Cardiol.* 2006; 40:553-561.
31. Yasmin, W, Strynadka, KD, and Schulz, R. Generation of peroxynitrite contributes to ischemia-reperfusion injury in isolated rat hearts. *Cardiovasc. Res.* 1997; 33:422-432.
32. Viappiani, S, Nicolescu, AC, Holt, A, Sawicki, G, Crawford, BD, Leon, H, van, MT, and Schulz, R. Activation and modulation of 72kDa matrix metalloproteinase-2 by peroxynitrite and glutathione. *Biochem. Pharmacol.* 2009; 77:826-834.
33. Wang, W, Sawicki, G, and Schulz, R. Peroxynitrite-induced myocardial injury is mediated through matrix metalloproteinase-2. *Cardiovasc. Res.* 2002; 53:165-174.

34. Schulz, R. Intracellular targets of matrix metalloproteinase-2 in cardiac disease: rationale and therapeutic approaches. *Annu. Rev. Pharmacol. Toxicol.* 2007; 47:211-242.
35. Chow, AK, Cena, J, and Schulz, R. Acute actions and novel targets of matrix metalloproteinases in the heart and vasculature. *Br. J. Pharmacol.* 2007; 152:189-205.
36. Matsumura, S, Iwanaga, S, Mochizuki, S, Okamoto, H, Ogawa, S, and Okada, Y. Targeted deletion or pharmacological inhibition of MMP-2 prevents cardiac rupture after myocardial infarction in mice. *J. Clin. Invest* 2005; 115:599-609.
37. Cheung, PY, Sawicki, G, Wozniak, M, Wang, W, Radomski, MW, and Schulz, R. Matrix metalloproteinase-2 contributes to ischemia-reperfusion injury in the heart. *Circulation* 2000; 101:1833-1839.
38. Jay, DJ, Garcia, E, Chow, AK, Cheung, PY, Ramirez, AL, and Schulz, R. Phosphorylation of cardiac troponin I affects its susceptibility to proteolysis by matrix metalloproteinase-2. *Can. J. Cardiol.* 2008; 24:0183.
39. Brilla, CG, Zhou, G, Rupp, H, Maisch, B, and Weber, KT. Role of angiotensin II and prostaglandin E2 in regulating cardiac fibroblast collagen turnover. *Am. J. Cardiol.* 1995; 76:8D-13D.
40. Coker, ML, Jolly, JR, Joffs, C, Etoh, T, Holder, JR, Bond, BR, and Spinale, FG. Matrix metalloproteinase expression and activity in isolated myocytes after

neurohormonal stimulation. *Am. J. Physiol Heart Circ. Physiol* 2001; 281:H543-H551.

41. Menon, B, Singh, M, and Singh, K. Matrix metalloproteinases mediate beta-adrenergic receptor-stimulated apoptosis in adult rat ventricular myocytes. *Am. J. Physiol Cell Physiol* 2005; 289:C168-C176.
42. Sasse, J and Gallagher, SR. Detection of proteins on blot transfer membranes. *Curr. Protoc. Immunol.* 2008; Chapter 8:Unit.
43. Krause, EG and England, PJ. Effect of isoproterenol on protein phosphorylation in myocardial ischaemia. *Gen. Physiol Biophys.* 1984; 3:193-199.
44. Maroko, PR, Kjekshus, JK, Sobel, BE, Watanabe, T, Covell, JW, Ross, J, Jr., and Braunwald, E. Factors influencing infarct size following experimental coronary artery occlusions. *Circulation* 1971; 43:67-82.
45. Bartel, S, Krause, EG, and Karczewski, P. Metabolic and contractile changes in ischaemic rat hearts after isoproterenol administration: effect of reperfusion. *Biomed. Biochim. Acta* 1986; 45:S215-S218.
46. Fert-Bober, J, Leon, H, Sawicka, J, Basran, RS, Devon, RM, Schulz, R, and Sawicki, G. Inhibiting matrix metalloproteinase-2 reduces protein release into coronary effluent from isolated rat hearts during ischemia-reperfusion. *Basic Res. Cardiol.* 2008; 103:431-443.
47. MacGowan, GA, Du, C, Cowan, DB, Stamm, C, McGowan, FX, Solaro, RJ, Koretsky, AP, and Del Nido, PJ. Ischemic dysfunction in transgenic mice

expressing troponin I lacking protein kinase C phosphorylation sites. *Am. J. Physiol Heart Circ. Physiol* 2001; 280:H835-H843.

48. McDonough, JL, Arrell, DK, and Van Eyk, JE. Troponin I degradation and covalent complex formation accompanies myocardial ischemia/reperfusion injury. *Circ. Res.* 1999; 84:9-20.
49. Di, LF, De, TR, Salamino, F, Barbato, R, Melloni, E, Siliprandi, N, Schiaffino, S, and Pontremoli, S. Specific degradation of troponin T and I by mu-calpain and its modulation by substrate phosphorylation. *Biochem. J.* 1995; 308 (Pt 1):57-61.
50. Li, P, Hofmann, PA, Li, B, Malhotra, A, Cheng, W, Sonnenblick, EH, Meggs, LG, and Anversa, P. Myocardial infarction alters myofilament calcium sensitivity and mechanical behavior of myocytes. *Am. J. Physiol* 1997; 272:H360-H370.

CHAPTER 7

CONCLUSIONS

7.1: Conclusions

Cardiovascular diseases are the leading cause of death and claimed over 17.1 million lives worldwide in 2004 alone¹. By 2030, this number is projected to be 23.6 million, with many of these new deaths occurring in low and middle income countries which are adopting a more Westernized diet and lifestyle. Ischemic heart disease accounts for a significant proportion of cardiovascular diseases and results in significant morbidity and mortality¹. Consequently, a thorough understanding of the pathophysiology that underlies ischemic heart disease is not only essential to ease the strain on the already taxed health care system, but also to reduce the number of lives lost.

Though great inroads have been made in terms of prolonging the life of those who have suffered ischemic heart disease, little is still known about the mechanism that is responsible for initiating and propagating the damage to the heart. Recently, MMPs have been the focus of much research, particularly in light of the fact that they have been shown to play significant roles in the initiation, propagation and recovery from ischemic heart disease. Elucidation of the regulation of MMP proteolytic activity, particularly intracellular MMP activity, is pivotal to the understanding of how MMPs mediate ischemic damage.

As such, this thesis as a whole has focused on the intracellular regulation of MMP-2 activity. Chapter 2 was the first instance that describes the inhibition of MMP-2 activity by Cav-1. Both an *in vitro* degradation assay, as well as a knockout mouse model demonstrated that Cav-1 is capable of inhibiting MMP-2 activity. CSD was capable of *in vitro* inhibition of MMP-2 proteolysis of an internally quenched fluorogenic substrate in a concentration dependent manner. Cav-1^{-/-} mouse hearts also demonstrated

significantly increased zymographic MMP-2 activity when compared with Cav-1^{+/+} hearts. These results are consistent with the hypothesis that Cav-1 is responsible for maintaining MMP-2 in a membrane localized and inhibited configuration, though this did not eliminate a role of extracellular MMP-2. No evidence of increased extracellular MMP-2 proteolytic activity was found in the Cav-1^{-/-} mouse hearts.

Co-localization of MMP-2 and Cav-1 was also demonstrated using immunohistochemistry and this was further elaborated on in Chapter 3. Whether Cav-1 exists in cardiomyocytes has been a subject of much debate, though the confocal micrographs in Chapters 2 and 3 reveal the presence of Cav-1 on the plasma membrane of cardiomyocytes. Additionally, in Chapter 3, MMP-2 was found to be co-localized with Cav-3, a muscle specific caveolin, in the heart.

The fact that Cav-1^{-/-} hearts demonstrated perturbed MMP-2 localization also lends credence to the hypothesis that Cav-1 may play a role in MMP-2 regulation. Confocal immunohistochemistry in both Chapters 2 and 3 reveals that Cav-1^{-/-} cardiomyocytes have a more diffuse cytoplasmic distribution of MMP-2 when compared with Cav-1^{+/+} hearts, which demonstrate MMP-2 localization to the Z-lines and plasma membrane. Whether this may be due to a direct effect of Cav-1 anchoring MMP-2 to specific locales, or an indirect effect of perturbed tubulin in Cav-1^{-/-} hearts is not known. The possibility of tubulin perturbations in Cav-1^{-/-} hearts is particularly intriguing given that MMP-2 is able to degrade α - tubulin in an *in vitro* assay (Chapter 2) and that tubulin is responsible for the transport of MMP-2 to the plasma membrane in preparation for extracellular export². If MMP-2 does indeed degrade tubulin in Cav-1^{-/-} as a result of Cav-1 disinhibition of MMP-2 activity, this would also explain the increased MMP-2 activity in Cav-1^{-/-} cardiomyocytes, since MMP-2 transport to the extracellular milieu

would be inhibited. However, an increase in intracellular MMP-2 protein would also be expected, but was not observed, suggesting that other factors that influence MMP-2 activity, such as post-translational modifications, may be involved.

To determine whether the increased MMP-2 activity in Cav-1^{-/-} hearts translated to functional changes in hearts, Cav-1^{-/-} hearts were examined using an isolated working mouse heart model in Chapter 4. Aerobic perfusions showed no differences in function between Cav-1^{-/-} and Cav-1^{+/+} hearts and thus, the hearts were subjected to increasing preload pressure to determine whether a physiological stressor would reveal functional differences that may not have otherwise been apparent. It was found that though lower preload challenges did not reveal functional differences between Cav-1^{+/+} and Cav-1^{-/-} hearts, at higher preloads, it was evident that the Cav-1^{-/-} hearts did not respond in the same manner as Cav-1^{+/+} hearts. Cav-1^{+/+} hearts did not respond to increasing preloads with an increased cardiac output and cardiac work, as the Cav-1^{-/-} hearts did, but instead maintained a fairly consistent cardiac output and work with the varying preload pressures. Interestingly though, Cav-1^{-/-} hearts responded to increasing preload pressures with increasing coronary flow. The differences in functional response of the Cav-1^{+/+} and Cav-1^{-/-} isolated hearts to isoproterenol were less remarkable and may be confounded by the fact that these same hearts had previously been exposed to a preload challenge.

Because there were not marked differences between Cav-1^{+/+} and Cav-1^{-/-} hearts exposed to physiological or pharmacological challenges, we hypothesized that a stronger oxidative stress may be necessary in order to activate MMP-2 in Cav-1^{-/-} hearts to cause the degradation of intracellular MMP-2 substrates. In Chapter 5, isolated Cav-1^{-/-} and Cav-1^{+/+} working mouse hearts were subjected to I/R injury, which has previously

been shown to affect Cav-1 distribution in the intestine³ and kidney⁴, with Cav-1 migrating to the cytoplasm from the plasma membrane. We hypothesize that this migration would lead to disinhibition of the MMP-2 that is docked at the membrane in preparation for exocytosis, allowing MMP-2 to degrade its intracellular substrates. Additionally, Cav-1 null mice were also shown to be more susceptible to ischemic brain injury⁵. Though Cav-1^{+/+} and Cav-1^{-/-} hearts did not demonstrate functional differences following either 15 or 17 min of global, no-flow I/R, Cav-1^{-/-} hearts unexpectedly demonstrated preserved TnI and α -actinin, when compared with Cav-1^{+/+} hearts.

As a result of previous work from the Schulz lab that showed altered phosphorylation states of TnI can change TnI's susceptibility to MMP-2 proteolysis⁶, Chapter 6 was initiated to examine whether this is also the case in an *ex vivo* isolated working heart model. Though functional results were equivocal, PhosTagTM acrylamide electrophoresis showed that I/R and β -adrenergic stimulation result in different phosphorylation states of TnI with isoproterenol administration resulting in the appearance of an additional, more highly phosphorylated form of TnI.

7.2: Limitations

7.2.1: Experimental design limitations

The experimental design of the isolated heart perfusions in Chapter 4 has been particularly problematic. Because the isolated hearts were exposed sequentially to both a preload and a pharmacological challenge, the biochemical results obtained at the end of the perfusion period cannot be definitively attributed to either challenge. Additionally, since the preload challenge preceded isoproterenol administration, the functional measures during the adrenergic stimulation may also be confounded.

The reason the study was designed in this manner, however, was for practical reasons. The isolated working heart model is a costly experimental technique, particularly as there is an extremely narrow margin for operator error, and large physiological variability, which necessitates the use of a large number of animals. The expense of this technique is further magnified by the use of genetically modified animals. Ideally, separate groups of animals would have been used for the preload challenge and for the pharmacological challenge, with each group being processed separately for biochemistry following perfusion, though in reality, this could be cost prohibitive.

The experimental design for Chapter 5 also has limitations. The addition of Cav-1^{+/+} and Cav-1^{-/-} aerobic control hearts could add to the aid in interpreting the biochemical results. If these aerobic groups were included, it would be possible to ascertain whether the decrease in protein and activity levels were the result of the I/R, or whether it was an artifact of perfusion.

The experimental design for Chapter 6 could also be improved upon. The intent of Chapter 6 was to elucidate the susceptibility of specific phosphorylation states of TnI and moving directly into an isolated working heart model may have been premature. Further *in vitro* work with TnI mutants that are either constitutively phosphorylated or unphosphorylatable⁷ would serve to better clarify the ability of MMP-2 to degrade specifically phosphorylated states of TnI before moving into a more complex tissue model.

7.2.2: Technique limitations

Each experimental technique has specific limitations and it is essential that they be recognized in order to prevent over- or misinterpretation of data.

In vitro degradation techniques, such as those used in Chapter 2 are fundamentally limited, as are all *in vitro* techniques, by virtue of the fact that they are not performed in a physiologically relevant environment. Though one of the greatest strengths of *in vitro* techniques is the fact that it eliminates many of the confounding variables that may lead to ambiguation of results, this simplicity is also its greatest weakness. The ability of MMP-2 to degrade tubulin, as in Chapter 2, in an *in vitro* situation, for example, does not necessarily translate into proteolysis in an *in vivo* situation, particularly as physiological compensatory mechanisms are lacking in an *in vitro* experiment. Despite this, however, *in vitro* techniques provide insight into the mechanisms that may underlie the control of MMP-2 activity and are effective, economical tools to use prior to initiating more resource and time consuming *in vivo* experiments.

Though genetically modified animal models can be a powerful tool in the elucidation of the function of specific proteins involved in cardiac pathologies, a number of factors when using these models must be considered. Firstly, though the Cav-1^{-/-} mouse model specifically targets the elimination of the Cav-1 gene, other proteins may also be inadvertently affected which may complicate interpretation of data. Additionally, compensatory mechanisms may be present to counteract the effect of the missing protein. In the case of the Cav-1^{-/-} mice, as a result of the structural and functional similarities between Cav-1 and Cav-3, it was entirely possible that Cav-3

expression may be increased to compensate for the lack of Cav-1 (an examination of the Cav-1^{-/-} hearts prior to the initiation of any of the studies in this thesis showed that Cav-3 protein is not increased in Cav-1^{-/-} mice).

Gelatin zymography has been extensively used to determine MMP-2 and MMP-9 activity in many biological samples, though interpretation of zymographic results is not without caveats. The protocol for zymography runs gel electrophoresis under reducing conditions and consequently, MMPs would, in theory, be dissociated from any inhibitory complexes (eg. TIMPs, caveolin etc.). Interestingly though, results from Chapter 2 clearly indicate that Cav-1^{-/-} hearts have considerably more MMP-2 activity than Cav-1^{+/+} hearts and the Cav-1^{+/+} and Cav-1^{-/-} gelatinolytic activities are observed at the same molecular weights. Different MMP-2 post-translational modifications may be able to explain these discrepancies in MMP-2 zymographic activity, as phosphorylation or glutathiolation of a protein is not easily detectible as a change in molecular weight by conventional SDS-PAGE. Additionally, gelatin zymography relies on MMP-2's ability to degrade an artificial substrate (gelatin) and may not necessarily be indicative of MMP-2 activity on other substrates.

Though Western blots are a commonly used biochemical technique, it is also not without limitations. The quality of a Western blot is often determined by the quality of antibody available against the protein of interest, the abundance of the protein in the sample and the presence of interfering substances in the sample. For instance, clean, quantifiable Western blots are more likely to be obtained from samples obtained from cell culture, when compared with a whole heart homogenate, likely due to the larger number of other substances such as proteins, polysaccharides and lipids in tissue

samples. A number of commercially available antibodies are available for the proteins of interest in the studies performed in this thesis. Monoclonal antibodies were preferred, when available, due to the fact that they generally result in better signal to noise ratio, and higher specificity. However, in low abundance proteins, such as MMP-2 following long perfusion periods (Chapters 4 and 5), a polyclonal antibody may have been more useful as more epitopes of MMP-2 would be recognized and polyclonal antibodies typically have higher avidity to the target protein. Additionally, use of a secondary antibody and ECL detection methods to amplify the signal to detectable levels renders the Western blotting technique a semi-quantitative method, rather than one that is fully quantifiable. Additionally, post-translational modifications of the protein of interest may also affect antibody binding in an unpredictable manner. One of the major caveats of Western blot interpretation is that it is important to keep in mind that Western blots only approximately indicate the abundance of a protein and not its activity. Because of the fact that Western blots are run under denaturing and reducing conditions, proteins that are naturally inhibited by other non-covalently bound proteins, or are normally protected from degradation due to their tertiary structures, may appear in Western blots as degradation products due to the release of inhibitory proteins and relaxation of tertiary structures. Finally, Western blots only indicate the relative abundance of a protein and does not provide any information on the localization of the protein, which may be significant in terms of its function.

Immunohistochemistry has the advantage over Western blots in this particular aspect, as it is able to detect the localization of a protein *in situ*. As well, immunohistochemistry also does not use denaturing or reducing conditions, and thus, the results are more representative of proteins in their native forms. However, like

other techniques that rely heavily on antibodies, the interpretation of immunohistochemical results is reliant on the specificity of the antibody that is used. Non-specific binding of the antibody could easily lead to misinterpretation of results. Additionally, immunohistochemistry is not readily quantifiable and thus it is difficult to compare the levels of proteins between two or more samples. Finally, interpretation of immunohistochemistry results is highly dependent on the field of view that is chosen. The disadvantages and caveats of immunohistochemistry are thoroughly reviewed elsewhere⁸.

The isolated working mouse heart was developed as a simplified model to study cardiac function and is extensively used, particularly in the evaluation of metabolic parameters (reviewed in ⁹). However, a number of caveats must be considered before translating the results obtained with this technique to an *in situ* heart. As it is an *ex vivo* model, the isolated working mouse heart is not under the influence of neurohumoral factors, as it would be *in vivo*, thus functional parameters do not necessarily mimic an *in situ* heart. For example, in a normal conscious mouse, heart rate ranges from approximately 500-600 beats per min¹⁰, while in the isolated working heart studies presented in this thesis, the heart rates were between 300-400 beats per min. Additionally, the function of the isolated working mouse heart is greatly dependent on the composition of the buffers used to perfuse the heart. There is little agreement between different research groups as to which is the most appropriate buffer system to use. As fatty acids are a major source of energy for the heart, some research groups routinely add fatty acids to their isolated working heart perfusion buffers. However, albumin, which is used to bind fatty acids in such buffers, also has antioxidant properties (reviewed in ¹¹), which may confound results when examining models such as I/R which

generate significant oxidative stress. Operator skill also plays a significant role in the use of this technique. Use of the isolated working mouse heart model requires considerable fine motor skills and keen eyesight. Coupled with this is the necessity to work rapidly in order to prevent the nearly instantaneous deterioration or preconditioning of the organ. Consequently, inter-operator variability is considerable.

7.3: Future directions

Though the work presented in this thesis was the first to demonstrate regulation of MMP-2 by Cav-1, a great deal of work still remains to be done in order to more fully elucidate the mechanisms of intracellular MMP-2 regulation.

To begin with, the nature of the Cav-1 / MMP-2 interaction needs to be more fully explored. Though Chapter 2 had examined the theoretical Cav-1 / MMP-2 binding sites, using a molecular technique such as yeast two-hybrid could empirically determine where on the MMP-2 protein Cav-1 binds. It was also shown that MMP-2 and Cav-1 co-localize by immunohistochemistry, however a demonstration of an interaction between these two proteins in the heart (e.g. by immunoprecipitation), would lend credence to the hypothesis that Cav-1 can regulate intracellular MMP-2 activity.

Further investigation of the Cav-1^{-/-} mouse heart is also necessary. As other groups have shown, the Cav-1^{-/-} hearts develop significant pathologies as the mice age, including dilated cardiomyopathy and cardiac hypertrophy¹²⁻¹⁴. Many of these pathologies have also been associated with changes in MMP-2 activity^{15;16}.

Consequently, a thorough exploration of Cav-1^{-/-} hearts from older mice may give insight into the regulation of MMP-2 by Cav-1.

Besides its role in cardiac I/R injury, MMP-2 has been shown to play significant roles in the development and progression of a number of other cardiovascular diseases (reviewed in ^{16,17}). Though the role of Cav-1 has not been extensively examined in these diseases, it is possible that Cav-1 may play a role in the regulation of MMP-2. Consequently, it becomes important to examine whether Cav-1 production and/or distribution is perturbed in other models of cardiovascular disease, in order to determine whether Cav-1 plays a role in the regulation of MMP-2.

Clinical examination of the role of Cav-1 regulation of MMP-2 would be the ultimate goal of this line of research. Alterations of Cav-1 have already been demonstrated in humans in different pathologies. For example, patients with pulmonary hypertension have been shown to have reduced levels of Cav-1 in their lungs¹⁸, and this may be significant, particularly as MMP-2 has been shown to be elevated in a rat model of pulmonary hypertension and is correlated with its severity¹⁹. Also, patients with failing hearts that were treated with mechanical unloading not only demonstrate improved structure and function in what is deemed “reverse remodeling”²⁰, but this mechanical unloading also increases Cav-1 expression in the heart²¹. This is consistent with our hypothesis that Cav-1 may be responsible for the regulation of MMP-2 activity, which has been shown to play a major role in heart remodeling^{22,23}. An examination of tissue from a human heart that was exposed to a stunning injury, as in the case of patients undergoing cardiopulmonary bypass for coronary artery grafting, for distribution of Cav-1 would greatly expand our

understanding of the conditions during which Cav-1 regulation of MMP-2 may be important.

Additionally, though this thesis has centered on Cav-1 regulation of MMP-2 in the intracellular milieu, this does not exclude a role of Cav-1 regulation of extracellular MMP-2. Indeed, a number of studies have shown that Cav-1 is perturbed in cancer models, and this consequently leads to an increase in extracellular gelatinase activity and cancer cell invasion²⁴. This may also be the case in the heart, where Cav-1 may play important roles in extracellular MMP-2 regulation, though the preliminary studies in Chapter 2 reveal no significant alterations in extracellular collagen levels between Cav-1^{+/+} and Cav-1^{-/-} mouse hearts.

Finally, additional work needs to be performed in order to more fully understand how the phosphorylation state of TnI changes with isoproterenol administration and/or I/R. 2D electrophoresis and/or mass spectrometry of heart samples exposed to β -adrenergic agonists and/or I/R injury could more fully reveal the specific different phosphorylation states of TnI. Interestingly, preliminary studies have shown that TnI may actually be able to regulate MMP-2 activity. TnI was added to the OmniMMP assay outlined in Chapter 2 in hopes that TnI would become a competitive substrate. Instead, it was found that the addition of TnI to this assay accelerated MMP-2's ability to degrade the OmniMMP substrate.

In conclusion, this thesis has centered on the exploration of the role of Cav-1 in the regulation of MMP-2 activity. The results presented here are the first to demonstrate that Cav-1 knockout can not only affect cardiac MMP-2 activity, but also how this altered MMP-2 activity may or may not affect intracellular MMP-2 substrates.

Subsequent studies will further reveal the molecular mechanisms that underlie the complex interactions between these two proteins and clinical examination may eventually lead to a novel avenue of therapeutic intervention for cardiovascular diseases.

7.4: References

1. World Health Organization. World Health Organization: Cardiovascular Diseases. World Health Organization, Fact sheet 317 .
<http://www.who.int/mediacentre/factsheets/fs317/en/index.html>. Updated 2009. Accessed on April 7, 2010.
2. Schnaeker, EM, Ossig, R, Ludwig, T, Dreier, R, Oberleithner, H, Wilhelmi, M, and Schneider, SW. Microtubule-dependent matrix metalloproteinase-2/matrix metalloproteinase-9 exocytosis: prerequisite in human melanoma cell invasion. *Cancer Res.* 2004; 64:8924-8931.
3. Li, Q, Zhang, Q, Wang, C, Liu, X, Qu, L, Gu, L, Li, N, and Li, J. Altered distribution of tight junction proteins after intestinal ischaemia/reperfusion injury in rats. *J. Cell Mol. Med.* 2009; 13:4061-4076.
4. Mahmoudi, M, Willgoss, D, Cuttle, L, Yang, T, Pat, B, Winterford, C, Endre, Z, Johnson, DW, and Gobe, GC. In vivo and in vitro models demonstrate a role for caveolin-1 in the pathogenesis of ischaemic acute renal failure. *J. Pathol.* 2003; 200:396-405.
5. Jasmin, JF, Malhotra, S, Singh, DM, Mercier, I, Rosenbaum, DM, and Lisanti, MP. Caveolin-1 deficiency increases cerebral ischemic injury. *Circ. Res.* 2007; 100:721-729.
6. Jay, DJ, Garcia, E, Chow, AK, Cheung, PY, Ramirez, AL, and Schulz, R. Phosphorylation of cardiac troponin I affects its susceptibility to proteolysis by matrix metalloproteinase-2. *Can. J. Cardiol.* 2008; 24:0183.

7. Gomes, AV, Liang, J, and Potter, JD. Mutations in human cardiac troponin I that are associated with restrictive cardiomyopathy affect basal ATPase activity and the calcium sensitivity of force development. *J. Biol. Chem.* 2005; 280:30909-30915.
8. Fritschy, JM. Is my antibody-staining specific? How to deal with pitfalls of immunohistochemistry. *Eur. J. Neurosci.* 2008; 28:2365-2370.
9. Barr, RL and Lopaschuk, GD. Methodology for measuring in vitro/ex vivo cardiac energy metabolism. *J. Pharmacol. Toxicol. Methods* 2000; 43:141-152.
10. Sheward, WJ, Naylor, E, Knowles-Barley, S, Armstrong, JD, Brooker, GA, Seckl, JR, Turek, FW, Holmes, MC, Zee, PC, and Harmar, AJ. Circadian control of mouse heart rate and blood pressure by the suprachiasmatic nuclei: behavioral effects are more significant than direct outputs. *PLoS. One.* 2010; 5:e9783.
11. Roche, M, Rondeau, P, Singh, NR, Tarnus, E, and Bourdon, E. The antioxidant properties of serum albumin. *FEBS Lett.* 2008; 582:1783-1787.
12. Cohen, AW, Park, DS, Woodman, SE, Williams, TM, Chandra, M, Shirani, J, Pereira de, SA, Kitsis, RN, Russell, RG, Weiss, LM, Tang, B, Jelicks, LA, Factor, SM, Shtutin, V, Tanowitz, HB, and Lisanti, MP. Caveolin-1 null mice develop cardiac hypertrophy with hyperactivation of p42/44 MAP kinase in cardiac fibroblasts. *Am. J. Physiol Cell Physiol* 2003; 284:C457-C474.
13. Murata, T, Lin, MI, Huang, Y, Yu, J, Bauer, PM, Giordano, FJ, and Sessa, WC. Reexpression of caveolin-1 in endothelium rescues the vascular, cardiac, and

- pulmonary defects in global caveolin-1 knockout mice. *J. Exp. Med.* 2007; 204:2373-2382.
14. Zhao, YY, Liu, Y, Stan, RV, Fan, L, Gu, Y, Dalton, N, Chu, PH, Peterson, K, Ross, J, Jr., and Chien, KR. Defects in caveolin-1 cause dilated cardiomyopathy and pulmonary hypertension in knockout mice. *Proc. Natl. Acad. Sci. U. S. A* 2002; 99:11375-11380.
 15. Roldan, V, Marin, F, Gimeno, JR, Ruiz-Espejo, F, Gonzalez, J, Feliu, E, Garcia-Honrubia, A, Saura, D, de la, MG, Valdes, M, and Vicente, V. Matrix metalloproteinases and tissue remodeling in hypertrophic cardiomyopathy. *Am. Heart J.* 2008; 156:85-91.
 16. Chow, AK, Cena, J, and Schulz, R. Acute actions and novel targets of matrix metalloproteinases in the heart and vasculature. *Br. J. Pharmacol.* 2007; 152:189-205.
 17. Schulz, R. Intracellular targets of matrix metalloproteinase-2 in cardiac disease: rationale and therapeutic approaches. *Annu. Rev. Pharmacol. Toxicol.* 2007; 47:211-242.
 18. Zhao, YY, Zhao, YD, Mirza, MK, Huang, JH, Potula, HH, Vogel, SM, Brovkovich, V, Yuan, JX, Wharton, J, and Malik, AB. Persistent eNOS activation secondary to caveolin-1 deficiency induces pulmonary hypertension in mice and humans through PKG nitration. *J. Clin. Invest* 2009; 119:2009-2018.

19. Frisdal, E, Gest, V, Vieillard-Baron, A, Levame, M, Lepetit, H, Eddahibi, S, Lafuma, C, Harf, A, Adnot, S, and Dortho, MP. Gelatinase expression in pulmonary arteries during experimental pulmonary hypertension. *Eur. Respir. J.* 2001; 18:838-845.
20. Barbone, A, Holmes, JW, Heerdt, PM, The', AH, Naka, Y, Joshi, N, Daines, M, Marks, AR, Oz, MC, and Burkhoff, D. Comparison of right and left ventricular responses to left ventricular assist device support in patients with severe heart failure: a primary role of mechanical unloading underlying reverse remodeling. *Circulation* 2001; 104:670-675.
21. Uray, IP, Connelly, JH, Frazier, OH, Taegtmeier, H, and Davies, PJ. Mechanical unloading increases caveolin expression in the failing human heart. *Cardiovasc. Res.* 2003; 59:57-66.
22. Matsusaka, H, Ide, T, Matsushima, S, Ikeuchi, M, Kubota, T, Sunagawa, K, Kinugawa, S, and Tsutsui, H. Targeted deletion of matrix metalloproteinase 2 ameliorates myocardial remodeling in mice with chronic pressure overload. *Hypertension* 2006; 47:711-717.
23. Hayashidani, S, Tsutsui, H, Ikeuchi, M, Shiomi, T, Matsusaka, H, Kubota, T, Imanaka-Yoshida, K, Itoh, T, and Takeshita, A. Targeted deletion of MMP-2 attenuates early LV rupture and late remodeling after experimental myocardial infarction. *Am. J. Physiol Heart Circ. Physiol* 2003; 285:H1229-H1235.

24. Han, F and Zhu, HG. Caveolin-1 regulating the invasion and expression of matrix metalloproteinase (MMPs) in pancreatic carcinoma cells. *J. Surg. Res.* 2010; 159:443-450.